KERNFORSCHUNGSANLAGE

Program of
Research and Development
on the

Thorium Utilization in PWRs

Final Report (1979–1988)

GERMAN-BRAZILIAN COOPERATION
IN SCIENTIFIC RESEARCH AND TECHNOLOGICAL DEVELOPMENT

GERMAN-BRAZILIAN COOPERATION
IN SCIENTIFIC RESEARCH AND TECHNOLOGICAL DEVELOPMENT

Program of Research and Development on the THORIUM UTILIZATION IN PWRS

Final Report (1979–1988)

PROGRAM PARTNERS

The program effort has been undertaken jointly by the companies

- KERNFORSCHUNGSANLAGE JÜLICH
  Gesellschaft mit beschränkter Haftung
- SIEMENS Aktiengesellschaft, Unternehmensbereich KWU
- NUKEM GmbH

on the German side and

- NUCLEBRAS Empresas Nucleares Brasileiras SA

on the Brazilian side.

The main working areas covered by the program partners were

- irradiation fuel testing and cold reprocessing studies by KFA
- nuclear fuel design and strategy calculations, fuel development and storage as well as irradiation fuel testing by SIEMENS UB KWU
- fuel development and irradiation fuel testing by NUKEM
- all areas by NUCLEBRAS

Herausgegeben von der Kernforschungsanlage Jülich GmbH
ZENTRALBIBLIOTHEK
Postfach 1913 · D-5170 Jülich
Telefon 02461/61-0 · Telex 833556-70 kfa d

Titelsatz: Graphische Betriebe der KFA

Druck: WEKA-Druck GmbH, Linnich

Jül-Spez-488
ISSN 0343-7639

ISBN 3-89336-019-0

NUCLEBRAS/CDTN 600/88
NUKEM FUE-88003
SIEMENS UB KWU, U 642/88/080

Abstract

Detailed investigations performed for a standard 1,300 MW_e PWR show that $(Th,U)O_2$ and $(Th,Pu)O_2$ fuels can be inserted in 3 and 4 cycle operating schemes without modifications in the fuel assembly or core design. The most important aspects of the fuel cycle have been covered. Ex-gel pelletizing of $(Th,U)O_2$ fuel making use of available LWR and HTR fuel manufacturing technology was demonstrated. The most promising application for Th-based fuels at present was proved to be the use of recycle plutonium in extended burnup once-through fuel cycle. The program was performed in a cooperative way between Brazilian and German partners.

Authors

NUCLEBRAS/CDTN

R.B. Pinheiro*, F.A.N. Carneiro, F.S. Lameiras*, R.A.N. Ferreira, W.B. Ferraz, M.S. Dias, M.L.L. Soares, E.P. de Andrade, H.A. Mascarenhas, A.M.M. dos Santos, L.C.M. Pinto, A. Santos, S.A.C.Filgueras, M.J. de O. Lopes.

SIEMENS KWU/Nuclear Fuel Cycle

M. Peehs*, G. Schlosser, F. Wunderlich, H. Gross, W. Doer, M. Gaertner, G. Kaspar, H. Finnemann, D. Porsch.

NUKEM

M. Hrovat, M. Kadner.

KFA-Jülich

V. Maly*, K. Reichardt, B.G. Brodda, E. Zimmer.

* Persons responsible for editing.

Acknowledgments

The report presents a joint activity of the program partners KFA, NUCLEBRAS, Siemens Group KWU and NUKEM. Besides the persons named above, many others have participated by valuable contributions and comments.

The following persons contributed to the initiation and progress of the program: Mr. S.C. Valadao, Mr. V. Andrade, Dr. S. Paiano, Mr. P.E.Cardoso on the NUCLEBRAS side, Dr. P. Engelmann and Dr. D.H. Leushacke (KFA), Dr. H. Märkl and Dr. H. Stehle (Siemens, UB KWU), Dr. H. Huschka (NUKEM) on the German side.

On the German side the program has been funded in part by the Federal Ministry of Research and Technology (BMFT).

Table of Contents

	Abstract	I
	Authors	II
	Acknowledgments	III
	Table of contents	IV
0.	**Executive Summary**	1
0.1	Introduction	1
0.2	Technical results	2
0.3	Program evaluation	3
1.	**Introduction**	5
1.1	**Program Objectives**	5
1.2	**State of the Art on Thorium Use in Power Reactors**	6
1.2.1	General Objectives	6
1.2.2	Overview on major national programs	7
1.2.3	Technical summary from the current programs	10
1.2.4	Special experience in former FRG-program used in the present joint activities	14
	References	17
	Table	21
2.	**Technical Results**	23
2.1	**Nuclear Core Design and Strategy Calculations**	23
2.1.1	Nuclear design programs	23
2.1.2	Nuclear fuel cycle studies	24
2.1.3	Nuclear design of an irradiation testing in the power reactor Angra-1	27
2.1.4	Strategy assessment of possible contribution of Th-fuel for PWRs in Brazil	28
2.1.5	Conclusions	29
	References	30
	Tables	31
	Figures	36
2.2	**Thermal and Mechanical Fuel Rod Design**	51
2.2.1	Design criteria for PWR $(Th,U)O_2$ fuel rods	51
2.2.1.1	Temperatures	52
2.2.1.2	Rod internal pressure	52
2.2.1.3	Strain	52
2.2.1.4	Corrosion	53
2.2.1.5	Hydrogen uptake	53
2.2.1.6	Elastic buckling and plastic deformation under external over pressure	53
2.2.1.7	Cladding tube stresses	54
2.2.1.8	Dynamic loads	54
2.2.2	Design related material properties of $(Th,U)O_2$ pellets	54

2.2.2.1 Thermal conductivity ... 54
2.2.2.2 Thermal density ... 56
2.2.2.3 Thermal expansion ... 56
2.2.2.4 Melting point ... 57
2.2.2.5 Theoretical density ... 57
2.2.3 Design related phenomena on $(Th,U)O_2$ pellets ... 58
2.2.3.1 Densification ... 59
2.2.3.2 Swelling ... 59
2.2.3.3 Relocation ... 59
2.2.3.4 Fission gas release ... 59
2.2.3.5 Restructuring ... 60
2.2.4 Design related materials properties and phenomena of Zircaloy-4 cladding tubes ... 60
2.2.4.1 Thermal conductivity ... 60
2.2.4.2 Thermal expansion ... 61
2.2.4.3 Mechanical properties ... 61
2.2.4.4 Creep ... 61
2.2.4.5 Axial growth ... 62
2.2.4.6 External corrosion ... 63
2.2.5 Thermal and mechanical design of a Th-fuel rod ... 64
2.2.5.1 Th-CARO approach for $(Th,U)O_2$ fuel rod behaviour ... 64
2.2.5.2 Th-CARO performance calculations for $(Th,5\%U)O_2$ test fuel rods ... 64
2.2.5.3 Design calculations for $(Th,5\%U)O_2$ pathfinder test fuel rods ... 65
2.2.6 Conclusions ... 68
References ... 68
Tables ... 72
Figures ... 73

2.3 **Technology Development for $(Th,U)O_2$-PWR Fuel** ... 103
2.3.1 Basic technology for $(Th,U)O_2$-pelletizing ex-gel ... 103
2.3.1.1 Conversion process ... 103
2.3.1.2 Pelletizing ... 104
2.3.2 Objectives, problems and solutions ... 104
2.3.2.1 Requirements for PWR-fuel pellets ... 104
2.3.2.2 Scoping studies ... 105
2.3.2.3 Solution investigated ... 105
2.3.3 Pellet specification and quality assurance requirements ... 107
2.3.3.1 $(Th,U)O_2$ specification ... 107
2.3.3.2 Quality assurance requirements ... 108
2.3.4 Description of $(Th,U)O_2$-pelletizing technology ex-gel ... 110
2.3.4.1 Process description ... 110
2.3.4.2 Results from process validation ... 112
2.3.5 Conclusions ... 113
References ... 114
Tables ... 115
Figures ... 121

2.4 **Transfer of $(Th,U)O_2$ Fuel Technology to $(Th,Pu)O_2$ Technology** ... 145
2.4.1 Plutonium simulation by means of cerium ... 145
2.4.2 Basic technologies for plutonium processing ... 147

2.4.2.1 The mixed oxide concept 147
2.4.2.2 The master-mix concept 149
2.4.3 Objectives, problems and solutions 149
2.4.3.1 Requirements for PWR-fuel pellets 149
2.4.3.2 Scoping studies 150
2.4.3.3 Solutions to be investigated 150
2.4.4 Conclusions 152
References 153
Tables 154
Figures 156

2.5 **Irradiation Testing** 169
2.5.1 Irradiation experiments in the material test reactor FRJ-2 169
2.5.1.1 Objectives, facilities and procedures 169
2.5.1.2 Test fuel rod manufacturing and quality control 172
2.5.1.3 Pre-irradiation measurements 174
2.5.1.4 Irradiation data 174
2.5.1.5 Post-irradiation examination 174
2.5.2 Pathfinder irradiation technology 175
2.5.2.1 Objectives, facilities and procedures 175
2.5.2.2 Irradiation strategy 176
2.5.3 Conclusions 177
Reference 177
Tables 178
Figures 183

2.6 **Fuel Storage and Reprocessing** 195
2.6.1 Spent fuel storage assessment 195
2.6.1.1 Description of the spent fuel storage assessment 195
2.6.1.2 Description of the EOL conditions of a Th-fuel pin 195
2.6.1.3 Storage performance predictions of a representative spent Th-fuel pin 195
2.6.2 Reprocessing studies for $(Th,U)O_2$ PWR fuel 196
2.6.2.1 Dissolution and feed adjustment of $(Th,U)O_2$ fuel with Zircaloy clad 197
2.6.2.2 Solvent extraction by THOREX process 199
2.6.3 Conclusions 206
References 207
Tables 209
Figures 211

0. Executive Summary

0.1 Introduction

The cooperative R&D Program on "Thorium Utilization in Pressurized Water Reactors" was carried out by NUCLEBRAS/CDTN on the Brazilian side and KFA-Juelich with the participating companies Siemens UB KWU and NUKEM on the German side. It was directed towards the improvement of knowledge in this field and actually aimed at fulfilling the „Governmental Agreement on Cooperation in the Field of Science and Technology" from 1969 and the „Memorandum of Understanding between KFA and NUCLEBRAS" from 1978.

The program was motivated by the fact, determined in numerous R&D activities, including those in Brazil and Germany, that thorium fuels can improve the resource utilization in thermal reactors and may supplement conventional uranium-based fuels. The thorium cycle technology was, however, not so mature as to permit well-founded feasibility statements in this area.

The original objectives of the program running since mid 1979 were

a) to analyze and prove thorium utilization in pressurized water reactors;
b) to design PWR fuel element and core for the Th-fuel cycle;
c) to manufacture, test and qualify Th/U and Th/Pu fuel elements under operating conditions;
d) to study spent fuel treatment and to close the thorium fuel cycle by reprocessing spent Th-containing PWR fuel assemblies.

The transfer of R&D methodology for the PWR fuel cycle presented the other main objective of the program.

The program was directed by the Coordinating Committee (CCM) consisting of two representatives from each participating country. The program managers, who met once or twice a year, jointly formulated the working program and supervised the progress. Task managers were assigned by each participating organization and shared the technical responsibility.

The program was planned to run in three phases. In the program Phase 1 (1979 through 1983) the technological basis for further work on $(Th,U)O_2$ fuel for PWR was established and the feasibility of the chosen fuel cycle concept was proven in principle. In Phase 2 the main objectives were the demonstration of the feasibility of PWR $(Th,U)O_2$ fuel, nuclear core design and initiation of the development of $(Th,Pu)O_2$ fuel and improving knowledge on spent fuel treatment. The demonstration of the $(Th,Pu)O_2$ fuel was intended to follow in Phase 3.

In the course of time, the objectives and scope of the program were adapted to the actual needs in the contributing countries. The effort was concentrated more on the development of the fuel fabrication, its qualification and testing as well as on the transfer of R&D know-how in this area. The activity related to the spent fuel treatment was

reduced, in particular when the advantageous features of the once-through Pu/Th fuel cycle with high burnup were confirmed.

Phase 2 of the program was focussed on the intended irradiation of a pathfinder fuel assembly in a Brazilian power reactor. It was also recognized that the major benefits in the Th-PWR application result from the Th/Pu fuel. Since Brazil decided not to reprocess spent PWR fuel, the most beneficial Th application was no longer a short term issue. Thus due to a Brazilian priority decision the partners agreed to terminate the program at a pre-determined decision point in the middle of Phase 2.

0.2 Technical Results

Nuclear core design and strategy

The program covered major portions of the PWR fuel cycle including the relevant parts of nuclear core design. The Siemens standard 1,300 MW_e PWR was used as the reference reactor, also providing a good basis for the know-how transfer. First, Siemens' standard nuclear core design codes were adapted for the use of thorium and validated. The results of nuclear core design show that the present design Siemens-type PWR can accommodate Th-based fuels without any changes or restrictions in the fuel assembly or core design. Operation of the reactor in three and four batches was investigated in open and closed fuel cycles. Moreover, partial core load with Th-fuel and successive switch-over from U to Th fuel is also practicable. Beside the determination of optimum shuffling patterns, basic three-dimensional safety calculations also show sufficient safety margins. Th/Pu based fuels show a possibility of extending the burnup even beyond the 4-year cycle operation.

In the strategy field beside the code development, the accompanying studies of thorium cycle potential have also provided insight into the possible introduction of Th-fuels in the long-term reactor strategy in Brazil.

Fuel technology

The merging of the standard LWR pelletizing process with the chemical ex-gel process developed for the HTR fuel was successful. The combination of a chemical ex-gel conversion process resulting in calcined unsintered $(Th,U)O_2$ kernels, with a mean diameter of about 0.3mm, with standard pelletizing techniques using an adapted compaction pressure, provided $(Th,U)O_2$ fuel pellets with adequate homogeneity, microstructure and geometrical shape, satisfying the usual PWR specifications. These pellets have been reproducibly manufactured in Germany and Brazil in kg charges and the results confirmed in a round robin test. In most steps of the production process standard equipment could be used. Thus, no major difficulties are expected for scale-up from pilot scale to production capacity.

The transfer of knowledge to the $(Th,Pu)O_2$ fuel production was performed on a laboratory scale using cerium as a substitute for plutonium. The dust-free ex-gel fabrication process is particularly attractive for this application. Results of a laboratory-scale investigation indicate that the master-mix fuel concept can also be realized.

Fuel design and modelling

Data and models for the thermal and mechanical fuel rod design were derived from theoretical considerations and experimental results for the newly developed oxidic Th-fuels for use in standard PWR fuel design. Design values were successfully verified by predicting the fuel behaviour in irradiation experiments performed in the FRJ-2 reactor at KFA, Juelich. Good agreement between predicted and measured values was reached. On this basis the design of a test fuel assembly for the Angra-1 reactor was prepared including the licensing report for the experimental fuel.

Irradiation testing

The irradiation testing of the previously developed fuel was performed in FRJ-2 reactor up to 10 MWd/kgHM under conditions covering the loads of a PWR. The ex-gel $(Th,U)O_2$ fuel behaviour satisfied the requirements. Extensive post-irradiation examination and evaluation of the series of experiments provided a comprehensive data base for further development effort and substantially improved knowledge on in-pile fuel behaviour.

On the basis of these experiments an irradiation program up to four cycles for four segmented rods and one full scale rod with burnups up to 45 MWd/kgHM was prepared using a pathfinder fuel assembly approach for a commercial power reactor including the preparation of the licensing documents.

Spent fuel treatment

Computer calculations based on newly developed methods were performed in order to identify differences between Th and U based fuels in storage performance. The intermediate and direct final storage does not present additional problems in comparison with the standard UO_2 fuel.

Laboratory investigations on reprocessing spent thoria fuel were focussed mainly on work with unirradiated fuel. To a limited extent hot laboratory work on dissolution was performed. The application of presently known reprocessing techniques for thoria fuels to the fuels developed in this program seems possible.

0.3 Program Evaluation

R&D progress

The results of the program confirm in detail that the newly developed thoria based fuels can be used in present PWRs of Siemens design. No changes in the fuel assembly and in the core design are needed. This holds both for $(Th,U)O_2$ and $(Th,Pu)O_2$ fuels in 3 and 4 batch operation. The latter fuel shows high burnup potential beyond the four-cycle scheme. In this case the inserted fissile Pu is strongly depleted and the once-through put-away cycle becomes very attractive.

The fuel manufacturing was developed on a pilot scale for kg-amounts of $(Th,U)O_2$ using adequate spin-off from fully established HTR and LWR fuel manufacturing. Due to the understanding of the key process parameters and using mostly standard equipment, full-scale production seems feasible after a short development period.

The status of the $(Th,U)O_2$ fuel testing and modelling permits a design of pathfinder fuel test which can be subjected to licensing. This would be a necessary step before insertion of $(Th,U)O_2$ fuel on a large scale.

As far as the technology development and transfer for the Th/U fuel are concerned, the program objectives were accomplished.

However, large scale demonstration of Th/U fuel in a power reactor, fabrication and qualification of Th/Pu fuel as well as closing the fuel cycle would require substantially more effort than presently desirable.

For $(Th,Pu)O_2$ fuel a basic knowledge considering the requirements for the transfer of the $(Th,U)O_2$ fuel fabrication technology was developed. The assessment of the back end of the fuel cycle shows that Zircaloy-4 clad PWR fuel can be handled in the storage regardless of the specific ceramic fuel included.

Cooperation and technology transfer

The contents of the final report and numerous joint publications and reports confirm that successful cooperation and technology transfer took place in the course of this program.

In the first phase of the program the build-up of the research capacity in the nuclear fuel technology area at NUCLEBRAS/CDTN resulted in steadily increasing Brazilian participation in the R&D effort. In the second program phase each partner's contribution consisted in delivering his share of the work package in a balanced way.

The technology transfer is documented in the technical part of the report. This transfer was enhanced by the fact that in most areas techniques used for a standard UO_2-fuelled PWR had to be modified thus requiring an active understanding and assimilation of the R&D know-how.

So far as the nuclear core design and the technology development and transfer for the Th/U fuel are concerned, the original program objectives were accomplished.

Conclusions

The utilization of thorium in PWRs presents a long term option providing in some respects interesting results. The most attractive application for Th-based fuels at present is the use of recycle plutonium in an extended burnup once-through fuel cycle.

From the point of view of cooperation and technology transfer, the program experience shows the importance of using hardware oriented goals, clear definitions of required outputs and sufficient communication including joint work on interacting tasks.

1. Introduction

1.1 Program Objectives

The cooperative Research and Development program on "Thorium Utilization in Pressurized Water Reactors between Empresas Nucleares Brasileiras S.A. – NUCLEBRAS through its R & D center (Centro de Desenvolvimento da Tecnologia Nuclear – CDTN) on the Brazilian side and Kernforschungsanlage Juelich GmbH with the participation of the companies Siemens AG-Group KWU and NUKEM GmbH, sponsored in part directly by the Federal Ministry for Research and Technology (BMFT) on the German side aimed at fulfilment in practice of the „Governmental Agreement on the Cooperation in the Field of Science and Technology of 1969" [1–1] and the „Memorandum of Understanding between KFA and NUCLEBRAS of 1978" [1–2].

The program was motivated by the fact known from numerous R & D activities among others in Brazil and Germany that thorium fuels can provide better resource utilization in thermal reactors compared with the conventional uranium based fuels. The thorium cycle technology was, however, not so mature as to permit well based feasibility statements in this area. By using the standard Pressurized Water Reactor (PWR) as a reference plant an efficient way had been chosen for demonstration of the technological feasibility by concentration on the problems specific for the thorium fuel cycle, providing also a way for assimilation of PWR-fuel cycle know-how. At the same time, the potential of the standard PWR with respect to the advanced fuel cycles was demonstrated.

The program work was initiated mid 1979 with the general objectives:

a) to analyze and prove the thorium utilization in PWRs,

b) to design the PWR fuel element and core for the different Th-fuel cycles,

c) to manufacture, test and qualify Th/U and Th/Pu fuel elements under operating conditions,

d) to study the closing of thorium fuel cycles by reprocessing of spent Th-containing PWR fuel elements.

Technology transfer by joint work on these tasks presented another major objective of the program.

Three phases were foreseen at the start of the program. In Phase 1 the main objective consisted in the adaptation of the existing methods and technologies to PWR thoria fuels. In Phase 2 the R & D effort should concentrate on demonstrating the behaviour of $(Th,U)O_2$ fuel behaviour in a current power reactor, followed by the demonstration of $(Th,Pu)O_2$ fuel in Phase 3.

The program utilized as much as possible the existing technologies and the available know-how combining the techniques and equipment used for standard PWR with those developed for the High Temperature Reactor (HTR). In the area of the nuclear core design the incorporation of thorium relevant data and routines in the standard design codes had to be performed first. An advanced ex-gel fuel manufacturing technol-

ogy has been developed utilizing the direct pelletizing of sol-gel derived mixed oxide kernels. The irradiation testing provided data for modification of the standard thermal and mechanical fuel design code. In the back-end of the fuel cycle the original intention to verify and upgrade the available reprocessing techniques has been redirected towards a closer look at the storage related problems in the last program period. The program has covered nearly the entire scope of the nuclear fuel cycle.

After confirmation of the feasibility of the developed fuel fabrication concept the program effort has concentrated on the application of the results to a standard KWU 1,300 MW_e PWR similar to the Angra-2 nuclear power plant under construction in Brazil. This objective has permitted clear and well measurable goals in all working areas being set.

This also enhanced the know-how development and the assimilation of the R & D techniques for the PWR fuel cycle by NUCLEBRAS.

The R & D activity included the modification of the processes and methods for an advanced type of fuel which had to satisfy the well known requirements of an existing reactor system.

The close cooperation between the program partners strongly contributed to the program success. In the initial phase the major flow of know-how was directed from Germany to Brazil mostly in connection with long term Brazilian delegations to Germany. Later, each partner has been contributing the results of his effective utilization of resources and balanced know-how flow had been achieved.

The program results proved that thoria based fuels can be inserted in unmodified fuel assemblies into a standard 1,300 MW_e of KWU type. Potential use of thorium containing fuel in a standard PWR appears particularly attractive in case of insertion of high burnup $(Th,Pu)O_2$ fuel in once through mode.

The advanced fuel fabrication process provides in a reproducible way fuel satisfying the PWR specifications. Its behaviour has been tested with good results up to 10 MWd/kgHM in a research reactor (FRJ-2, in Juelich) providing also a basis for planning of power reactor testing and validating the Th-related design codes. The spent fuel storage does not need any change in the treatment compared to standard UO_2-fuel.

The program was terminated by mid 1988 after 9 years of successful cooperation before entering the pathfinder demonstration phase with a $(Th,U)O_2$ fuel bearing test assembly in a commercial PWR. This major goal has not been achieved due to changes in R & D priorities within NUCLEBRAS.

1.2 State of the Art on Thorium Use in Power Reactors

The assessment of the worldwide activities on the Th-based nuclear fuel is based in part on the results of the IAEA Technical Committee Meeting discussing the current status and perspectives in this field [1–3].

1.2.1 General objectives

Conventional nuclear power plants can be designed for operation either in the U/Pu

cycle, in Th/HEU* cycle or in Th/Pu cycle. The main advantage of the Th-based fuel cycles in thermal reactors is that it has a higher neutron yield of ^{233}U, in comparison with the neutron yield of ^{239}Pu in the U/Pu cycle. Those benefits may be equalized by commercial disadvantages, due to the requirement of HEU and the problems related to reprocessing and refabrication in a closed fuel cycle since full remotization is needed. The once-through put-away cycle by the use of Th/Pu fuel offers the possibility, when applied to PWR systems, to avoid these problems.

1.2.2 Overview on major national programs

In the following the status and results of the major national programs will be summarized shortly (see also Tab.1.1).

FRG [1–4]

The development of thorium fueled reactors has been closely connected in the Federal Republic of Germany with the activities related to the High-Temperature Reactor. The 15 MW_e AVR-Reactor has been successfully operated since 1967 with graphite based coated-particle oxidic thorium fuel. Burnups of 15–20% fima have been reached for a significant portion of the fuel showing good structure and hardly any defects. Up to now about 2,000 kg of thorium heavy metal have been fabricated and inserted in the reactor. The 300 MW_e demonstration THTR plant in Schmehausen also using thorium based coated particle $(Th,U)O_2$ fuel has been in operation since 1986 showing good fuel behaviour under irradiation. Related to this reactor program, activities directed to spent fuel treatment concentrate presently on the intermediate and direct storage of the $(Th,U)O_2$ fuel.

Based on the fabrication techniques developed for HTR-fuel the technology used for the production of the pressfit kernels used in the present program has been derived.

Another effort in FRG has been concentrated on the development of the heavy water moderated Thorium Breeder Reactor. This activity incorporated beside nuclear core design and fuel development also an irradiation program, in the course of which vipac $(Th,U)O_2$ fuel was irradiated up to 5% fima showing good fuel behaviour. Some of the results have been utilized in the present program.

The recycling of plutonium and thorium oxidic fuel was investigated in a few fuel assemblies in the Lingen BWR in the early seventies. The task was terminated in 1973 after changes in the boundary conditions.

USA [1–3]

Three extended thorium-fuel reactor programs have been undertaken in the USA. These are the Molten Salt Breeder Reactor (MSBR) and the Light Water Breeder Reactor (LWBR). A third, the High Temperature Gas Cooled Reactor, has utilized thor-

*HEU — Highly Enriched Uranium — uranium enriched e.g. to 93. w/o ^{235}U.

ium since 1976 in the 300 MW_e Ft.St.Vrain power plant. The behaviour of the graphite based coated particle fuel with $(Th,U)C_2$ is good. Because of problems with some components the Ft. St. Vrain reactor did not reach a satisfactory performance until now.

The study and development of molten-salt reactors was begun in the USA at the Oak Ridge National Laboratory in 1947. The potential of MSBR for civilian power production was recognized and a development program was established in 1956. The Molten Salt Reactor Experiment was operated from 1969. It was fueled with a ^{235}U-^{238}U mixture during the initial two years of operation and with ^{233}U during the remaining 1.5 years of operation. The successful operation of the molten salt reactor and the favourable projected system characteristics attracted significant US industry and utility interest. The development of molten-salt reactors was interrupted in 1973. The program was resumed briefly in 1974 but finally terminated in mid 1976.

The second major reactor concept utilizing thorium was the Light Water Breeder Reactor. The concept, then called seed-blanket, was originally introduced in 1951 as a means of minimizing the separative work required for the fuel of a light water reactor. The seed-blanket concept was employed in the design of the first commercial PWR plant at Shippingport.

It was long thought to be impractical to breed with light water however, since the eta value of ^{233}U is only slightly lower in the epithermal region, while that of ^{235}U and ^{239}Pu are greatly reduced, the thorium cycle appeared to be most attractive for a thermal breeder. After preliminary work in the early 1960s indicated the feasiblity of breeding in a light water seed-blanket core on the thorium cycle, the US- Atomic Energy Commission authorized a demonstration in the Shippingport plant. Full-power operation of the demonstration cores began in December 1977.

The reactor operated on thorium and ^{233}U cycles until 1982 at which time it was shut down. It is understood that the spent fuel is presently being reprocessed to provide an accurate check of theoretical predictions.

France [1–5]

For some years Electricité de France (EDF) has been carrying out studies concerning the thorium cycle. These studies began in 1969 in relationship to the High Temperature Reactor and have been performed jointly with the Commissariat à l'Energie Atomique (CEA), the Nuclear Studies Center at Saclay for theoretical studies concerning designs and code developments, the Nuclear Center at Cadarache for the integral experiments made necessary by the search for improvements in the accuracy of the basic nuclear data. These studies were completed in the field of molten salt reactors from 1975 and more recently in the field of light water reactors.

With regard to the PWRs, the studies were first concerned with the use of plutonium with thorium to start the cycle. A satisfactory solution has been obtained by recycling the plutonium with thorium as from the first core loading. The solution proposed consists of loading the whole reactor with Th/Pu assemblies from the first core and no longer using the standard checker-board loading scheme where the fuel assemblies are loaded in rings. Two positive aspects appear: burnable poisons are no longer necessary and the fuel assemblies are no longer divided into several zones (as with plu-

tonium recycle together with uranium in reloadings). There are two rather negative characteristics: the second generation plutonium may be used only in fast breeder reactors (FBRs) and the conversion factor is rather small. Nevertheless the proposed solution gives acceptable pin power peak and temperature coefficients.

Satisfactory solutions have also been obtained for cores loaded with Th-^{233}U assemblies. The main problem is, in this case, the moderator temperature coefficient.

Japan [1–6]

No thorium fuel reactor is currently planned to be built in Japan, but basic R & D works are under way to pursue the possible diversification of nuclear fuel resources through thorium utilization in the future.

The Japan Atomic Energy Research Institute started in 1975 basic R & D works on thorium and thorium-uranium mixed oxides to develop laboratory scale fabrication methods, examine irradiation behaviour and to measure physico-chemical properties of these fuels.

Microsphere and pellet-type fuels have been investigated taking into account potential applications of the acquired data for the fabrication and performance analyses of both types of nuclear fuels. The main accomplishments are the following:

a) development of new sol-gel process to prepare crack-free kernels fuel with better sphericity aiming at HTGR applications and to prepare starting material for making high-density pellets with varying Th/U ratios;
b) measurement of fission-gas release/irradiation-induced damage and data analyses to predict irradiation stability and densification mechanism;
c) measurement of new data on equilibrium oxygen potential/stoichiometry and its effect on chemical behaviour of burn-up simulated $(Th,U)O_2$.

The Research Program on thorium fuel has been continued since 1980 on the university basis, under the support of Grant-in-Aid for Energy Research of the Ministry of Education, Science and Culture of the Japanese Government. The main results have been published in the English report „Research on Thorium Fuel (SPEY 9, 1984)" [1–6]. It covers nuclear data evaluation, reactor physics experiments, fuel fabrication, irradiation, actinides production/separation and down-stream process development, and molten salt reactor engineering.

USSR [1–7]

The use of Th is regarded in the USSR as a contribution to assure the fuel supply to its extended nuclear power program. The conclusion is as follows: the most radical means for solving the fuel problem is the application of fast breeder reactors in combination with improved fuel utilization characteristics of the thermal reactors. Among the ways of realizing the improved fuel balance in the thermal reactors emphasis should be placed on the use of the ^{233}U/Th cycle. The available estimates of fuel utilization by the thermal reactors on U/Th cycle are indicative of its attractiveness.

The USSR investigations confirmed that thorium utilization contributes noticeably to the extension of the nuclear fuel resources. Combination of the uranium-plutonium

and thorium cycles ensures long-term fuel supply, makes the nuclear energy production more flexible and, at realistic requirements with regard to the level of fast reactor breeding, enables the self-sustaining regime to be realized in the future.

India [1–8]

For India which has rather limited known reserves of uranium and a vast reserve of thorium, its special interest in utilization of thorium in its reactors is obvious. Studies have shown that Th in radial blanket region of FBRs has only marginal neutron economic penalty compared to complete uranium cycles.

Therefore fabrication and supply of blanket assemblies containing thorium oxide pellets of the required quality for full core of the Indian Fast Breeder Test Reactor, is one of the important tasks of the Nuclear Fuel Complex at Hyderabad. Performance test of these assemblies under actual operating conditions of FBRs, followed by reprocessing studies, will be of great value for the Indian program of utilization of thorium in the envisaged FBRs.

Brazil

In the period 1965-1970 technical and economic studies were conducted in the country aiming at the conceptual development of a heavy-water cooled and moderated pressurized reactor, with prestressed concrete reactor vessel, fueled with thorium-plutonium [1–9, 1–10]. In support of the theoretical studies a subcritical heavy water facility was constructed as well as a thermal-hydraulic test loop.

This program was closed in 1970 due to the Brazilian Government's decision favouring the pressurized light water reactor (PWR) concept.

1.2.3 Technical summary from the current programs Th-resources [1–11]

Thorium occurs in association with uranium and rare earth elements in diverse rock types. It occurs as veins of thorite, uranothorite and monazite in granites, syenites and pegmatites. Monazite also occurs in quartz-pebble conglomerates, sandstones and fluviatile or beach placers. Thorium occurs along with rare earth elements in bastnaesite and in the carbonatites.

Present knowledge of the thorium resources in the world is poor because of inadequate exploration efforts arising out of insignificant demand. The total known world reserves of thorium in reasonable assured resources category are estimated at about 1.16 million tonnes. About 31% of this (0.36 million tonnes) is known to be available in the beach and inland placers of India. The possibility of finding primary occurrences in the alkaline and other acidic rocks is good in India. The other countries having sizeable reserves are Brazil, Canada, China, Norway, USSR, USA, Burma, Indonesia, Malaysia, Thailand, Turkey and Sri Lanka.

Fundamental investigations:

In general fundamental investigations are concerned with preparing the base for studying the physical properties of nuclear reactors, with either mixed uranium-thorium fuel cycle or Th-based fuel. The dependencies of ^{233}U, ^{232}U, ^{233}Pa and fission product build up upon integral thermal neutron fluxes have been studied in the high flux Epithermal Thorium Reactor (ETR) [1–12], including detailed correlation between above mentioned values and fast to thermal flux ratios in wide range. These results are helpful in assessing breeding potential of Th-based fuel for different reactor types. The evaluations of nuclear cross section data are still important in optimization and comparison studies for thermal and fast reactors. French work [1–5] on revising and reevaluations of ^{232}Th and ^{233}U data revealed that the value of ^{232}Th absorption in thermal range is apparently well known, though absorption cross section seems to decrease more rapidly than the 1/v-law. Accurate experimental values are desirable to improve temperature coefficients forecast. The most desirable future work is in the high energy range. The knowledge of ^{233}U cross section is presently not as good as that of ^{232}Th.

Reactor core and blanket concepts regarding Th-based fuel reactors strategy investigation, reactor core and blanket design are still important for successful development of Th-based fueled reactors [1–5 to 1–7, 1–13 to 1–17].

The current state of the reactor and fuel cycle facility development suggest in the USSR the combination of the uranium-plutonium and uranium-thorium cycles for nuclear power. Transition to the U/Pu closed cycle, development of spent fuel regeneration and plutonium accumulation paves the way for introduction of fast breeder reactors which are to be the basis of future nuclear fuel breeding [1–7, 1–8]. In case of acute need fuel supply problems could be eased by transition of the thermal reactors to utilization of the ^{233}U accumulated in the fast breeder reactor blankets [1-7]. This idea is supported by Indian plans [1–8] for ^{232}Th investigations in blankets of fast test reactors. Another possibility [1–5, 1–13 to 1–18] is to use Pu/Th cycle in unmodified PWRs as an active Pu-store. The main goal of this work is to find a real way for opening the Th-cycle in present reactors. The solution proposed consists of initial loading the whole PWR-type reactor with Th/Pu assemblies. Besides, it is an attractive way for storage of plutonium in case of rather slow development of FBRs. ^{233}U can also be used in Spectrum Shift Control Reactors. Corresponding optimizing neutronics calculations are made, including pin power peak, moderator temperature coefficient, etc.

The results of the program presented in this report show that standard PWR may use $(Th,U)O_2$ fuel and even $(Th,Pu)O_2$ fuel without any changes in the fuel assembly as well as within the reactor system. A favourable strategy to avoid the need of early reprocessing and to strive for worthmentioning savings in uranium might be the use of $(Th,Pu)O_2$ fuel in the once-through put-away-cycle with strongly extended burnups.

Status of thorium fuel fabrication technology:

Pelletizing ThO_2-based fuel pellets out of calcinated kernels seems to present the most attractive fuel fabrication process at present. It has been under development since the late seventies [1–20 to 1–28].

For fabrication of thoria kernels the sol-gel process has been developed. On the basis

of this technology a procedure for production of pelletized fuel for water cooled reactors has been developed.

External gelation of thorium sols is used in order to produce gel kernels which could be calcinated suitable for pelletization and sintering. Heavy metal nitrate feed solutions of lower molarity were found to be more suitable. Calcium nitrate was added to the feed solution in order to have around 0.4 w/o CaO „sintering aid". Also carbon black is added to the sol prior to gelation. The pores formed in the sol-gel kernels after burning off the carbon black particles reduce the crushing strength of the kernels and facilitate pelletization.

The pelletizing of ex-gel-kernels not only avoids dust generation and is easy to remotize but also produces high density pellets of desired microstructure at compaction pressures and sintering temperatures, which may be even lower than for the conventional UO_2 manufacturing.

ThO_2-pellets can also be manufactured by the classical pelletizing process extruded from adequate pretreated powder. The relevant experience is described in detail in the open literature. All ThO_2-based fuel in the US-programs since the early fifties had been produced by pelletizing from different powders until 1978. Other sophisticated approaches such as duplex pellet manufacturing were exercised in the laboratory scale. The necessary powders have been produced by nearly all known and applicable processes. The experience from India in fabrication of thoria-pellets ex-oxalate powder was concentrated on powder granulation and on pressing parameters as well as on sintering by the use of Mg-dopant (approx. 500 ppm) as a sintering aid. The objective of this work was to improve the fabrication reliability for fast breeder blanket elements for the fast reactor at Kalpakkam, India.

The extrusion processes were also investigated. However it seems that this approach is not very promising.

An economic and viable recycling method for rejected sintered pellets and pellet scrap needs to be developed for pellet production.

In-pile performance:

A number of irradiation tests was performed in water-moderated reactors to evaluate the in-pile behaviour of various $(Th,U)O_2$ containing fuel rods fabricated by either pelletizing, vipac or sphere-pac.

Fuel performance was extensively studied within the Oak Ridge National Laboratory irradiation program which started in 1961. The first initial results on the performance characteristics were found to be favourable [1–29, 1–40]:

a) all thoria based fuels in general performed better compared to urania based fuels;
b) sol-gel derived $(Th,U)O_2$-fuel meets the basic performance requirements of a nuclear fuel;
c) vibratorily compacted $(Th,U)O_2$-fuel rods perform as well as those containing pressed-and-sintered pellets at moderate heat ratings up to 300 W/cm and burnup levels about 40,000 MWd/t HM.

The work was continued by investigating the performance of $(Th,U)O_2$ fuel under different test conditions such as:

a) high burnups and moderate heat ratings [1–30, 1–31];

b) high burnups and intermediate heat ratings [1–32,1–33, 1–35];

c) moderate burnups and high heat ratings [1–30, 1–32,1–35,1–36]

d) processing variables affecting the irradiation performance [1–30, 1-32, 1-36].

Additionally, special irradiation test programs had been performed under the Light-Water Breeder Reactor program and in the Halden Boiling Heavy Water Reactor and in power reactors:

a) LWBR-irradiation program [1–37, 1-38];

b) Halden Boiling Heavy Water Reactor [1–39];

c) $(Th,U)O_2$ and $(Th,Pu)O_2$ fuel element performance in power reactors [1–30, 1–32, 1–34, 1–37, 1–38, 1–40, 1–42];

All these tests demonstrate that the in pile performance of thoria fuel is satisfactory under water reactor conditions. Assessing the use of thoria fuel e.g. in PWRs other parameters than the in-pile performance are of decisive influence.

Interim storage of spent ThO_2-based nuclear fuel:

There are no reports available in the open literature about results on ThO_2-based spent fuel storage performance of LWR-type fuels. However it is known that the end-of-life condition of a ThO_2-based spent fuel rod corresponds to that of a UO_2 fuel rod. Therefore no spent fuel problems should arise [1–43].

Reprocessing [1–3, 1–13, 1–19]:

There is a lot of experience available on thorium based fuels reprocessing extensively described in the open literature. Under the aspects of thorium use in PWR, the reprocessing of Zircaloy-4 clad spent thoria fuel is of special interest. The available experience of this issue is limited.

The results of the present program show that the reprocessing of Zircaloy clad spent LWR-fuel with $(Th,U)O_2$-fuel is principally feasible using reprocessing schemes derived from experience gained in the context with HTR work and in combination with a chop-leach technique using the THOREX solvent. Cold dissolution experiments have shown that in the dissolution of $(Th,U)O_2$ fuels by THOREX solution, the Zircaloy clad is also dissolved to some extent and, besides this the dissolution time is 30% increased if Zircaloy cladding is present. However work with irradiated fuel shows that the dissolution time may be decreased with increasing burnup by about 50%. For an optimization of the solvent extraction processes, distribution data covering the whole range of interest have been evaluated, interpolations and extrapolations are possible by a computer program. Considerations about the radioactivity of reprocessed ^{233}U fuel from power reactors on the one side and the experience gained so far with the THOREX process variants on the other side lead to the proposal of a single-cycle THOREX process for PWR application.

Refabrication:

For refabrication of ^{233}U bearing HTR fuel kernels, the sol-gel process has been developed. The process starts with a solution containing $Th(NO_3)_4$ and $UO_2(NO_3)_2$. The kernel production is completed in a few steps and besides ammonia and water no other chemicals are necessary. In conjunction with the chemical process, equipment for continuous and remotely controlled operation was developed [1–44, 1–49].

Beside the fabrication of LWBR core the only refabrication experience with pelletized Th/U fuel is available from a former program in the ITREC plant in Italy. The hot operation started in July 1975, with the reprocessing of 20 Th/U spent fuel elements, irradiated in the Elk-River (USA) reactor. For this first campaign the maximum cooled and less irradiated elements were chosen. The refabrication had to be carried out in a hot cell fitted with adequate shielding, using remotely-operated equipment and techniques. All equipment of the main chemical processing was installed in modular units (the Rack Removal System), an arrangement which provides for the remote-controlled removal (after appropriate decontamination) of the individual mobile unit (rack) for maintenance work and modification of components and equipment.

The pellets were fabricated ex Th-U-oxalates powder, green pellets were obtained by cutting extruded cylinders into pellets. Sintering was performed in H_2/Ar atmosphere between 1,600 and 1,700° C. About 90% of the pellets met the specification. After loading the pellets into the Zircaloy-4 cladding the second end plugs were remotely TIG-welded. All welds were routinely X-rayed. The fuel pins were assembled into a Halden type fuel element.

1.2.4 Special experience in former FRG-program used in the present joint activities

$(Th,U)O_2$ kernel fabrication: For the preparation of spherical particles, powder and wet-chemical processes can be employed. Wet-chemical processes have proven to be very suitable for the production of fuel kernels for HTR fuel elements. A special wet chemical process using the gel precipitation has been developed at NUKEM/HOBEG up to the production scale, according to which all current types of spherical nuclear mixed-oxide feed and breed particles (mostly called kernels), containing high melting uranium and thorium oxides or carbides, respectively, can be fabricated by only slight changes in the composition of the feed solution and of some process parameters.

Pellet fabrication of standard UO_2: The fabrication of UO_2 pellets from the feed material uraniumhexafluoride (UF_6) and aqueous solution of uranylnitratehexahydrate (UNH) consists of two processing areas:

a) the production of UO_2 powder by a chemical process, called conversion, and
b) the fabrication of UO_2 pellets from UO_2 powder by powder metallurgical methods, called pelletizing.

For the conversion there are three alternatives of industrial manufacturing processes. Two of them are wet conversion processes, where intermediate products are precipitated from aqueous solutions. These uranium compounds are ammonium diuranate (ADU) or ammonium uranyl carbonate (AUC). The third class of such processes is the

dry conversion where UF_6 is directly processed into UO_2 powder. The latter processes can only start with the feed material UF_6, whereas the wet conversion processes can start either with UF_6 or UNH.

There are also three alternatives for the pelletizing which are combined with the distinct conversion processes. Two of them use dry granulation and prepressing methods with ex-ADU and ex-dry conversion powder. In the third process direct pelletizing with ex-AUC powder is used. In this process no intermediate product during the pelletizing step and no granulate are necessary. Additionally, with the direct pelletizing process the scrap recycling (U_3O_6) can easily be integrated.

At Siemens/RBU, the UO_2 powder is produced by the AUC conversion route, and consequently the direct pelletizing process is applied for pellet production.

$(Th,U)O_2$-pellet fabrication by standard procedures: Within the D_2O-Th-program, in addition to fabrication of vibratorily compacted mixed-oxide fuel, 250 kg $(Th,U)O_2$-fuel was manufactured in 1964. The fuel was needed to perform a critical experiment. The fuel consisted of pellets having the dimensions of 10.0 $\pm$ 0.1 mm in diameter and 13.0 $\pm$ 0.1 mm in length, with 97.5% ThO_2 and 2.5% UO_2. The uranium was 93% enriched in ^{235}U. The specified pellet density was 8.8 $\pm$ 0.2 g/cm^3.

The fuel was manufactured in the normal production lines of UO_2. The fabrication process comprised the steps powder mixing, pressing and sintering in hydrogen atmosphere. The defined specifications could be reached. However, the homogeneity, the structure and the geometrical shape were inadequate under the aspect of using this fuel as reactor fuel. Nevertheless, the manufactured fuel could be used because it was only applied to a critical experiment.

Irradiation testing of vipac $(Th,U)O_2$ fuel of the D_2O-Th-program: The objective of the irradiation program using the experience from out-of-pile studies can be summarized as follows:

a) investigation of the irradiation behaviour of vibro-compacted fuel up to 60,000 MWd/t HM
b) influence of the rating, power cycling and ramping on the performance of vibro-compacted fuel;
c investigation of fission gas release from vibro-compacted fuel;
d) investigation of the relocation behaviour of vibro-compacted fuel especially under the aspect of restructuring the virgin fuel columns and of equilibrium structure;
e) investigation of redistribution of uranium in the mixed oxide fuel;
f) investigation of the thermal conductivity of restructured vibro-compacted fuel;
g) to check if there is any evidence for fuel rod failure mechanisms being typical for vibro-compacted fuel;
h) to provide spent fuel to investigate the dissolving characteristic and the refabrication feasibility of Zircaloy clad vibro-compacted Th/U mixed-oxide fuel.

The irradiation program was performed up to 50,000 MWd/t HM. During the irradiation of the seven experiments (each with two test rods) heat ratings up to 680 W/cm, power ramps between 520 and 650 W/cm and special cycling programs could be realized

without typical fuel rod failures. Failures occurring could be attributed to the formation of deposits due to impurities in the capsule.

During post-irradiation examination, none of the fuel rods showed significant diameter changes or fuel swelling. The gamma-scan values agreed with those calculated for the power distribution prior to the experiments. The fission gas release rate was between 25 and 61%. The characteristic fuel structures i.e. the non-relocated outer fuel region, the sintered kernel region, the fully restructured inner fuel zone and possible formation of central voids will appear within a few days of irradiation. Afterwards the changes in the fuel columns are very small. Relocation of the fissile uranium towards the cooler outer fuel zone was verified during the post-irradiation examination.

Reprocessing: For reprocessing studies, sections of a D_2O-Th-Breeder-Reactor fuel rod (RBE-30) were supplied to HOECHST. The fuel rod contained vibratorily compacted $(Th,U)O_2$-kernels in a Zircaloy-4 cladding. The fuel rod achieved a burnup of 2,660 MWd/t HM and was cooled for dissolution tests up to 96 days and for extraction 158 days. The fuel rod was cut at KFA into about 10 mm long sections. Fuel ranging in size from approximately 0.5 mm to 5 mm could be poured from the cut fuel sections. The size of kernels before irradiation had been smaller than 0.8 mm. Therefore, the irradiation apparently produced only localized sintering of the fuel near the axis of the rod. However the general experience has shown that most fuels cannot be poured freely from the sheared cladding sections but must be dissolved out by THOREX-reagent. Therefore, the Zircaloy-4 cladding was placed into the dissolver solution together with the fuel in order to investigate the amount of Zircaloy being dissolved. The reprocessing tests showed that the dissolution of the fuel took 40–50 hours during which 17% of the Zircaloy-4 were also dissolved. The feed adjustment and extraction using the acid THOREX process with an acid deficient feed solution were performed without problems.

References

[1-1] Rahmenvertrag über Zusammenarbeit in der wissenschaftlichen Forschung und technologischen Entwicklung zwischen der Regierung der Bundesrepublik Deutschland und der Föderativen Republik Brasilien vom 9.6.1969 (Bezug: Artikel 1, Absatz 3).
Acordo Geral sobre Cooperacao nos Setores da Pesquisa Cientifica e de Desenvolvimento Tecnologico, assinado pelos Governos da Republica Federativa do Brasil e da Republica Federal da Alemanha, Bonn, 9.6.1969.
(Cobertura: Artigo 1, Paragrafo 3).

[1-2] Memorandum of Understanding between KFA and NUCLEBRAS on Cooperation in the Field of High Temperature Reactors and Gas Cooled Fast Breeder Reactors and the Thorium Cycle in High Temperature Reactors and Light Water Reactors as well as in Gas Cooled Fast Breeder Reactors. March 8, 1978.

[1-3] IAEA-TECDOC-412
"Th-Based Nuclear Fuel: Current Status and Perspectives"
Proceedings of a TCC-meeting
Vienna, December 1985

[1-4] KFA, NUCLEBRAS, KWU, NUKEM.
Program of Research and Development on the Thorium Utilization in PWRs- Final Report for Phase 1 (1979-1983).
May 1984, Juel-Spez.-266

[1-5] G.Gambier, H.Schaeffer
"Th-Cycle in Unmodified PWR's"
IAEA-TECDOC-412 p. 45
Vienna, December 1985

[1-6] "Research on Th-Fuel"
The ministry of education, science and culture
Japan SPEY 9, January 1984

[1-7] I.S. Slesarev et al
"Th-Utilization in Solving the Nuclear Power Fuel Problem"IAEA-TECDOC-412 p. 59
Vienna, December 1985

[1-8] P. Balakrishna et al
"Th-Oxide Blanket Fabrication for Indian FBR-Test Reactor"
IAEA-TECDOC-412 p.73
Vienna, December 1985

[1-9] Salvo Brito, S. de; Lepecki, W.P.S.
Preliminary Assessment of Heavy-Water Thorium Reactor in the Brazilian Nuclear Programme.
In: IAEA CONFERENCE ON HEAVY-WATER POWER REACTORS.
Vienna, Austria, September 1967.

[1-10] Salvo Brito, S. de et al.
Projeto "Instinto" – Relatorio Final: Periodo 1966/67.
Instituto de Pesquisas Radioativas, Belo Horizonte, December 1967.

[1-11] K.M.V. Jayaram
"An Overview of World Th-Resources, Incentives for Further Exploration and Forecast for Th-Requirements in the Near Future"
IAEA-TECDOC-412 p. 7
Vienna, December 1985

[1-12] J.H.Zhang et al
"Basic Research on Utilization of Th-Based Nuclear Fuel"
IAEA-TECDOC-412 p. 67
Vienna, December 1985

[1–13] M. Peehs, G. Schlosser, R.B. Pinheiro, V.Maly, M. Hrovat
"Th-Utilization in PWR's: Status of Work in the Cooperative Brazilian/German Program"
IAEA-TECDOC-412 p.27
Vienna, December 1985

[1–14] M. Peehs, G.Schlosser
"Prospects of Th-Fuel Cycles in a Standard PWR"
SIEMENS Forschungs- und Entwicklungsberichte
Band 5, Nr. 4, p. 199, 1986

[1–15] V. Maly, R.B. Pinheiro
Technology Transfer within the KFA/NUCLEBRAS Cooperative Program Th-Utilization in PWR's
ICONT III Conf.
Madrid/Spain, Oct. 1985

[1–16] G. Schlosser, E.P. Andrade, Carneiro F.A.N.
"Brazilian-German Investigations of Th-Utilization in KWU-Type PWR's-Results of Nuclear Core Design", IAEA
Technical Committee in Advanced Light and Heavy Water Reactor Technology
IAEA-TECDOC-344/85, pp. 135-145
Vienna/Austria, November 26-29, 1984

[1–17] Program of Research and Development on the Thorium-Utilization in PWR's
Final Report for Phase 1, 1979-1983, Juel-Spez.-266, May 1984

[1–18] D. Porsch, E.P. Andrade, G.Schlosser
Deutsch-Brasilianische Studie zur nuklearen Auslegung von DWR mit Th-Brennstoff
Jahrestagung Kerntechnik, Tagungsber. pp. 27-30
München, 1985

[1–19] E. Zimmer, C. Ganguly
„Reprocessing and Refabrication of Th-Based Fuel"
IAEA TECDOC-412, p. 89
Vienna, 1985

[1–20] M. Peehs, W. Doerr, M. Hrovat
Development of a Pelletized (Th,U)O_2-Fuel for LWR- Application
IAEA Advisory Group Meeting on Advanced Fuel Technology and Performance
IAEA-TECDOC-352/85, pp. 175-185
Wuerenlingen/Switzerland, December 1984

[1–21] P.E. Cardoso et al
Development of Alternative Fuel for PWR
III Congresso Brasileiro de Energia
Rio de Janeiro, October, 1984

[1–22] H. Huschka et al
Coated Fuel Particles, Requirements and Status of Fabrication Technology
Nucl. Technol. 35, pp. 238-241, 1977

[1–23] P.E. Hart, C.W. Griffin, K.A. Hsieh, R.B. Matthews, G.D.White
ThO_2-Based Pellet Fuels – Their Properties, Methods of
Fabrication, and Irradiation Performance: A Critical Assessment of the State of the Technology and Recommendations for Further Work Battelle Pacific Northwest Labs.
Richland, WA (USA), PNL-3134, September 1979

[1–24] R.B. Matthews, P.E. Hart
Hybrid Pellets: An Improved Concept for Fabrication of Nuclear Fuel
Battelle Pacific Northwest Labs.
Richland, Wa (USA), PNL-3134, September 1979

[1–25] R.B. Matthews, N.C. Davis
Fabrication of ThO_2 and ThO_2-UO_2 Pellets for Proliferation Resistant Fuels
Battelle Pacific Northwest Labs.
Richland, WA (USA), PNL-3210, October 1979

[1–26] R.B. Matthews, P.E. Hart
Nuclear Fuel Pellets Fabricated from Gel-Derived Microspheres
Battelle Pacific Northwest Lab.
J.Nucl.Mater. ISSN 0022-3115 v. 92 (2/3), p. 207-206
Richland, WA (USA), September 1980

[1–27] S.M. Tiegs, P.A. Haas, R.D. Spence
Sphere-Cal Process: Fabrication of Fuel Pellets from Gel Microspheres
Oak Ridge National Lab.
TN (USA) ORNL/TM-6906, p. 46, September 1979

[1–28] C. Ganguly, H. Langen, E. Zimmer, E.R. Merz
Sol-Gel Microsphere Pelletization Process for Fabrication of High-Density ThO_2-2% UO_2 Fuel for Advanced Pressurized Heavy Water Reactors
Nucl. Technol. ISSN 0029-5450, v. 73 (1), p. 84-85
April 1986

[1–29] D.J. Cameron
"A Review of the Potential for Actinide Redistribution in CANDU Thorium Cycle Fuels"
AECL-5962, February 1978

[1–30] C. Ganguly, private communication.

[1–31] A.R. Olsen, J.H. Coobs, J.W. Ullmann
"Current Status of Irradiation Testing of Thorium Fuels at Oak Ridge National Laboratory"
Thorium Fuel Cycle Symp. Gatlingburg, pp. 475-494, 1966

[1–32] A.R. Olsen, D.B. Trauger, W.O. Harms, R.E. Adams, D.A. Douglas
"Irradiation Behaviour of Thorium Alloys and Compounds"
ORNL-TM-1142, June 1965

[1–33] A.R. Olsen, J.D. Sease, R.B. Fitts, A.L. Lotts
"Fabrication and Irradiation Testing of Sol-Gel Fuels at Oak Ridge National Laboratory"
ORNL-TM-1971, pp. 29-48, September 1967

[1–34] A.R. Olsen
„Irradiation of Thoria-Base Bulk Oxide Fuels"
ORNL-4170, pp. 220-223, November 1967

[1–35] A.R. Olsen, J.W. Ullmann, E.J. Manthos
„Irradiation of Oxide Fuels"
ORNL-4001, pp. 102-112, October 1966

[1–36] A.R. Olsen, R.B. Fitts
„Irradiation of Bulk Oxide Fuels"
ONRL-4275, pp. 121-134, January 1969

[1–37] J.E. McCauley
„Irradiation-Induced Structural Changes Obtained in ThO_2-UO_2 Fuel"
Trans. Am. Nucl. Soc., 13, pp. 35-36, June-July 1979

[1–38] J.E. McCauley
„Observations on the Irradiation Behaviour of a Zircaloy-4 Clad Rod Containing Low Density ThO_2-5, 3% UO_2-Pellets"
WAPD-TM-664, December 1969

[1–39] G. Kjaerheim, E. Rolstad
„In-Core Study of Fuel/Clad Interaction and Fuel Centre Temperature"
HPR-107, January 1969

[1–40] C.F. Reinke, L.A. Neimark, R. Carlander, J.H. Kittel
„Metallurgical Evaluation of Failed BORAX-IV Fuel Elements"
pp. 112 and
L.A. Neimark, R. Carlander
„Irradiation of X8001 Aluminium Alloy-Clad, Lead-Bonded ThO_2-UO_2-Pellets"
ANL-6330, pp. 105-108, Ann. Rep. for 1960

[1–41] C.J. Baroch, W.N. Bishop
„Performance of ThO_2-UO_2 Fuel in Indian Point Reactor"
Trans. Am. Nucl. Soc. 11, pp. 494, see CONF-681 101 1968

[1–42] M.D. Frehsley, H.M. Mattys
„Properties of Sintered ThO_2-PuO_2"
HW-76300, pp. 2.6-2.8, December 1962
HW-76559, pp. 11-6-11, January 1963

[1–43] M. Peehs, J. Fleisch
LWR Spent Fuel Storage Behaviour,
J. Nucl. Mat. 137, pp. 190-202, 1986

[1–44] R.E. Booksbank et al
„The Impact of Kilorod Perational Experience on the Design of Fabrication Plants U^{233} Th-U-Fuel"
ORNL Th – Fuel Symposium
Gatingburg 1966

[1–45] J.D. Sease et al
„Remote Fabrication of Th-Fuel"
ORNL Th-Fuel Symposium 1966

Table 1.1: List of major activities worldwide in the area of Th-based nuclear fuels

Country	Program		Directed towards					Areas of R and D						
	termi-nated	run-ning	HTR	HWR	LWR	FBR	Other	Basic research	Stra-tegy	Core design	Tech-nology	Irra-diation	Repro-cessing	Refabri-cation
ARGENTINA		X		X				X	X		X			
AUSTRIA		X	X	X	X	X		Dynamic System Analysis Fuel cycle (by lite-rature)	X					
AUSTRALIA	1980	X						X						
BRAZIL*	1970			X					X	X				
CANADA		X		X					X					
CHINA	1971	X	X					X			X		X	
		X			X			X	X			X		
FRANCE	1979/82		X				X		X	X	X	X	X	
		X			X	X		X	X	X				
FRG*		X	X	X						X	X	X	X	X
FRG/BRAZIL JOINTLY	1988				X				X	X	X	X	X	
INDIA		X		X		X		X	X		X	X	X (Planned)	
ITALY	1974				X			X					X	X
JAPAN		X	X				X	X	X	X	X		X	
PAKISTAN	1983							X			X			
ROMANIA		X		X			X	X	X	X				
USA	1982	X	X		X		X	X	X	X	X	X	X	X
USSR		X	X		X	X		X	X	X				

*See below FRG/BRAZIL jointly

2. Technical Results

2.1 Nuclear Core Design and Strategy Calculations

Utilization of thorium-based fuels in thermal reactors is aimed at the production and fission of ^{233}U. The purpose of this study is an assessment of the most economic way to make use of the attractive properties of all possible thorium-based fuels in present commercial PWRs. With unchanged PWR geometry related to fuel assembly and core the present optimum in power generating costs can be achieved in following the trend for maximum burnup and minimum efforts for fuel supply and for reprocessing. The KWU PWR of 1,300 MW_e of Angra-2 type was the reference reactor for the study. Its design data are presented in Table 2.1.1.

The utilization of thorium as fuel implies the need for initial fissile materials. This may be ^{235}U as natural fissile material or the artificial nuclides ^{239}Pu and ^{241}Pu extracted during reprocessing of burnt uranium-based fuels.

The use of thorium mixed with high enriched uranium (Th/HEU) and thorium-plutonium (Th/Pu) mixed oxide fuels in an unmodified pressurized water reactor (PWR) were studied. The choice of Th/HEU was established because of its high potential to breed ^{233}U.

Reactor core nuclear design calculations for the following options were performed:

	Th/HEU fuels	**Th/Pu fuels**
Once through fuel cycle	3 and 4 batch cores	3 and 4 batch cores
Recycle option	Recycling of ^{233}U and ^{235}U 3 and 4 batch cores	Recycling of ^{233}U and Pu 3 and 4 batch cores
Insertion of Th fuel assemblies in a U-core	3 batch core	3 batch core

To prepare the insertion of first thorium-based fuel assemblies into a power reactor it was seen necessary to design a special irradiation test uranium fuel assembly including some thorium-based test rods. It was planned to insert this assembly in the power reactor of Angra-1.

The results on nuclear core design were finally used to study the economic chances of the various Th-fuels to penetrate the future market of fuel assemblies and to improve the uranium resource utilization. Additionally, the question at which time Th-fuelled reactors should be introduced into a nuclear growth scenario was answered by these strategy calculations.

2.1.1 Nuclear design programs

The computer programs of the nodal reactor analysis system SAV79A [2.1-1] were

used for the design of cores containing Th/U and Th/Pu fuel. The main constituents of the SAV-system are:

a) **FASER** is a one dimensional spectral depletion code of MUFT/THERMOS type based on LASER [2.1-2]. From an 85 energy group library (50 for the fast region and 35 for the thermal) effective few group cross sections (2 to 10 energy groups) can be calculated as a function of burnup, boron concentration, fuel and moderator temperature and moderator density. For the application to thorium a new version was established called Th-FASER. Within this version the basic cross section library was extended by the nuclides of the thorium chain. The resonance calculation was adjusted to thorium treatment.

b) **MULTIMEDIUM** is a two dimensional transport depletion code (up to 10 energy groups) for fuel assembly calculations in a homogenized pinwise representation. In the frame of this work it is used for neutronic fuel assembly design and to calculate heterogeneous form functions.

c) **MEDIUM** is a multidimensional nodal reactor depletion code. The diffusion equation in 2 energy groups is solved by a burnup corrected variant of NEM (Nodal Expansion Method). Feedback of the fuel temperature, moderator density and xenon is applied to the neutron flux solution.

d) **PINPOW** calculates the pinwise power, burnup and flux distribution from the nodal reactor solution by using a modulation technique.

For safety analysis the **PANBOX** code system [2.1-3] is used. The system consists of the following codes:

a) **DIEB** processes a file prepared by the depletion program MEDIUM and generates an input file for BOXER and IQSBOX.

b) **BOXER** is a multidimensional nodal two-group diffusion program especially suited for the calculation of quasi-stationary power distributions under transient xenon conditions and the analysis of load follow behaviour.

c) **IQSBOX** is a coupled neutronics/thermal-hydraulics space-time kinetics program for the analysis of stationary and transient power distributions under off-nominal core and boundary conditions.

d) **PANDA** processes an output file produced by IQSBOX and generates data for comparison with experimental results or for use in core simulators.

In this study the codes DIEB and IQSBOX were used for the analysis of a steam line break accident. IQSBOX is fully consistent to MEDIUM under normal operating conditions if the same options are used. For the analysis of off-nominal conditions more sophisticated thermal/hydraulic models are provided. The calculations of DNB's and centerline fuel temperatures are based on pinwise power distributions reconstructed from the interpolated nodal solution modulated by heterogeneous assembly functions precalculated by MULTIMEDIUM.

2.1.2. Nuclear fuel cycle studies

In all once-through options it was admitted that the first core would be designed with a full load of thorium fuel. For the reloads, the make-up fissile material is made by the ad-

dition of new HEU, in the case of Th/HEU cycle, or by the addition of Pu from a PWR operating in the uranium once-through mode in the case of Th/Pu cycle. For the recycle cases the recycling started at the beginning of cycle 4 with fissile material unloaded from the first cycle of the same reactor. It was assumed a period of 2 years for spent fuel to be cooled, reprocessed and refabricated. The complement of fissile material in the reloads was done with new HEU, in the case of Th/HEU cycle, or with Pu from PWR operating in the U once-through mode in the case of Th/Pu cycle. Calculation was done cycle by cycle. The fuel balance took into account losses of 5 w/o for the first recycled batch and later on 2.5 w/o of losses.

Thorium/Uranium fuel cycles

In the Th/HEU cycle only a small part of the reloads had to be completed with make-up fissile material. That is the reason why it was decided to mix reprocessed and fresh fissile material and to fabricate only one type of fuel for the recycling reloads.

In each case the enrichment in fissile material for the reloads was determined in such a way that the cycle lengths were of approximately 280 EFPD (equivalent full power days). As an example, Figure 2.1/1 presents the loading pattern in the equilibrium core and the power distribution at BOC obtained. The preliminary density of the mixed oxide fuel considered was 9.4 g/cm^3. The use of the experimental pellet density equal to 9.5 g/cm^3 and of Zircaloy-4 for guide tubes caused an extended cycle length of more than 300 EFPD in the final calculation of the Th/HEU fuel cycle options.

Table 2.1.2 summarizes the main results at equilibrium of Th/HEU cycles analysed. The calculations were done looking for an acceptable BOC power distribution which however can be improved without great effort. It was found that the desired cycle length can be achieved with reasonable enrichments. Substantial savings of natural uranium resources can be obtained only with the recycle option.

The high concentration of soluble boron at BOC-1 causes a positive moderator temperature coefficient indicating the need of a burnable poison. This may be avoided by gradually switching over from a U- to a Th/HEU-core by successive Th-fuel reloads. In the beginning of equilibrium cycles the moderator temperature coefficient is slightly positive at hot zero power in the mixed recycle mode only. This is of no significance, because with increasing coolant temperature and decreasing boron concentration the coefficient soon assumes negative values. Table 2.1.3 shows the relevant reactivity coefficients for Th/HEU-cores at the beginning of equilibrium cycles under hot zero power conditions. The results of reactivity balance calculations for equilibrium cycles have shown that there is always sufficient reactivity shutdown margin (Figure 2.1/2) for a moderator temperature decrease up to about 100°C. In case of a main steam line break accident even a further reduction of coolant temperature has to be assumed. The analysis of this accident therefore requires more detailed investigations. These have been made in this study for the Th/Pu core which regains criticality already after a decrease in coolant temperature of about 50°C.

Thorium/Plutonium fuel cycles

Also in the case of Th/Pu fuel cycle it is possible to achieve the desired cycle length with reasonable enrichments in fissile material. Figure 2.1/3 presents the loading pattern and power distribution of equilibrium core obtained. Table 2.1.4 summarizes the main results of the burnup calculations.

The boron concentrations at BOC are similar to those calculated in the Th/HEU cycle, except for the first cores of all options analysed, when these concentrations are higher due to the high Pu content of the fuel. The presence of the ^{233}U at the beginning of subsequent cycles results in lowering the values for the critical boron concentrations. The calculations of moderator temperature coefficient (Table 2.1.5) indicate that, at hot full power conditions, this coefficient is always negative, from the beginning to the end of all cycles (including the first core) in all options analysed. Results of reactivity balance calculations (Figure 2.1/4) indicated a potential return to criticality for a decrease in the moderator temperature in the range of 50° C. As mentioned above, this case therefore was adopted for a detailed steam line break analysis.

The analysis demonstrates that the accident is controlled and that the core is at no time endangered, as safety-related parameters do not exceed permitted limits. In all calculations including even simultaneous extreme variation of all thermal – hydraulic parameters in the most adverse direction – the minimum DNBR remains markedly above, the maximum fuel central temperature markedly below the respective value reached during normal operation.

This result was obtained under a lot of conservative assumptions which lead to maximum core subcooling, minimum shutdown reactivity and maximum reactivity release. Thus it can be concluded that similar results hold for other Th-designs.

Insertion of thorium fuel assemblies in a U-core

It is to be anticipated that the realistic way of introducing Th-fuel to a PWR would be via a partial and later on complete Th-fuel assembly reload [2.1-4, 2.1-5]. Results gained so far in the cooperative program show that no changes of the Th/HEU fuel assembly (FA) design – in comparison with the standard U-fuel assembly – to be loaded into a U-core are necessary. The use of Pu instead of HEU also reveals some interesting features. Figure 2.1/5 shows the relative energy production of Th/Pu-isotopes inserted in a standard PWR core. However, the high fission cross sections of Pu combined with a high thermal flux of neighbouring U-fuel assemblies would cause unacceptable power peaking [2.1-4, 2.1-5]. Thus Th/Pu-MOX fuel assemblies – as used for Pu recycling via U/Pu-MOX assemblies – need 2 to 3 types of fuel pins with a different fissile material content as shown in Figure 2.1/6 to avoid local power peaking when loaded adjacently to U-fuel assemblies [2.1-4, 2.1-5].

Figure 2.1/7 shows pinwise power distribution in 1/8 of a Th/HEU and a Th/Pu fuel assembly calculated surrounded by U-fuel assemblies at beginning of the irradiation. The power peaking factor is lower than 1.15.

Figure 2.1/8 shows a possible loading for 16 Th/Pu assemblies per cycle in a U-core and the average power in each fuel assembly at the equilibrium cycle. The maximum average power of the Th/Pu FA is less than in the U FA. Table 2.1.6 shows main results until equilibrium cycle. As seen in this table the main characteristics of the uranium core remain unchanged.

Figure 2.1/9 shows power history of Th/Pu rods for the equilibrium cycle. As it can be seen, the rod with the maximum linear power over the whole period of irradiation is lower than the design value.

2.1.3 Nuclear design of an irradiation testing in the power reactor Angra-1

With the objective of verifying the performance of the Th/U fuel in a power reactor, it was planned to irradiate 4 segmented rods and 1 full scale rod in a fuel element reloaded in the Angra-1. With this test a realistic burnup can be obtained and because the neutronic spectrum in the Angra-1 core is well known, the nuclear design (relative to power density and burnup) of the Th/U fuel can be checked, too.

As it is common at KWU for such irradiation tests the top end piece of this fuel element should have a cross-shaped cut-off. This allows fuel rod examination during shut down without problems. In a general way, the whole design of the Th/U test rod followed that of the uranium rod of Angra-1: the outside diameter, the active length and the same average linear heat generation were kept.

The test rods were planned to be inserted in a reload fuel assembly of Angra-1 (Figure 2.1/10), at the beginning of cycle 4. At the end of each of the following cycles one Th/U rod would be withdrawn and in its place inserted a dummy rod of aluminum oxide (a fuel rod of Angra-1 with Al_2O_3 pellets) to restrain power peakings in the surrounding positions.

The design of the test rods was made in a way to keep pinwise and assemblywise power distribution and reactivity the same as in the fuel assembly containing only UO_2 rods.

Firstly the Th/HEU fuel was investigated because it leads to higher breeding of ^{233}U, which is a better fuel than the other fissile isotopes in the thermal spectrum. Afterwards an alternate fuel had to be chosen as its substitute due to difficulties in obtaining HEU for the manufacture of the test rods. Two types of fuel were considered: one mixing thorium with MEU*) and the other with LEU+).

The rods with Th/HEU fuel were designed and a content of 4.1 w/o of ^{235}U in the heavy metals was found. Figure 2.1/11 shows a comparison of K_{oo}'s of Th/HEU and UO_2 (3.3 w/o of ^{235}U) cells of Angra-1 the U-cell is more reactive until 520 EFPD and from this point on, less reactive. A calculation of the reload fuel assembly with and without test rods has shown no significant difference in reactivity.

A comparison of corresponding power distributions in both fuel assemblies was made (Figure 2.1/12). The tendency is to lower the power in a maximum of 7% in the positions of substitution. At the end of irradiation this test rod reaches a burnup that compared to the U-rod deviates only in 4.0%. Therefore the influence of the Th/HEU rods may be considered as negligible.

Two alternatives for reloading the test fuel assembly were investigated for different levels of power and are shown in Figure 2.1/13. The power histories of the correspondent hot rods are shown in Figure 2.1/14 their maximum linear power is far away to offer any risk to such rods.

---

*) MEU Medium Enriched Uranium, uranium enriched up to 20 w/o ^{235}U

+) LEU Low Enriched Uranium, uranium enriched e.g. to 3.3 w/o ^{235}U

The alternative fuels were investigated too. The Th/LEU was discarded at the very beginning because of the low burnup reached at the end of irradiation. Then, calculations were done to determine the content of MEU in the mixture (Th,MEU)O_2 in a way to get, as close as possible, the same burnup as U rods. The result obtained was a mixed fuel made of ThO_2 and UO_2, having 17.8 w/o of MEU in heavy metal. At 900 EFPD of irradiation it presents an insignificant burnup difference when compared to UO_2 fuel.

2.1.4 Strategy assessment of possible contribution of Th-fuel for PWRs in Brazil

Objectives, intentions, methods and main result

Strategy studies aim at offering the optimal allocation of power plants to meet a country's electrical energy demand. Within the program effort centered in searching the „best" Th-bearing Angra-2 type unmodified PWR option to penetrate in a forecasted Brazilian nuclear power demand, otherwise fulfilled by U/Pu fuelled Angra-2 type PWRs. For this purpose the following questions should be answered:

a) which of the Th-fuel cycle options is most advantageous in relation to actual boundary conditions;

b) how do Th-fuel cycles compare to usual U-fuel cycles in a system of PWRs with respect to resource utilization and economics;

c) at which time is the introduction of Th-fuel cycles possible or advantageous?

For clear answers a sound basis of results is necessary. The promising nuclear design results have been used to support the efforts on the other tasks of the program, and, in particular, the strategy studies. In the same way, for example, the technically feasible fuel data influence the nuclear design and enable in part the needed cost estimates.

Nuclear reactor strategy analysis – as part of the more general problem of energy planning – is concerned with determining optimum reactor mixes required to meet electrical energy demand. Figure 2.1/15 shows a forecast of the future development of nuclear capacity in Brazil over a period extending up to the middle of the next century. Up to the year 2000 the forecast is based on the (then) official nuclear implementation program. In the following decades it is characterized by moderately increasing growth rates assuming that nuclear energy will play an important role in the economic development of Brazil.

Most of the strategy programs are based on a linear programming model (LP model). In the FUKOMA code [2.1-6, 2.1-7] – utilized in strategy studies – an objective function that represents the present worth of the electrical energy costs is minimized subject to a set of linear restraints. The reactor strategy which provides the lowest costs is selected by the LP model APEX. FUKOMA then proceeds to calculate the material requirements of the optimum strategy.

In Phase 1 of this program the work under strategy studies was devoted especially to improve and to test the use of the strategy analysis procedure of FUKOMA, which had to be changed to treat the complex possibilities of Th-based fuel cycles [2.1-8].

In the present report, results of strategy calculations done with the FUKOMA code are presented. They include a comparative analysis on competition of different plants in meeting nuclear demand as assumed in the adopted scenario in the U/Pu and in the Th/Pu fuel-cycles, and on cumulative demand for natural uranium and separative work.

Calculations made use of updated results from the program's nuclear core design [2.1-8]. These results include plants operating in the thorium-plutonium (Th/Pu) fuel cycle, with Pu^- and Pu^+ ^{233}U-recycling modes, in the 3- or 4-batch reload schemes. For plants operating in the U/Pu fuel cycle the best available data from literature were utilized.

The main results from the strategy studies are given in Table 2.1.7 and can be summarized as follows

a) To profit from the real resource-savings advantages of thorium utilization in unmodified present day PWRs – with respect to the Th/Pu fuel option – one has to close the Th-fuel cycle and recycle the generated ^{233}U along with the residual Pu. If this is done, significant economies both in natural uranium and in separative work are obtained when compared to the once-through PWRs of the present time: approx. 33 % economy in U_3O_8, approx. 20% economy in SWU*.

b) Should the alternate option of not closing the Th-fuel cycle be chosen, the utilization of Th together with recycled Pu in present day PWRs offers sound economies approx. 29% in U_3O_8 and approx. 15% in SWU – when compared to once-through PWRs the U_3O_8 economy is yet somehow superior, while the SWU economy inferior, when the self-generating Pu recycling PWRs are used for comparison.

The relative savings are independent of the absolute consumption. This is also evident from Table 2.1.7.

2.1.5 Conclusions

The fuel assembly and core design studies of all foreseeable combinations of fissile materials with thorium show that

a) fuel assemblies of such fuels can be inserted in cores of present time PWRs: partial reloads of Th-based fuel assemblies can finally result in complete Th-cores;

b) standard PWR fuel assemblies and core configurations are to be foreseen to establish complete cores of such thorium based fuels including recycle fuels using the reprocessing fissile and fertile materials;

c) the safe and unrestricted operation under normal conditions can be demonstrated for the actual loadings. No evidence was found that the requirements for safe shutdown could not be fulfilled by a proper adjustment of the stored amounts of boron compensating for the reduced reactivity worth especially connected to the use of plutonium.

* SWU – Separative Work Units

d) Th/Pu fuel provides a potential for extended burn-up under the aspect of nuclear core design.

The overall conclusions of strategy studies on nuclear power implementation in Brazil, in the frames of the present program, are:

a) though the adopted nuclear power demand scenario excludes any suggestion with respect to the introduction date of Th-fuelled reactors the results of the strategy calculations clearly demonstrate that substantial savings in natural uranium and separative work units can be achieved in comparison with PWR once-through scenarios.

b) Evenso, if the Th-fuel cycle could not be closed in the near future a symbiosis of PWRs operating in U-mode and once-through Th/Pu-reactors seems to be at least competitive to self-generated Pu recycle PWRs.

References

[2.1-1] Koebke, K., B. Ehret, B. Mueller, M.R. Wagner, H.-J. Winter
Das KWU-Programmsystem zur nuklearen Kernauslegung und Brennelementeinsatzplanung von Druckwasserreaktoren
Jahrestagung Kerntechnik, 1984, p. 19

[2.1-2] C.G. Poncelet
LASER A Depletion Program for Lattice
Calculations based on MUFT and THERMOS WCAP-TM (1957)

[2.1-3] Finnemann, H., W. Gundlach
Space Time Kinetics Code IQSBOX for PWR and BWR.
Part I: Description of Physical and Thermohydraulic Models.
Atomkernenergie/Kerntechnik, vol. 37, no. 3, 1981, pp 176-182

[2.1-4] Schlosser, G., E.P. Andrade, F.A.N.Carneiro
Brazilian – German Investigations of Th-Utilization in KWU-Type PWR's Results of Nuclear Core Design
IAEA- TECDOC-344, Vienna, 1985, p. 135-146

[2.1-5] Porsch, D., E.P.Andrade, G.Schlosser
Deutsch-Brasilianische Studie zur nuklearen Auslegung von DWR mit Th-Brennstoff
Jahrestagung Kerntechnik, 1985, pp 27-30

[2.1-6] H. Maerkl
Untersuchungen über langfristig optimale Reaktorstrategien unter Berücksichtigung des begrenzten Umfangs der Uranreserven
Teil 1: Beschreibung des Optimierungsmodells
Nukleonik, 10. Bd., Heft 4, 207-217 (1967)

[2.1-7] H. Finnemann, W. Gutgesell, H. Maerkl
Investigations of Long-Term Optimum Reactor Strategies
Considering the Limited Extent of Uranium Resources
Part 2: Results of Model Calculations
Nukleonik, 12. Bd., Heft 6, 263-269 (1969)

[2.1-8] KFA-KWU-NUCLEBRAS-NUKEM
Program of Research and Development on the Thorium Utilization in PWRs.
Final Report for Phase 1 (1979-1983).
May 1984 (Jül-SPEZ-266, NUCLEBRAS/CDTN-471/84).

Table 2.1.1: Design data of a KWU standard PWR of 1.300 MWe

Fuel Rod Diameter (mm)	10.75
Lattice Pitch (mm)	14.30
Number of Fuel Rods per Fuel Assembly	16x16-20 (= 236)
Fuel Assembly Pitch (mm)	231
V_{H2O}/Vfuel (cell)	1.74
V_{H2O}/Vfuel (core)	2.05
Fuel Rod Linear Power (W/cm)	211
Number of Fuel Assemblies	193
Fuel Rod Active Length (mm)	3.900.0
Cladding Wall Thickness (mm)	0.725
Volume of the Spacer Grids per Fuel Assembly (cm^3)	831.62
Cladding Material	Zircaloy-4
Control Rod Guide Tube Material	SS-4550 Zircaloy-4*
Spacer Grid Material	Inc-718
Heavy Metal Mass per Fuel Assembly (kg)	485.365
Coolant Average Temperature (°C)	310
For the Present Study	
Mixed Oxide Density (g/cm^3)	9.4 (Th/Pu) 9.5 (Th/HEU)
HEU Isotopic Vector (w/o)	$^{235}U/^{239}U = 93.0/7.0$
Pu Isotopic Vector (w/o) (fresh PWR-Pu)	$^{239}Pu/^{240}Pu/^{241}Pu/^{242}Pu$ 60.1/23.4/12.4/4.1

*improved FA

Table 2.1.2: Main results of equilibrium Th/HEU fuel cycles

		3-batch core		4-batch core	
	unit	once-through	with recycling	once through	with recycling
Reload Batch (no. of FAS)	1	64	64	48	48
Reload Enrichment	w/o	4.2	3.9	4.8	4.5
Boron Concentration at BOC	ppm	1013	1138	988	1038
Cycle Length	d	319	306	310	293
Max. Average Power Form Factor BOC		1.29	1.44	1.30	1.28
EOC		1.33	1.35	1.24	1.23
Core Burnup BOC	MWd/kg	10.7	10.5	16.6	16.2
EOC		21.7	21.1	27.3	26.3
Average Burnup of Unloaded Batch	MWd/kg	33.7	32.0	43.8	42.4
Max. Average Burnup of Unloaded FA	MWd/kg	41.2	39.7	51.7	52.4
$^{233}U + {}^{225}U$ Loaded	g/kg	42.0	39.0	48.0	45.0
$^{233}U + {}^{233}Pa + {}^{235}U$ Unloaded	g/kg	24.7	24.4	24.3	24.1

Table 2.1.3: Reactivity coefficients for Th/HEU cores at HZP and at the beginning of equilibrium cycle

		once-through	mixed recycling
Moderator Temperature Coefficient (ppm/°C)			
	3 batch	− 2.17	+ 1.89
	4 batch	− 6.04	− 3.39
Reciprocal Boron Worth (ppm/%Δ°)			
	3 batch	−114.98	−121.07
	4 batch	−119.05	−111.62
Fuel Temperature Coefficient (pcm/°C)			
	3 batch	− 3.98	− 4.05
	4 batch	− 3.98	− 4.01

Table 2.1.4: Main results of equilibrium Th/Pu fuel cycles

		3-batch core		4-batch core	
	unit	once-through	with recycling	once-through	with recycling
Reload Batch (no. of FAS)	1	64	48	64	48
Reload Enrichment	w/o	4.4	4.2	5.0	4.6
Boron Concentration at BOC	ppm	1374	1521	1238	1422
Cycle Length	d	287	287	278	265
Max. Average Power Form Factor BOC		1.36	1.28	1.42	1.44
EOC		1.27	1.24	1.35	1.30
Core Burnup BOC	MWd/kg	10.4	11.4	16.8	16.4
EOC		22.0	22.9	27.8	26.9
Average Burnup of Unloaded Batch	MWd/kg	34.6	35.2	44.6	43.0
Max. Average Burnup of Unloaded FA	MWd/kg	43.4	48.0	54.3	50.8
$^{233}U + ^{235}U$ Loaded	g/kg	0.0	10.9	0.0	19.3
$^{239}Pu + ^{241}Pu$ Loaded	g/kg	44.0	31.1	50.0	26.7
$^{233}U + ^{233}Pa + ^{235}U$ Unloaded	g/kg	13.0	12.4	14.6	21.2
$^{239}Pu + ^{241}Pu$ Unloaded	g/kg	13.2	13.4	12.0	5.6

Table 2.1.5: Reactivity coefficients for Th/Pu fuel cycles at HFP and at the end of equilibrium cycle

		once-through	mixed recycling
Moderator Temperature Coefficient (pcm/°C)			
	3 batch	− 61.0	− 52.4
	4 batch	− 59.4	− 50.6
Reciprocal Boron Worth (ppm/%Δ°)			
	3 batch	−185.0	−171.1
	4 batch	−198.6	−168.0
Integral Doppler (%Δ°)			
	3 batch	1.01	1.06
	4 batch	0.94	1.03

Table 2.1.6: Main results of the reload of Th/Pu fuel assemblies in an uranium core until equilibrium

No. of Th/Pu-FAs in Core		0	16	2x16	3x16	3x16	3x16
Boron Concentration, BOC (ppm)		1101	1047	1099	1163	1160	1163
Cycle Length (FPD)		324	306	313	317	316	316
Max. Average Form Factor	BOC	1.37	1.34	1.33	1.36	1.36	1.36
	EOC	1.22	1.24	1.24	1.22	1.22	1.21
Cycle Burnup (MWd/kg)		11.6	11.3	11.5	11.8	11.7	11.7
Average Burnup of Unloaded Batch (MWd/kg)		35.1	35.1	34.6	35.3	35.5	35.5
Max. Average Burnup of Unloaded FA (MWd/kg)		43.1	41.6	42.0	41.7	41.2	41.4
Reload: 16 Th/Pu-FA	4.4 w/o Pu_{ples}						
48 U-FA	3.2 w/o ^{235}U						

Table 2.1.7: Main results of strategy calculations

Optimum* Tails Assay, w/o ^{235}U	Reactor Type: Fuel Cycle	Reactor Type: Reload Mode	U_3O_8: Annual 10^3t	U_3O_8: Cumulative 10^3t	U_3O_8: Δ%	SWU: Annual 10^6 kg	SWU: Cumulative 10^6 kg	SWU: Δ%
0.282	U	3 batch once-through	17.4	424	100	8.3	202	100
	U/Pu	3 batch recycle	12.5	311	73	5.7	146	72
	Th/Pu	4 batch once-through	12.4	306	72	7.0	172	85
	Th/U/Pu	4 batch recycle	11.1	288	68	6.3	162	80
0.249	U	3 batch once-through	16.4	399	100	8.9	217	100
	U/Pu	3 batch recycle	11.7	292	73	6.1	157	72
	Th/Pu	4 batch once-through	11.5	285	71	7.5	185	85
	Th/U/Pu	4 batch recycle	10.3	268	67	6.7	174	80
0.227	U	3 batch once-through	15.7	383	100	9.4	229	100
	U/Pu	3 batch recycle	11.3	281	73	6.5	166	72
	Th/Pu	4 batch once-through	11.0	272	71	7.9	195	85
	Th/U/Pu	4 batch recycle	9.8	256	67	7.1	183	80

*Corresponding costs and reductions in the uranium demand

US$/lb$U_3O_6$	US$/kg SWU	U_3O_8 (%)
30	140	100
60	200	94
90	240	90

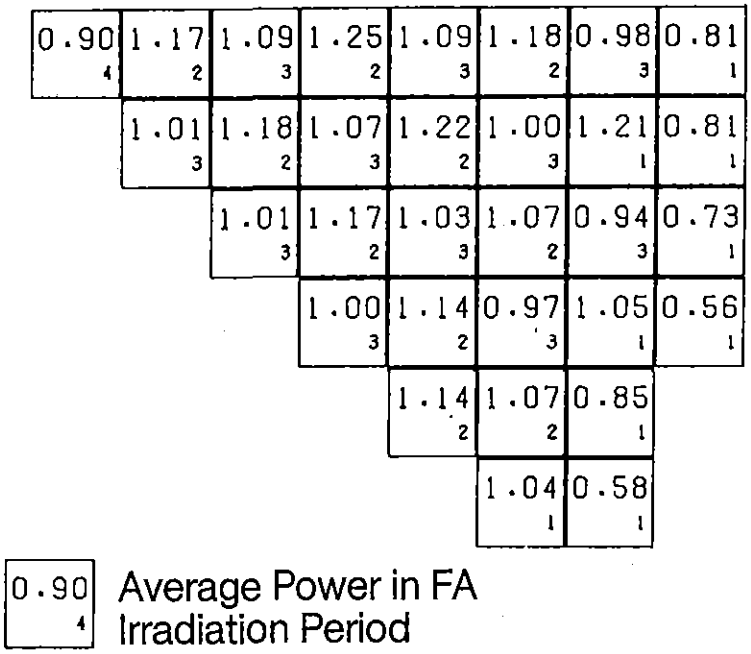

Fig. 2.1/1: Th/HEU, 3 Batch Core, Once Through Power Distribution at Beginning of an Equilibrium Cycle

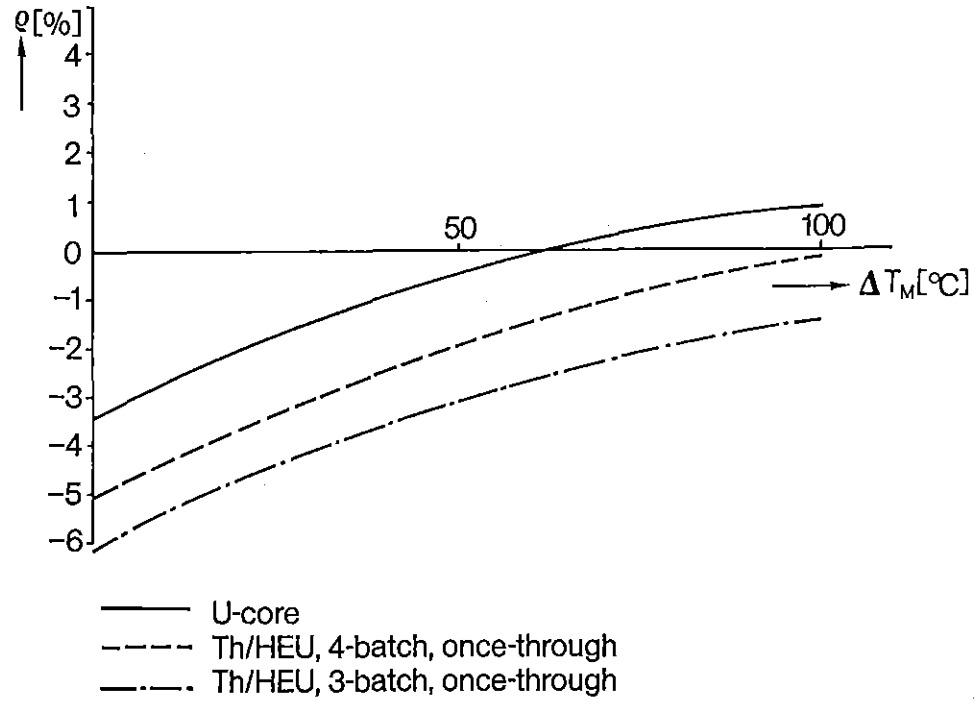

Fig. 2.1/2: Net Shutdown Reactivity in Function of Moderator Temperature Reduction (End of Equilibrium Cycle)

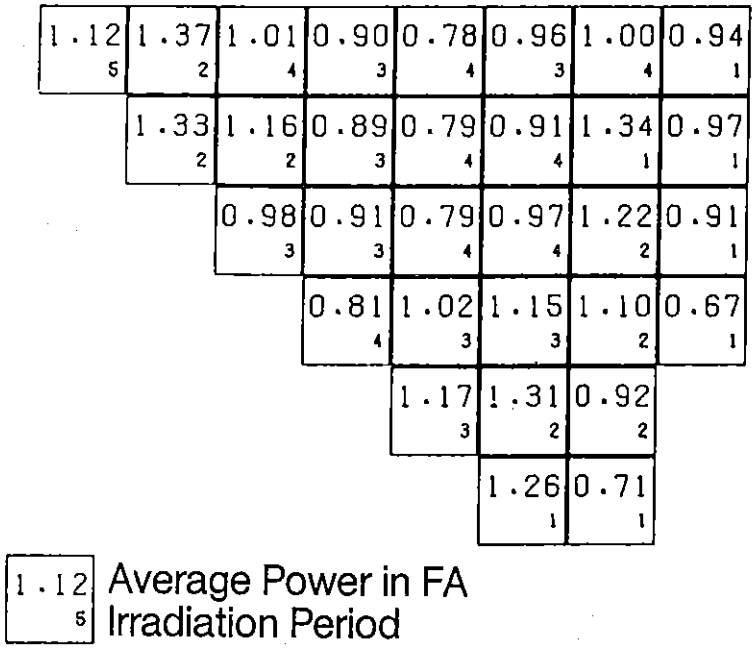

Fig. 2.1/3: Th/Pu, 4 Batch Core, Once Through Power Distribution at Beginning of an Equilibrium Cycle

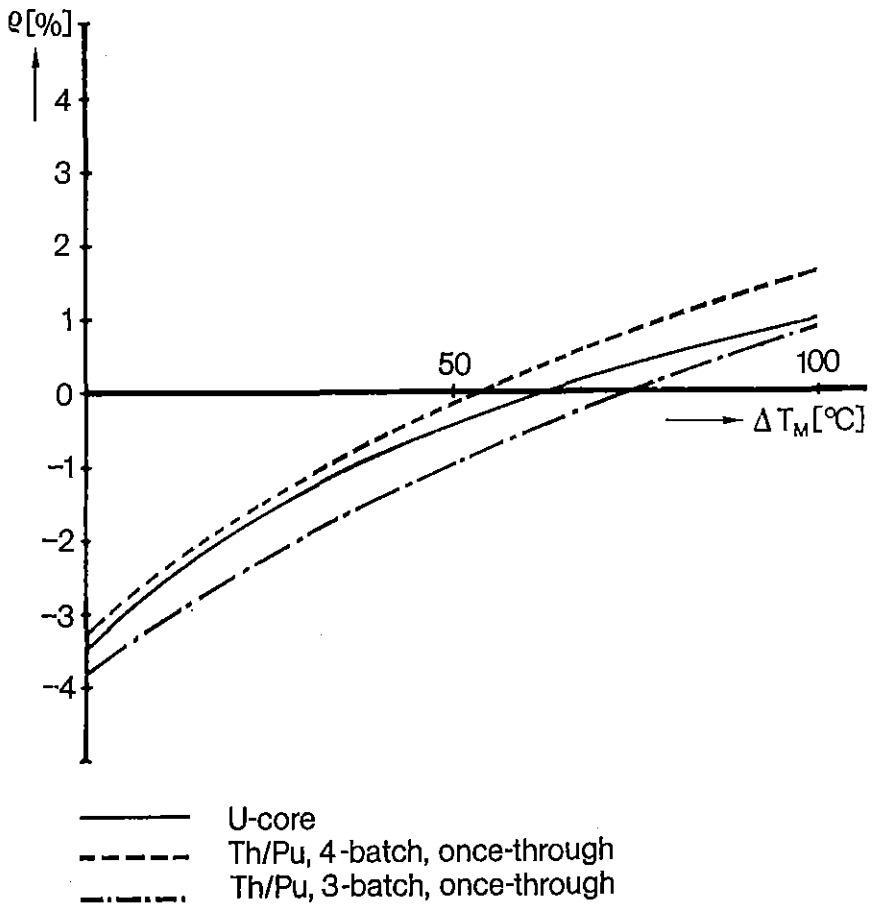

Fig. 2.1/4: Net Shutdown Reactivity in Function of Moderator Temperature Reduction (End of Equilibrium Cycle)

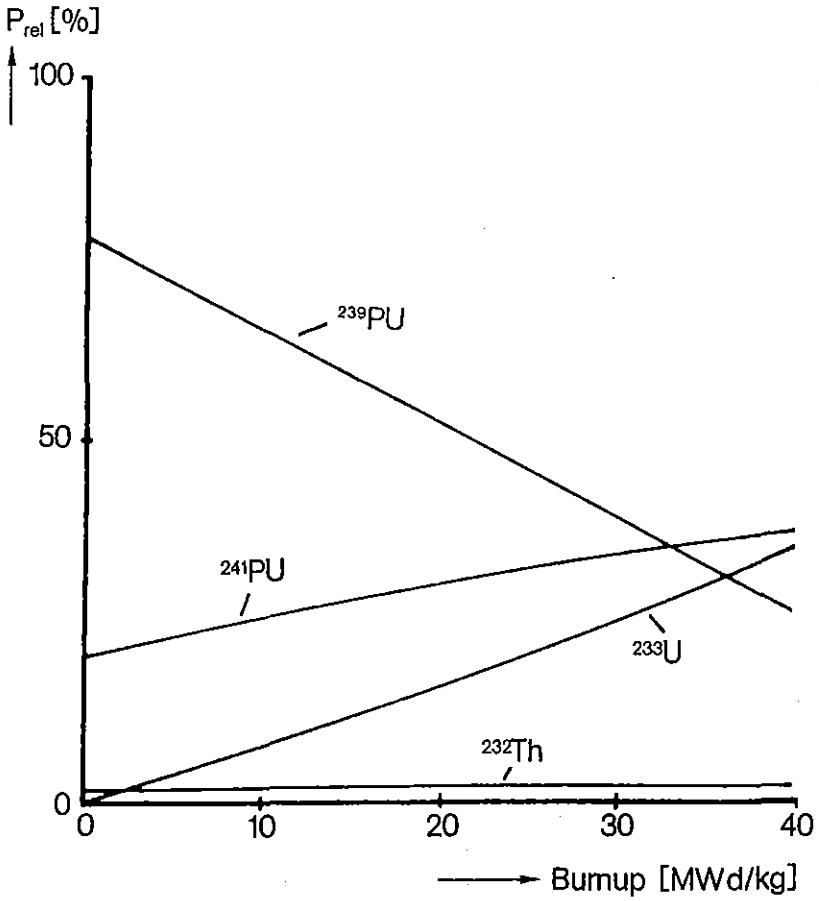

Fig. 2.1/5: Relative Energy Contribution of the Isotopes of Th/Pu Fuel

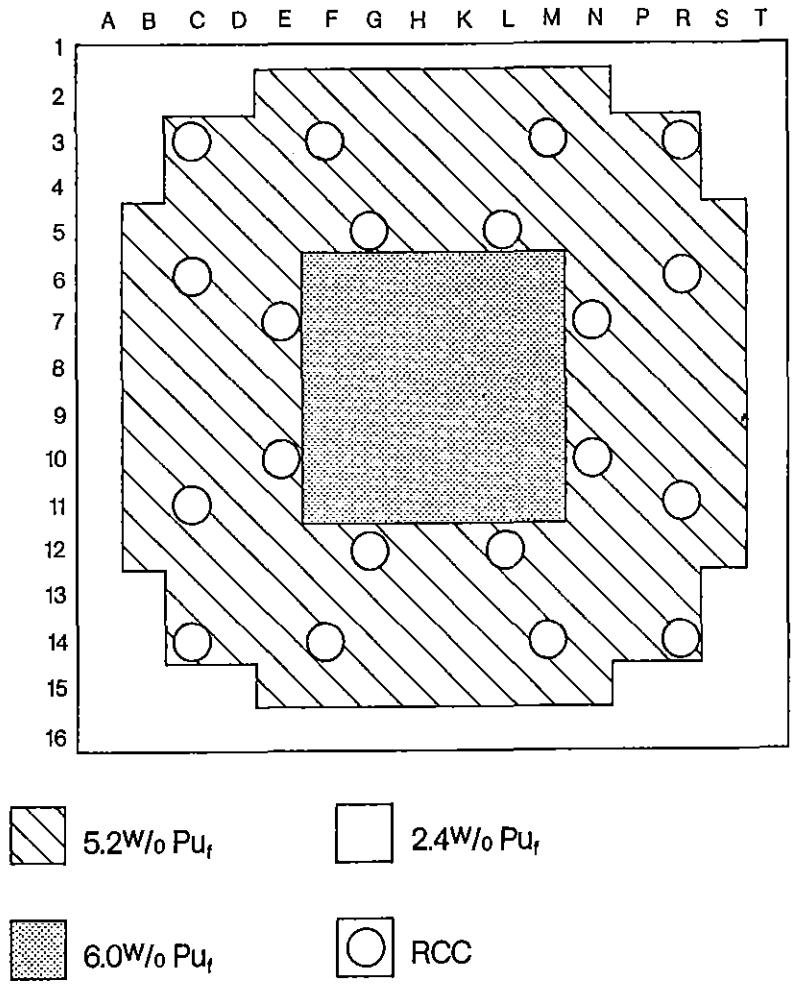

Fig. 2.1/6: Th/Pu Fuel Assembly with 3 Enrichment Zones

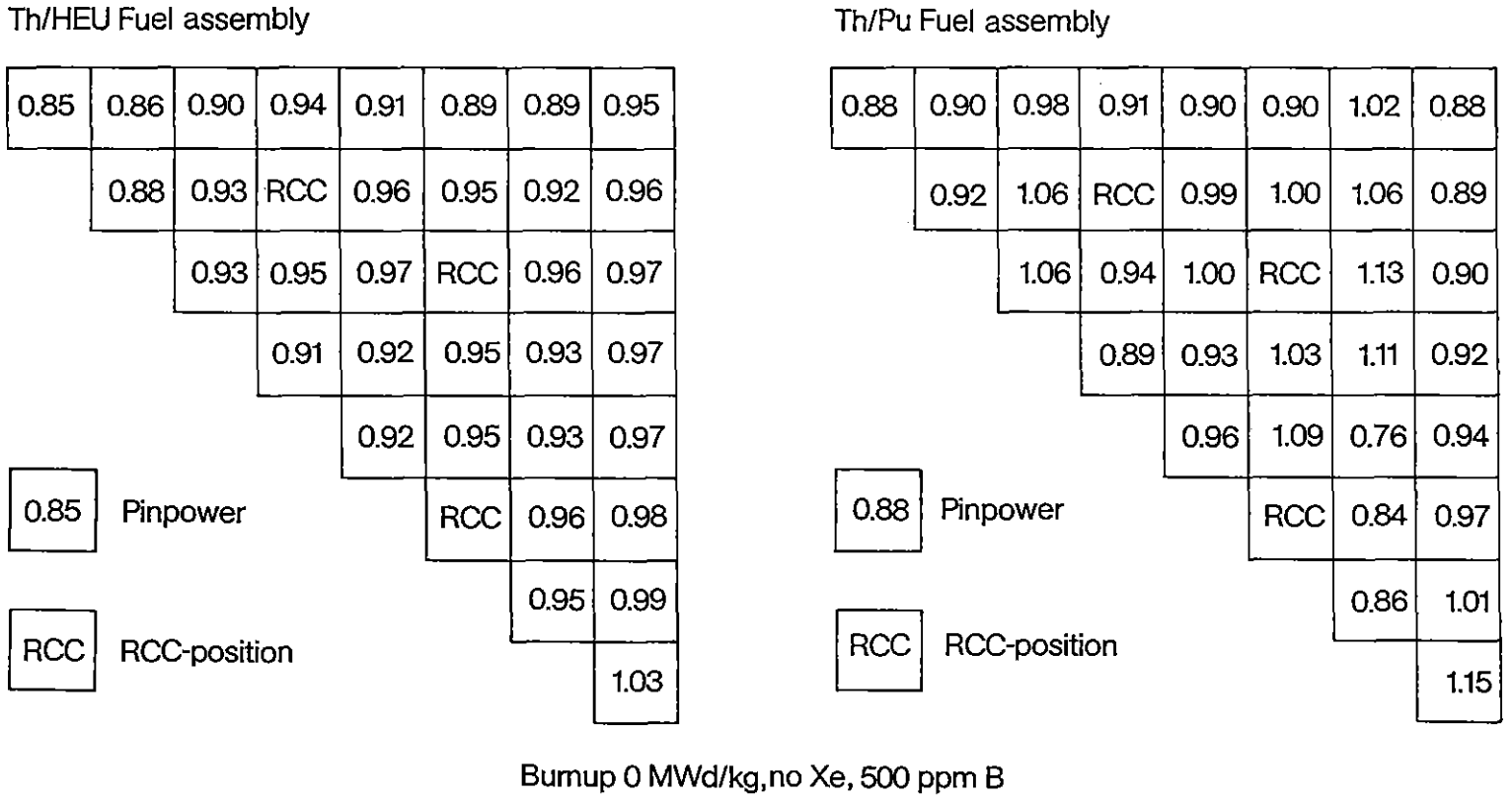

Fig. 2.1/7: Power Distribution in Th/HEU and Th/Pu Recycle Fuel Assembly Adjacent to Uranium Fuel Assemblies

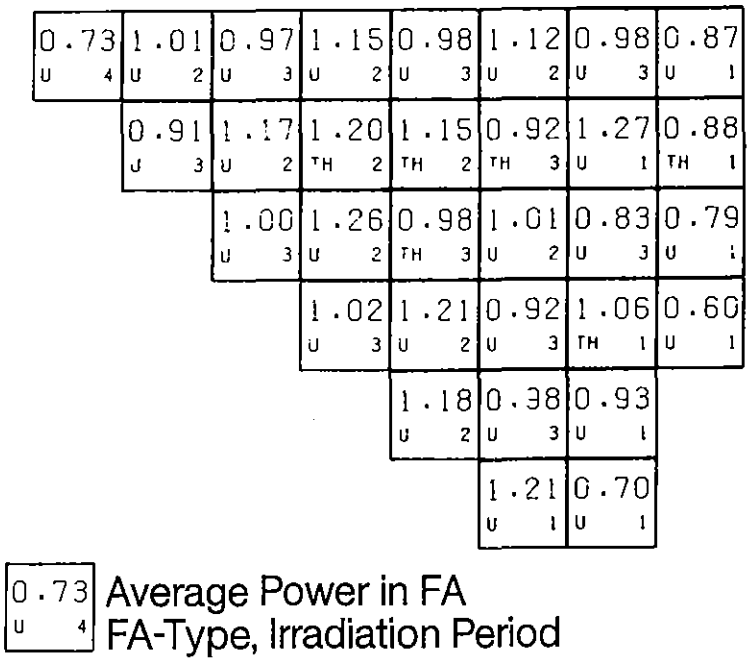

Fig.2.1/8: Equilibrium Core with a Reload of 48 U-FAs and 16 Th/Pu-FAs, Power Distribution at Begin of Cycle

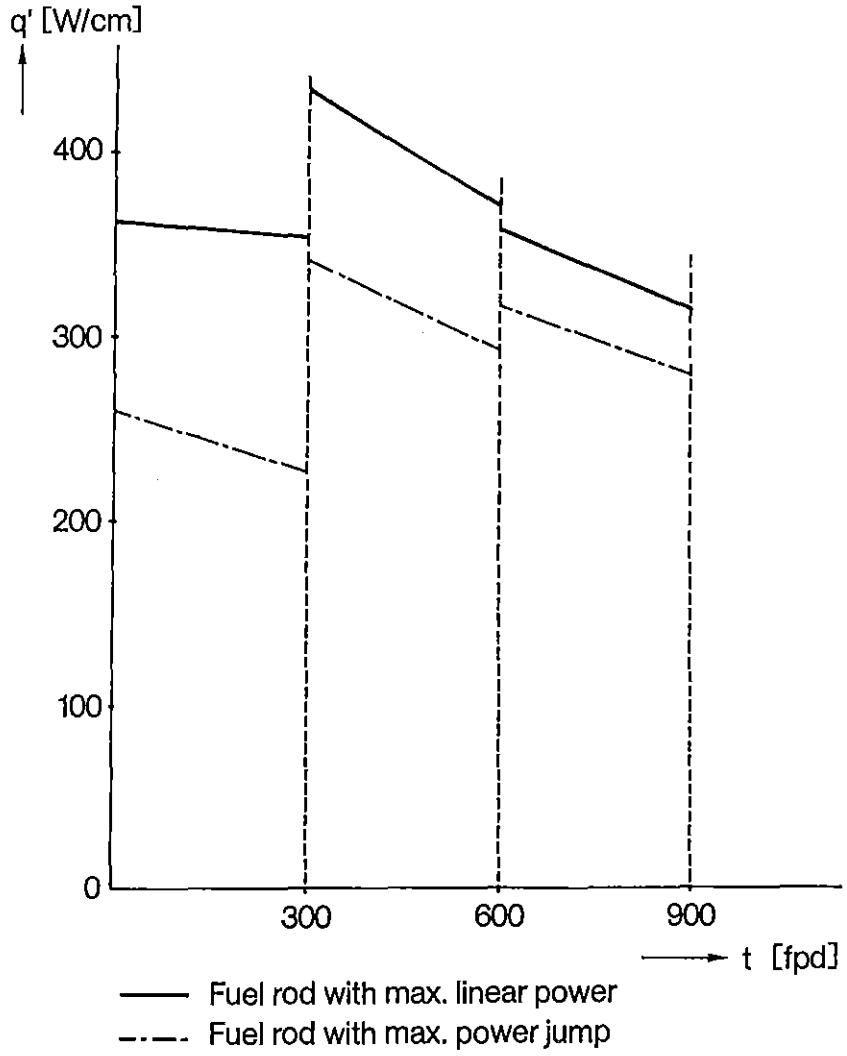

Fig. 2.1/9: Power History of Th/Pu Rods Equilibrium Cycle, 3 x 16 Th/Pu FA

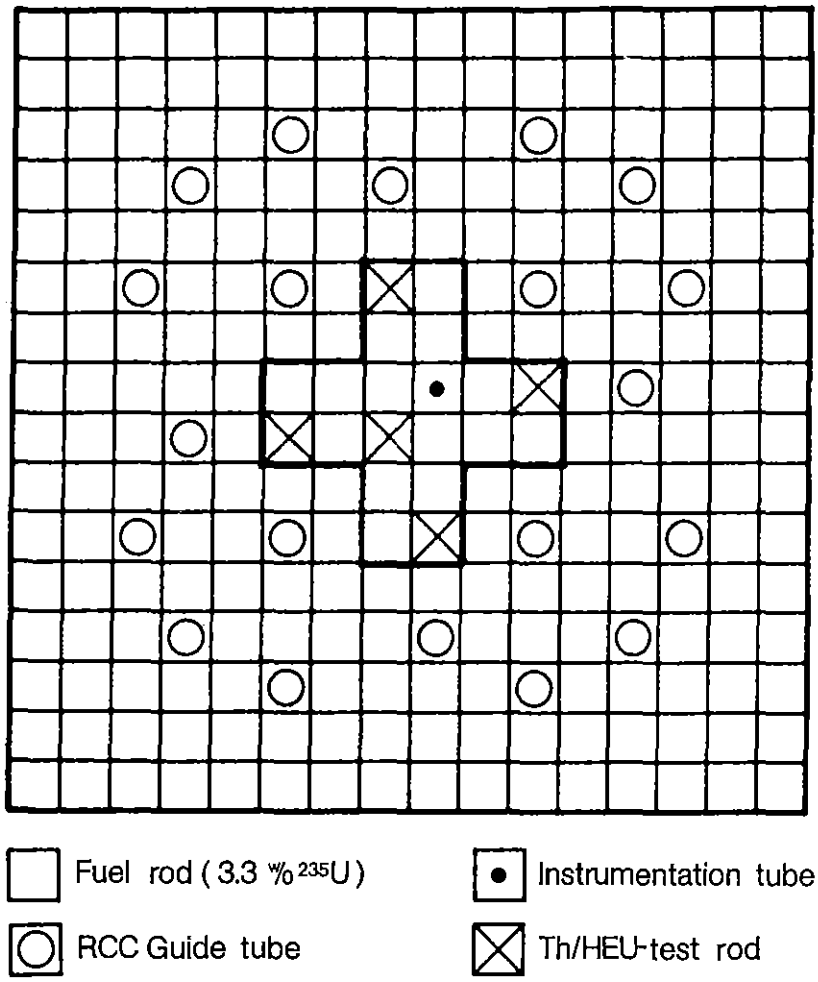

Fig. 2.1/10: Positioning of Test Fuel Rods in the Angra-1 Fuel Assembly

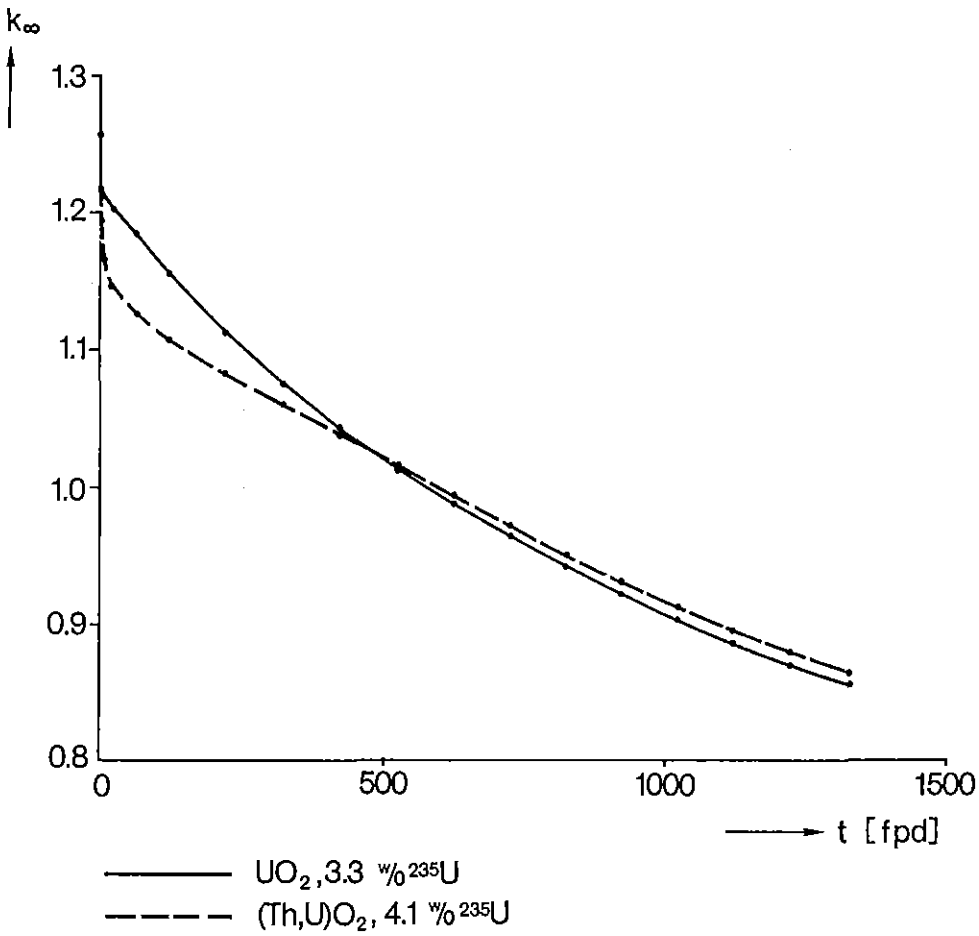

Fig. 2.1/11: Comparison of k_∞ of $(Th,U)O_2$ and UO_2 Cell of Angra-1 Type

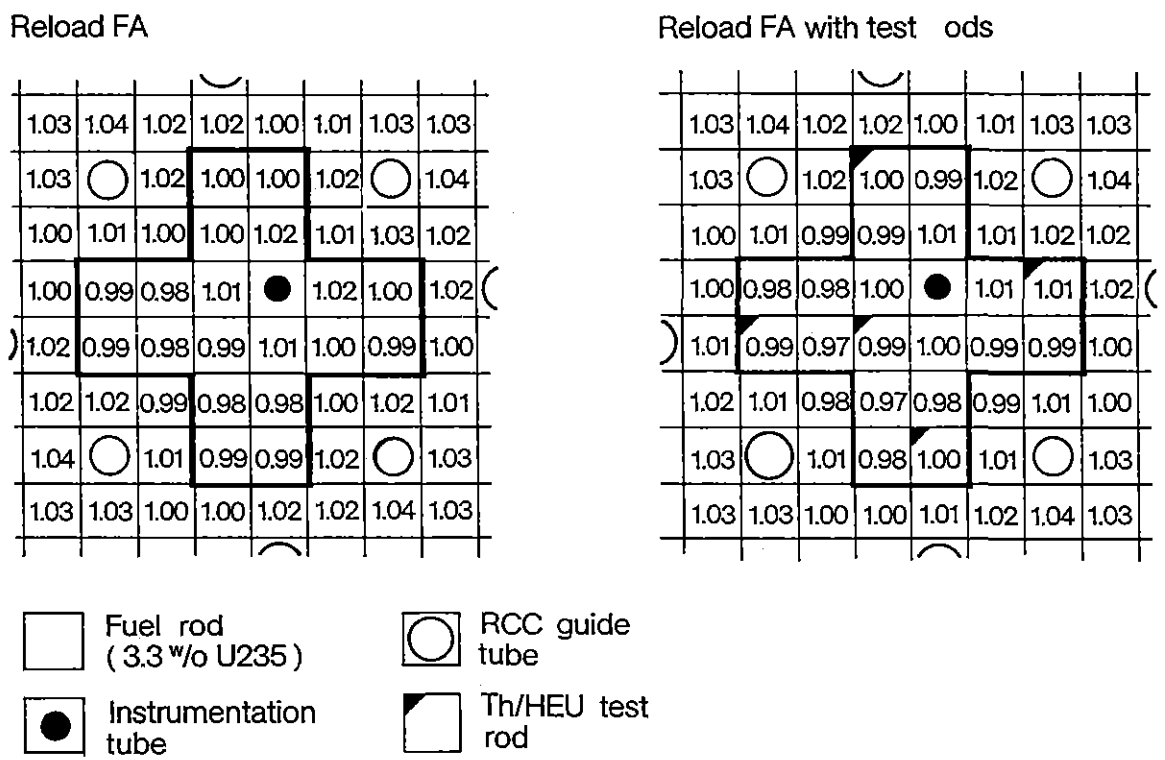

Fig. 2.1/12: Proposed Test Irradiation at Angra-1: Power Distribution in the Centre Part of a Reload Fuel Assembly and a FA with Th/HEU Test Rods

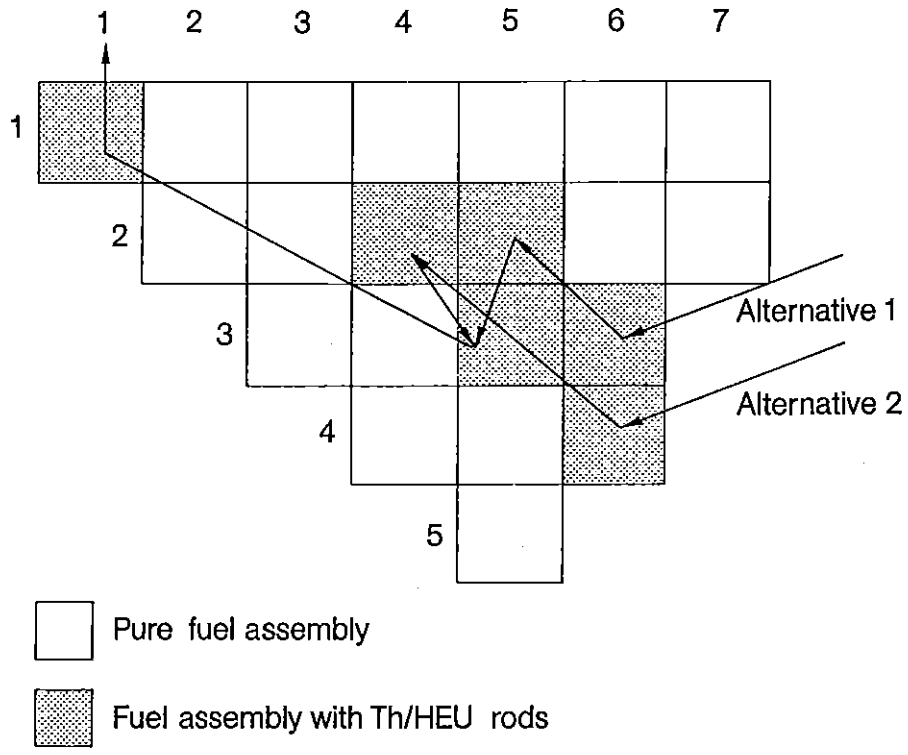

Fig. 2.1/13: Investigated Positions of the Test Fuel Assembly for 4 Periods of Irradiation

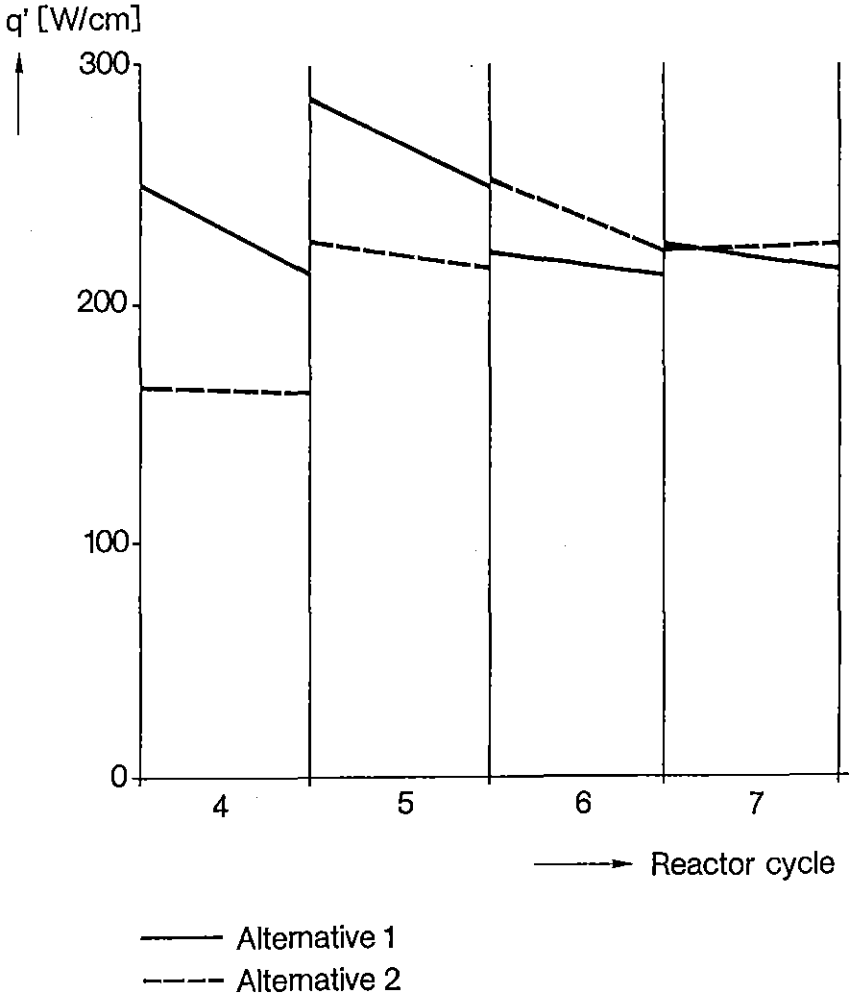

Fig. 2.1/14: Power History of Th/HEU Rods in a Reload FA of Angra-1

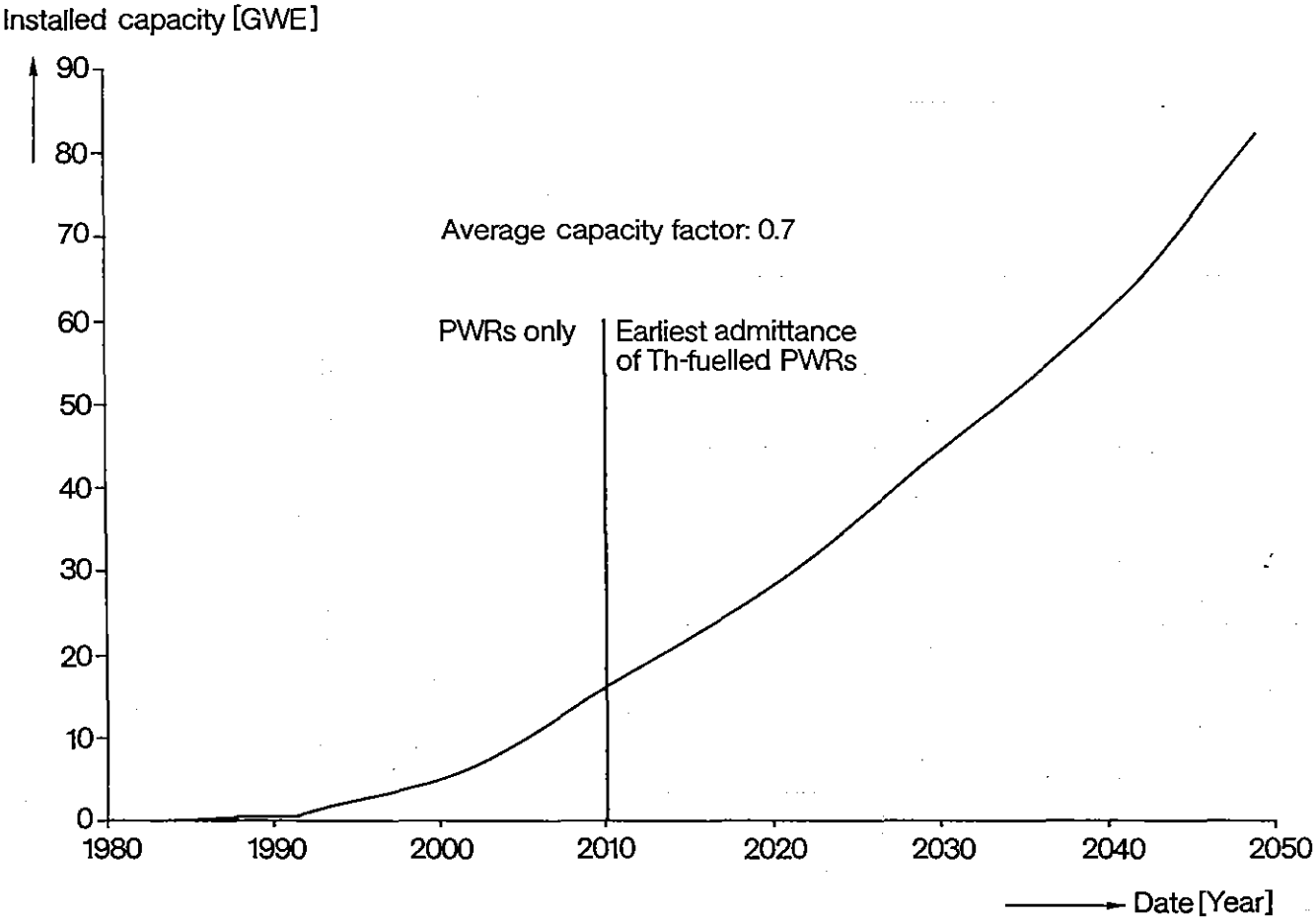

Fig. 2.1/15: Projected Power Demand in Brazil

2.2 Thermal and Mechanical Fuel Rod Design

The fundamental consideration in the safety-related design of nuclear power plants is the limitation of the release of radioactive products. The fuel rods with their gas-tight welded cladding tubes constitute an important barrier in this context.

In view of the large number of fuel rods in the reactor core, it is statistically not possible to preclude defects due to fortuitous factors in a small number of fuel rods. This is not necessary either, since the design of the plant ensures that a small number of defective fuel rods cannot cause the permissible rates of radioactive product release to the environment to be exceeded.

However, systematic defects arising under the conditions of authorized operation (normal operation and operational transients condition I and events of moderate frequency condition II, ANSI/ANS-57.5-1981 [2.2-1]) must be precluded.

The fuel rods comprise sintered thorium and uranium pellets with ground circumferential surface which are enclosed by a cladding tube made of Zircaloy-4. The fuel consists of a one-phase solid solution of thorium and uranium dioxide, the amount of uranium being approximatelly 5 w/o. The uranium is enriched about 93% with ^{235}U. The cladding tube is closed by means of end plugs and welded gas-tight. As in the standard UO_2 pellets, the end surfaces of the $(Th,5\%U)O_2$ pellets are dished to reduce the axial thermal expansion of the pellet stack.

The gaseous fission products released from the fuel matrix during the dwell time in the reactor are primarily accommodated in the gas plena at the end of the fuel rods. The upper plenum contains a spring which has to impart a certain degree of compression to the pellet stack so as to prevent axial moving of the pellet stack during fuel assembly transport. The spring permits axial displacement of the fuel pellet stack relative to the cladding tube during irradiation. The lower plenum (if existing) contains a supporting tube.

The fuel rods are internally prepressurized to reduce the strain induced by the coolant in the cladding tube in the core. Helium is used as the gas filling to assure fuel-to-cladding heat transfer.

Figure 2.2/1 shows a schematic diagram of the fuel rods.
Figure 2.2/2 shows a pellet.

2.2.1 Design criteria for PWR $(Th,U)O_2$ fuel rods

The fuel rod is exposed to certain loads during normal operation. It is necessary to limit these loads to ensure that the rod retains its mechanical integrity. To demonstrate the mechanical integrity design limits are defined. These design limits and the reasoning behind them are presented in brief in the following pages of this section. As construction and function of $(Th,U)O_2$ fuel rods and UO_2 fuel rods do not differ, the same design criteria are used for both rod types.

2.2.1.1 Temperatures

It has been demonstrated in numerous irradiation experiments that fuel rods can be operated for lengthy periods even with molten fuel without damage to the cladding tubes [2.2-2, 2.2-3].

The temperature limit for fuel rod design nevertheless requires that even under worst-case operating conditions, including maximum possible overload, the melting point of the fuel shall not be exceeded at the point of peak thermal power generation. This particular limit is specified to ensure that sudden shifting of molten fuel in the interior of the fuel rods can be positively precluded. Thanks to this limitation, there is also no danger of excessive cladding tube expansion as a result of an increase in the volume of the fuel due to melting and there is therefore no need to provide additional space (porosity, hollow pellets, etc.) in the fuel rod to accommodate any such volume increase.

2.2.1.2 Rod internal pressure

The fuel rod is filled with helium during manufacture. A filling pressure higher than atmospheric is applied. This improves heat transfer from the fuel to the cladding and reduces clad creepdown caused by coolant overpressure.

At the beginning of the dwell period, the temperature rise during power operation and the different degrees of expansion of the cladding tube and the fuel cause the filling pressure to rise to more than 100%. This internal pressure increases progressively during the residence time as fission gases are released. It must nevertheless be assured that the fuel-to-cladding gap cannot increase as a result of the internal pressure even at the end of the dwell time, i.e. that the rate of increase of the cladding tube diameter due to the maximum internal pressure must be less than the increase in pellet diameter due to fuel swelling (cladding non-lift-off design criterion). If this is not the case, i.e. if the gap grows wider, the reduced coefficient of heat transfer across the wider fuel-to-cladding gap gives rise to higher fuel temperatures and hence to increased fission gas release. This in turn causes the pressure in the fuel rod to build up still further and hence leads to continued widening of the gap. Another limit on the maximum permissible internal pressure is derived from the strain criterion explained in Section 2.2.1.3.

2.2.1.3 Strain

Given the manufacturing clearance between fuel and cladding, an operating clearance for the warmed-up condition at rated reactor power remains taking into account the elastic compressive strain in the cladding tube due to the coolant pressure and the different thermal expansion of the cladding and fuel. Owing to the difference between the coolant pressure on the outside and the helium pressure on the inside the cladding tube is subject to compressive stress and contacts onto the fuel due to creepdown. Once the cladding has come into contact with the fuel, fuel swelling causes the cladding tube to expand gradually until, in the extreme case, i.e. at very high burnup, the cladding tube may expand beyond its original beginning-of-life (BOL) dimensions. Consequently tangential deformation of the cladding is composed of creep-induced compressive strain and subsequent creep under tensile stress. The tangential strain

on the cladding tube is superposed with an axial strain since it is assumed that, once the cladding has come into hard contact with the pellets, it will be forced to expand axially as well due to swelling and thermal expansion of the fuel.Straining of the cladding by the fuel can also be caused by power ramps. So the following kinds of fuel-cladding interaction have to be considered in fuel rod design:

a) **fast power ramps**
Dependent on burnup, ramp height and final power the cladding can be strained due to the thermal expansion of the fuel during power ramps. In this case the cladding strain must be below the ductility of the cladding material by a safe margin (see also [2.2-4]).
Principally fast ramps can also cause a chemical/mechanical pellet clad interaction known as PCI/SCC. In this case the criterion just given is not valid.
PCI/SCC failures however can be precluded as operational regulations and/or the reactor power regulation system ensure that the reactor is not operated under conditions with the risk of PCI/SCC.

b) **long term interaction due to fuel swelling**
In this case stress relaxation at a low stress level takes place. The cladding is forced to creep outward with a stress exponent of less than 10 (about 4 for recrystallized cladding). Under these conditions irradiated Zircaloy-4 has a very high creep ductility. The cladding strain has to be below the creep ductility by a safe margin. This limit shall not be exceeded even if the cladding tube is caused to expand not by the fuel but by the internal gas pressure, provided that this pressure is higher than the external pressure exerted by the coolant.

2.2.1.4 Corrosion

Zircaloy-4 cladding tubes undergo corrosion at slow rates in reactor operation [2.2-5, 2.2-6]. This causes thinning of the cladding tube walls and impairs heat transfer to the coolant. In the case of thick layers enhanced local variation of layer thickness can cause cladding defects. Therefore maximum cladding corrosion has to be limited.

2.2.1.5 Hydrogen uptake

Part of the hydrogen released in the corrosion process diffuses into the Zircaloy-4 cladding tubes. This uptake must not exceed certain values since hydrogen in excessive quantities can reduce the ductility of the cladding tube metal.

2.2.1.6 Elastic buckling and plastic deformation under external overpressure

As a result of the difference between the external coolant and rod internal gas pressures, the fuel cladding tubes are generally subject to an external overpressure. A cladding tube under external overpressure may momentarily buckle elastically or, if the stresses exceed the yield point, may undergo plastic deformation.

To prevent elastic buckling and plastic deformation, the stipulation is that the maximum pressure difference shall exceed neither the pressure at which buckling takes place nor the pressure at which the membrane stress reaches the $Rp_{0.2}$ yield point.

2.2.1.7 Cladding tube stresses

In addition to the stresses imposed by the difference between the coolant and rod-internal pressures, a number of other stresses occur in the cladding tube, the overall effects of which must be limited.

The individual stresses in tangential, radial and axial direction are computed to calculate the equivalent stress in accordance with the energy of distortion theory.

The design limits are based on the yield strength $Rp_{0.2}$ and on the ultimate tensile strength Rm (see 2.2.4.3).

2.2.1.8 Dynamic loads

In the analysis of the dynamic stresses acting on the fuel rods, only the alternating bending stresses excited by the coolant flow forces are considered. The other dynamic loads (pressure fluctuations, thermal stresses, etc.) may be neglected on account of the low magnitude of fluctuations and/or the low number of stress cycles involved.

In [2.2-7] a design curve is given for irradiated Zircaloy-4 showing the permissible number of stress cycles as a function of the amplitude of the stresses taking into account the maximum possible mean stress.

The design curve was obtained on the basis of experimental results a safety factor is applied to the sustainable stress cycles and one of 2 to the stress amplitude, depending on which method yields the more conservative value.

With the above-mentioned safety factors taken into account, the permissible design value for the alternating bending stress (endurance limit) is obtained for irradiated Zircaloy-4 under the condition of maximum possible mean stress [2.2-7] and under operating conditions.

2.2.2 Design related material properties of $(Th,U)O_2$ pellets

The existing data of $(Th,U)O_2$ properties were reviewed to provide the data base required in the fuel design analysis of fuel irradiation.

2.2.2.1 Thermal conductivity

In oxide ceramics, heat can be transported by three different mechanisms:

a) conduction by phonons (lattice conduction),
b) conduction by photons (radiation),
c) conduction by electrons.

Phonon, or lattice conduction, above the Debye temperature can be represented by an equation of the form:

$$\lambda = \frac{1}{A + B.T}$$

where the constant A characterizes phonon impurity, or grain boundary collisions and

the constant B characterizes phonon-phonon collisions. A supplementary CT^2 term can be used to fit some oxide ceramic data. This term corresponds to complicated phonon-phonon collisions and has some theoretical justification [2.2-8].

Contributions from internal radiation heat transfer and electron charge carriers can become important at high temperatures. Indeed, in the UO_2, the observed increase in thermal conductivity with increasing temperature has been attributed to one or both of these factors.

Schmidt [2.2-9] attributed the so-called „excess" thermal conductivity of UO_2 at the higher temperatures to an increase in the heat capacity with increasing temperature. This interpretation is compatible with a significant electronic contribution to the total thermal conductivity if the anomalous increase in the heat capacity is due to energy absorption through electron excitation.

The experimental data of the $(Th,U)O_2$ thermal conductivity were reviewed and fitted through a three-term lattice conduction equation. The 312 experimental results used in the fitting cover the temperature range of room temperature until 1310° C, the UO_2 molar contents until 30% and were reported in the references [2.2-8, 2.2-10 to 2.2-17].

The high temperature component of the thermal conductivity was evaluated using the following relationship

$$\lambda = \alpha \cdot \rho \cdot C_p \qquad (1)$$

where

α = thermal diffusivity, evaluated at high temperature by extrapolation of the experimental results;

ρ = density, evaluated at high temperature by extrapolation of the thermal expansion results (section 2.2.2.3);

C_p = heat capacity (section 2.2.2.2)

A linear dependence of the UO_2-molar contents was supposed for this component.

Then, the thermal conductivity could be expressed by the following fitting, in W/m.° C:

$$\lambda = (1-\beta.p)\left[\frac{1}{A + \beta.t + C.t^2} + \frac{D.\exp(-E/k\,(t+273.15))}{(T+273.15)^2}\right]$$

where:

β = 2.5;
p = porosity fraction;
t = temperature in °C;
$A = 6.1973\times10^{-2} + 9.8982\times10^{-2}\,y - 6.4788\times10^{-2}\,y^3$;
$B = 1.7646\times10^{-4} + 5.5105\times10^{-5}\,y$;
$C = -2.0052\times10^{-8}\,y^2$;
$D = \exp[E/k.d_1(1-f_1y)]$
E = 2.6898 (1–0.4508 y) eV;
y = mole fraction of UO_2;
$k = 8.617\times10^{-5}$ eV/K;
d_1 = 1189.4 K
f_1 = 0.35333

The relative standard deviation is 7.3 %. Figure 2.2/3 shows measured versus calculated thermal conductivities.

Thermal conductivity measurement

The thermal conductivity measurements of the $(Th,5\%U)O_2$ ex-gel pellets were done to support the evaluation of the irradiation tests in FRJ-2.

The $(Th,5\%U)O_2$ thermal conductivity measurements were obtained through the above equation from thermal diffusivity measurements and supposing that the density is known from linear thermal expansion and the thermal capacity is known from literature data.

The thermal diffusivity was measured by the laser flash method. The measurements were performed on cylindrical pellets (radius r and thickness l) with different radius/length ratios as shown in Table 2.2.1.

Figure 2.2/4 shows the thermal conductivity measurements obtained at the KWU laboratory. In this figure is shown the thermal conductivity obtained from literature, too.

2.2.2.2 Thermal capacity

The thermal capacity of $(Th,U)O_2$ can be represented by a 3-term equation obtained by differentiation of the 3-term enthalpy equation. The enthalpy results cited in [2.2-18] and reported in the references [2.2-19, 2.2-20] were fitted by the following relationship:

$$H_T - H_{298.15}\ (J/mol) = C_1\theta\left[\frac{1}{\exp(\theta/T)-1} - \frac{1}{\exp(\theta/298.15)-1}\right] + C_2\left[T^2 - (298.15)^2\right] + C_3\exp(-E/RT)$$

where

θ = 387 K
C_1 = 71.151 J/mol.K;
C_2 = 4.1282×10^{-3} J/mol.K^2;
C_3 = $3.4608\times10^{+9}$ J/mol;
E = $3.24218\times10^{+5}$ J/mol;
R = 8.31434 J/mol.K

Figure 2.2/5 shows the $(Th,U)O_2$ enthalpy for different compositions. As can be seen, no significant difference is observed.

Then, the thermal capacity equation, for $(Th,U)O_2$ for molar fraction of UO_2 until 0.20, is as follows:

$$C_p = \frac{C_1\,\theta^2\exp(\theta/T)}{[\exp(\theta/T)-1]^2\,T^2} + 2\,C_2\,T + \frac{C_3\,E}{R\,T^2}\exp(-E/RT)$$

where the constants have the same meaning as above.

2.2.2.3 Thermal expansion

The linear thermal expansion is treated isotropically and was determined from a best fit

of experimental data for the temperature range 0 to 2,000°C and for mole fractions of UO_2 less than or equal to 0.50 [2.2-18, 2.2-21 to 2.2-27]. The obtained expression is given by:

$$\frac{\Delta l}{l}(\text{cm/cm}) = (8.1635\text{x}10^{-6} + 3.8325\text{x}10^{-6}\,y + 5.2423\text{x}10^{-6}\,y^2).$$
$$.(T\text{-}25)\,(1.2144\text{x}10^{-9} + 1.4936\text{x}10^{-10}\,y +$$
$$+ 1.5633\text{x}10^{-9}\,y^2).\,(T^2 - 25^2)$$

where T is the temperature in °C and y is the UO_2 molar fraction.

This equation is applicable over the temperature range observed, with a relative standard deviation of 4.8%. The number of experimental data used was 103.

Figure 2.2/6 shows the comparison between the calculated and experimental values.

2.2.2.4 Melting point

Melting points measurements on $(Th,U)O_2$ systems from references [2.2-28 to 2.2-33] and calculated values based on ideal solution behaviour [2.2-8], are shown in Figure 2.2/7. They are best fitted by the following equation

$$T_m(°C) = 3{,}352 - 506 \cdot y$$

where y, the molar fraction of UO_2, is ≤ 0.90.

2.2.2.5 Theoretical density

ThO_2 is generally completely miscible with UO_2 forming complete series of fluorite cubic solid solutions. It was obtained from an expression for theoretical density for $(Th,U)O_2$ solid solutions considering the E-an Zen expression for lattice parameter [2.2-34].

The theoretical density for $Th_{1-y}U_yO_2$ is given by:

$$\rho = m/V \qquad (1)$$

where m is the mass of solid solution and V is the unit cell volume of solid solution.

For $Th_{1-y}U_yO_2$, the molecular weight is given by:

$$M = M_2 + y\,(M_1 - M_2)$$

where

M = molecular weight of solid solution;

M_1 = molecular weight of UO_2 taking into account the enrichment, if present;

M_2 = molecular weight of ThO_2

y = molar fraction of UO_2

The number of metallic ions (Th^{4+} and/or U^{4+}) in CFC unit cell is 4 to 8 oxygen ions. Then, the cell contains 4 molecules of $Th_{1-y}U_yO_2$ and the mass of solid solutions can be written as:

$$m = \frac{4[M_2 + y\,(M_1 - M_2)]}{N_o} \qquad (2)$$

Where N_o is the Avogadro's number and the other terms have the same meaning as above.

The volume of $Th_{1-y}U_yO_2$ unit cell is given by the E-an Zen expression:

$$V = a_2^3 + y\,(a_1^3 - a_2^3) \qquad (3)$$

Substituting equation (2) and equation (3) into equation (1), the theoretical density for $(Th,U)O_2$ solid solution can be written as:

$$\rho(Th_{1-y}U_yO_2) = \frac{4\,[M_2 + y\,(M_1 - M_2)]}{N_o\,[a_2^3 + y(a_1^3 - a_2^3)]} \qquad (4)$$

where

a_1 = lattice parameter of UO_2,
a_2 = lattice parameter of ThO_2.

Figure 2.2/8 shows the measured lattice parameter [2.2-25, 2.2-28, 2.2-31, 2.2-32, 2.2-35] versus UO_2 contents and the estimation curve given by equation (3).

Another method based on molar density of the solid solutions components gives

$\rho = [M_2 + y(M_1 - M_2)] \cdot [m_2 + y(m_1 - m_2)]$
$\rho = M \cdot m$

where

m_1 = 4.05931×10^{-2} moles/cm^3 = molar density of UO_2;
m_2 = 3.78775×10^{-2} moles/cm^3 = molar density of ThO_2;
$M = M_2 + y(M_1 - M_2)$ = molecular weight of solid solution;
$m = m_2 + y(m_1 - m_2)$ = molar density of solid solution.

Example:

Calculation of theoretical density for $(Th_{0.95}\ U_{0.05})O_2$:

a_1 = 5.4693×10^{-8} cm
a_2 = 5.5970×10^{-8} cm
N_o = 6.023×10^{23}/mol
M_1 = 270.05 g/mol
M_2 = 264.04 g/mol

from equation (4), we have:

$$\rho(Th_{0.95}\ U_{0.05})O_2 = 10.046\ g/cm^3,$$

and from equation (5) results

$$\rho(Th_{0.95}\ U_{0.05})O_2 = 10.048\ g/cm^3.$$

2.2.3 Design related phenomena on $(Th,U)O_2$ pellets

$(Th,U)O_2$ pellets have been shown to have many more similarities than differences in relation to UO_2 pellets. So, the design related phenomena modelling base of UO_2 pel-

lets were adapted for $(Th,U)O_2$ pellets. The adaptation was performed in view of available information of the literature, theoretical and experimental studies and irradiation tests in the research reactor FRJ-2 in Juelich, Germany.

2.2.3.1 Densification

Densification occurs in the porous fuel under irradiation, causing a reduction in porosity and hence in pellet volume [2.2-36]. The magnitude and densification rate are markedly governed by the initial pore sizes.

The densification mechanisms that prevail in fuel of the pore size range of standard PWR fuel can be described with sufficient accuracy by a burnup dependent formula whose constants are calibrated against empirical densification values.

In the case of $(Th,U)O_2$ pellets, a careful determination of the irradiated fuel pellet density was carried out in order to get appropriated constants for the densification formula. Figure 2.2/9 shows the fuel dimensional variation considering superposition of densification and swelling in comparison with experimental points.

2.2.3.2 Swelling

The swelling rate on $(Th,U)O_2$ pellets was taken as follows [2.2-37]:

$$\frac{\Delta V^{(S)}}{V} = 1.25\%/[10\ \text{MWd/(kg U + Th)}]$$

where $\Delta V^{(S)}/V$ is the pellet volume increase due to swelling.

2.2.3.3 Relocation

Already at the first power rise the pellets split into cuneiform fragments owing to the steep radial temperature gradient. Accordingly this cracked fuel is able to undergo free thermal expansion. Beyond that the fuel fragments relocate in outward direction. This gives rise to an additional increase of the thermally effective pellet diameter. This radial relocation adapts itself to the available „space in the gap". This model is calibrated against fuel rods equipped with temperature instrumentation.

Taking into account the minor differences in the material properties of $(Th,U)O_2$ and UO_2, the linear heat rating at typical PWR conditions higher than the threshold power level required to initiate the cracking and the large scattering on the UO_2 relocation behaviour [2.2-38,2.2-39], a similar relocation behaviour to UO_2 is expected for $(Th,U)O_2$.

2.2.3.4 Fission gas release

A certain fraction of the fission gas produced is released from the fuel into the free volume of the fuel rod. The KWU fission gas release model is based on the following concept: the capacity of the fuel grain matrix for retaining fission gas is limited. The fission gas which can no longer be retained in the grain interior accumulates at the grain boundaries and from there it may be released via pathways that form in the network of grain boundaries. The model comprises – one sub-model for steady-state and one for transient release.

Results of fission gas release from 59 fuel rods containing $(Th,U)O_2$ were reported by Goldberg et al. [2.2-40, 2.2-41, and 2.2-42]. Analysis of these results showed that the thoria-based fuel rods have lower fission gas release than UO_2 rods under similar operating conditions.

However, this was not observed for the present ex-gel-C-$(Th,5\%U)O_2$ fuel irradiation testing. Fission gas release fractions measured from irradiated test fuel rods are comparable to the calculated ones according to the KWU model (U-based fuel):

Observed	Calculated
0.17%	0.18%
1.61%	1.01%

2.2.3.5 Restructuring

Formation of columnar grain by a sublimation-condensation phenomenon for UO_2 fuel is considered to occur at about 1800°C The phase transition solid-vapour of the fuel oxides occurs in the vapour pressure range 10^{-5} to 10^{-4} atm.

The sublimation temperature of 2,400°C for pure ThO_2 was determined from experimental in- and out-of-pile investigations. So, it is foreseen for $(Th,U)O_2$ mixed oxides a restructuring temperature range 1,800–2,400°C depending on the fuel composition. Based on the analysis of the literature survey [2.2-43, to 2.2-45] the following temperatures for $(Th,5\%U)O_2$ fuel were taken:

a) minimum temperature for onset of equiaxed grain growth equal 1,800°C;

b) minimum temperature for onset of columnar grain growth equal 2,100°C.

2.2.4 Design related material properties and phenomena of Zircaloy-4 cladding tubes

Zircaloy-4 is used as standard material for the cladding of fuel rods. It has low thermal neutron cross section and good mechanical properties as well as good corrosion resistance. For fuel rod design the properties of Zircaloy-4 are described in the following. Irradiation tests in the research reactor FRJ-2 in Juelich, Germany have shown that cladding behaviour of $(Th,U)O_2$ fuel rods is comparable to that of UO_2 fuel rods. So the same models can be used for both rod types.

2.2.4.1 Thermal conductivity

The thermal conductivity λ of Zircaloy-4 depends on temperature T as given in the following (in W/m·K):

$T = 20...800°C:$

$\lambda = 13.51 + 5.138 \times 10^{-3} \cdot T + 8.055 \times 10^{-6} \cdot T^2$

$T = 800...1{,}600°C$

$\lambda = 15.12 + 1.100 \times 10^{-3} T + 1.058 \times 10^{-5} T^2$

This dependency is illustrated in Figure 2.2/10.

2.2.4.2 Thermal expansion

The manufacturing process causes anisotropy of the cladding tubes. So their linear thermal expansion is different in the axial and radial direction. It depends on temperature T as follows (reference temperature 25°C)

Axial direction:
$\Delta l/l_o = 5.575 \times 10^{-6} T - 1.115 \times 10^{-4}$ for 100°C < T < 800°C.

Radial direction:
$\Delta l/l_o = 2.6412 \times 10^{-4} + 3.7099 \times 10^{-6} T + 7.4252 \times 10^{-9} T^3$ for 100°C < T < 600°C

This dependency is illustrated in Figure 2.2/11.

2.2.4.3 Mechanical properties

Young's modulus
The Young's modulus is temperature-dependent:

$$E = 99{,}408 - 65.4\ T \quad (N/mm^2)$$

Poisson's ratio
For fuel rod design a mean value of several measured data is used which is not dependent on temperature:

$$\delta = 0.3$$

Strength
Strength depends on material and condition of the cladding. PWR cladding tubes are in general cold worked and stress relieved or partly recrystallized. Typical figures for yield strength and ultimate tensile strength at operating temperature are:

	Stress relieved	Partly recrystallized
Yield strength $Rp_{0.2}$	320	250
Ultimate tensile strength Rm	400	340

Because of the heat input in the cladding during the welding process the region immediately adjacent to the welding zone shows a certain loss of strength. Therefore for this cladding condition, strength values for the fully recrystallized Zircaloy-4 tube are used conservatively.

It must be mentioned that calculating on the basis of specified values is conservative: the specified values are minimum values and due to irradiation the material undergoes a considerable increase of strength (Figure 2.2/12).

2.2.4.4 Creep

External overpressure causes compressive stresses in the cladding. Therefore it is forced to creep inward so that the diameters are reduced. This process depends on temperature and fast neutron flux.

Both influences are composed of a primary and a secondary term:

a) Thermally activated primary creep strain $\varepsilon_{p,th}$
b) Thermally activated secondary creep strain $\varepsilon_{s,th}$
c) Irradiation-induced primary creep strain $\varepsilon_{p,irr}$
d) Irradiation-induced secondary creep strain $\varepsilon_{s,irr}$

These components are superposed to get the total creep strain:

$$\varepsilon = \varepsilon_{p,th} + \varepsilon_{s,th} + \varepsilon_{p,irr} + \varepsilon_{s,irr}$$

Every component is a function of the secondary creep rate as:

$\varepsilon_p = C\dot{\varepsilon}_s (1 - \exp(k)/\bar{t})$
$\varepsilon_s = \dot{\varepsilon}_s \cdot t$

where:

C = strain-hardening constant of the material,
k = temperature function,
t = insertion time.

The secondary creep rate is

a) for thermally activated creep:

$$\dot{\varepsilon}_{s,th} = A_{th} \cdot \exp(K/\bar{T}_H)\, \tau^{1.87}$$

b) for irradiation-induced creep:

$$\dot{\varepsilon}_{s,irr} = A_{irr}\, \varphi^{0.85} \cdot \tau$$

where

A = creep constant;
τ = stress;
K = constant;
T_H = mean cladding temperature (absolute);
φ = fast neutron flux.

This creep model was described in [2.2-46]. It was calibrated with data from KWU measurements including post-irradiation examination results and with data from literature. Figure 2.2/13 shows a comparison between measured and calculated cladding tube outside diameter reductions.

2.2.4.5 Axial growth

Zircaloy-4 cladding tubes undergo axial growth during irradiation in the reactor.

This anisotropic growth effect is caused by neutron bombardment and is connected with the texture of the cladding tubes (differing accumulation of radiation-induced vacancies or interstitials on base surface of the hexagonal crystal lattice).

The axial growth of PWR cladding tubes is calculated with an exponential formula:

$$\Delta l/l = A \cdot (\Phi \cdot t)^n \quad (\%)$$

where:

$\emptyset \cdot t$= fast neutron fluences · 1.E-21
A,n = model constants

Figure 2.2/14 shows growth curves gained by experience.

2.2.4.6 External corrosion

The contact to the coolant causes an external corrosion of the fuel rod cladding tubes. Under PWR conditions the corrosion rate of Zircaloy-4 is governed by the metal/oxide interface temperature. It is enhanced by irradiation [2.2-5].

The corrosion layer starts growing proportionally to the cubic root of time. After a certain layer thickness is reached (transition point) a linear time dependency follows [2.2-6]:

Pre-transition: $(ds/dt)^3 = K_1^3 (-3\, T_{A1}/T_K)$

Post-transition: $ds/dt = F_I\, K_2 \exp(-T_{A2}/T_K)$

where:

s = cumulative corrosion layer thickness;
t = time;
K = corrosion constants;
T_A = Arrhenius temperatures (absolute);
T_K = interface temperature (absolute) metal/oxide;
F_I = irradiation factor.

Figure 2.2/15 shows KWU experience with oxide layers in PWRs.

Due to corrosion attack the thickness of the metallic cladding tube is reduced with increasing corrosion layer. As the corrosion products are less dense than the metal only about 2/3 of the layer thickness lie under the former metal surface.

Corrosion is caused by oxygen which was dissociated out of the coolant water. So free hydrogen remains which is absorbed by the cladding and forms hydrides [2.2-6]. Hydrogen content is calculated as follows [2.2-6]:

$$C_H = C_{H,o} + K \cdot \alpha \cdot s/h$$

where

$C_{H,o}$ = initial hydrogen in cladding tube wall;
K = constant;
α = hydrogen pick-up fraction;
s = corrosion layer thickness;
h = cladding wall thickness.

Figure 2.2/16 shows the development of the hydrogen pick-up fraction with growing corrosion layer thickness.

2.2.5 Thermal and mechanical design of a Th-Fuel rod

2.2.5.1 Th-CARO approach for $(Th,U)O_2$ fuel rods behaviour

The CARO-D Computer Code has been developed for the analysis of the fuel rod behaviour under the conditions of authorized operation. The code deals with the entire rod in its radial and axial extension. It is originally applicable to oxide pellet fuel (pure UO_2, mixed U/Pu oxide and fuel poisoned by neutron absorbers) enclosed in metallic cladding tubes for use in (light and heavy) water-moderated power reactors. In the frame of this program, the code has been adapted to handle $(Th,U)O_2$ fuel pellets.

Figure 2.2/17 shows a simplified flow chart of CARO-D.

Starting with the local coolant temperature, the radial temperature pattern is calculated by stepping opposite to the direction of radial heat flow.

Calculation of the temperature drop across the gap pellet/cladding takes into account thermal conductivity of the gas mixture, radial strains of the fuel and cladding tube, and gas extrapolation lengths at the solid/gas interface.

The calculated gas pressure depends on the individual temperatures in the free volumes, their dimensional changes, as well as the amount of fill gas and also of that which is released from the fuel in the course of exposure.

The code CARO-D comprises a set of interactive sub-models for handling the various mechanisms that determine fuel rod behaviour under inpile conditions. These are described in sections 2.2.3 and 2.2.4.

The adaptation of the CARO-D code (from the CARO-D5 version) resulted in the so-called Th-CARO version and included the $(Th,5\%U)O_2$ fuel pellets material properties as well as the interactive sub-models.

2.2.5.2 Th-CARO performance calculations for $(Th,5\%U)O_2$ test fuel rods

The Th-CARO version was verified against measured data from instrumented test fuel rods irradiated in the FRJ-2 research reactor in Juelich, Germany. These data can be grouped into temperature, fission gas release and dimensional changes.

Centreline temperatures

The model for fuel temperature calculation was calibrated against fuel rods equiped with temperature instrumentation. Figure 2.2/18 compares the fuel centreline temperatures calculated by Th-CARO version with those actually measured. The shown data cover linear heat generation rates up to 370 W/cm and burnups up to 9.6 MWd/(kg U+Th).

Fission gas release

The KWU fission gas release model for LWR fuel rods was applied to the $(Th,U)O_2$ test fuel rods without modifications. In Figure 2.2/19 the calculated values for fractional fission gas release are compared with the measured values for about 100 LWR fuel rods. The results of the figure comprise UO_2, $(U,Pu)O_2$ and $(Th,U)O_2$ fuel pellets.

Rod dimensional changes

The free volume in the fuel rod is calculated by the Th-CARO version as a result of dimensional changes in the fuel (densification and swelling) and in the cladding (creep and axial growth). Table 2.2.2 shows a comparison between the measured and calculated values for the inner free volume.

2.2.5.3 Design calculations for (Th,5%U)O_2 pathfinder test fuel rods

A test irradiation was designed for the Angra-1 reactor. Four segmented and one full-length fuel rod loaded with thorium based fuel pellets were designed to be inserted in a special carrier fuel assembly for up to four reactor cycles. Figures 2.2/20 and 2.2/21 show the test fuel rods. With exception of the length and the connection end pieces, there is no basic difference between a segment of the segmented fuel rod and a full-length fuel rod.
Table 2.2.3 shows a list of the individual calculations associated with each of the design limits to be complied with.

The codes used for the individual calculations are also shown in Table 2.2.3. The most important conservative assumptions in the calculations are explained in the parts dealing with the respective calculations.

Determination of power distributions

In the neutron physics calculations (section 2.1.3) two different positions to insert the special carrier fuel assembly were considered. For these design calculations the positions in reactor core that result in a lower power in the last two cycles were taken, because in this case a lower amount of fission products should be released. A more uniform power over all the dwell time is resulted in this case, too.

For the segmented rods, only the segment exposed to the highest load was considered.

The result of the maximum local linear power for the test fuel rods is shown in Figure 2.2/22 for the four reactor cycles.

Two kinds of calculations were performed: beginning-of-life calculations (BOL) and long-term calculations (referred in the following as end-of-life, EOL, too).

Beginning-of-Life calculations (BOL calculations)

The BOL calculations were performed by means of the CARO-D computer code to demonstrate that under conditions of authorized operation the fuel will not melt and the cladding tube will not be tangentially strained beyond the design limit. For this purpose, various conservative input data records were used for each calculation, the most important assumptions of which are shown below:

Data batch	1	2
Cladding tube diameter	max.	min.
Pellet diameter	min.	max.
Rod free gas volume	min.	max.
Fuel density	min.	min.
Fill gas pressure	max.	min.
Helium absorption*	–	max.
Fission gas release*	max.	min.
Fuel densification	max.	min.
Fuel swelling*	min.	max.
Cladding creepdown*	min.	max.
Radial relocation	min.	max.

* These models are inoperative at BOL.

Data batch 1 yields the maximum fuel rod centre temperature and data batch 2 yields the maximum interaction between fuel and cladding tube.

Maximum fuel temperature

The fuel centre temperatures and the temperature profile in the pellet calculated conservatively with data batch 1 on the basis of the maximum linear heat generation rate at BOL are shown in Figures 2.2/23 and 2.2/24 as a function of the local linear power.

The worst case for pellet-cladding tube interaction calculated conservatively with data batch 2 on the basis of the maximum linear heat generation rate is shown in Figure 2.2/25.

No pellet-cladding tube interaction is expected.

End-of-Life calculations (EOL calculations)

For the calculation of the long-term behaviour of the fuel rods, the same conservative combinations of the input data for CARO-D were used.

Data batch 1 yields the highest fission gas release and maximum rod internal gas pressure. Data batch 2 yields the maximum interaction between cladding tube and fuel. Here, however, fission gas release is minimal, the highest rod internal pressure is also minimal. An overload factor in case of data batch 1 is taken into account as a safety margin.

Figures 2.2/26 and 2.2/27 show the highest fission gas release and the highest rod inner pressure, respectively, from batch 1. The fuel rod centre temperatures resulting from data batch 1 are shown in Figure 2.2/28.

The interaction between fuel pellets and cladding tube in the radial direction calculated with data batch 2 is shown in Figure 2.2/29 for the segment with the highest load.

The total expansion of the fuel is obtained from the sum of the thermal expansion and the changes in diameter due to densification and swelling.

The total expansion of the cladding is obtained from the sum of the creep induced de-

formation, thermal expansion, compressive strain and diametral cold as-filled clearance.

The determination of the axial strain in the cladding tube is based on the assumptions that the cladding is forced to expand in the axial direction by the expanding fuel proceeding from the point of hard contact. In addition, the irradiation-induced axial growth of the cladding tube, which reduces the plastic strain in the axial direction is taken into consideration from the time when the hard contact is reached. The individual strains in the axial direction are shown in Figure 2.2/30.

For $\varepsilon_{a,pl}$ the following applies:

$$\varepsilon_{a,pl} = \varepsilon_{a,tot} - \varepsilon_{a,irr} - \varepsilon_{a,el}$$

where

$\varepsilon_{a,pl}$ = axial plastic strain;
$\varepsilon_{a,tot}$ = total axial strain;
$\varepsilon_{a,Irr}$ = irradiation-induced axial growth;
$\varepsilon_{a,el}$ = axial elastic strain components.

The equivalent plastic strain $\varepsilon_{e,pl}$ is calculated from the plastic strains in the axial and tangential directions according to the following equation:

$$\varepsilon_{e,pl} = \frac{2}{\sqrt{3}} \sqrt{\varepsilon_{a,pl}^2 + \varepsilon_{t,pl}^2 + \varepsilon_{a,pl} \cdot \varepsilon_{t,pl}}$$

According to these results the warm pellet-cladding diametral clearance should increase after about 1,000 days of irradiation time. As a consequence an excessive increase of the fuel centre temperature and rod inner pressure were calculated (Figures 2.2/28 and 2.2/27).

These calculations were based on results of test irradiations in the research reactor FRJ-2 at KFA Juelich. Only burnups up to 9.6 MWd/kgHM were achieved in these irradiations. The fuel design parameter set concerning densification, swelling, fission gas release and relocation were obtained from the performance calculations as described in section 2.2.5.2. In the design calculations the validity of these parameter sets was extrapolated to up about 60 MWd/kgHM. Data on the fuel performance at high burnups are necessary to support the conclusions of these design calculations. Additionally, results from best-estimate calculations of temperatures, fission gas release and internal pressures have been included in Figures 2.2/26 to 2.2/28.

Stress Analysis

Steady-State Stresses

The stress analysis calculations were performed by means of the SPAN program. Two cases were investigated:
a) fuel rod with the highest cladding tube temperature;
b) reactor at hot standby.

The calculations were performed conservatively for the beginning of life when the pressure difference at the cladding is at its maximum and strength has not yet increased by neutron irradiation.

The external and internal cladding tube temperatures and the fuel rod internal pressure obtained from the Th-CARO calculations were used in the determination of the stresses.

These calculations showed that the pressures developed in the cladding tube are securely below the design limits.

Cyclic Stresses

The maximum cyclic bending stress calculated by means of the SPAN program showed that there is a very wide safety margin, especially since the stresses have been calculated conservatively.

2.2.6 Conclusions

The fuel rod design studies on Th/U based fuel rods have provided the following results:

a) a material properties database worked out from the open literature and data collected from own measurements made on ex-gel-C-(Th,5%U)O_2 fuel pellets,

b) a model for a fuel pellet, adapted from the available Siemens UB KWU model for UO_2 fuel pellets with data obtained from the open literature and from in-pile and post-irradiation examination in the Jülich FRJ-2 research reactor,

c) a computer code for fuel rod design and performance prediction, validated with irradiation testing of ex-gel-C-(Th,5%U)O_2 fuel rods in the FRJ-2 reactor.

The design analysis of ex-gel-C(Th,U)O_2 test fuel rods could be safely introduced in a pressurized water power reactor for a pathfinder irradiation test.

References

[2.2-1] ANSI/ANS-57.5-1981 American National Standard for Light Water Reactors Fuel Assembly Mechanical Design and Evaluation

[2.2-2] A. S. Bain
Post Irradiation Structures in UO_2 Quenched or Slowly Cooled from the Melt. AECL – 2587

[2.2-3] GEAP – 3771
High Performance Program of GE (Series of numerous separate reports)

[2.2-4] NUREG – 0800
Standard Review Plan for the Review of Safety Analysis Reports for Nuclear Power Plants
U.S. Nuclear Regulatory Commission, July 1981

[2.2-5] H. Stehle, W. Kaden, R. Manzel
External Corrosion of Cladding in PWR's Nuclear Engineering and Design, 33 (1975), p. 155

[2.2-6] H. Stehle et. al.
Factors Contributing to the In-Reactor Waterside Corrosion of Zircaloy
6th International Conference on Zirconium in the Nuclear Industry, Vancouver, June 1982

[2.2-7] W.J. O'Donnell, B. F. Langer
Fatigue Design Basis for Zircaloy Components Nuclear Science and Engineering, 20,p.1-12 (1964)

[2.2-8] J. Belle and R.M. Berman
„The High-Temperature ex-Reactor Thermal Conductivity of Thoria and Thoria- Urania Solid Solutions (LWBR/AWBA Development Program)".
WAPD-TM-1530, Dec./1982

[2.2-9] H.F. Schmidt
„Some Considerations of the Thermal Conductivity of Stoichiometric Uranium Dioxide at High Temperatures".
J. Nucl. Mater., 78:225-227, 1978.

[2.2-10] M. Murabayashi
„Thermal Conductivity of Ceramic Solid Solutions".
J. Nucl. Sci. Tech. 7(11):559-563, Nov./1970

[2.2-11] M.Murabayashi et al.
„Thermal Conductivity of ThO_2-UO_2 System".
J. Nucl.Sci.Tech. 6(3): 128-131, March/1969

[2.2-12] J.C. Weilbacher
„Thermal Diffusivity of Uranium Oxide and Thorium Oxide at High Temperature"
High Temperatures High Pressures, 4:431-438 (1972)
„Thermal Diffusivity Measurements of Mixed Oxides of Uranium and Plutonium"
CEA-R-4572, 1974.

[2.2-13] R.M.Berman et al.
The Thermal Conductivity of Polycrystalline Thoria-Urania Solid Solutions: (LWBR- Development Program).
WAPD-TM-908,Dec./1972

[2.2-14] W.D. Kingery. In: Y.S. Touloukion (ed.):
„Thermophysical Properties of Matter"
vol.2: "Thermal Conductivity Nonmetallics Solids"
p.415 , IFI/PLENUM, 1970.

[2.2-15] C.Ferro et al.
„Thermal Properties of Ceramic Materials", paper presented at the Italian-Polish Meeting, Warsaw, May-Jun./1970, RT/ING (70) 23

[2.2-16] G.P. Marino
„Porosity Correction Factor for the Thermal Conductivity of Porous Materials"
WAPD-TM- 807, 1970

[2.2-17] D.A. Himes
„Thermal Conductivity Model for $(Th,U)O_2$ to Melting"
in: Fuels and Materials Performance, Trans. Am. Nucl. Soc., 30:174-175, 1978

[2.2-18] S. Peterson C.E. Curtis
„Thorium Ceramics Data"
Manual. ORNL-4503, vol.1, 1970

[2.2-19] D.F. Fischer et al.
„Enthalpy of Thorium Dioxide to 3400 K"
J. Nucl. Mat. 102:220-222, 1981

[2.2-20] D.F. Fischer et al.
„Enthalpies of Thoria-Urania from 2300 to 3400 K"
J. Nucl. Mat. 118:342-348, 1983

[2.2-21] J.R. Springer et al.
„Fabrication, Characterization and Thermal-Property Measurements of ThO_2-UO_2 Fuel Materials"
BMI-X-10210, oct./1967.

[2.2-22] P.T.B. Shaffer
„Oxides"
In: Plenum Press Hand-Books of High-Temperature Materials N.1
New York, Plenum Press, 1963, P. 308-387

[2.2-23] K. Hirata et al.
„High Temperature Thermal Expansion of ThO_2, MgO and Y_2O_3 by X-ray Diffraction"
in: Journal of Mat. Science, 12 : 838-839, 1977. Letters.

[2.2-24] O.J.Whitemore N.N. Ault.
„Thermal Expansion of Various Ceramic Materials to 1500°C"
In: Journal of the American Ceramic Society, 39 (12) : 443-444

[2.2-25] C.P. Kempter R.O. Elliot
„Thermal Expansion of (UN), (UO_2), (ThO_2, UO_2) and (ThO_2)"
The Jornal of Chemical Physics, 30 (6) : 1524-1526, Jun, 1959.

[2.2-26] B. Ohnysty F.K. Rose
„Thermal Measurements on Thoria and Hafnia to 4500°F"
In: Journal of the American Ceramic Society,47 (8): 398-400, August, 1964.

[2.2-27] L.R. Weissert G. Schileo
„Fabrication of Thorium Fuel Elements"
Published by American Nuclear Society, 1968, p.33

[2.2-28] R.E. Latta et al.
Solidus and Liquidus Temperatures in the UO_2-ThO_2 Systems
J. Nucl. Mat., 35: 347-349, 1970.

[2.2-29] R.E. Latta R.E. Fryxell
„Determination of Solidus- Liquidus Temperatures in the UO_2+x System ($-0.50 < x < 0.20$)"
J. Nucl. Mat. 35: 195-210, 1970.

[2.2-30] K. Benz
„Thorium-Thorium Dioxide Phase Equilibria"
J. Nucl. Mat. 29: 43-49, 1969.

[2.2-31] W.A. Lambertson et al.
„Uranium Oxide Phase Equilibrium Systems : IV, UO_2-ThO_2"
J. Am. Ceram, Soc. 36: 397-99, 1953.

[2.2-32] J.A. Christensen
„UO_2-ThO_2 Phase Studies"
Quart. Progr. Rept. Research and Development Programs, HW- 76559, pp. 11.5-6, May/1963.

[2.2-33] M.H. Rand
„I. Thermochemical Properties"
In: Thorium: Physical-Chemical Properties of its Compounds and Alloys, ed. O. Kubaschewski, IAEA, Vienna, vol. 13, Special Issue No. 5, 1975.

[2.2-34] E-an Zen
„Validity of Vegard's Law",
Am Mineral., 41(5/6): 523-24,1956.

[2.2-35] I. Cohen R.M. Berman
„A Metallographic and X-ray Study of the Limits of Oxygen Solubility in the UO_2-ThO_2 System"
J. Nucl. Mat. 18: 77-107, 1966.

[2.2-36] H. Assmann & H. Stehle
„Thermal and In-Reactor Densification of UO_2: Mechanisms and Experimental Results"
Nucl. Eng. Des. , 48(1): 49-67, June 1978.

[2.2-37] S.A. Rabin et al.
„Irradiation Behavior of High Burnup ThO_2-4.45% UO_2 Fuel Rods."
Tennessee, U.S., Oak Ridge National Lab., Oct./1965 (ORNL-3837).

[2.2-38] L. A. Walton J.E. Matheson
„FUMAC" A New Model for Light Water Reactor Fuel Relocation and Pellet-Cladding Interaction.
Nuclear. Techn. , 64, 127-138, 1984.

[2.2-39] H. Devold
„Comparison of ThO_2 and UO_2 Mixed Oxide Fuels"
OECD Halden Reactor Project.

[2.2-40] I.Goldberg et al.
„Fission Gas Release from ThO_2 and ThO_2-UO_2 Fuels" (LWBR Development Program).
WAPD-1350, Aug./1978

[2.2-41] I.Goldberg et al.
„Fission Gas Release and Grain Growth in ThO_2-UO_2 Fuel Irradiated at High Temperature" (LWBR Development Programm)
WAPD-TM-1350 Addendum, Jul/1979

[2.2-42] I. Goldberg et al.
„Fission Gas Release from High-Burnup ThO_2 and ThO_2-UO_2 Fuels Irradiated at Low Temperature"
(LWBR/AWBA Development Program).
WAPD-TM-1350 Addendum 2, may/1982.

[2.2-43] L.A. Neimark
„Recrystalization of ThO_2-UO_2 During Irradiation"
Trans. Amer. Nucl. Soc., 5 (1): 226-228,1962.

[2.2-44] M. S. Dias,
„Producao e liberacao de gases de fissao em varetas combustiveis a base de (Th,U)O_2"
Anexo B, Dissertacao mestrado, EEUFMG,CCTN, Belo Horizonte, junho de 1982.

[2.2-45] „Irradiation performance of thoria-urania fuel materials"
Quarterly technical report no. 1, May/Sep.,1964 (TID 4500)

[2.2-46] G. Senski & A. Kunick
„A Phenomenological Thermal and Irradiation Creep Model for Zircaloy"
5th. International Conference on Structural Mechanics in Reactor Technology, Berlin, August, 1979, paper C3/3.

Table 2.2.1: Radius/length ratios of cylindrical pellets used for thermal diffusivity measurement by the laser flash method.

Probe	(%TD)	0 (mm)	1 (mm)	r/l
A	94.91	9.42	6.73	0.700
B	95.05	9.503	8.265	0.575

Table 2.2.2: Comparison of measured and calculated free volume at end-of-life

Fuel Rod	Measured (cm^3)	Calculated (cm^3)
TT80	2.22 ± 0.06	2.05
TDT81	2.21 ± 0.04	2.01
TT82	$2.13 + 0.04 - 0.06$	2.04
TDT83	$2.19 + 0.06 - 0.04$	1.97
TDT85	2.15 ± 0.09	1.98

Table 2.2.3: List of individual calculations

Design calculation	Data Batch	Computer Code
Beginning-of-life (BOL)	1	Th-CARD-D
Beginning-of-life (BOL)	2	Th-CARD-D
End-of-life (EOL)	1	Th-CARD-D
End-of-life (EOL)	2	Th-CARD-D
Stress analysis	–	SPAN
Elastic buckling	–	–
Plastic deformation	–	–

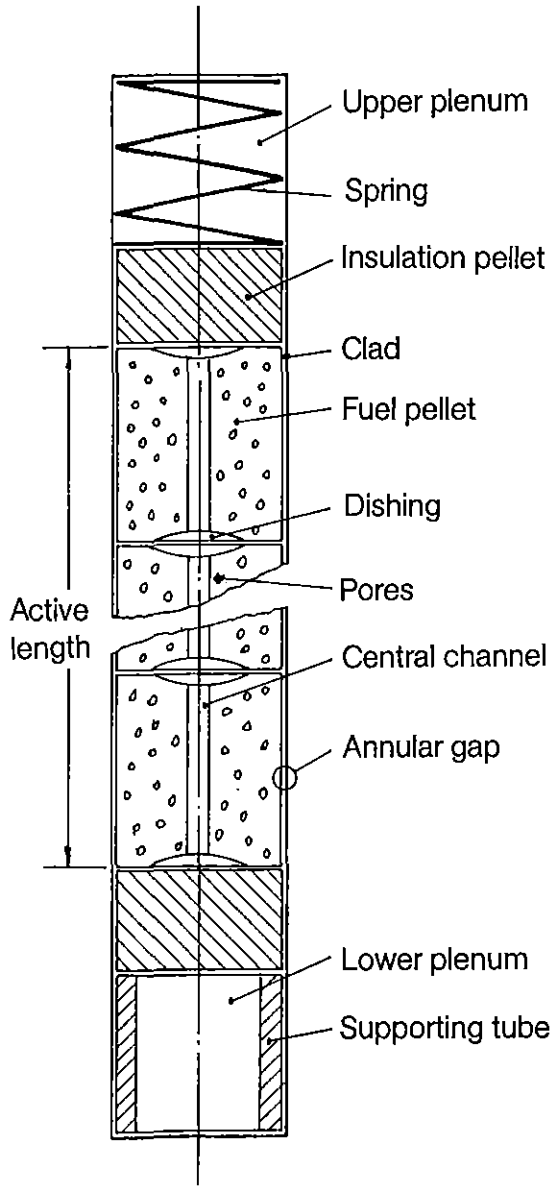

Fig. 2.2/1: Schematic Diagram of the Fuel Rod

D_0 pellet diameter
H_0 pellet height
D_I diameter of central channel
V_D dishing volume
R_D dishing radius

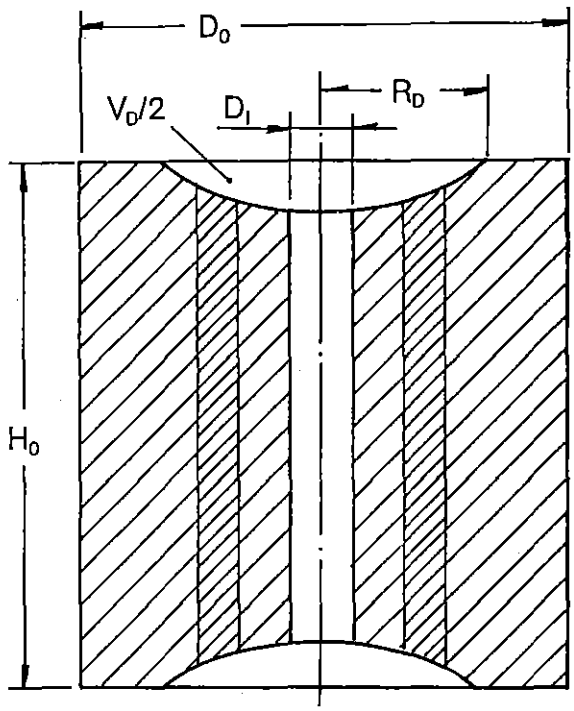

Fig. 2.2/2: Fuel Pellet Sketch

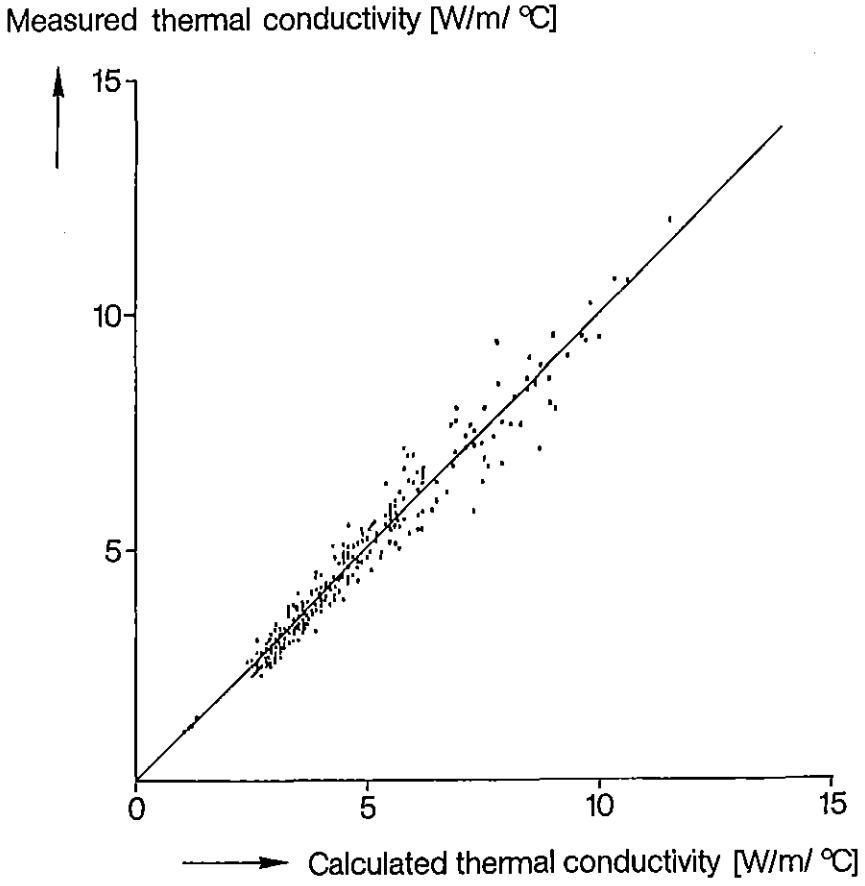

Fig. 2.2/3: Measured Versus Calculated Thermal Conductivity of $(Th,U)O_2$

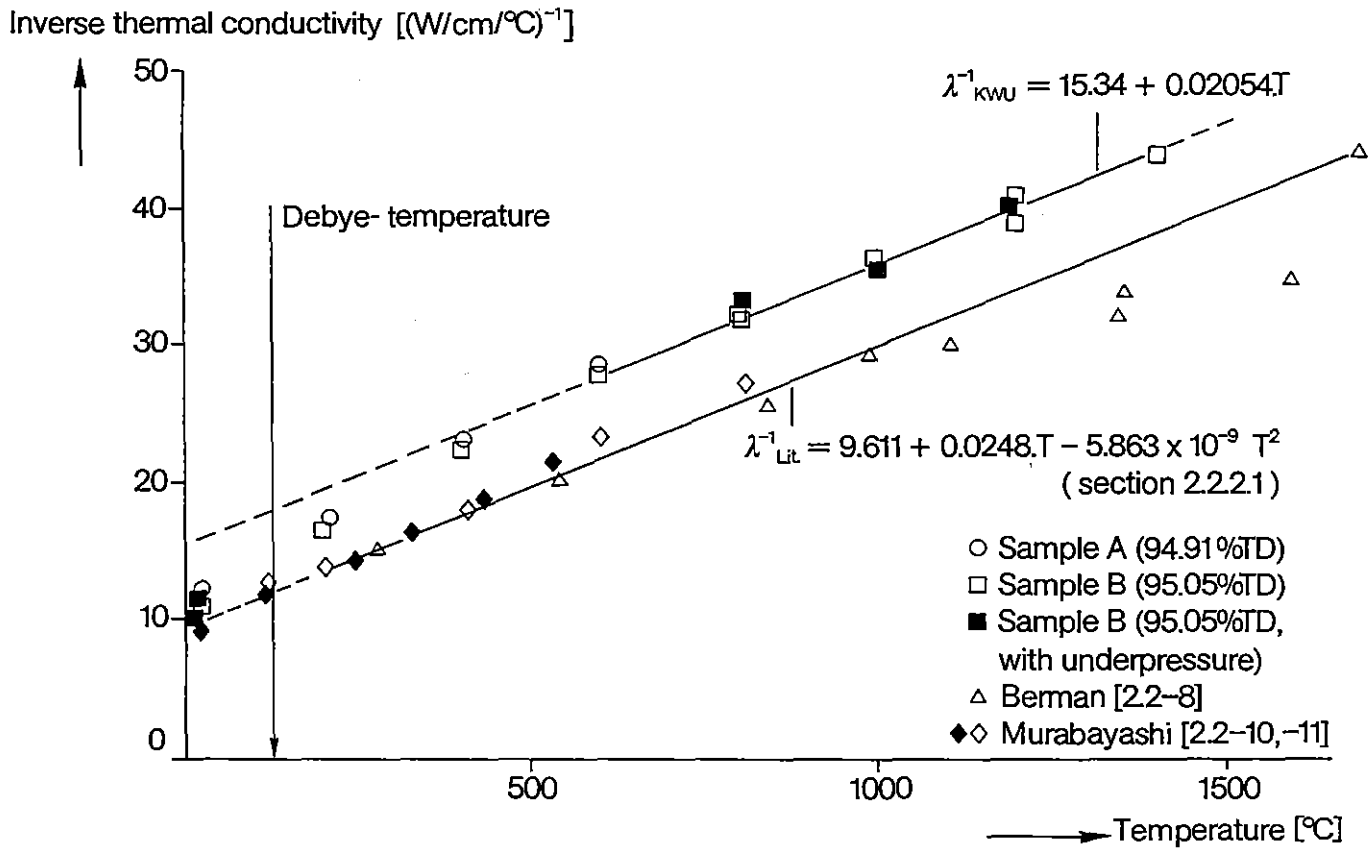

Fig. 2.2/4: Comparison of Thermal Conductivity of (Th,5% U)O_2 Samples

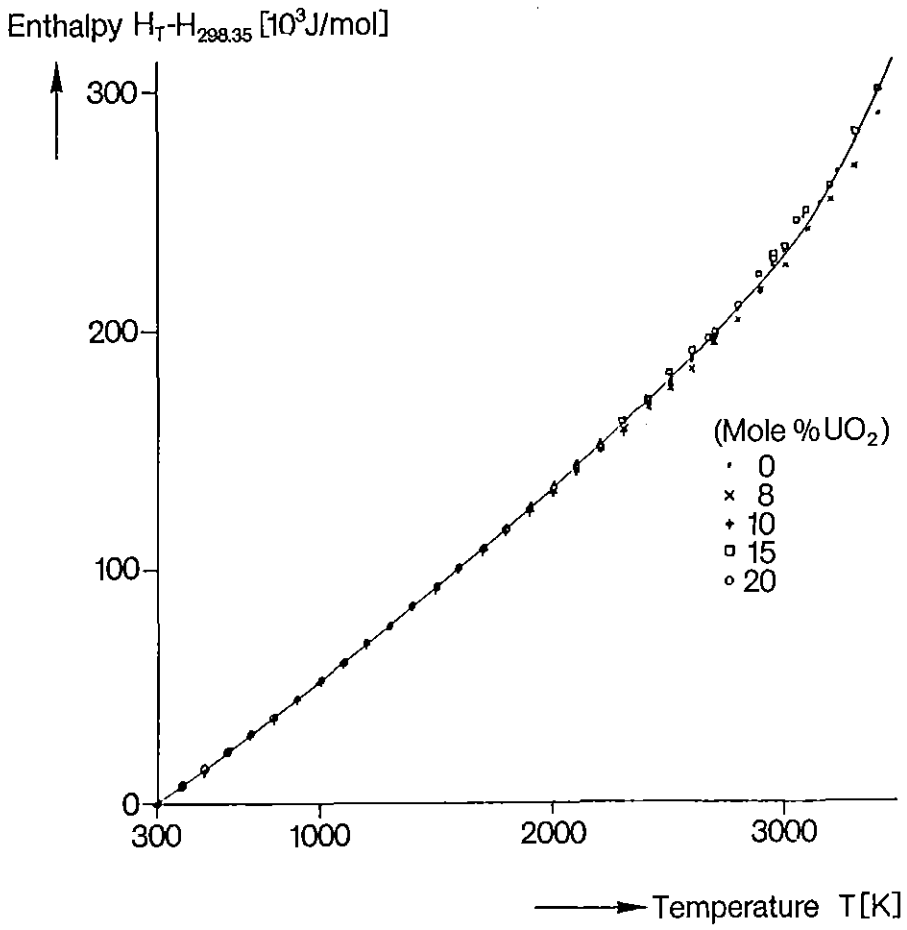

Fig. 2.2:5: Enthalpy of (Th,U)O_2 Solid Solution

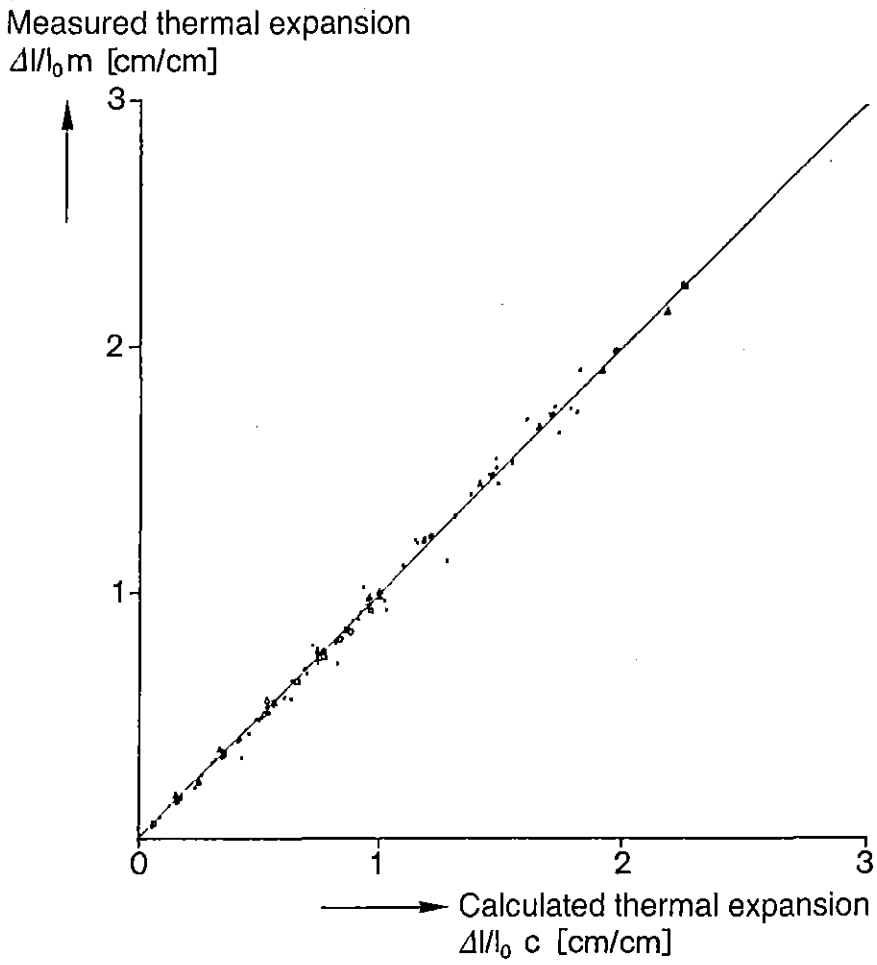

Fig. 2.2/6: Measured Versus Calculated Thermal Expansion of $(Th,U)O_2$

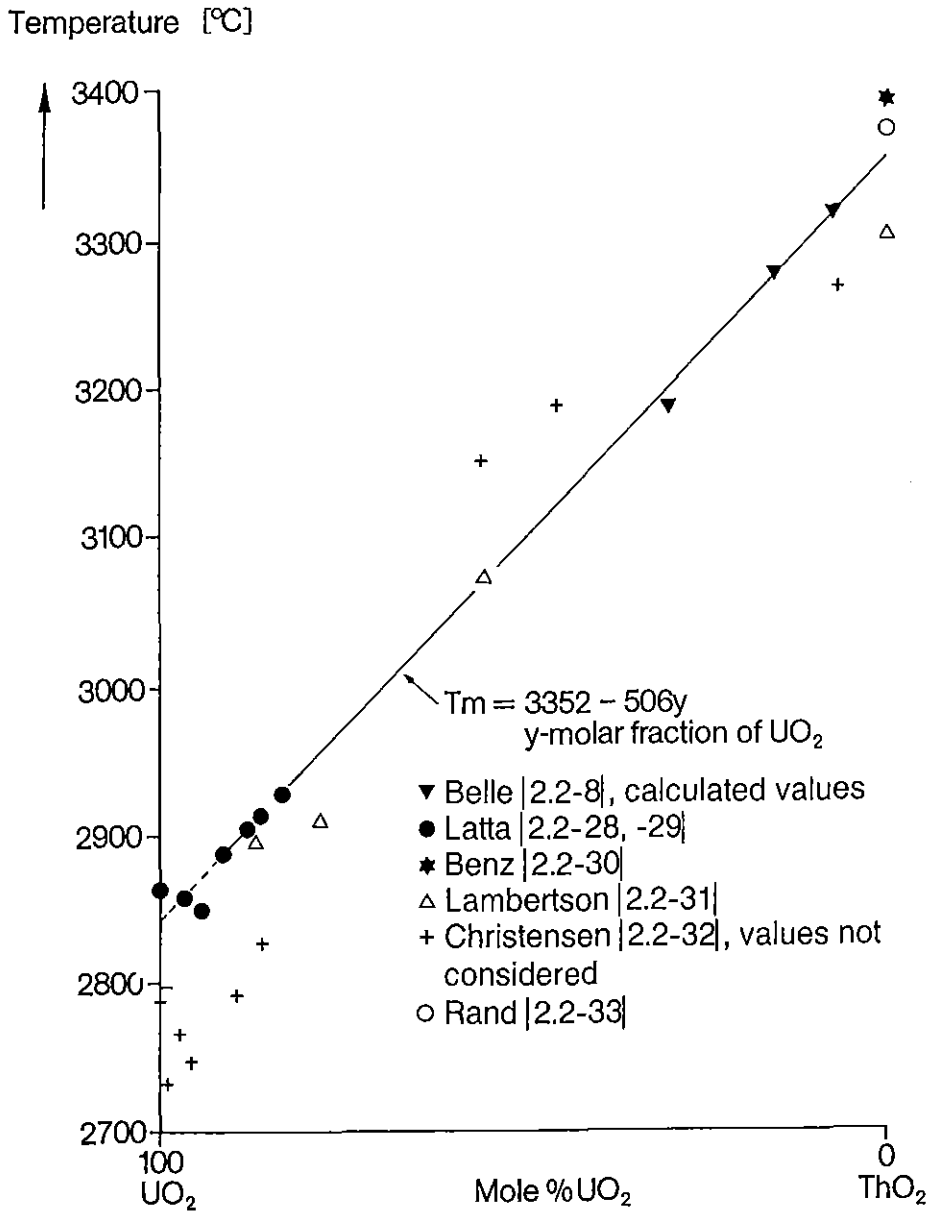

Fig. 2.2/7: Melting Point of Thorie-Urania Solid Solutions

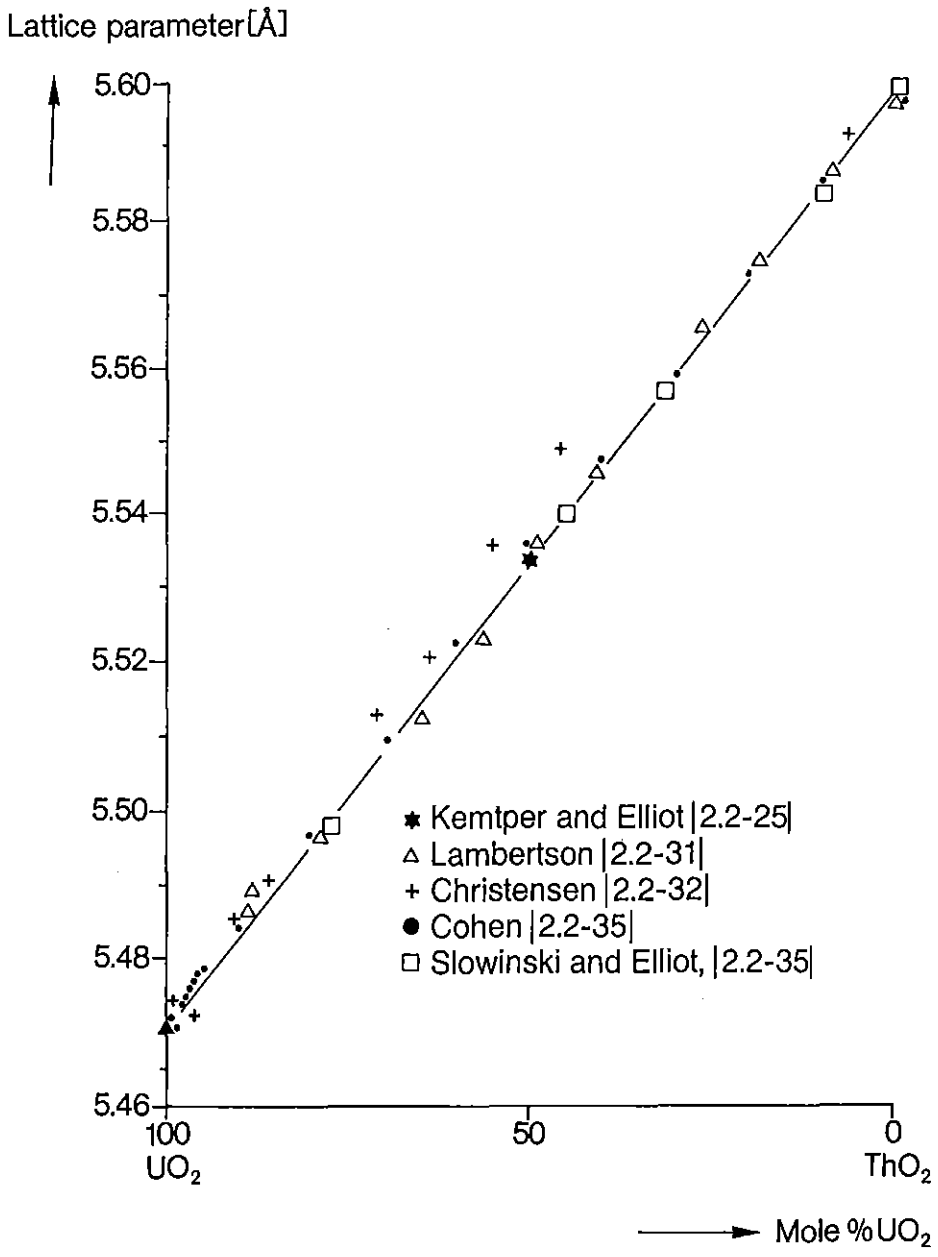

Fig. 2.2/8: Lattice Parameter of $(Th,U)O_2$ Solid Solutions

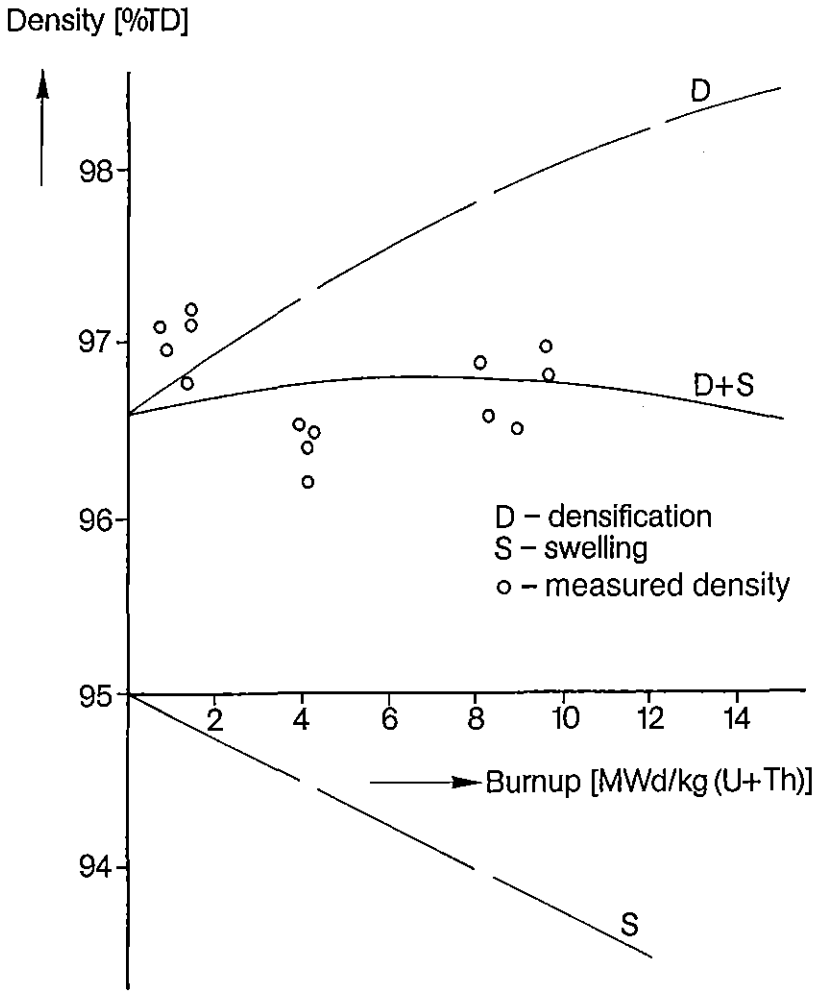

Fig. 2.2/9: Density Evolution of the (Th,U)O_2-Fuel During Irradiation

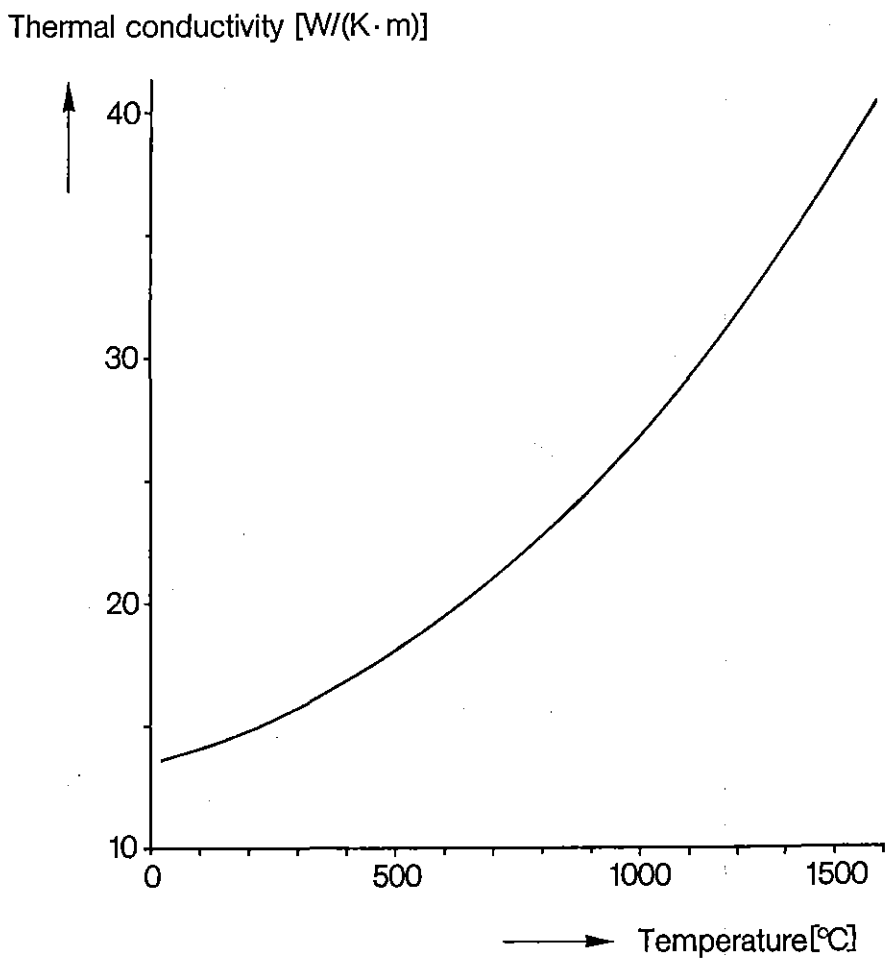

Fig. 2.2/10: Thermal Conductivity of the Zircaloy-4 Cladding Tube Material Versus Temperature

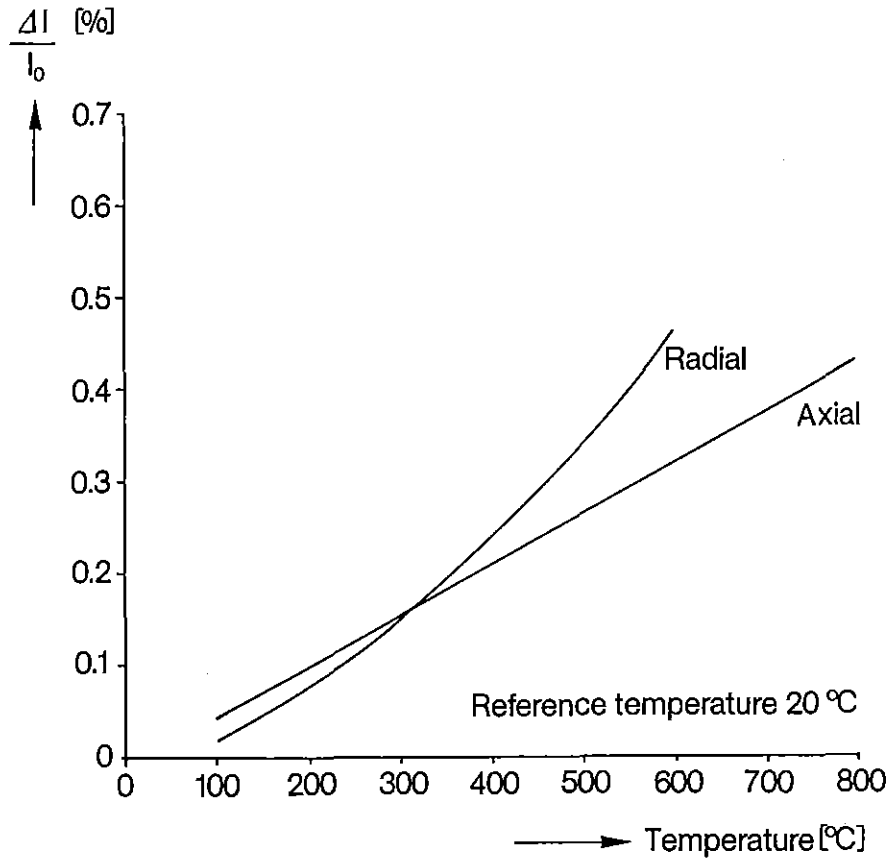

Fig. 2.2/11: Thermal Expansion of the Zircaloy-4 Cladding Tube Material

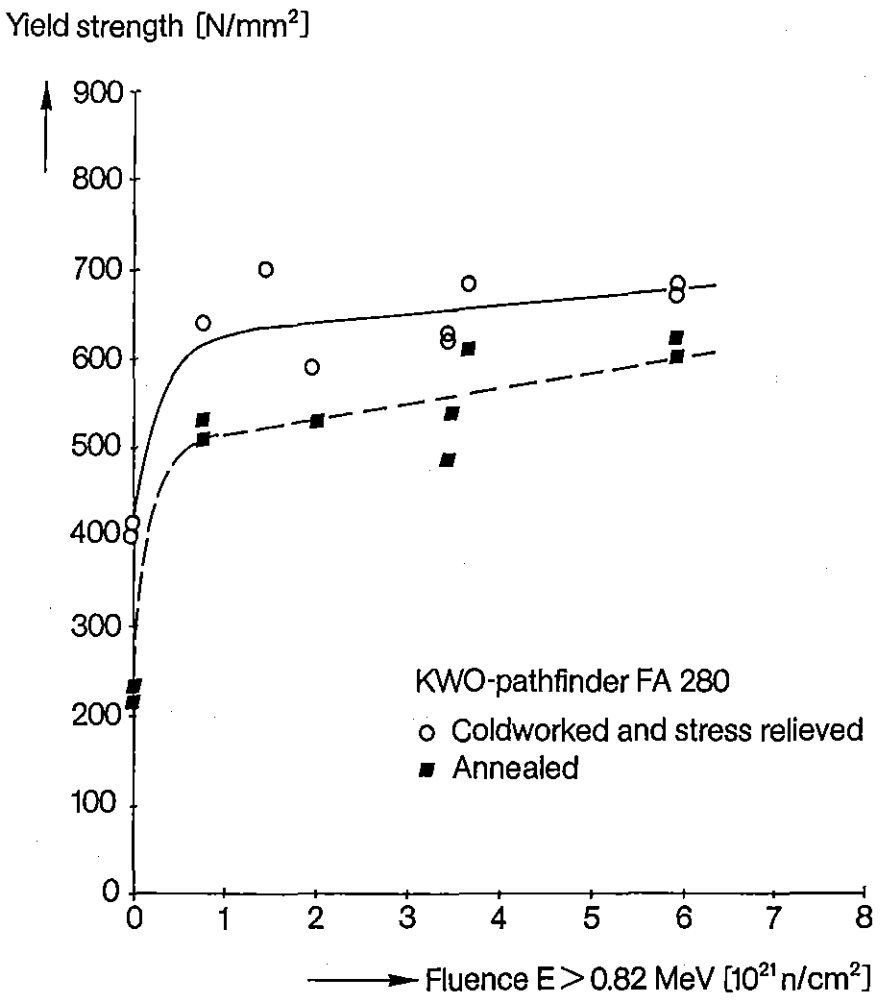

Fig. 2.2/12: Yield Strength of Zircaloy-4 Cladding

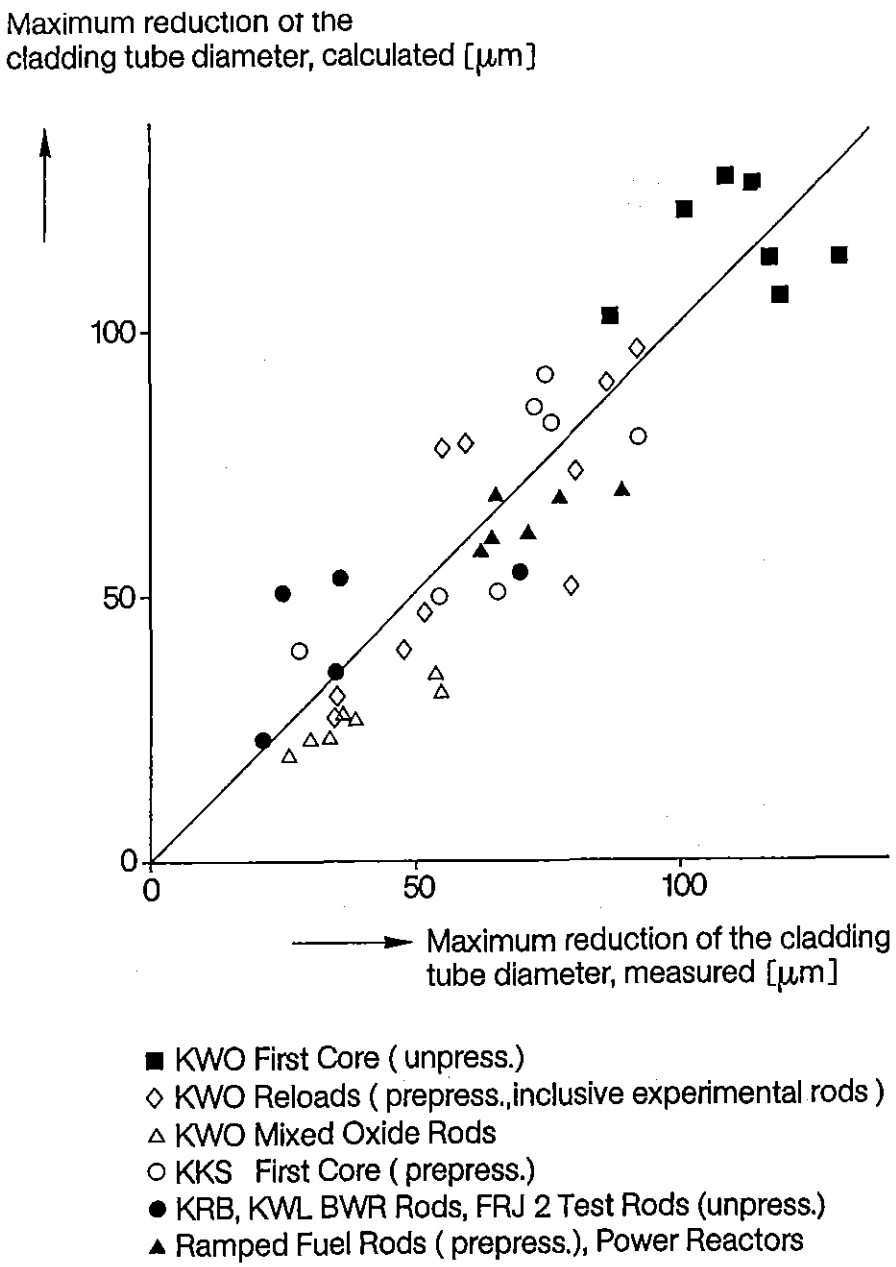

Fig. 2.2/13: Maximum Reduction of the Cladding Tube Outside Diameter, Measured Versus Calculated With CARO-D (Best Estimate Values)

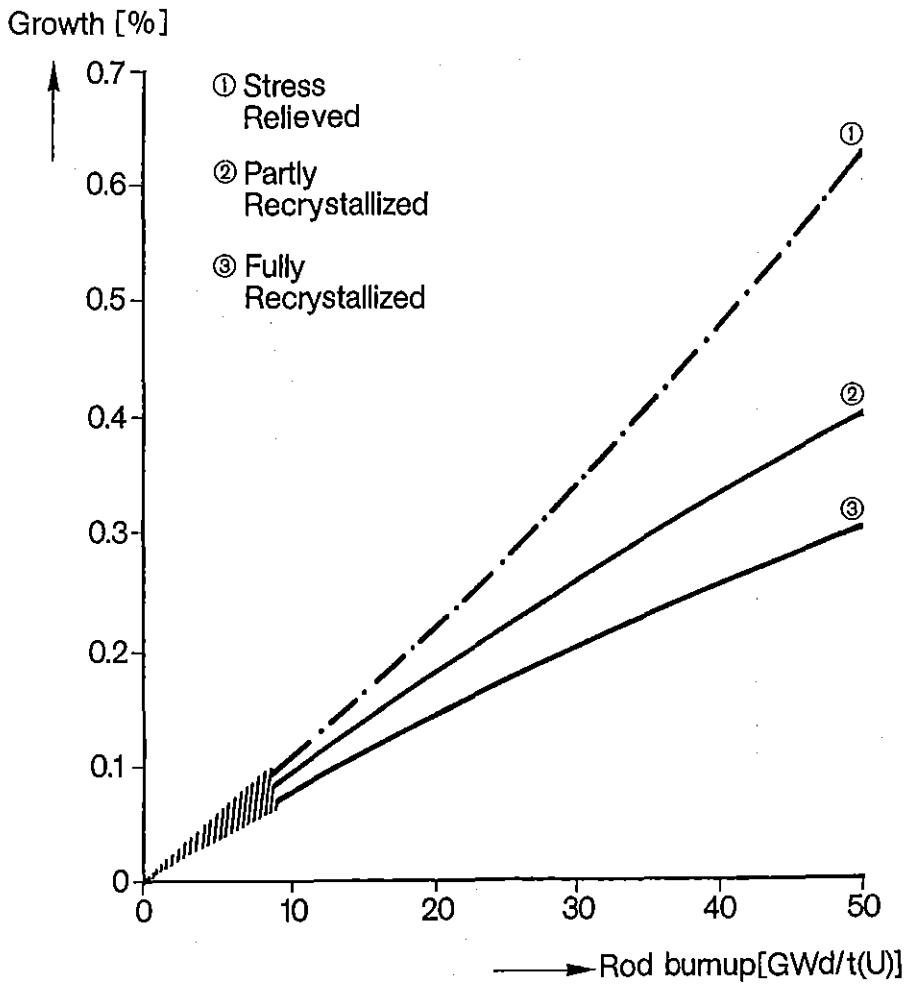

Fig. 2.2/14: Irradiation Growth of Fuel Rod Cladding of Different Degrees of Recrystallization

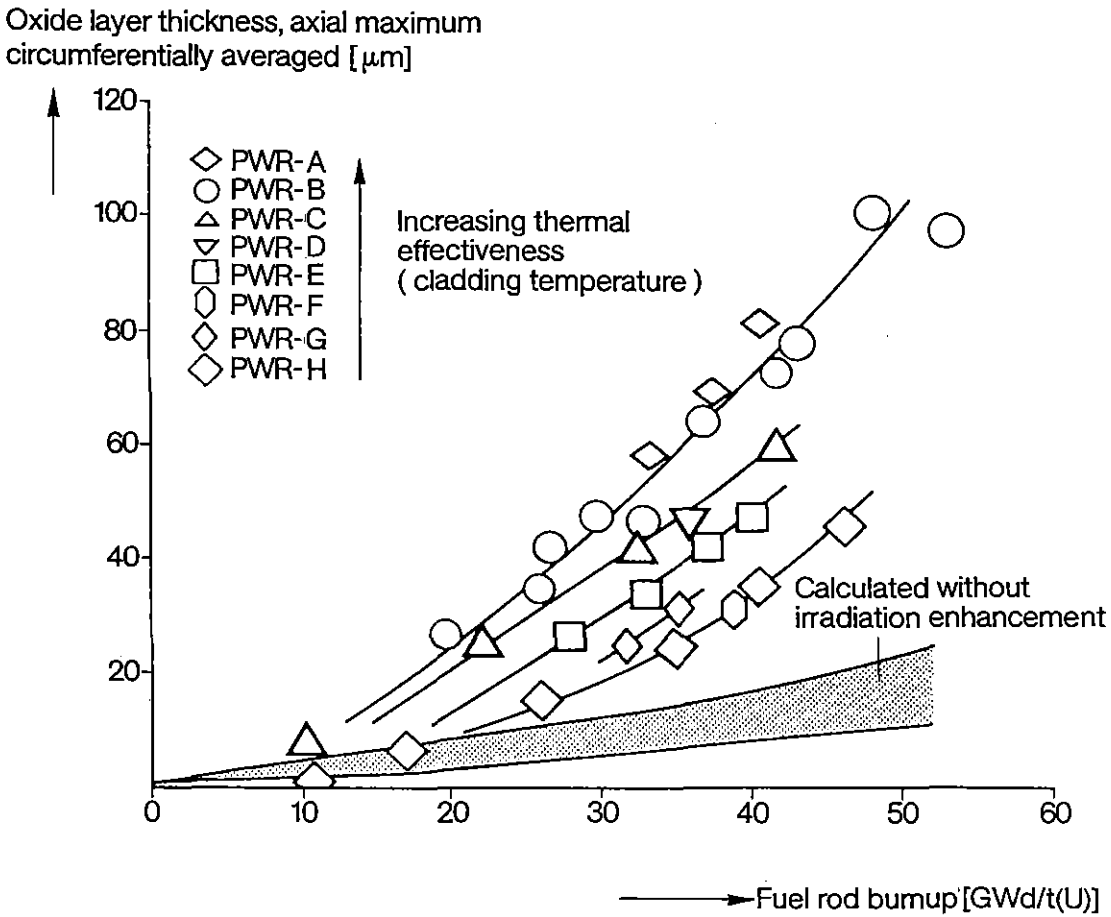

Fig. 2.2/15: Oxide Layer Thickness on PWR Fuel Rods With Comparable Power History

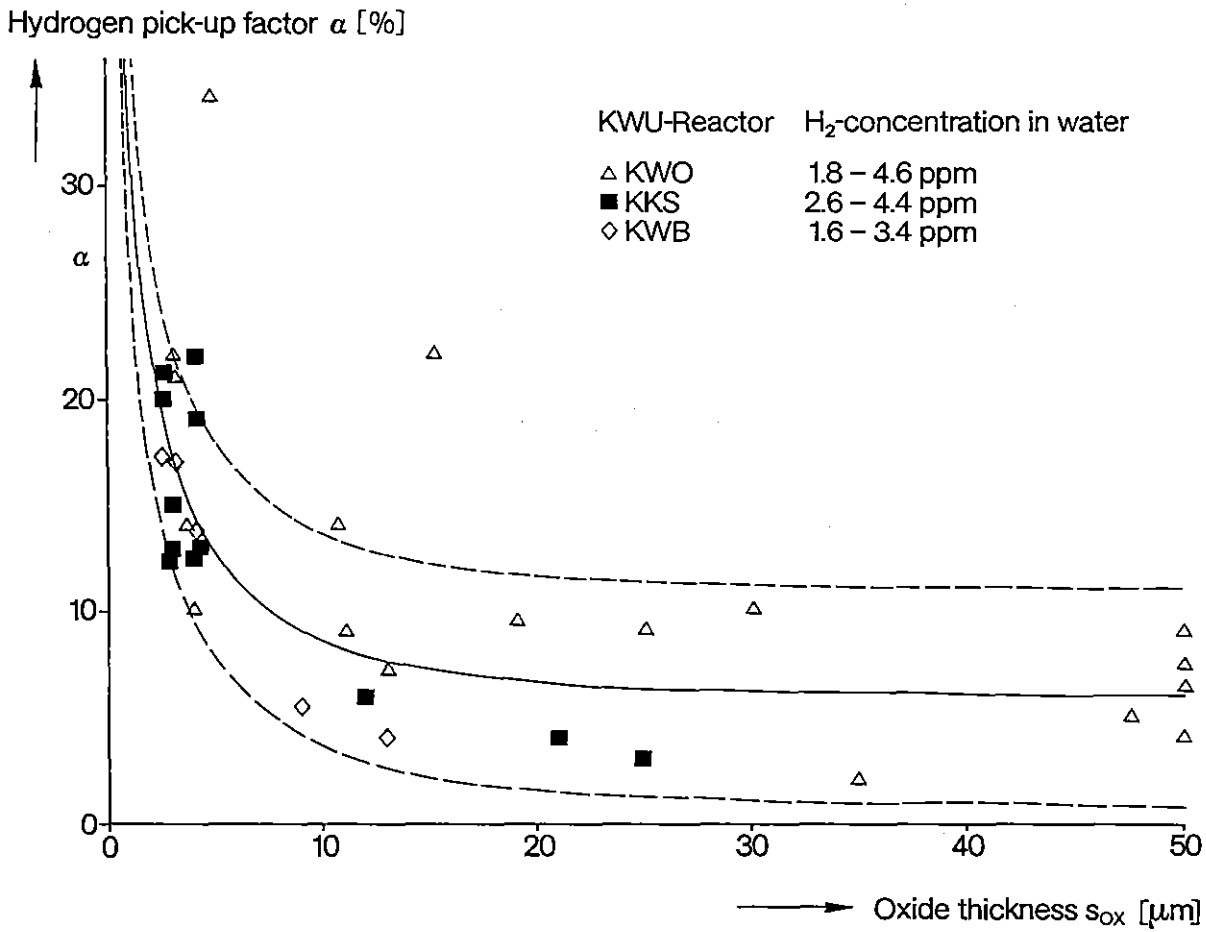

Fig. 2.2/16: Hydrogen Pick-up Versus Oxide Thickness for KWU-PWR-Fuel Rod Cladding

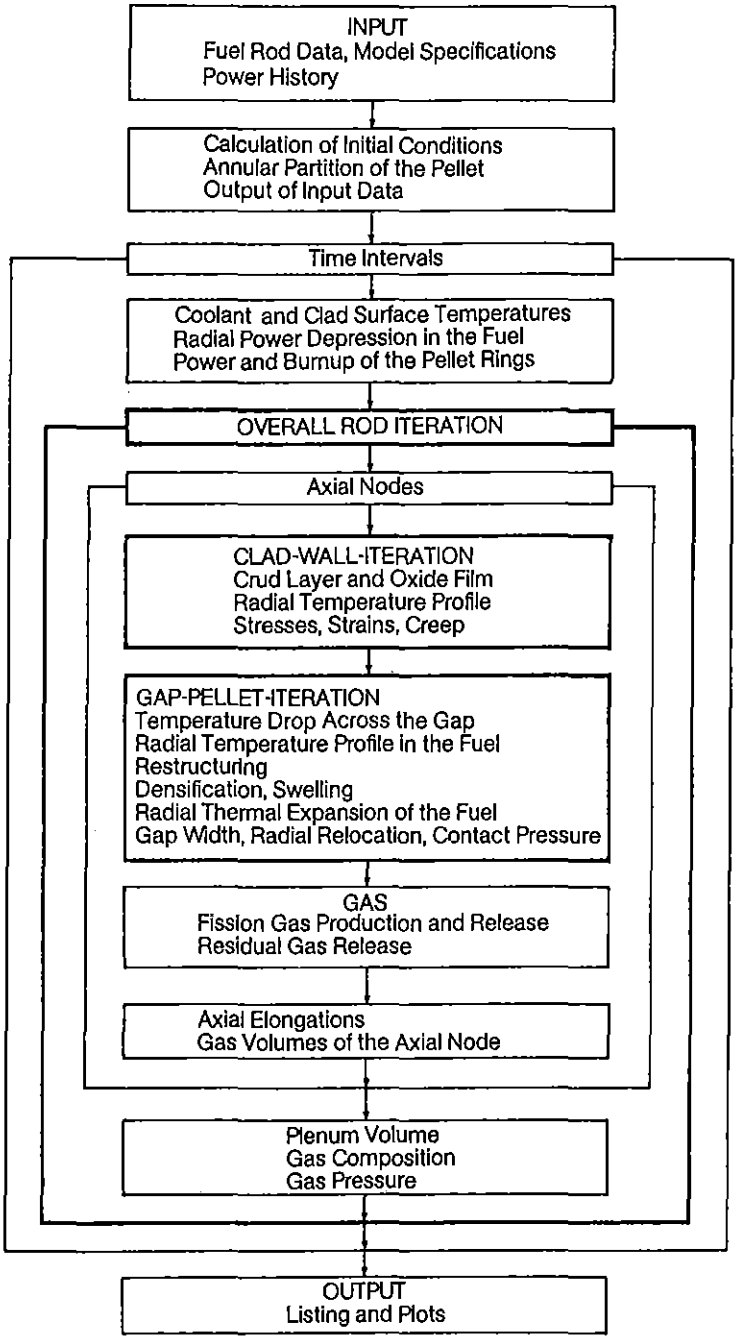

Fig. 2.2/17: Program Flow of CARO-D

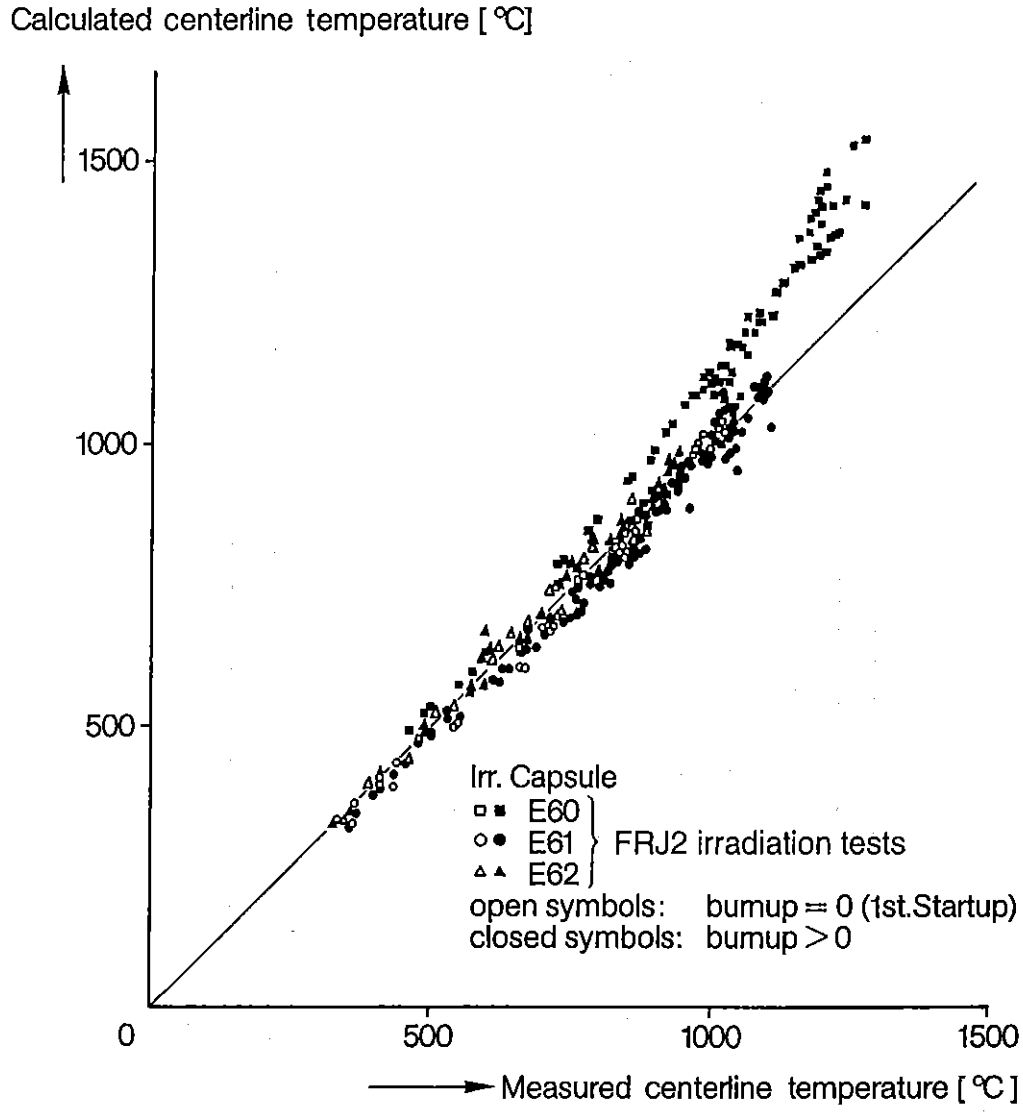

Fig. 2.2/18: Centerline Temperature, Calculated Versus Measured Values

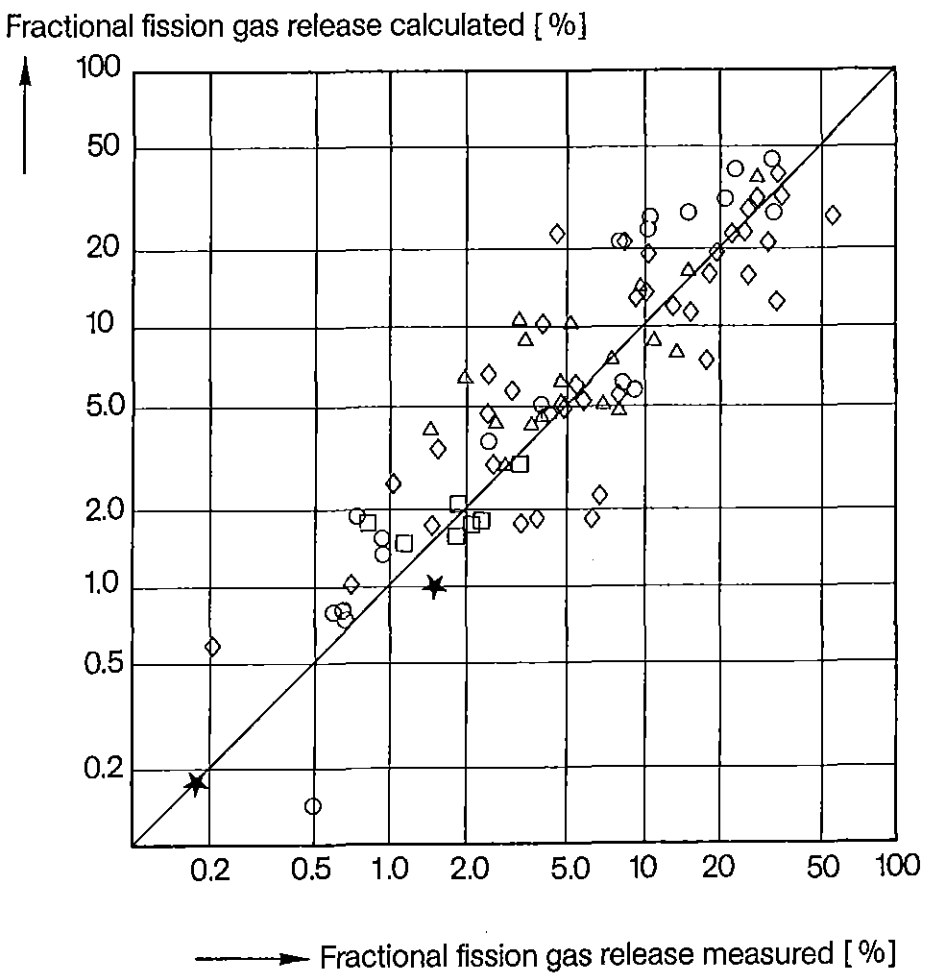

Fig. 2.2/19: Fission Gas Release, Calculated Versus Measured Values

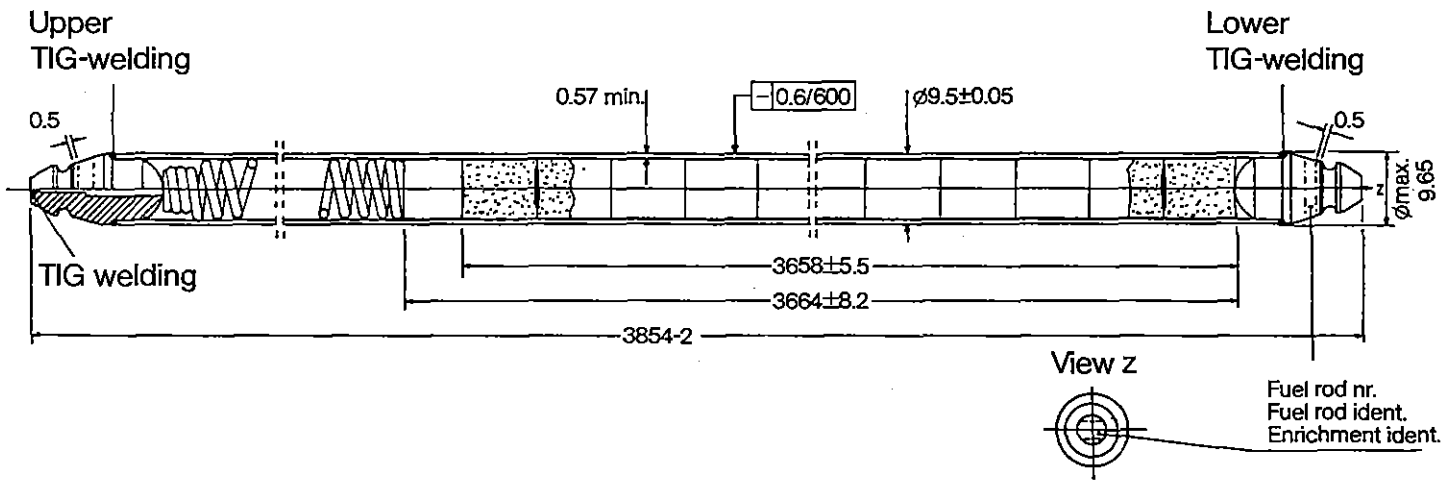

Fig. 2.2/20: Full-Scale Test Fuel Rod

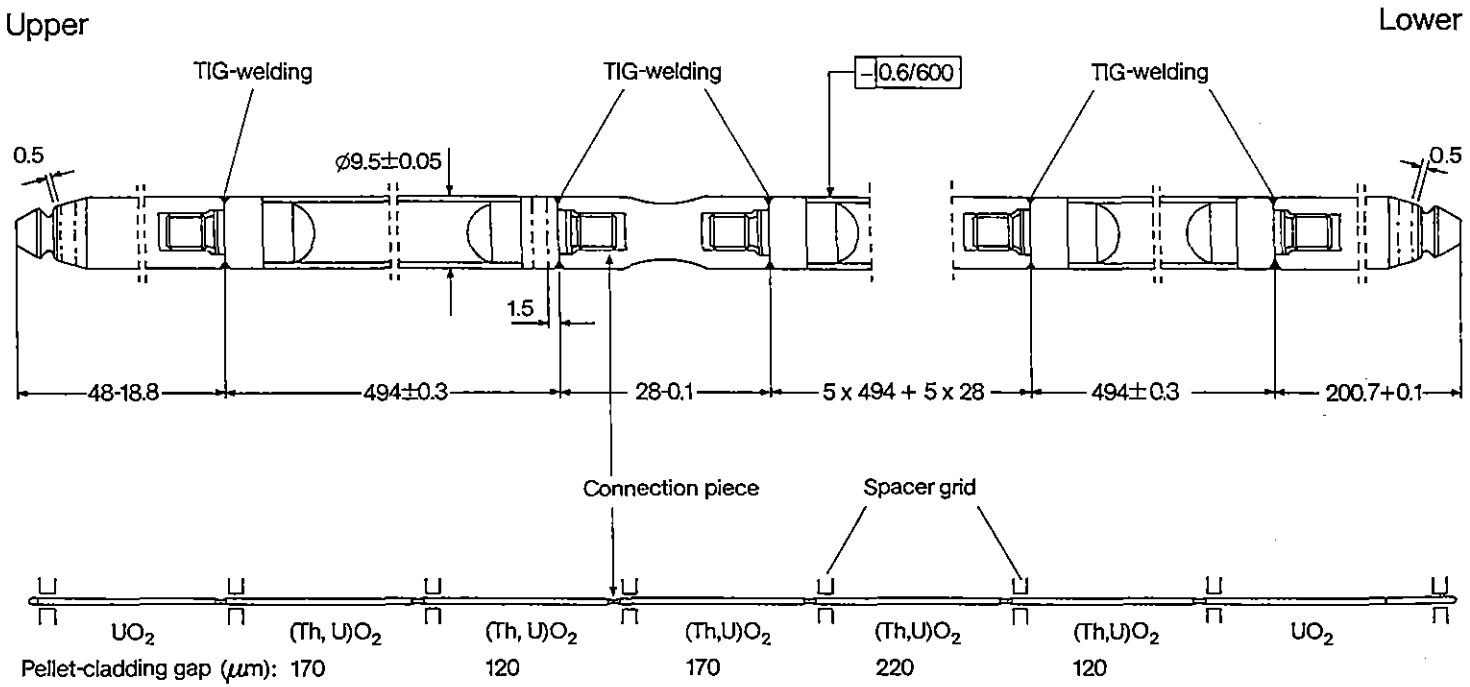

Fig. 2.2/21: Segmented Test Fuel Rod

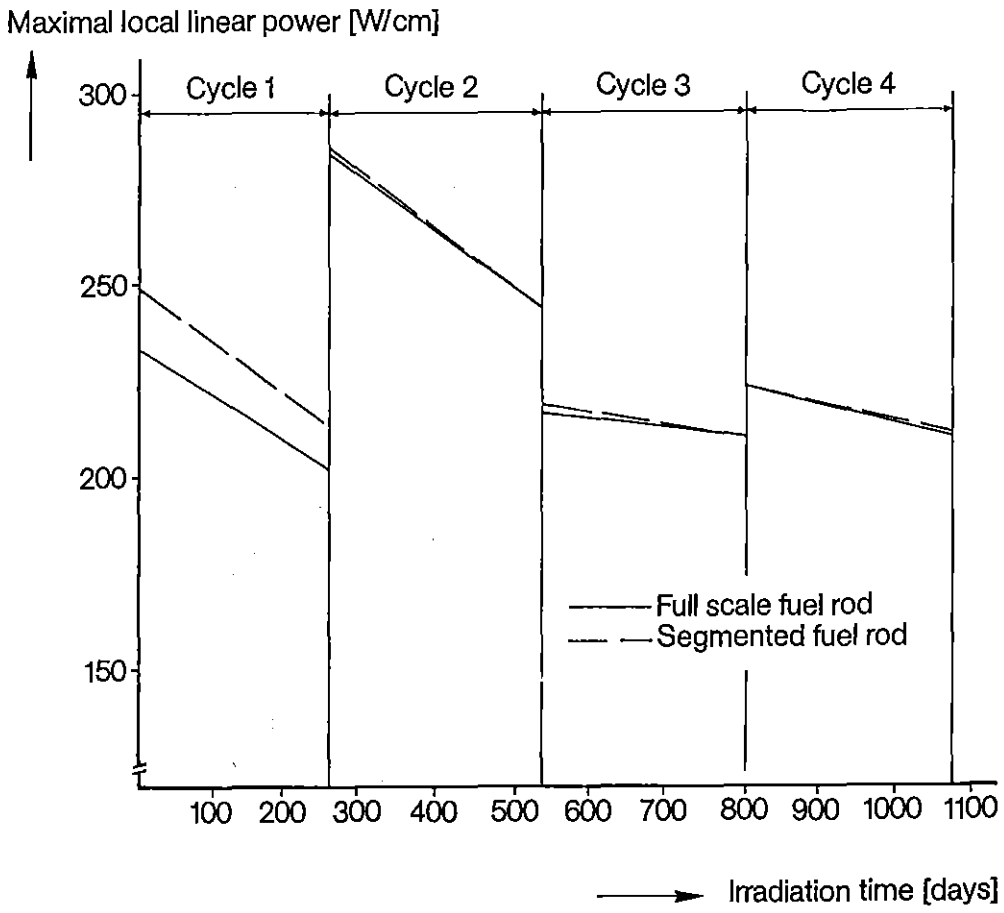

Fig. 2.2/22: Power Histories of Th/U Test Fuel Rods

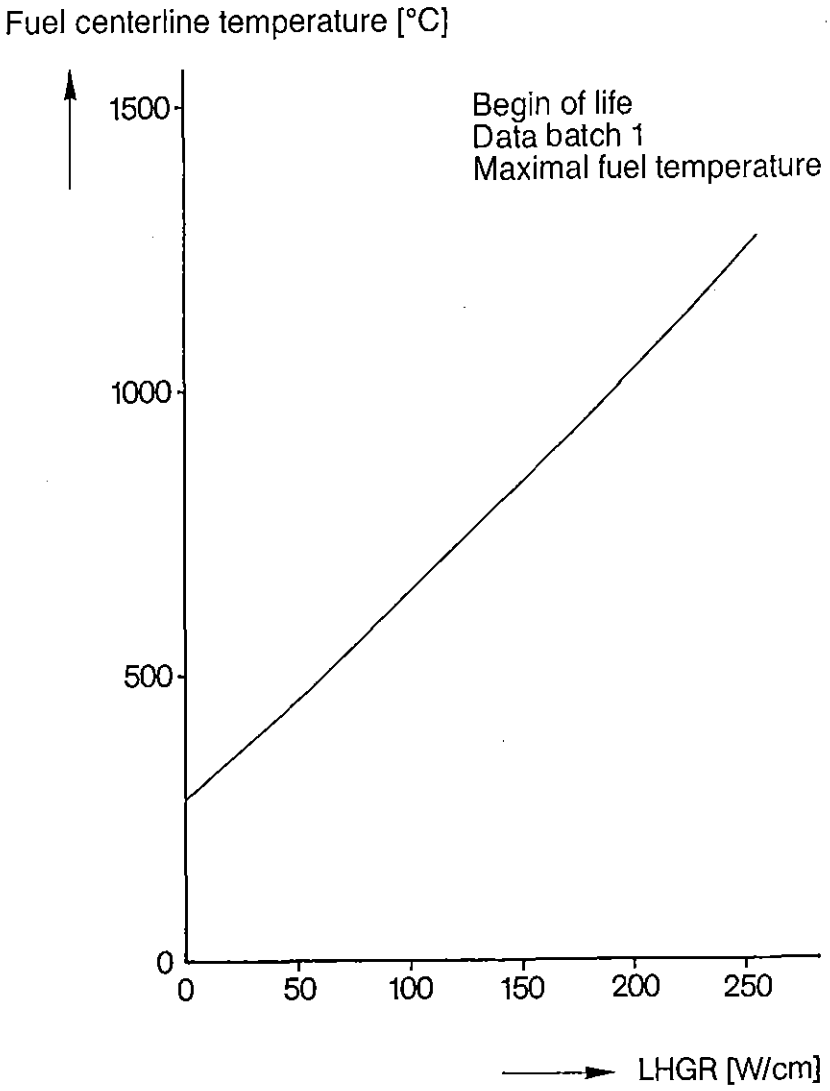

Fig. 2.2/23: Fuel Centerline Temperature as a Function of Local Linear Power of Th/U Test Fuel Rods

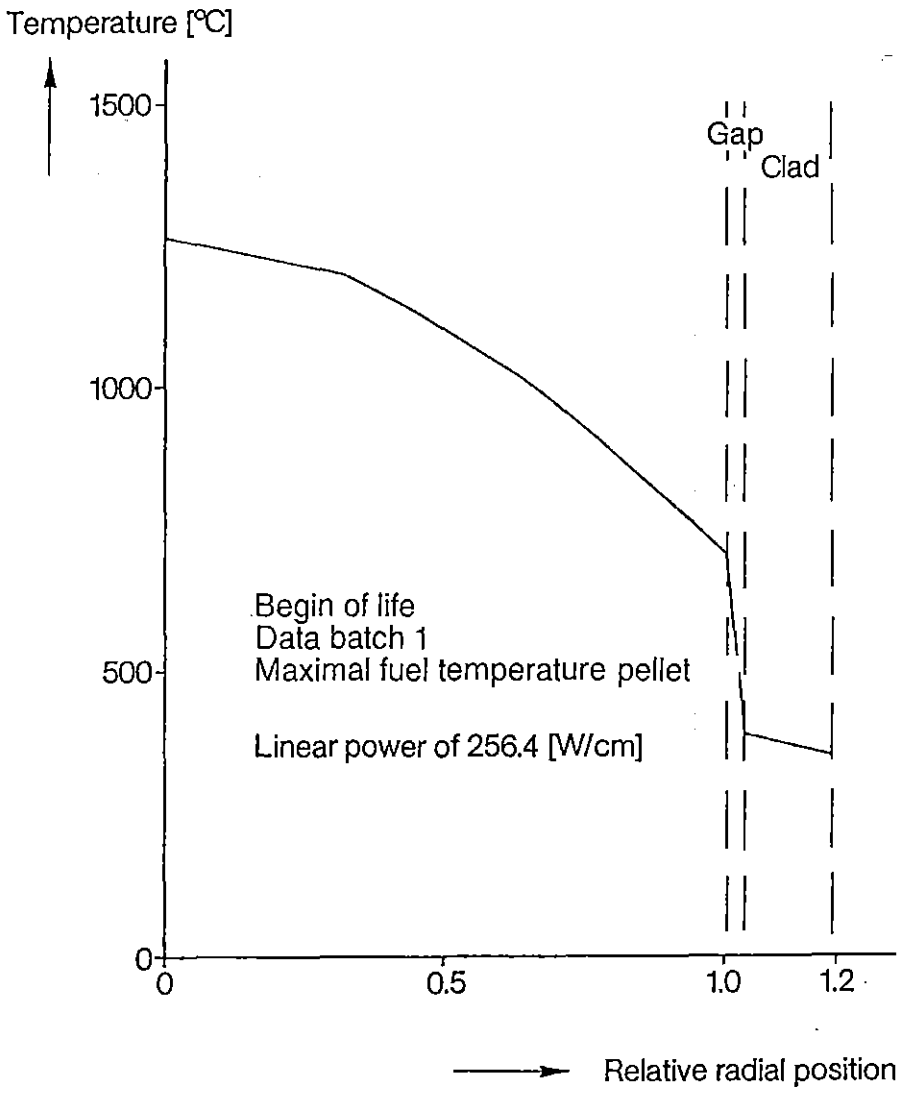

Fig. 2.2/24: Radial Temperature Profile in the Fuel Rod

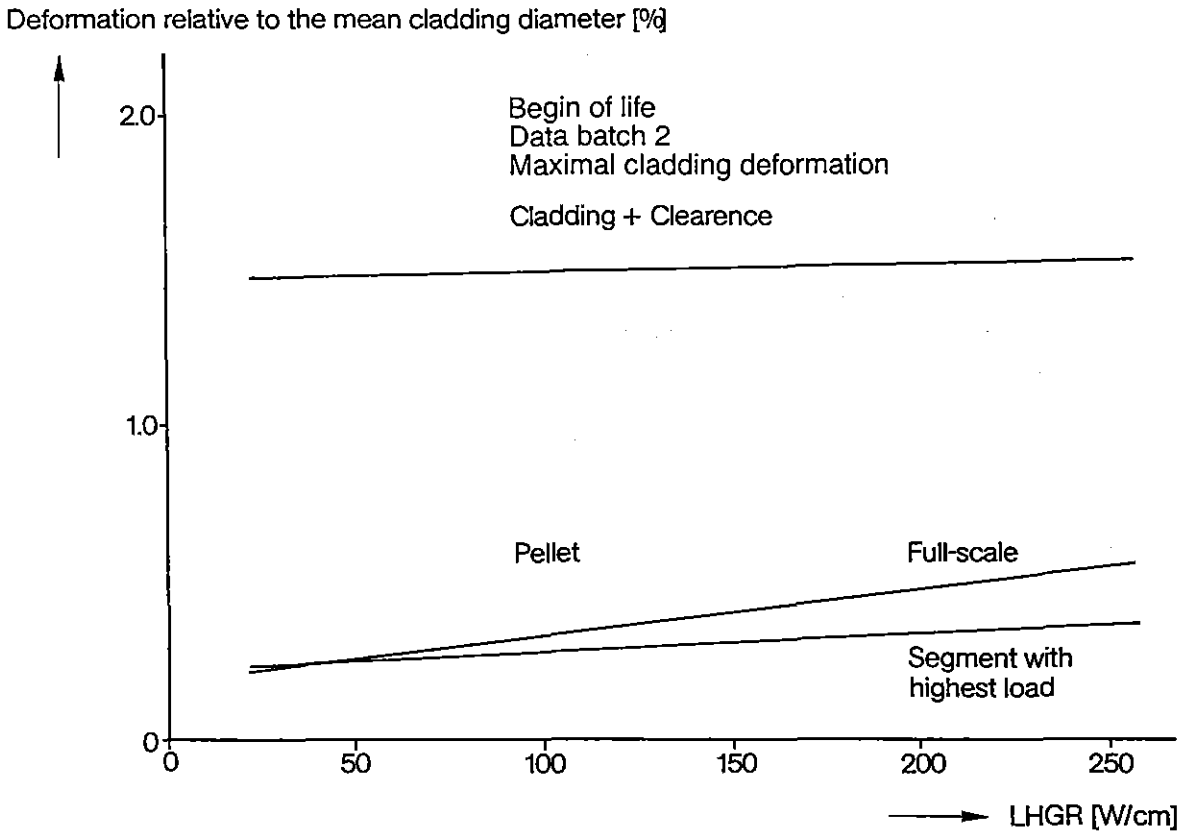

Fig. 2.2/25: Relative Diametral Change of the Fuel Pellet and Cladding Tube as a Function of the Local Linear Power at BOL in Th/U Test Fuel Rods

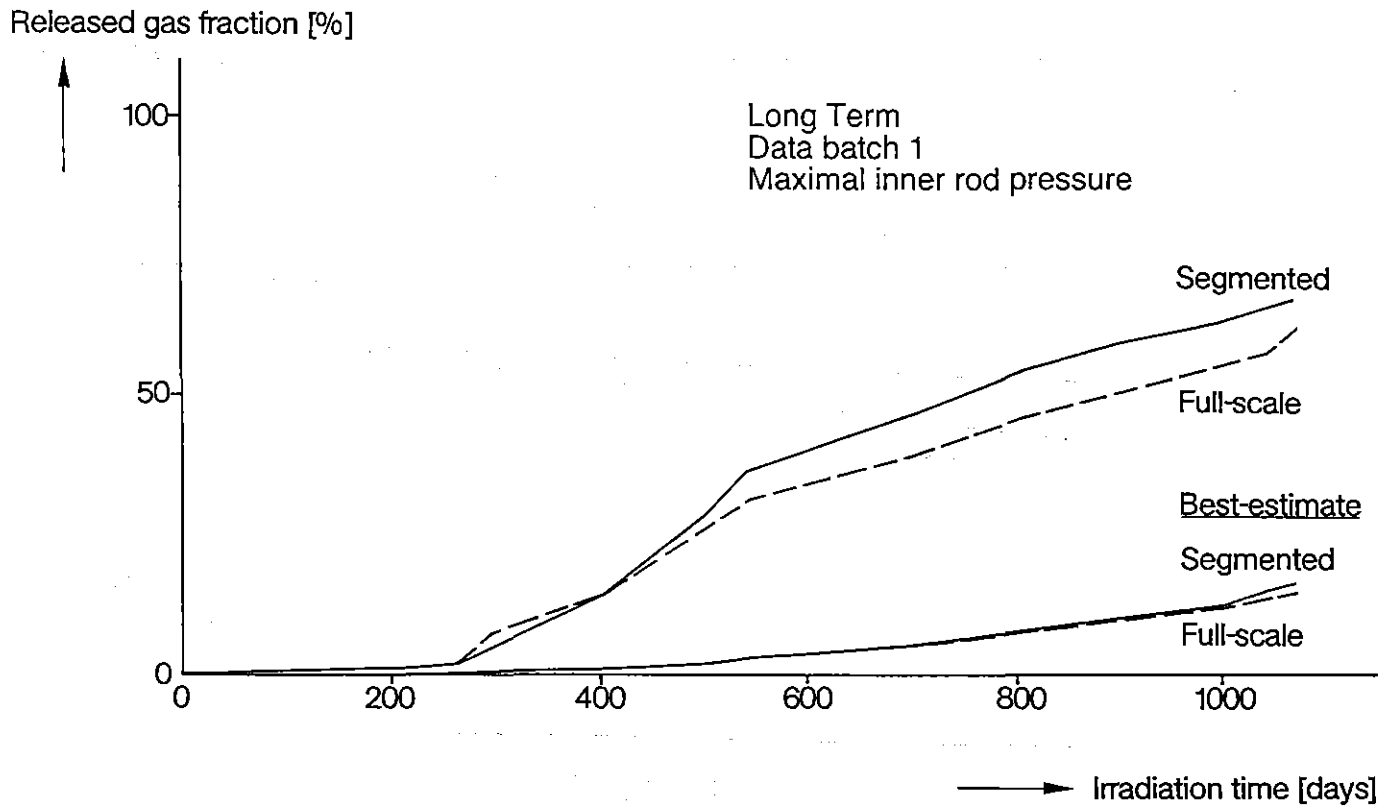

Fig. 2.2/26: Highest Fission Gas Release Fraction of Th,U-Test Fuel Rod

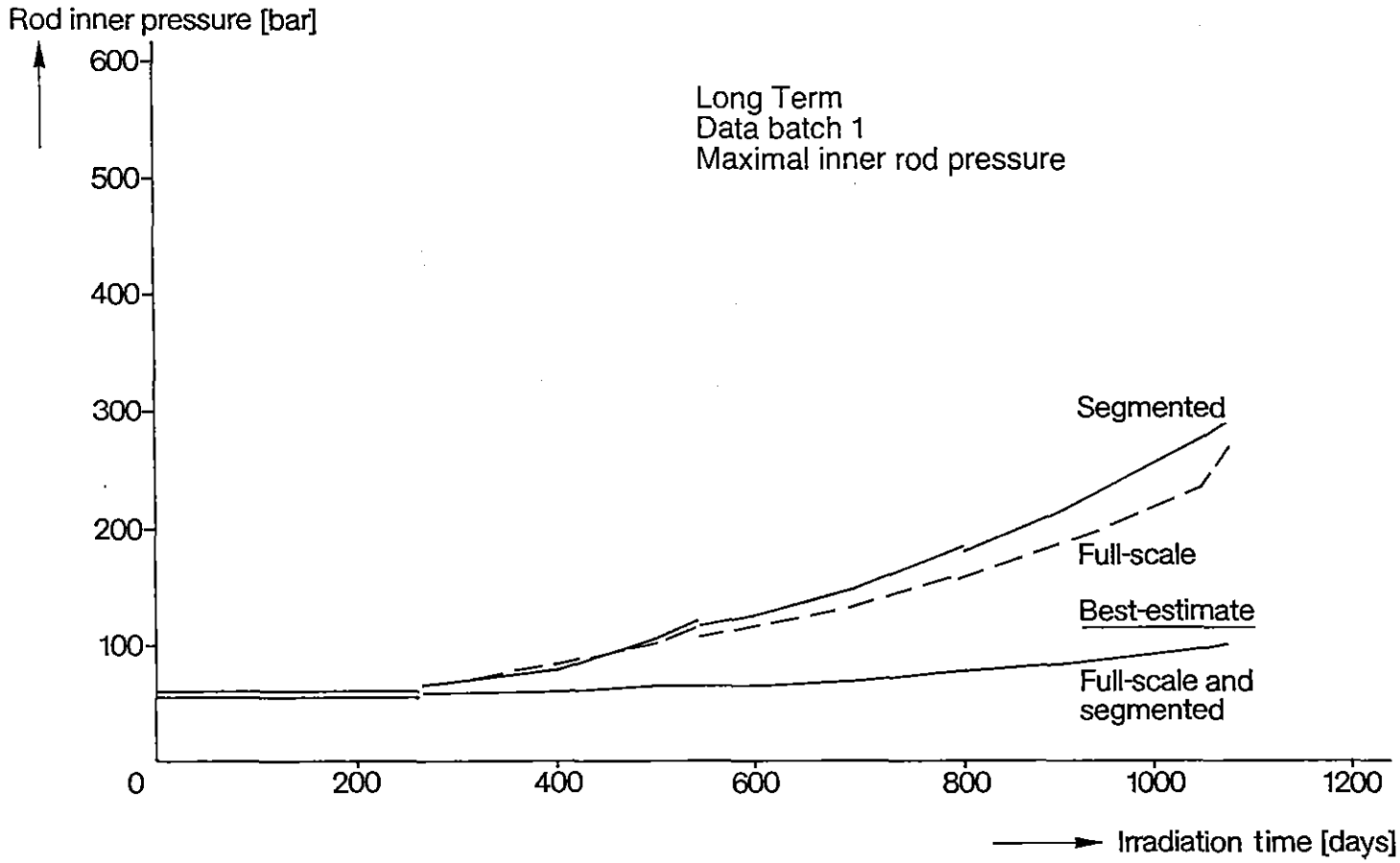

Fig. 2.2/27: The Highest Rod Inner Pressure of Th,U-Test Fuel Rods

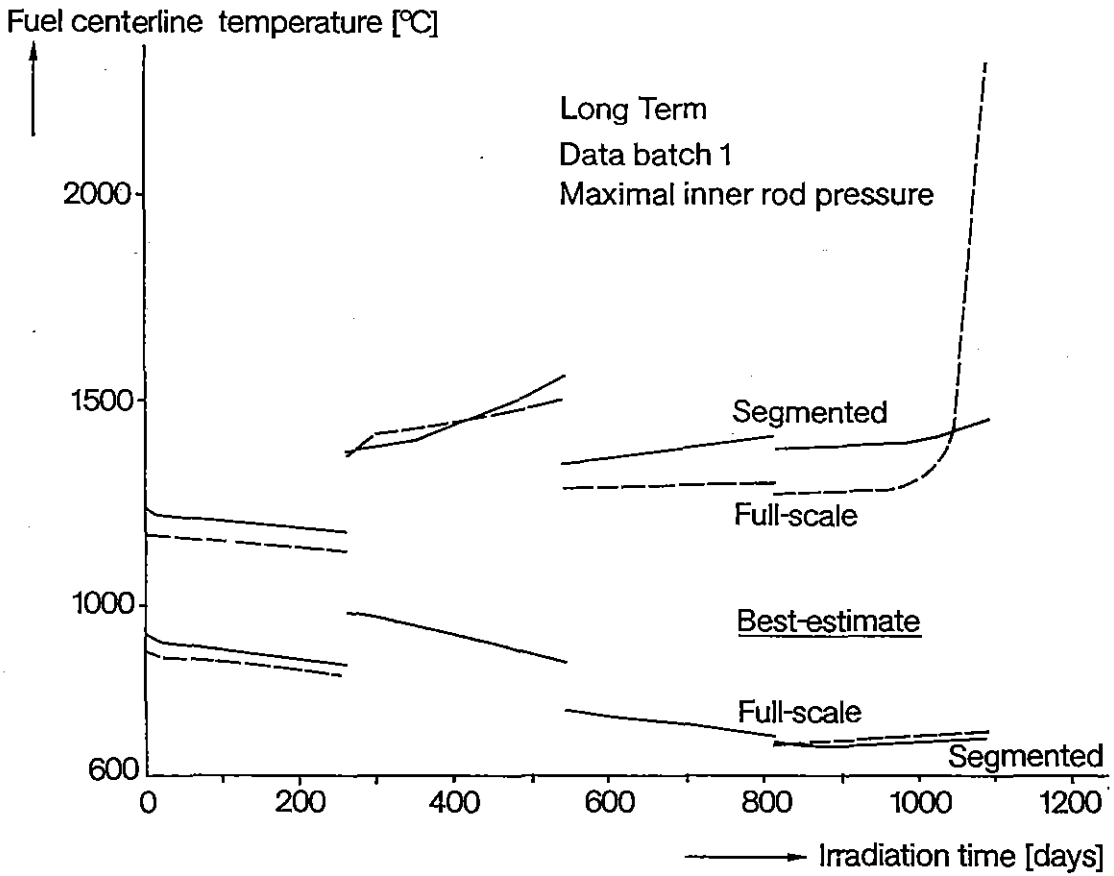

Fig. 2.2/28: Fuel Rod Centerline Temperatures as a Function of the Irradiation Time of Th,u-Test Fuel Rod

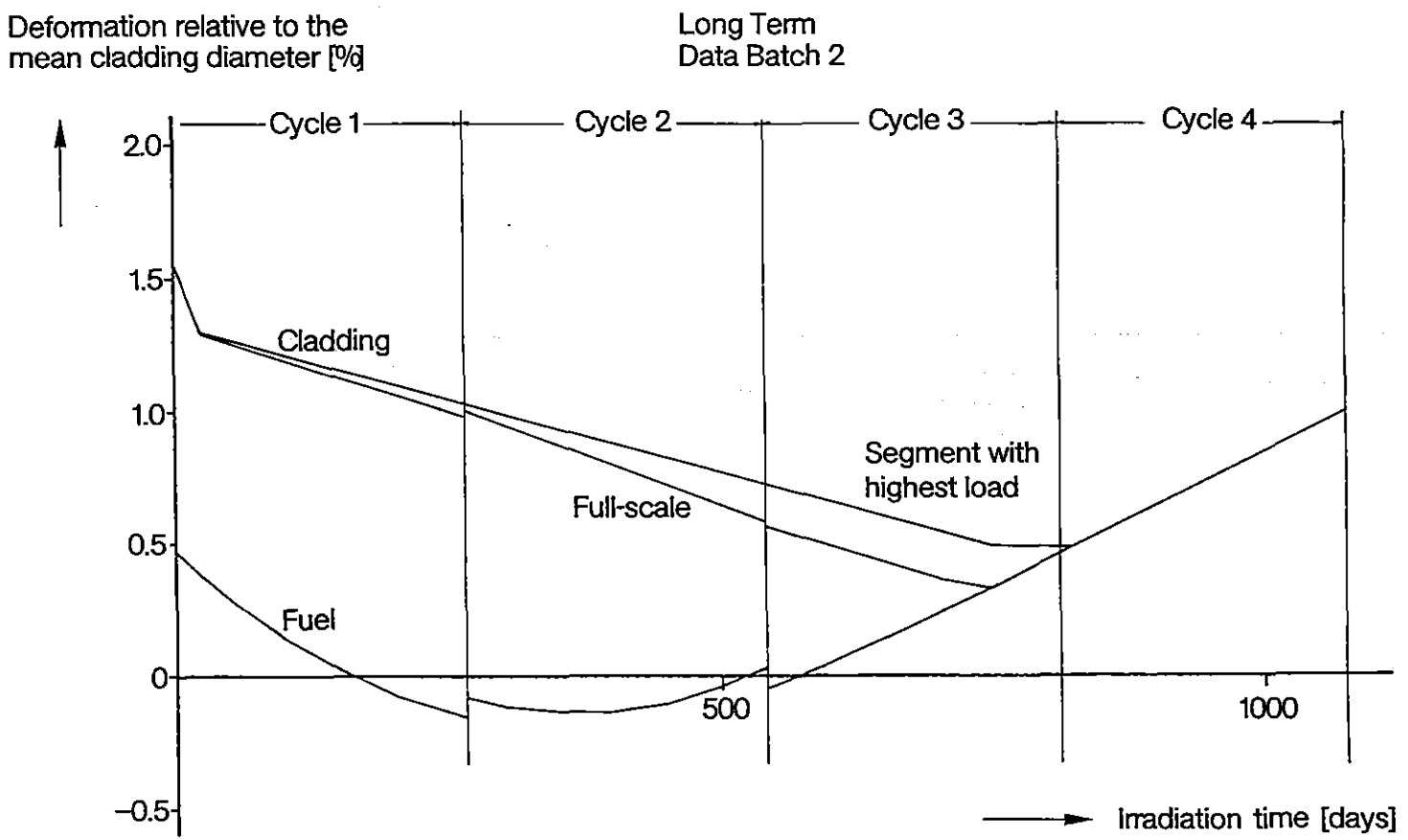

Fig. 2.2/29: Relative Diametral Change

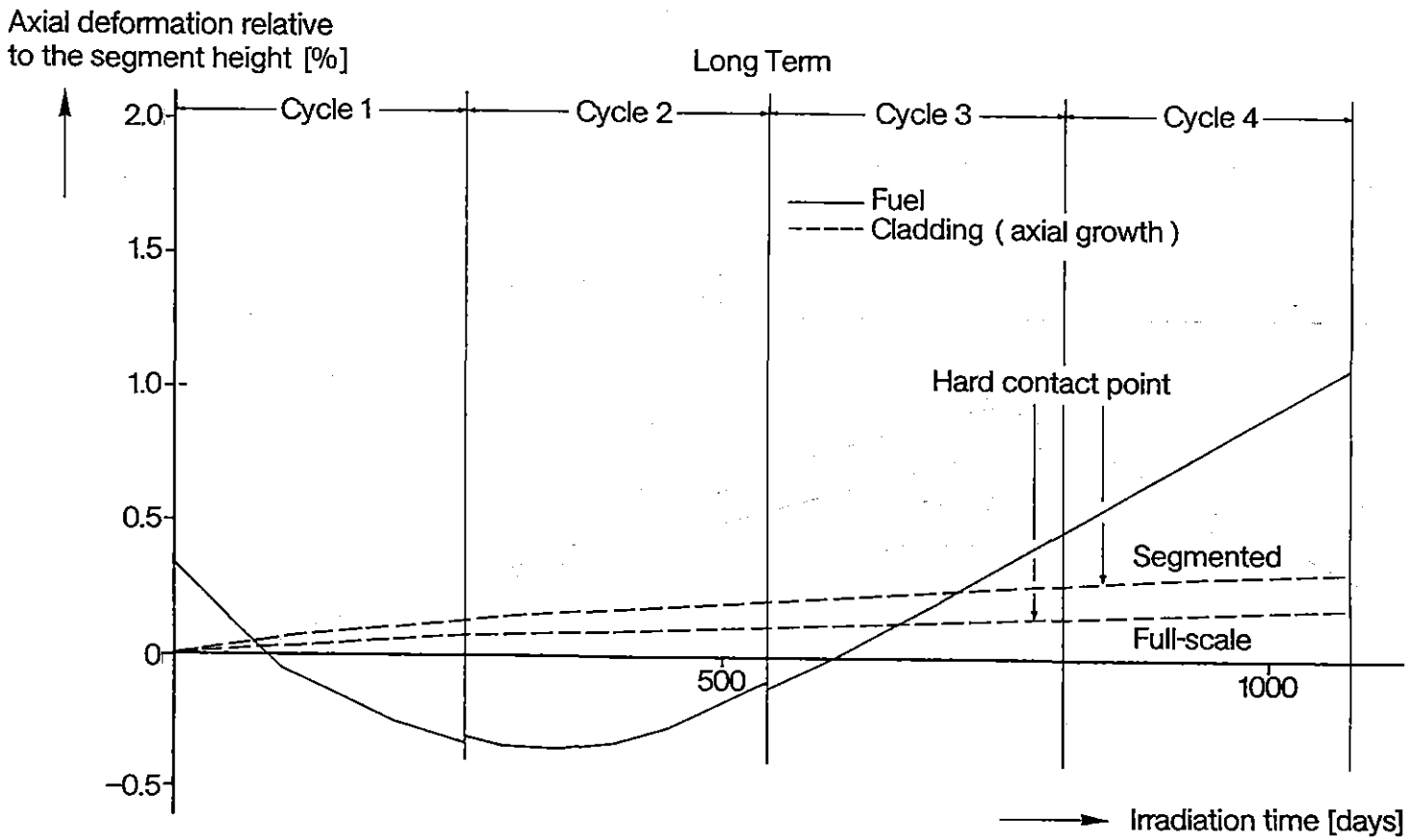

Fig. 2.2/30: Relative Length Change

2.3 Technology Development for $(Th,U)O_2$-PWR Fuel

The aim of this task was the development of a reliable process for the manufacturing of $(Th,U)O_2$ fuel pellets meeting the operational PWR requirements. This should be performed using available fabrication technology as much as possible.

2.3.1 Basic technology for $(Th,U)O_2$ pelletizing ex-gel

Within the former D_2O-Th-Program $(Th,U)O_2$ fuel pellets were manufactured in 1964. The fuel was needed to perform a critical experiment [2.3-1].

The fuel was manufactured in the normal Light Water Reactor (LWR) production lines for UO_2. The fabrication process comprised the steps powder mixing, pressing and sintering in hydrogen-atmosphere. The defined specifications could be reached. However, the homogeneity, the structure and the geometrical shape were inadequate under the aspect of using this fuel as a reactor fuel.

To overcome these difficulties it was emphasized to use :

> the chemical ex-gel conversion process resulting in calcined unsintered$(Th,U)O_2$ particles where both constituents ThO_2 and UO_2 form a perfect solid solution

in combination with:

> standard pelletizing techniques.

Selecting this combination offers the possibility to use the available manufacturing equipment and quality assurance programs from commercial High Temperature Reactor (HTR) and LWR fuel production without modification, especially (Figure 2.3/1):

a) the kernel fabrication lines from HTR;

b) the pressing, sintering and grinding equipment from LWR.

2.3.1.1 Conversion process

For the preparation of spherical particles wet-chemical processes have proven to be very suitable for the production of fuel kernels for HTR fuel elements. A special wet-chemical process which employs the gel precipitation has been developed up to the production scale, according to which all current types of spherical nuclear mixed-oxide feed and breed particles (mostly called kernels), containing high melting uranium and thorium oxides and carbides, respectively, can be fabricated by only slight changes in the composition of the feed solution and some process parameters.

For production of mixed-oxide Th/U kernels aqueous solutions of uranyl nitrate, thorium nitrate and polyvinyl alcohol (PVA) as auxiliary material are homogeneously mixed in a specified ratio. Using mechanical vibration of an eletromagnetic vibration system this feed solution is passed through nozzles, generating jets of liquid in air which are dispersed into uniform droplets. The surfaces of the droplets are hardened by chemical reaction with ammonia gas which are collected in ammonia solution where the external gelation reaction is completed.

Subsequently, the kernels are treated with aqueous ammonia thus eliminating the reaction by-product ammonium nitrate. Drying and calcining are performed in air, whereby the thorium oxide hydrate is dehydrated and ammonium diuranate and the PVA are thermally decomposed (Figure 2.3/2).

2.3.1.2 Pelletizing

As far as UO_2 pelletizing is concerned there are two alternatives for the fabrication of green pellets due to the powder properties from the different powder conversion processes (Figure 2.3/3):

a) the granulation process by adaptation of the powder flowability for powder transport and filling of the pressing tools sometimes in combination with the addition of internal lubricants to improve the pressing characteristics;

b) the direct pelletizing taking the powder directly from the conversion to the pressing without additives or any conditioning of the powder to the process needs.

The method of direct pelletizing, successfully used for commercial LWR-fuel production from UO_2-powder ex-AUC-process in several countries, was chosen for the present application.

Since the sintering activity of the as-produced $(Th,U)O_2$ green pellets is very high, the mixed oxide pellets can be sintered in H_2 at a maximum temperature of 1,750° C in reasonable sintering times (Figure 2.3/4). This proves that standard pressing equipment and sintering lines from commercial UO_2-production are suitable for $(Th,U)O_2$ pelletizing. However, two problem areas could be identified where the R + D effort was concentrated, as described in the following.

2.3.2 Objectives, problems and solutions

2.3.2.1 Requirements for PWR-fuel pellets

The basic requirements a water cooled reactor fuel has to meet can be subdivided into the following features [2.3-2]:

a) optimum content and homogeneous distribution of fissile and fertile material according to reactor physics calculation;

b) limited amounts of atoms with parasitic neutron absorption;

c) high melting point and high chemical stability;

d) limited chemical interaction with the cladding and compatibility with the coolant;

e) high thermal conductivity, small thermal expansion;

f) dimensional stability under irradiation;

g) high fission product retention.

Some of these properties are inherent to the oxide fuel material like c), d) and e) in the case of UO_2 and ThO_2. Other required characteristics such as fissile/fertile distribution,

the dimensional stability and the fission product retention are governed by the manufacturing process. The use of a gelation process for $(Th,U)O_2$ fabrication guarantees the completely homogeneous distribution of Th and U in the fuel. The dimensional stability and the fission product retention are mainly related to the fuel density and microstructure; the target values of these properties are given in Table 2.3.1 (see [2.3-3]).

The development of a $(Th,U)O_2$ manufacturing process has to be done with the aim that these pellet properties can be safely adjusted.

2.3.2.2 Scoping studies

The two basic processes to be used for $(Th,U)O_2$ pellet manufacturing have both proven to be very reliable in large scale fuel production – the ex-gel conversion for HTR-fuel and the direct pelletizing for LWR-fuel. The combination of both offers the unique possibility to use the existing manufacturing equipment and quality assurance programs for commercial PWR and HTR [2.3-3 to 2.3-6].

First investigations showed the feasibility of this combined fabrication route [2.3-7]. Two major areas of concern have been identified in these preruns:

a) the improvement of the fuel microstructure, especially to avoid the so-called „blackberry" structure;

b) the adjustment of the pore size distribution due to requirements given in Table 2.3.1.

For the improvement of the pellet microstructure an adaptation of both processes to each other is necessary and can be performed in three possible ways, Figure 2.3/5:

a) adaptation of the kernel properties to the requirements of direct pelletizing;

b) adaptation of pressing and sintering conditions to the kernels as precipitated;

c) or a partial adaptation of both.

The adaptability of the pelletizing steps, pressing and sintering, has been investigated in some scoping studies. The variation of parameters and the influence on the pellet properties are summed up in Table 2.3.2. Only a minor potential of adjusting the pellet properties has been found. It turned out very soon that standard ex-gel-kernels are not suitable for direct pelletizing.

Thus, main efforts have been done to adapt the kernels' properties. This adaptation mainly consisted in:

a) lowering the mechanical strength in order to facilitate the disintegration of kernels during pressing and

b) lowering the sintering activity to get a homogeneous pore structure (the „internal" sintering of the kernels should be prevented).

2.3.2.3 Solution investigated

The high mechanical strength of the kernels as optimized for HTR application is disadvantageous in the case of compactation: high pressing forces are needed, and the

non-complete disintegration of the kernels during pressing leads to the „blackberry" pellet structure.

Considerable efforts were done to obtain softer kernels. All development work with respect to kernel softening is summed up in Table 2.3.3. The steps 1 through 5, consisting in an optimization of the composition of the feed solution and of the heat treatment had some beneficial effect on the kernel strength, but they all resulted in a not totally satisfactory microstructure.

The most effective way of „softening" the kernel has been found by comparison with UO_2 powder from the AUC conversion process as can be seen in mercury porosimeter measurement in Figure 2.3/6, the UO_2 ex-AUC powder reveals an inner pore structure with two pore fractions:

a) a fine size pore fraction of about 100 nm diameter, which gives about 99% of the specific surface area of the powder (sinter pores);

b) a coarse pore fraction of about 1-5 µm diameter; these pores act as notches for the crushing process during compactation (press pores).

The idea to introduce such press pores in the ex-gel-kernels, too, could successfully be verified by adding decomposable pore formers already to the feed solution. Such substances are encased in the kernels during pouring, decompose during the following heat treatment and form pores in this way. The use of carbon black as pore forming additive was successfully tested and introduced as a process step. The efficacy of carbon black is demonstrated by Hg porosimeter results (Figure 2.3/6) as well as by tests of the kernels crushing strength. This test has been developed to get a measure for the mechanical strength of the kernels. It consists in crushing single kernels by a slowly moving punch and recording the force of crushing in dependence on punch position. As can be seen in Figure 2.3/7, unadapted kernels show a brittle fracture at a high force, whereas soft kernels break at low forces successively into different fragments, which is comparable to the behaviour of UO_2 ex-AUC powder.

The use of carbon black needs a treatment of the kernels after the precipitation to remove the carbon – the C-content in the pellet is specified at a very low level (see section 2.3.3). This carbon removal is effectuated during the calcination in air, where the carbon black oxidizes to CO_2 leaving the kernels easily. On the other hand, the calcination is the final step for the adjustment of the sintering activity mainly via controlling the specific surface area. The calcination parameters have been optimized with respect to both requirements.

The removal of carbon as shown in Figure 2.3/8 is dependent on calcination temperature and time, whereas the specific surface area can only be controlled by the calcination temperature, see Figure 2.3/9. Since specific surface area of not more than 10 m^2/g is desirable, a temperature of 900 through 950°C is necessary. At such high temperatures, the carbon removal is a fast process thus a short calcination time of about 2 hours is sufficient.

Using the pelletizing conditions as given in Table 2.3.2, a good progress in the microstructure improvement and in the adjustment of the pore size distribution could be achieved. This step by step optimization is demonstrated in Figures 2.3/10 and 2.3/11.

2.3.3 Pellet specification and Quality Assurance requirements

Satisfactory in-pile behaviour of nuclear fuel can only be achieved by close cooperation between all stages of design, technology, manufacturing and the evaluation of operational experience within a closed system of an „Engineered Quality Assurance System" [2.3-8].

The fuel specification and the quality control system are both important parts of this Integrated Quality Assurance Circuit at KWU, shown in Figure 2.3/12.

Fuel design ensures a safe margin between the in-pile requirements and the technical properties of the fuel, which are fixed in the fuel specification. Quality assurance has to guarantee an appropriate product quality in accordance with the specification.

2.3.3.1 $(Th,U)O_2$ specification

Basis for the specification of $(Th,U)O_2$ hybrid fuel has to be the LWR standard specification for UO_2. UO_2 has proven its reliability in wide-spread use in power reactors over a long time.

Those characteristics of the fuel pellets which are related to their fabrication can be subdivided into four categories [2.3-9], according to the hierarchical system in Figure 2.3/13:

a) type and percentage of fissile, fertile and nuclear poison material (e.g. B, Gd);

b) chemical purity and stoichiometry;

c) density and microstructure;

d) pellet geometry and surface conditions.

Fertile and fissile content

The nominal fertile and fissile contents of LWR fuel and their acceptable tolerances are given by neutron physical calculation and design. In the case of LWR-UO_2, ^{235}U enrichments up to about 4 wt% are usual. In $(Th,U)O_2$, HEU or MEU are to be used (depending on the U/Th ratio) in order to ensure an appropriate overall fertile content.

Neutron absorbing species like Gd or B are limited to $\leq$ 1 ppm totally (see Table 2.3.4) if not used as burnable poison material.

Chemical purity and stoichiometry

Requirements in the category of chemical purity and stoichiometry aim at the following:

a) Minimization of impurities that might trigger or support defect mechanisms. This relates to the hydrogen content, mainly from the adsorbed moisture, which can lead to hydride induced „sunburst" defects, or to the halides fluorine and chlorine, which can act as catalysts for the local depassivation of the tubing oxide film. These defect-sensitive impurities have to be kept in the $(Th,U)O_2$ specification within the same limits as in the LWR standard specification (see Table 2.3.4) [2.3-10].

b) Limitation of the impurities which might be brought into the fuel during manufactur-

ing in order to ensure a good process control. In the case of ex-gel-hybrid fuel mainly C because – of the use of organic precipitation aids and S as impurity in the soot used as pore former have to be recognized.

c) Minimization of deviations in stoichiometry to ensure basic properties such as thermal conductivity and creep behaviour within narrow limits and to limit the internal oxidation of the cladding tube. Both aspects are also true for $(Th,U)O_2$ fuel. A summary of the specified chemical properties of $(Th,U)O_2$ is given in Table 2.3.4.

Density and microstructure

Many basic properties of the fuel depend on its density, e.g. thermal conductivity, elastic moduli and creep behaviour. Since on the other hand a residual porosity is necessary to compensate for the in-pile swelling of the fuel, a density of 95% TD for LWR fuel is considered to be the best compromise.

A good in-pile dimensional behaviour, i.e. an optimal compensation of the fuel swelling by in-pile densification, can be ensured by an average pore size of between 1 and 5 µm. Pores larger than 10 µm diameter are assumed to be helpful for increasing the PCI resistance at high burnups, but the amount of these coarse pores should be limited to $\leq$ 20 volume %.

The grain size may affect the mechanical properties of the fuel and the release of fission gas during operation. An average grain size between 5 and 25 µm has shown to be suitable.

In mixed oxide fuel, the oxide phase structure plays an important role with respect to the dimensional changes and on the behaviour of fission products in the fuel. In the case of $(Th,U)O_2$ fuel ex-gel, a complete homogeneity of Th and U is garanteed due to the gelation process. Thus, a specification of the oxide phase structure is not necessary.

Pellet geometry and pellet surface

Centerless grinding of the pellets is common practice in order to keep the narrow limits of pellet diameter: this is important in order to minimize the gap between pellet and cladding for constant heat transfer. For the same reason, the roughness of the ground pellet surface Ra is specified to be lower than 2 µm.

The pellet surface may show different types of defects as cracks, chips and pores. Although there is no clear „risk threshold" regarding these defects it is practise to established „go – no go" standards and to a 100 % check.

2.3.3.2 Quality assurance requirements

Quality assurance for $(Th,U)O_2$ is realized – as is usual for all nuclear fuels – by process and product control:

a) **process control** by implementation and surveillance of production procedures which automatically yield a product with high quality, and

b) **product control** by the specification of appropriate quality control plans and by the application of adequate testing procedures.

The successful control of the manufacturing process is possible because of the detailed knowledge of the influence of the process parameters on the quality of the intermediate (kernels) and final product (pellet) and because of the well known interdependency between the kernel properties and the pellet characteristic. As examples, the relationship between the calcination temperature and the specific surface area and the influence of the kernels density on the density and microstructure of the pellets should be mentioned. In order to ensure the observance of the optimal process parameters, a formal framework of process manuals has been settled with a detailed description of all single fabrication steps.

The Quality Control Plan for the product control of $(Th,U)O_2$ kernels and pellets consists of:

a) a set of testing techniques appropriate for all specified quality control data;

b) a fixation of the testing frequency (scope of testing) of those data.

The methods of testing have been described in detail in the quality control manuals. From the methods of chemical analysis, which are listed in [2.3-11] in a survey, only those for the determination of the Th and U content and of the O/M ratio shall be mentioned here:

a) For the **Th- and U-content** the oxide is dissolved in nitric acid by addition of hydrofluoric acid. The Th is precipitated as thorium oxalate, dried and calcined to ThO_2 at 1,100°C in air. The U-content can be measured by potentiometric titration according to the modified Davies-Gray method as being applied for pure UO_2 and other binary oxides.

b) The **U-content** can also be measured by a method which is a combined analysis for U and O/U ratio in ThO_2-UO_2 fuel [2.3-9]. Samples are dissolved in a neutral medium which does not change the valency of U, i.e. phosphoric acid-hydrofluoric acid by addition of $Al_2(SO_2)_3$.

c) **O/M-ratio** is calculated from the determination of the O/U-ratio by controlled-potential coulometry taking into account that the Th is always tetravalent whereas the U changes from the tetravalent state into the hexavalent state by oxidation.

The **Quality Control Plan** for $(Th,U)O_2$ pellets – like for other ceramic fuel – consists of

a) the definition of the test lots,

b) the fixation of appropriate testing frequencies.

The test lot definition takes into account, by which process step the property to be tested is mainly governed. For example, the thorium and uranium content check relates to a precipitation lot (see Table 2.3.4).

Further-on, a „delivery lot" has been defined for the control of enrichment, and a grinding lot for the check of diameter and surface roughness.

Defining the testing frequencies, credit can be taken from the process control system which allows to lower the scope of testing by controlling the manufacturing steps and by a check of the intermediate products. Concerning the sintered pellet density for instance, control of the sintering parameters, the green density and the kernel propert-

ies „density" and „specific surface area" yields a safe adjustment of pellet density, which consequently can be checked to a lower extent.

For the quality control performance in praxis, all these controls described above should be documented and compiled in a so-called „Manufacturing and Inspection Sequence Plan" (Figure 2.3/14). It comprises:

a) the current numeration and denomination of all manufacturing and inspection steps;

b) the number of manufacturing and inspection manuals to be applied;

c) the inspection method;

d) the scope of testing;

e) the type of documentation.

2.3.4 Description of $(Th,U)O_2$ pelletizing technology ex-gel

2.3.4.1 Process description

Production of ex-gel-C-$(Th,U)O_2$ kernels

Gel kernels with carbon black are manufactured by means of the gel precipitation technique developed by NUKEM GmbH [2.3-12]. In this technique, isolated drops of heavy metal solution are formed. These drops are partially hardened when they pass through ammonia atmosphere. The hardening is completed after immerging into an aqueous ammonia solution. These hardened droplets are called gel kernels.

The gel kernels production steps are:

a) preparation of the feed-solution components;

b) preparation of the feed-solution;

c) pouring;

d) washing.

The flowsheet on Figure 2.3/15 shows the steps of gel kernels production and characterization.

Preparation of the feed-solution components

The feed-solution components are:

a) preneutralized thorium nitrate solution;

b) uranyl nitrate solution or U_3O_8 solution;

c) PVA solution;

d) carbon black;

e) alcohol.

The preneutralized thorium nitrate solution is prepared first through dissolution of the thorium nitrate salt in deionized water followed by a preneutralization with NH_3-solution. The solution is characterized by determining the density, thorium concentration, pH value, conductivity, NH_4^+ content and HNO_3 content.

The uranyl nitrate solution is prepared by dissolution of the uranyl nitrate salt in deionized water at the required concentration. It is analysed for density, concentration, pH and conductivity.

If the U_3O_8 solution is required instead of uranyl nitrate salt, it is necessary to dissolve the U_3O_8 in nitric acid. Finally, the uranium concentration and acidity are adjusted. The final solution is characterized according to the uranyl nitrate solution.

The PVA solution is prepared by dissolution of the PVA in deionized water at the required concentration. It is checked by density, concentration and visual aspect.

The carbon black should fulfil the requirements with respect to specific surface, particle size and ash content.

Preparation of the feed-solution

The feed solution is prepared by mixing preneutralized thorium nitrate solution, PVA solution, uranyl nitrate solution, carbon black and alcohol. The content range of each component is specified according to the desired characteristics of the calcined kernels.

Pouring

The pouring is performed with the equipment shown in Figure 2.3/16. The double wall recipient is loaded with the feed-solution and is then pressurized to let the feed-solution flow to the nozzle. By vibrating drops are generated. In the upper side of the column an NH_3 atmosphere is held to harden the droplets. The droplets hardening is completed at the bottom of the column filled with ammonia solution. The kernels are collected in the vessel at the bottom of the column.

The gel kernels' diameter is controlled by adjusting the feed-solution flow, the vibration frequency and nozzle diameter.

Washing

The washing is performed by agitating the gel kernels in a dilute ammonia solution as many times as necessary to get this solution free of NO_3 ions. After the washing, the gel kernels are submitted to the following steps:

a) drying;
b) sieving;
c) calcining.

The flowsheet on Figure 2.3/17 shows the steps of calcined kernels' production and characterization.

Drying

The drying of the gel kernels is performed by heating to separate them from the washing solution. This step should be performed immediately after the washing to avoid undesirable aging of the gel kernels.

Sieving

If kernel agglomerates are formed during the drying it is necessary to carry out the sieving to smash these agglomerates to single kernels.

The sieving equipment consists in a sieve stack of increasing mesh (from the bottom to the top end) assembled in a vibratory table. The agglomerated dried kernels are filled in the top sieve and by turning on the vibratory table they fall through the other sieves smashing the agglomerates. The kernels are finally collected in the last sieve through which they cannot pass.

Calcination

The calcination of the dried kernels is necessary to eliminate the auxiliary materials of the casting and to set up the desired physical and chemical properties. Two kinds of calcination are available: on tray and in rotating chamber (see Figures 2.3/18 and 2.3/19). The calcination on tray has the advantage of taking only a short time. Its drawback is a greater scattering of the kernel properties. The calcination in the rotating chamber has the advantage of getting a small scattering of the kernel properties. Its drawback is a longer calcining time to avoid the formation of dust. The calcined kernels are characterized by measuring their physical (density, specific surface and fracture strength) and their chemical (carbon and sulphur contents) properties.

Pelletizing

The pelletizing is carried out in three steps:

a) pressing;
b) sintering;
c) grinding.

The pelletizing parameters are fixed by means of a pelletizing prerun for each calcining batch.

The pressing is carried out directly without any pretreatment of the kernels like milling, precompactation and granulation and without the use of pressing aids.

The sintering is carried out according to standard UO_2 procedure for PWR (reducing atmosphere, 1,700–1,750°C, 2–3 h).

The grinding is performed in a centerless grinding machine according to the standard UO_2 procedures for PWR.

2.3.4.2 Results from process validation

In order to demonstrate the validation of the final commitment on:

a) process parameter fixation,

b) quality control and manufacturing manuals,

c) manufacturing and examination sequence plan,

four batches of pellets were manufactured according to the flowsheet of Figure 2.3/20.

The results of the calcined kernels characterizations are collated in Table 2.3.5. With

exception of the specific surface and sulphur content, the kernel characteristics have been kept with variations of less than 10%. According to the previous experience, such variation range of the kernel properties are sufficient to assure the manufacturing of pellets with the required properties.

A pelletizing prerun was done to fix the appropriate working compactation pressure for each calcining batch. The results are shown in Figure 2.3/21. The working compactation pressure ranged between 45 and 55 kN/cm^2.

Thirty pellets from each calcining batch were pressed and sintered. The results of the physical and chemical characterizations are shown in Tables 2.3.6 and 2.3.7, respectively. The length of the pellets was settled at 10 mm instead of 11 mm, as specified, due to a human failure.

Typical pore and grain structures are shown in Figure 2.3/22. A representative pore size distribution is shown in Figure 2.3/23. The microstructure analyses identified cracks in some pellets, as shown in Figure 2.3/24. The grain size (10-15 μm) meets the specification (4-25 μm) and is even within the scope for high-burnup fuel; 10 μm).

Within the chemical analyses scope, all batches have met the specifications. The sulphur content has been kept at a very low level (<20 ppm). The carbon content has been kept within the specified range (<100 ppm).

The visual inspection has shown metallic crystals on the surface of the dishing of some pellets. The cause of this has been an unexpected interaction of the pellets with the molybdenum sintering boat. This is probably due to the uncontrolled oxygen potential of the sintering atmosphere that has existed during all sintering runs. The unexpected cracks identified by the microstructure analyses could be linked with the oxygen potential, too.

2.3.5 Conclusions

The technology development for (Th,U)O_2 PWR fuel allows the following main conclusions:

a) the gel precipitation process has successfully been adapted to the specific requirements of the direct pelletizing. This has been achieved mainly by the subsequent heat treatment of the kernels. The parameters of direct pelletizing of standard UO_2 fuel (pressing, sintering and grinding) could be kept almost unchanged,

b) the design criteria for (Th,U)O_2 fuel pellets for PWR application were settled in the fuel specification and a fabrication manual,

c) a complete quality assurance system was successfully applied both to the fabrication of FRJ-2 irradiation test fuel and to the fabrication of fuel for the manufacturing process validation test at CDTN/NUCLEBRAS.

References

[2.3-1] H. Kuehn, M. Peehs, K. Reichardt
„Thermische Brueterstudie Teil 2 – Entwicklung, Herstellung und Bestrahlung von $(Th,U)O_2$-Brennstäben mit sphärischen Sol-Gel-Partikeln"
Forschungsbericht BMWF Inv. Reaktor 37, April 1969

[2.3-2] Stehle, H., Assmann, H., Maier, G.
IAEA/CNEA Intern. Seminar on Heavy Water Reactor Fuel Technology
San Carlos de Bariloche, June 1983

[2.3-3] Peehs, M., Doerr, W., Hrovat, M.
Development of a pelletized $(Th,U)O_2$-fuel for LWR application
IAEA Advisory Group Meeting on Advanced Fuel Technology and Performance
EIR Wurenlingen/Switzerland, Dec./1984

[2.3-4] Peehs, M., Schlosser, G., Pinheiro, R.B., Maly, V. Hrovat, M.:
Th-Utilization in PWR's
IAEA Techn. Comm. on Utilization of Th-Based Nuclear Fuel – Vienna, Dec. /1985

[2.3-5] Huschka, H. et. al.
Nucl. Technol. 35 238 (1977)

[2.3-6] Assmann, H., Peehs, H., Doerr, W.,
J. Am. Cer. Soc. 67 631 (1984)

[2.3-7] "Program of Research and Development on the Thorium- Utilization in PWR's"
Final Report for Phase 1 1979-1983, May 1984 Juel. Spez. 266
ISSN-0343-7639- NB/CDTN-471/84-KWU B 22/84/35 – NUKEM F u.E. 83075

[2.3-8] Guidebook on Quality Control of Water Reactor Fuel, Techn. Rep. Series no. 221
IAEA, Vienna/Austria, 1983

[2.3-9] H. Assmann, J. Nucl. Mat. 106 (1982) 15

[2.3-10] H. Assmann, M. Peehs, H. Roepenack
3. Conf. on „Characterization and Quality Control of Nuclear Fuels"
Karlsruhe, May 25-27, 1987, to be published in J. Nucl. Mat.

[2.3-11] „Program of Research on Development on the Thorium Utilization in PWR's"
Final Report for Phase 1, 1979 – 1983 May 1984 Juel. Spez. 266
ISSN-0343-7639-NB/CDTN – 471/84-KWU B 22/84/35 – NUKEM F u.F. 83075, Fig. 2.3./15

[2.3-12] Kadner, M. & Baier, J.
Production of fuel kernels for high-temperature reactor fuel elements.
Kerntechnick 18. Jahrgang (1976) no. 10

Table 2.3.1: Design criteria for $(Th/U)O_2$ fuel for PWR application

Criteria	Values	Aims
Average pore size of pores distributed by a log.-nom. Gaussian function	2.5–3.5 µm	optimization of swelling/ shrinkage behaviour in-pile
Scattering factor of the distribution	0.25–0.30	
Shape factor*	0.7	
Open porosity	1%	minimization of fission gas release
Grain Size	10 µm	
Density	9.40–9.70 g/cm^3	optimization of PCI behaviour

*$1/F = \frac{\text{Circumference of a pore in the micro-section}}{\text{Circumference of a circle with identical area}}$

Table 2.3.2: Influence of the variation of pressing and sintering parameters on the properties of $(Th,U)O_2$-ex-gel pellets

Fabrication Step	Investigated Parameter	Influence on the Pellet Properties
Pressing	high pressing forces	high sintered density low open porosity
	use of internal lubricants	crack susceptibility
	lubrication with S-base lubricant	homogeneous microstructure „blackberry" structure
	pressing speed	no conclusive influence on the pellet properties
	pressing sequence	
Sintering	atmosphere: H_2 CO_2 Air	adjusting the O/Me ratio
	increasing sintering temperature and time	high sintered density low open porosity

Table 2.3.3: Final status of adaptation of $(Th,U)O_2$ ex-gel-kernel properties to the PWR-pressing and sintering technology

Step	Investigated Parameter	Objective	
1	Minimization of PVA-Content 30 g/l → 5 g/l feed solution	Decrease of crack susceptibility of pellets	by decrease the PVA-content of feed solution
2	Aging conditions		by extraction the PVA from as cast kernels
3	US treatment of as cast kernels		by US-washing of kernels after aging
4	Drying/calcination conditions 80–1.000°C t: 2–100 h	Minimizing of crushing strength to provide:	by optimization of drying procedure
5	Variation of heavy metal content 300 g/l → 120 g/l	– high green and sinter density – good microstructure	by decreasing the heavy metal content of feed solution
6	Use of pore former material: C amount 50 g/l → 10 g/l		by use of pore formers
7	Addition of a stabilizer for carbon black	Stabilization of the carbon black	by use of THFA

Table 2.3.4: Quality Control plan for chemical purity of $(Th,U)O_2$ pellets

Specified Material Characteristics	Specified Values or Tolerance Limits[1)]	Scope of Testing[2)]
Th + U content	≧ 87.7 wt%	1/K
U content	± 0.1 wt%	1/K
^{235}U	± 10% rel.	1/D
Oxygen/Metal ratio	1.99 – 2.05	1/S
Hydrogen equivalent content	≦ 10 Nmm^3/g Oxide	1/2S
Residual gas content	≦ 40 Nmm^3/g Oxide	1/2S
Impurities content	[3)]	
F	≦ 10 ppm	1/K
Cl	≦ 15 ppm	1/K
N	≦ 30 ppm	1/K
Ca	≦ 100 ppm	1/K
Si	≦ 100 ppm	1/K
Ni	≦ 50 ppm	1/K
Fe	≦ 100 ppm	1/K
C	≦ 100 ppm	1/S
S	≦ 100 ppm	1/S
Boron equivalent value (B, Cd, Dy, Eu, Gd, Li, Sn)	≦ 1 ppm	1/K

Remarks: [1)] according to specification

[2)] K = daily production of the kernel manufacturing line
S = daily production of the sintering line
D = delivery lot

[3)] weight ppm related to Th + U

Table 2.3.5: Calcined kernels characterization

Batch	Apparent Density g/cm^3	Specific Surface m^2/g	Fracture Strength N/kernel	Diameter µm	C ppm	S ppm
P-2201-A	4.2	6.6	1.3	316	95	106
P-2201-B	4.2	6.3	1.1	307	103	73
P-2202-A	4.1	6.6	1.1	307	93	96
P-2202-B	4.1	4.6	1.1	308	92	86
P-2203-A	4.3	4.4	1.3	274	103	64
P-2203-B	4.1	6.1	1.2	273	91	98
P-2204-A	4.1	5.6	1.1	294	103	152
P-2204-B	4.2	5.3	1.3	289	105	130

Table 2.3.6: Physical characterization of ex-gel-C-(Th, 5%U)O_2 fuel pellets process validation test

Property	Scope	Unit	Specified	Observed
Density and Thermal Stability				
Density xi s1	1 x sintering run (AQL = 1.0)	g/cm^3	9.55 ± 0.15	9.54; 0.03
s2				9.57; 0.02
s3				9.59; 0.04
s4				9.60; 0.04
s5				9.58; 0.02
s6				9.56; 0.04
s7				9.64; 0.02
s8				9.64; 0.02
Thermal Stability				
(Resintering test)	1 x sintering run	g/cm^3	≦ 0.20	≦ 0.08
Microstructure				
Pore structure	1 x sintering run			three batches rejected due to fractures and too large macropore fraction
Mean grain size	1 x sintering run	µm	5–25	12–19
Dimensional Requirements				
Diameter xi s1	1 x retification run (AQL = 1.0)	µm	9.11 ± 0.01	9.108; 0.001
Length xi s1	1 x 2 sintering runs (AQL=4.0)	µm	11 ± 1	10.07; 0.03
s2				10.00; 0.03
s3				10.04; 0.07
s4				9.87; 0.05
Dishing xi s1 volume	1 x 2 sintering runs (AQL=4.0)	µm	16 ± 4	17.42; 0.89
s2				17.61; 0.62
s3				18.32; 0.85
s4				17.80; 1.11
Surface Properties				
Surface roughness Ra	3 x rectification runs	µm	2	1.23 1.00 1.25
Surface integrity	10%			Pellets compared to standard: [1]approx. 50% with metallic crystals on one dishing surface [2]1 pellet with a too large surface pore

Table 2.3.7: Chemical characterization of ex-gel-C-(Th, 5%U)O_2 fuel pellets

	Scope	Unit	Specified	Observed
Chemical Composition				
Th Content	1 x Casting run	w/o		> 83.2
U Content	1 x Casting run	w/o		4.37 – 4.45
Heavy metal	1 x Casting run	w/o	≧ 87.77	> 87.8
U Content of heavy metal	1 x Casting run	w/o	5.1 ± 0.1	5.0 – 5.1
Stoichiometry	1 x sintering run	Mol O/Mol U	2.00 – 2.02	2.00 – 2.01
Moisture + H_2-content	1 x 3 sintering runs	$Nmm^3/g(Th,U)O_2$	10	< 20
Impurity Content	1 x 5 sintering runs	µg/g		
F			10	< 5
Cl			15	< 10
C			100	< 86
S			100	< 20
Ca			100	< 30
Ni			50	< 5
Fe			100	< 91

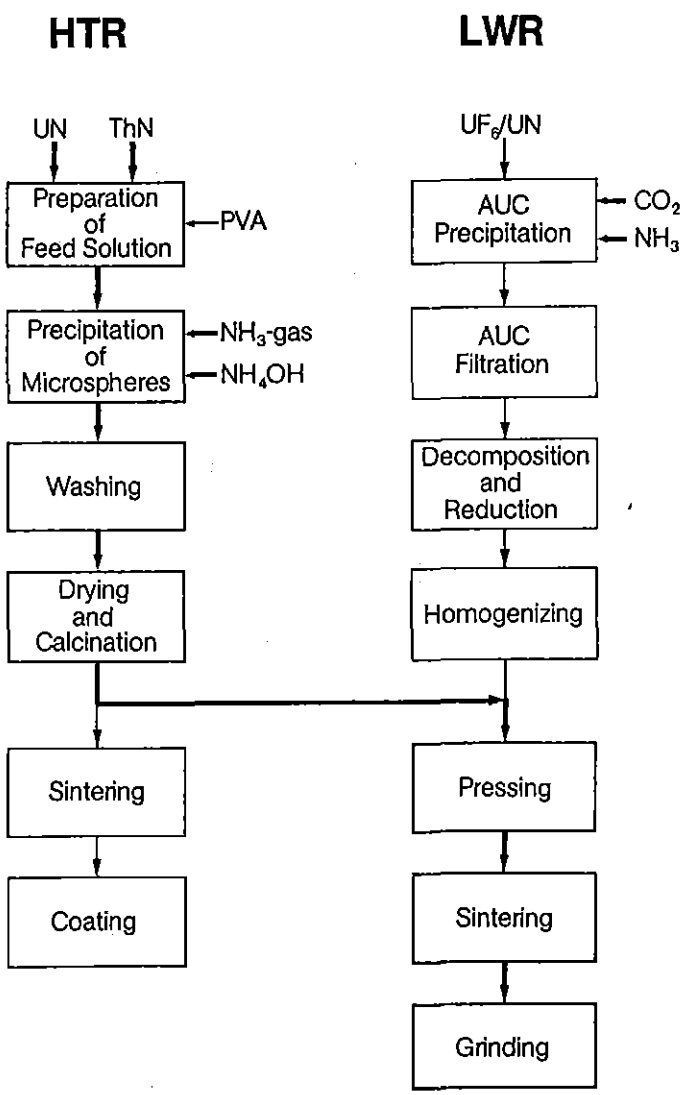

Fig. 2.3/1: Combination of Available Technologies for the Manufacturing of Mixed-oxide Fuel

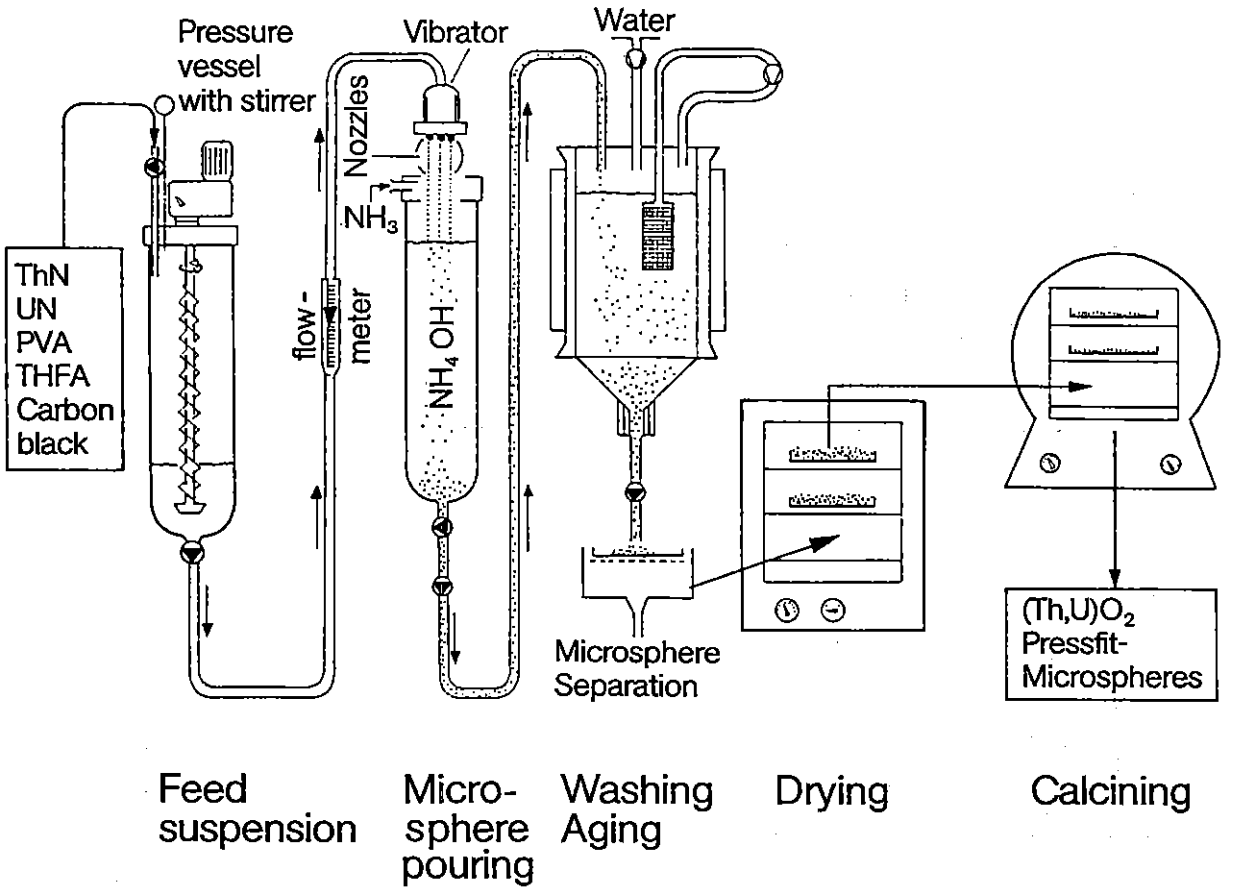

Fig. 2.3/2: Flowsheet of Microsphere Production Process

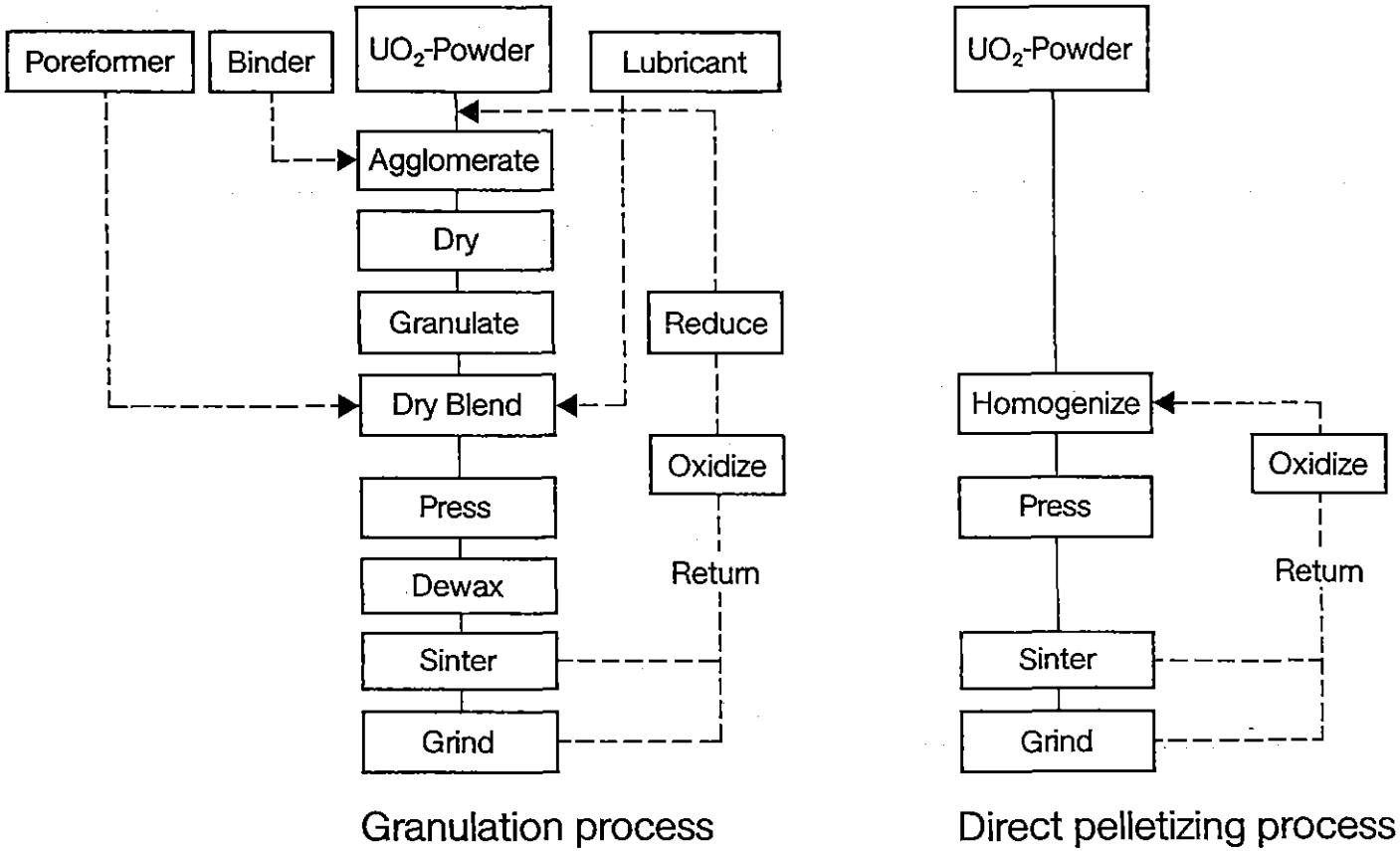

Fig. 2.3/3: UO_2 Pelletizing Processes

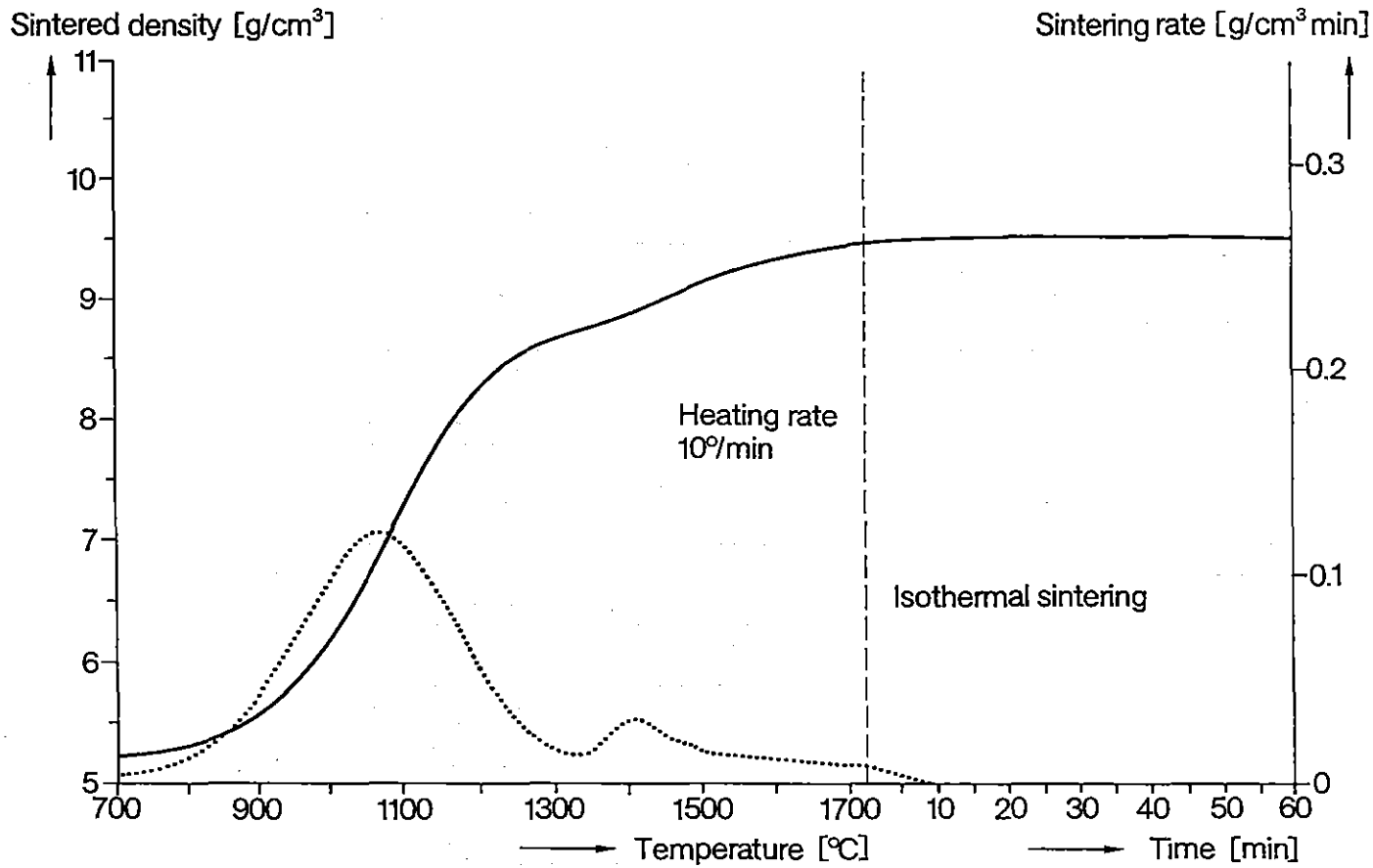

Fig. 2.3/4: Sintering Kinetics of $(Th,U)O_2$ ex-Gel-Pellets with Carbon Addition

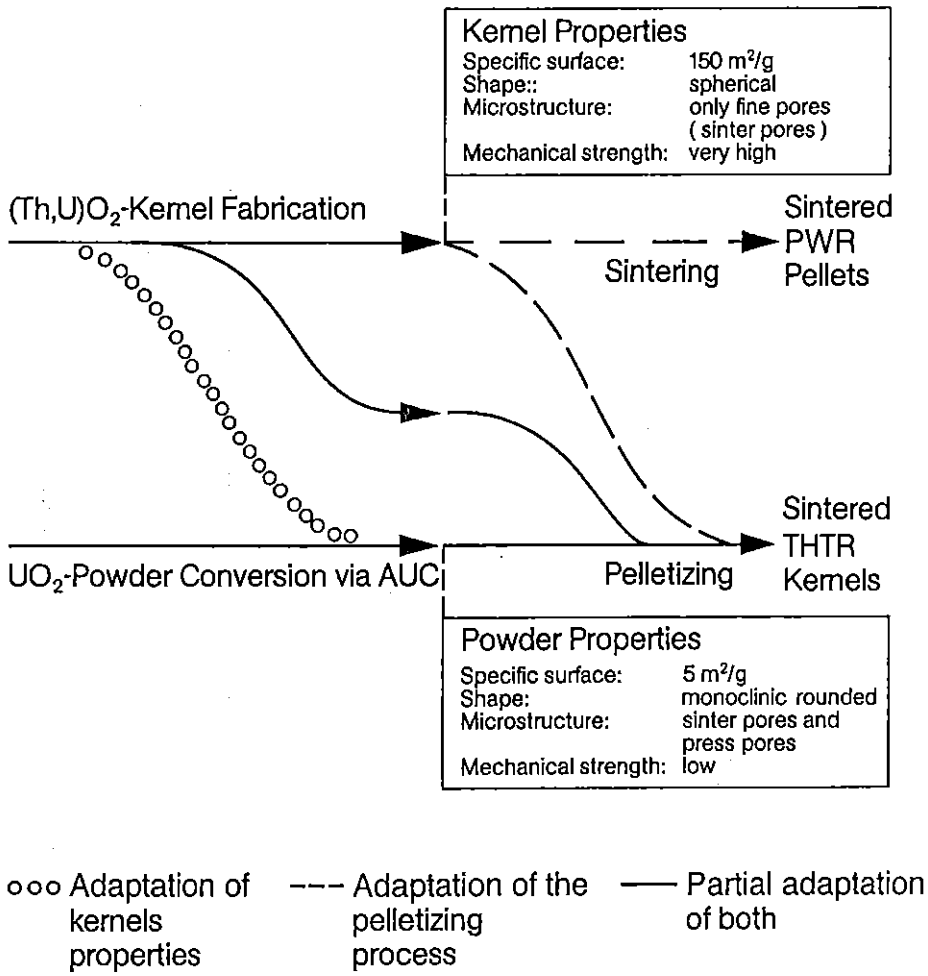

Fig. 2.3/5: Possible Ways of Combining Ex-Gel Kernel Fabrication and PWR-Fuel Pelletizing

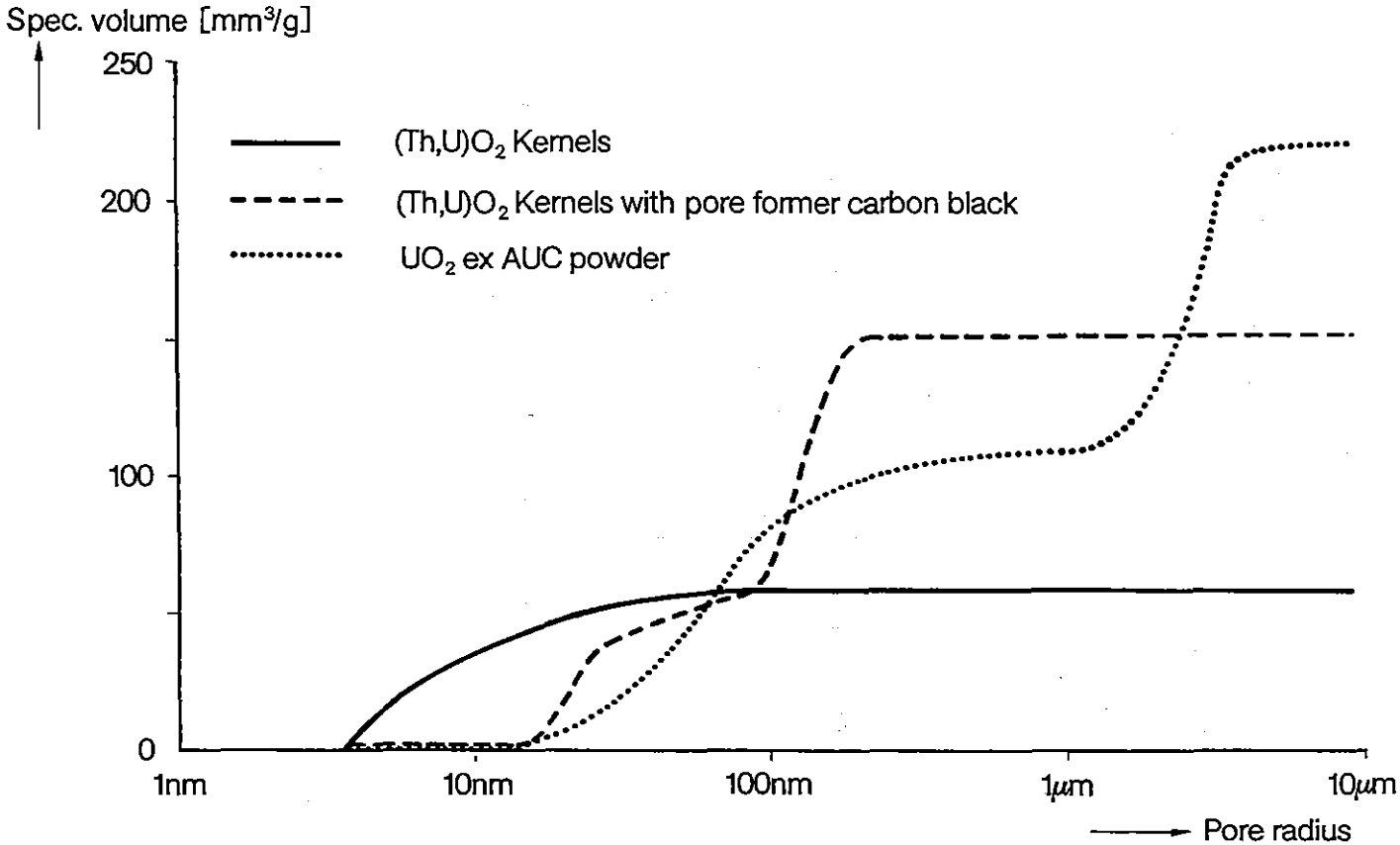

Fig. 2.3/6: Pore Structure of $(Th,U)O_2$-ex Gel Kernels in Comparison to UO_2-ex AUC Powder

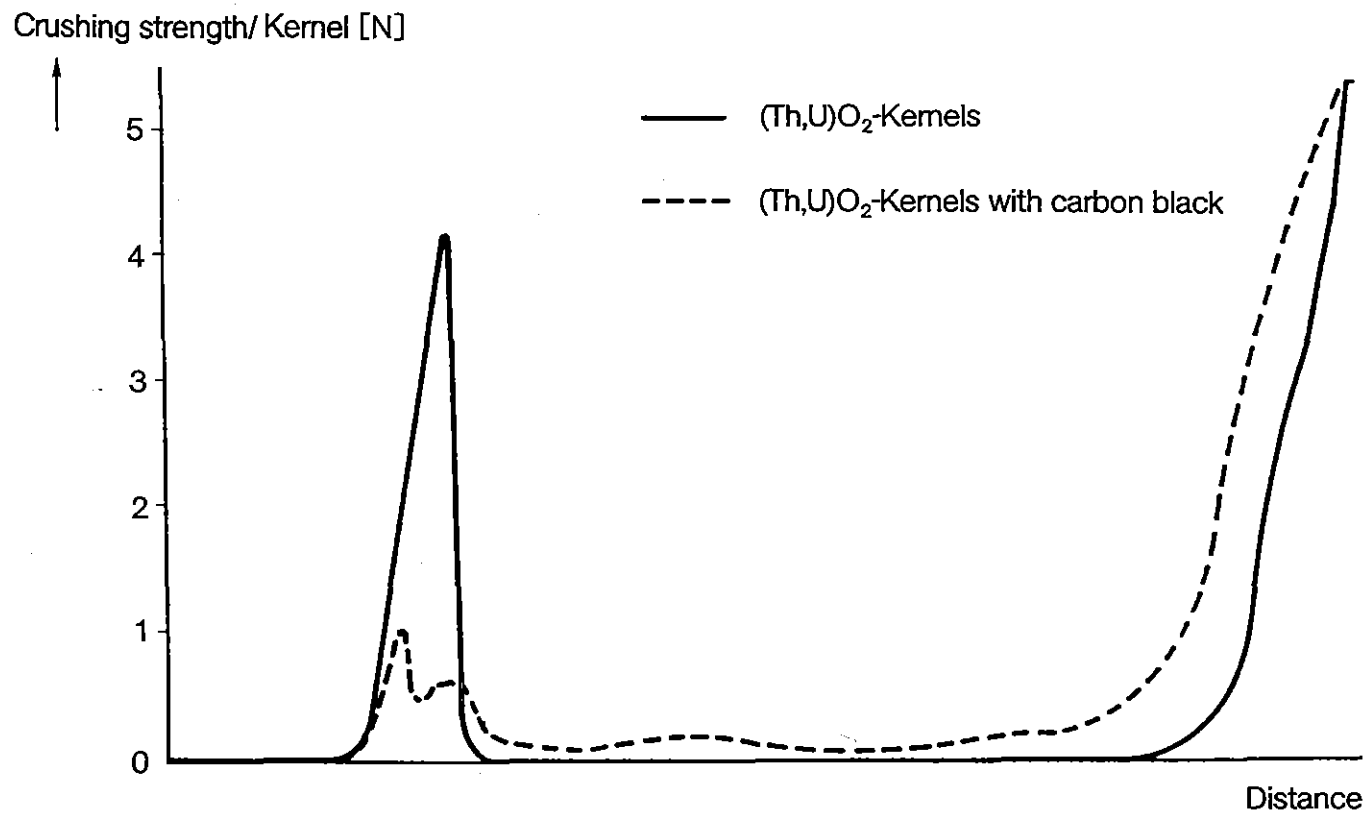

Fig. 2.3/7: Fracture Kinetics of $(Th,U)O_2$ Kernels

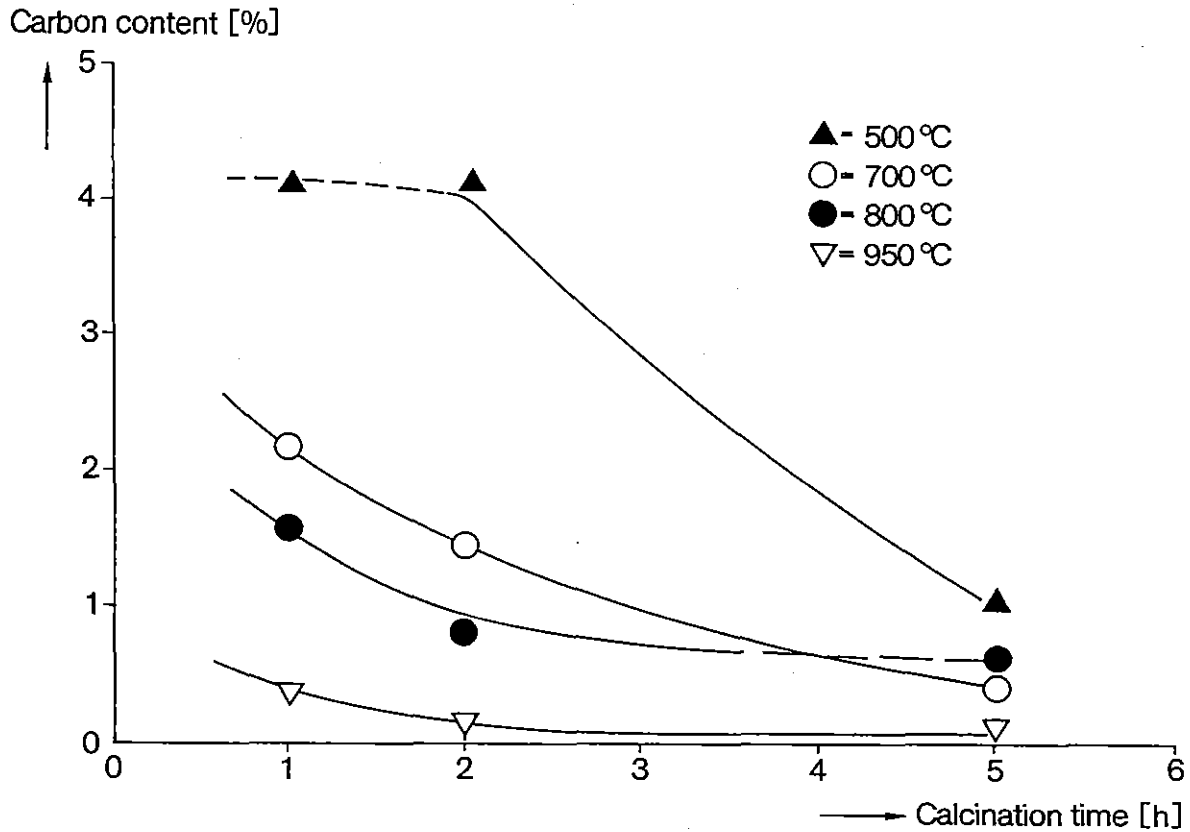

Fig. 2.3/8: Decrease of C-Content in $(Th,U)O_2$-Kernels During Calcination

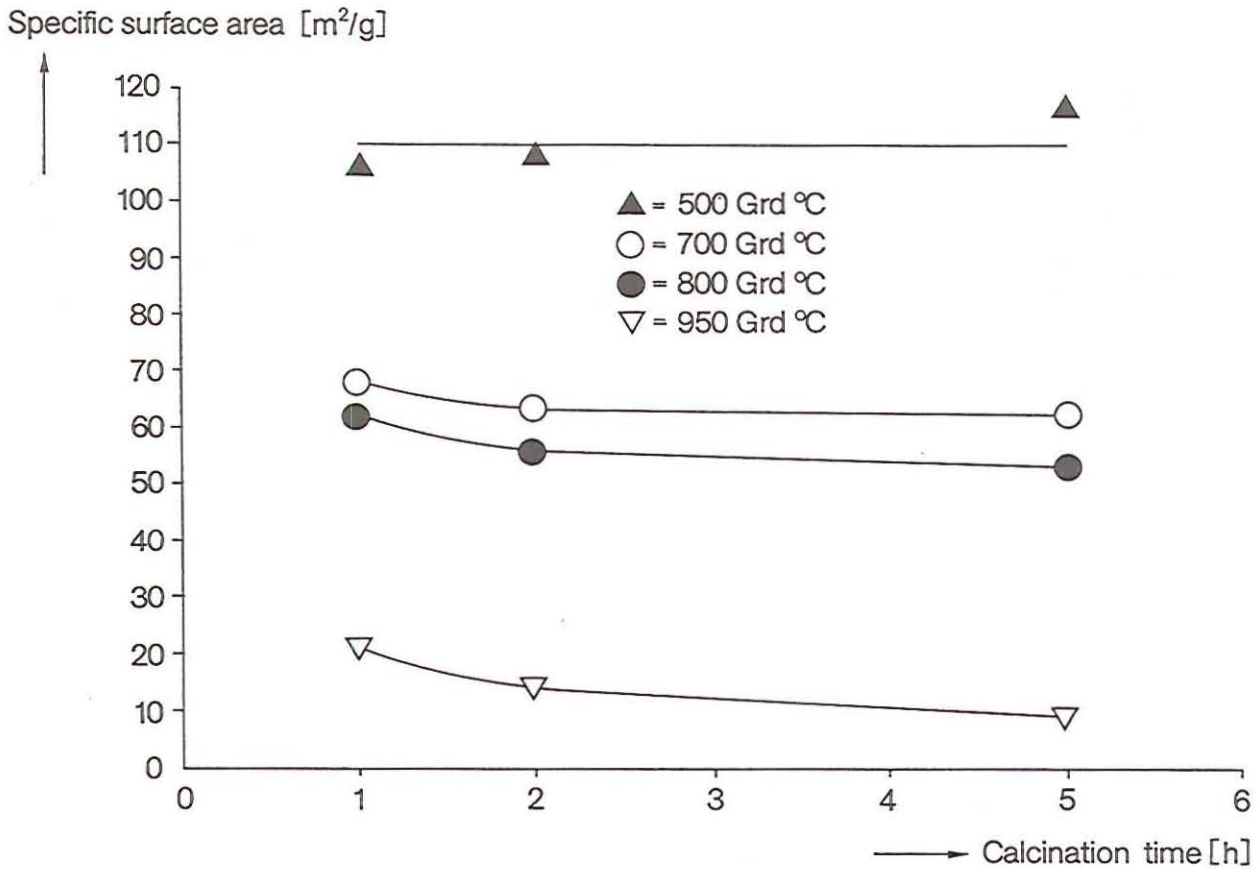

Fig. 2.3/9: Adjustment of Specific Surface Area During Calcination

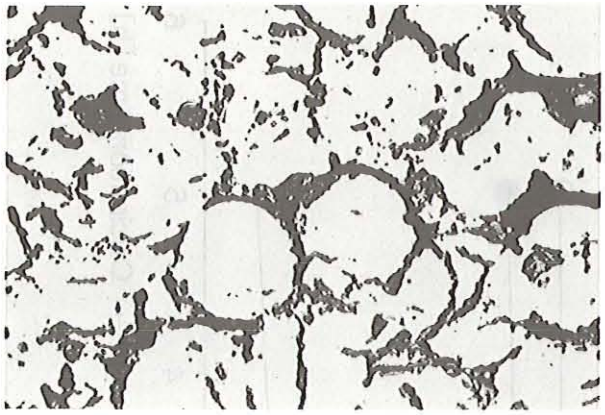

Standard Kernels

30g PVA/l
calcined at 300°C
green density 4,1 g/cm^3
sintered density 8,95 g/cm^3

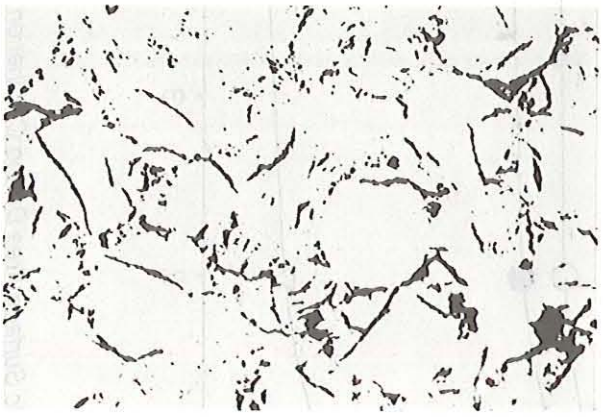

First Optimization

5g PVA/l
calcined at 300°C
green density 5,34 g/cm^3
sintered density 9,32 g/cm^3

Final Optimization

Kernels with Carbon
30g C/ l
10g PVA/ l
calcined 300°C
calcined 800°C
green density 5,42 g/cm^3
sintered density 9,60 g/cm^3

V=100

Fig 2.3/10: Adaption of the Porestructure of (Th,U)O_2-Pellets ex-Gel-Microspheres on LWR-Requirements

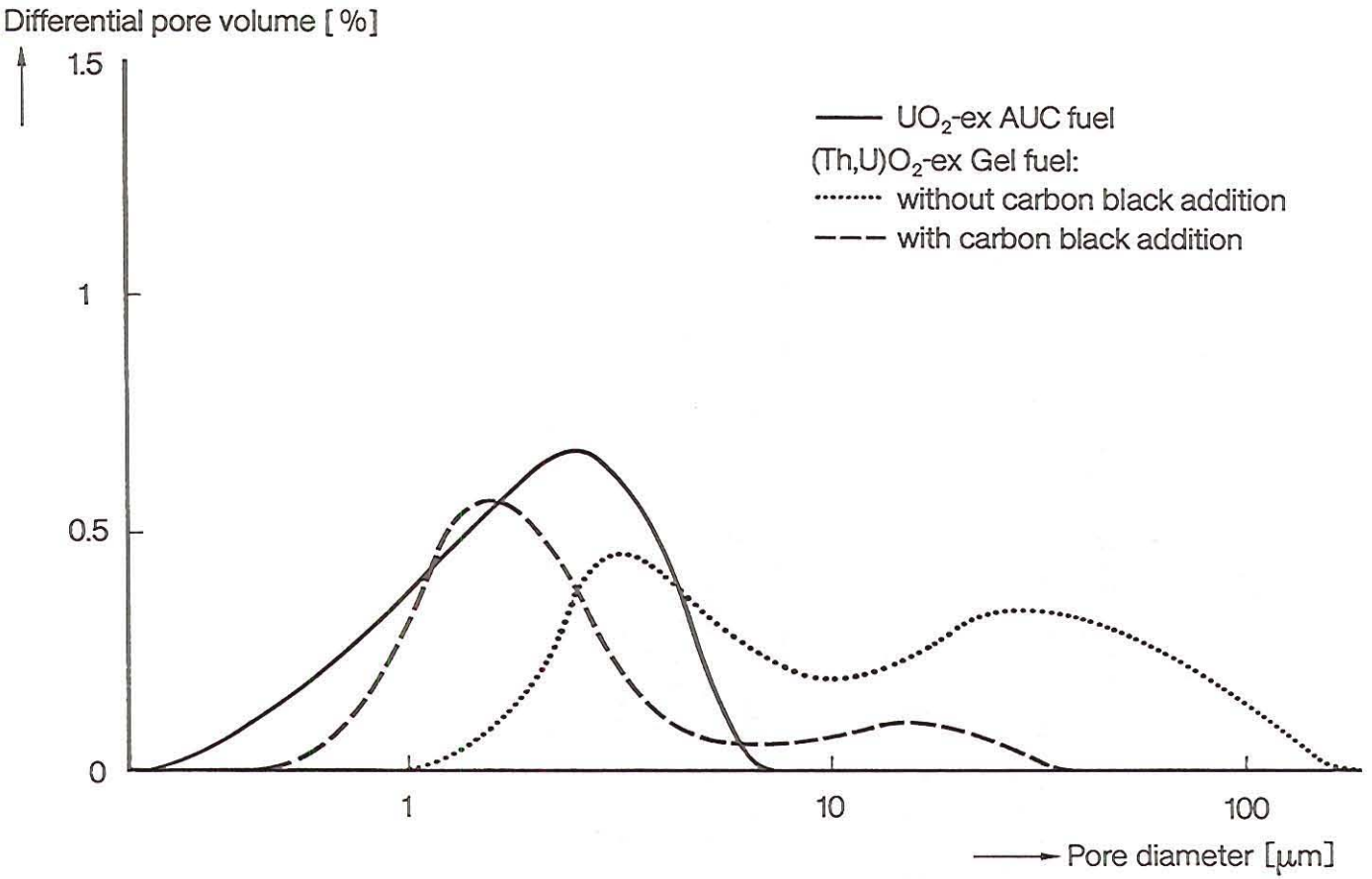

Fig. 2.3/11: Pore Size Distributions of $(Th,U)O_2$-Pellets at Different Stages of Optimization; Comparison with UO_2-ex AUC Fuel

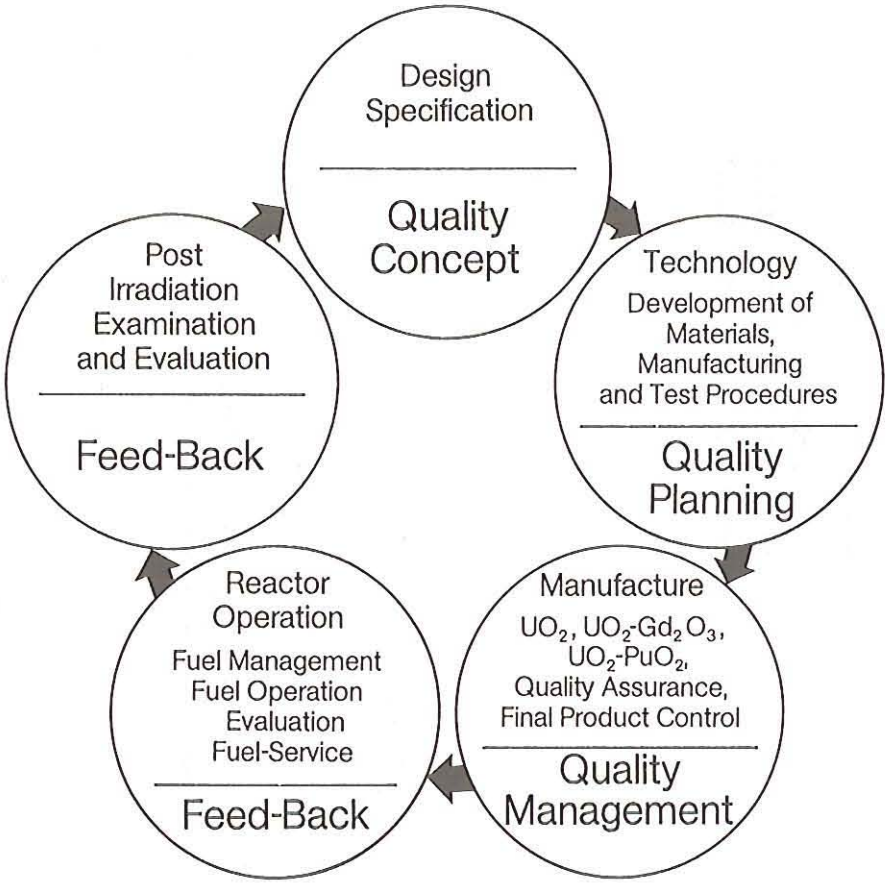

Fig. 2.3/12: Integrated Quality Assurance Circuit for Nuclear Fuel at SAG/KWU Group

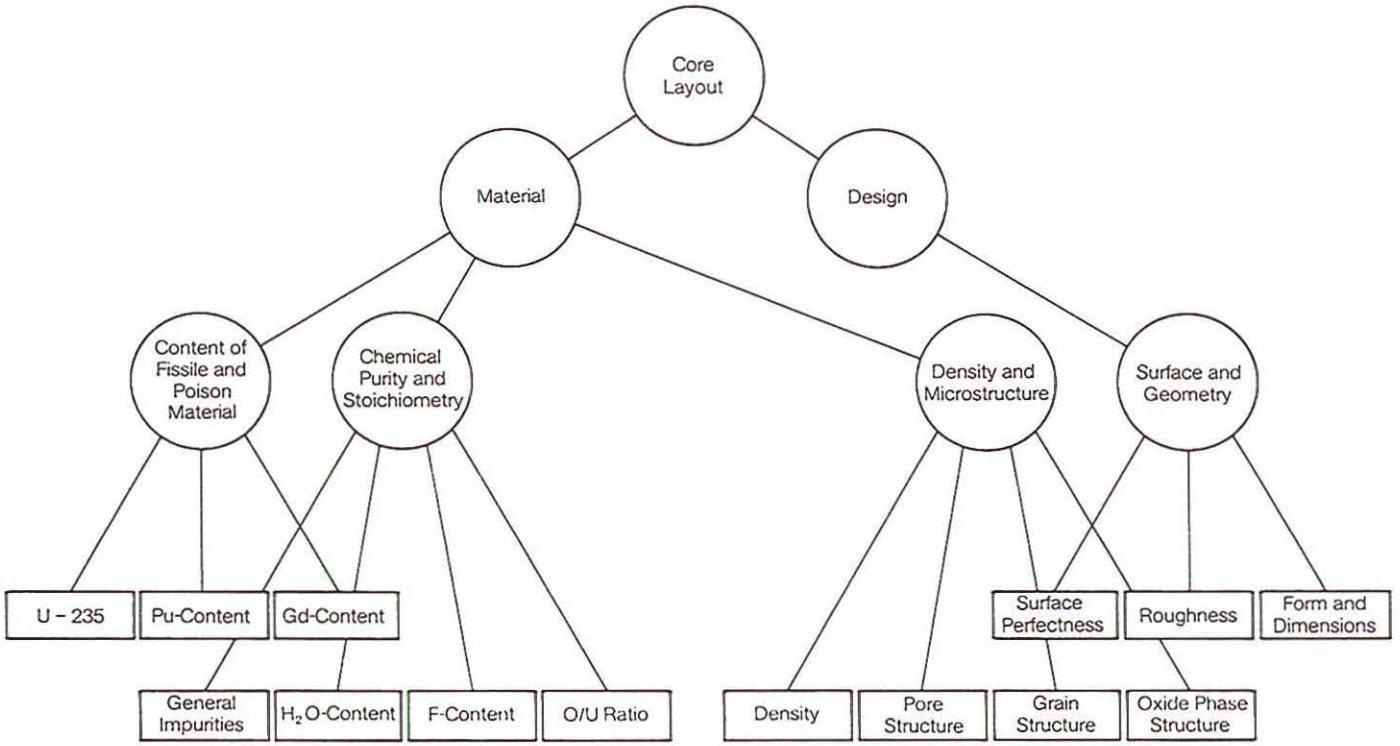

Fig. 2.3/13: Hierachical System of the Requirements Placed on Oxide Fuel for Water Reactors

NUCLEBRÁS	MANUFACTURING AND EXAMINATION SEQUENCE PLAN	ORDER Nº:	CODE:	Nº	
CDTN	PRODUCT	DRAWING Nº	SPECIFICATION Nº	CONTENTS	PAGE Nº
				REVISION	DATE

PROD. STEP	INSPEC. STEP	PARAME TER	PRODUCTION STEP / INSPECTION STEP, QUALITY CHARACTERISTICS	PROCEDURE Nº DOCUMENTS	PRODUCTION-CONTROL METHOD EQUIPMENT	SCOPE	INSPECT BY U	P	G	O	STD. DIN50049	REV.
	1		U-235 Check test		1 X delivery of enriched U							
2			Uranium solution preparation									
3			Casting	TS-011								
4			Drying	TS-026	Board							
5			Sieving	TS-027								
6			Calcination	TS-028	Rotating camera							
	7		Kernel density	TS-023	Pipette method	1 X calcination run					Only for fabrication control	
	8		Specific surface	TS-035	BET	1 X calcination run					"	
	9		Fracture strength	TS-034		30 kernels X calcination run					"	
	10		C + S contents	AT-021; At-022	LECO	1 X calcination run					"	
	11		Kernel diameter	TS-012		30 kernels X calcination run					"	
12			Pelletization prerun	TS-030		5 points with 2 pellets/point						
13			Pressing	TS-031								
14			Sintering	TS-032								

REV.	PREPARED	REVIEWED	REVIEWED	REMARK
DATE				
NAME				

LEGEND: U - Subsupplier
P - Inspection by CDTN
G - Supervision by experts, customers
O - Others

Fig. 2.3/14: Manufacturing and Inspection Sequence Plan of NB/CDTN

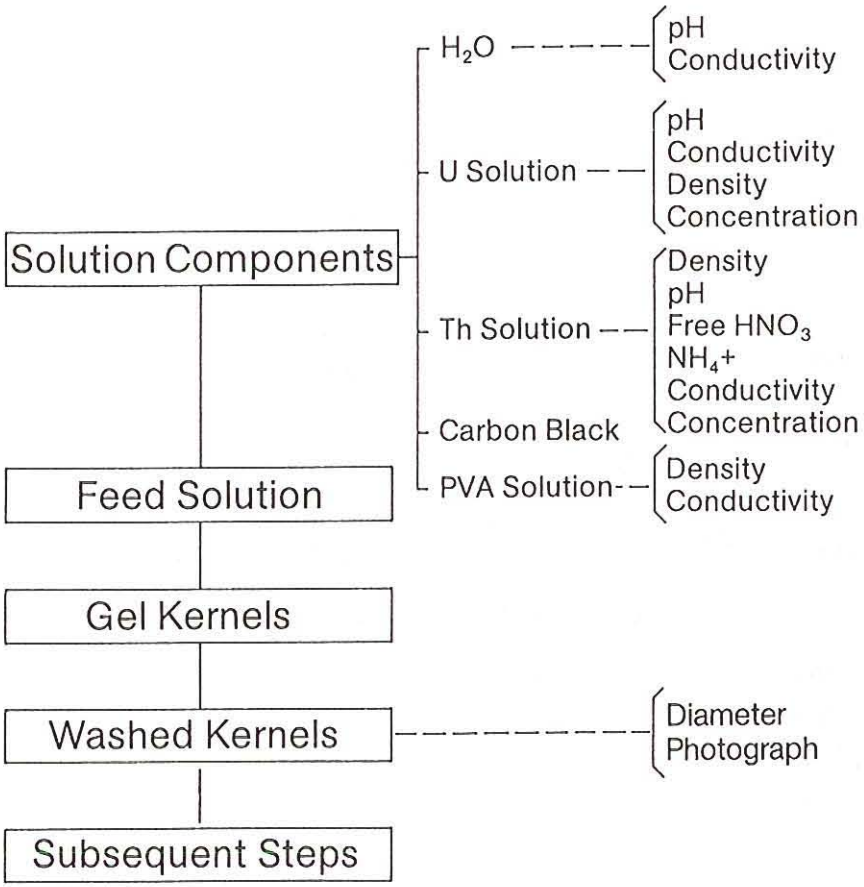

Fig. 2.3/15: Production and Characterization Steps of Gel Kernels

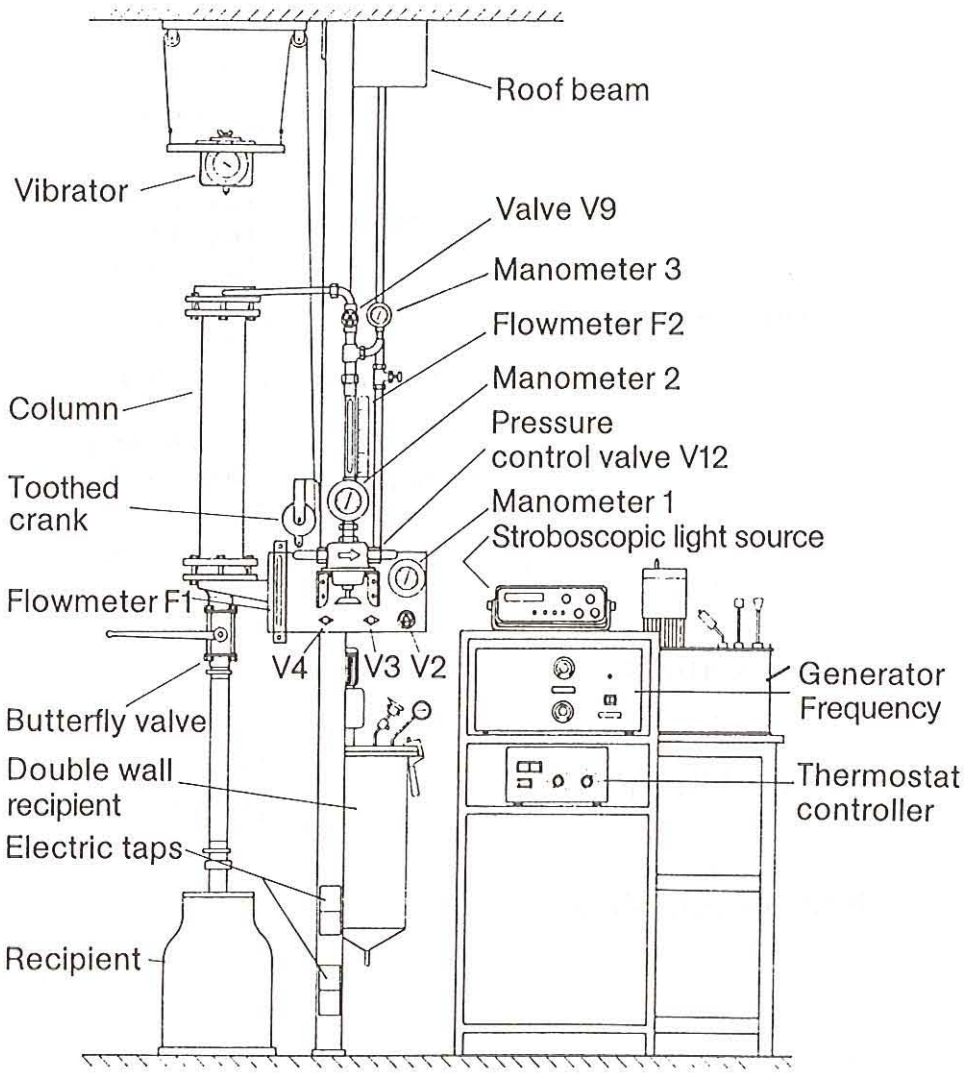

Fig. 2.3/16: Schematic Figure of the Precipitation Column

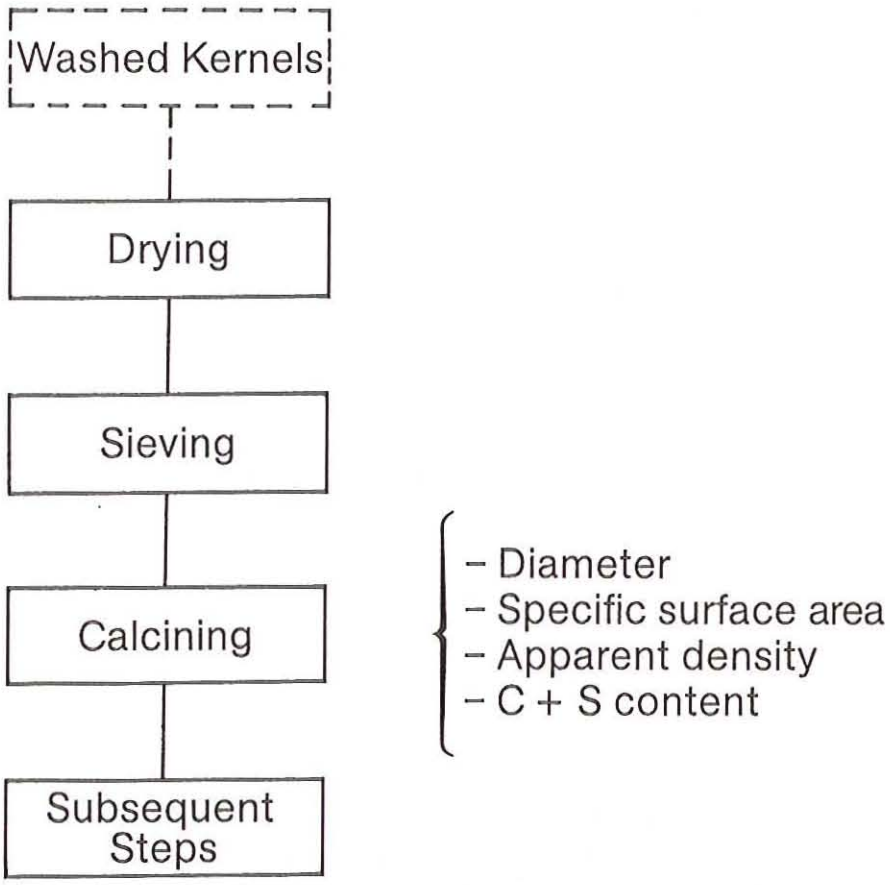

Fig. 2.3/17: Production and Characterization Steps of Calcined Kernels

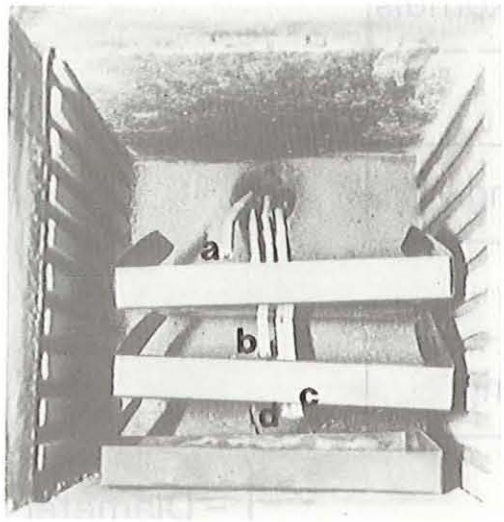

a – Chromel - Alumel temperature record thermocouple
b – Chromel - Alumel temperature record thermocouple
c – Chromel - Alumel temperature record thermocouple
d – Chromel - Alumel temperature control thermocouple

Fig. 2.3/18: Calcination: Arrangement of the Trays and Thermocouples Inside the Muffle Furnance

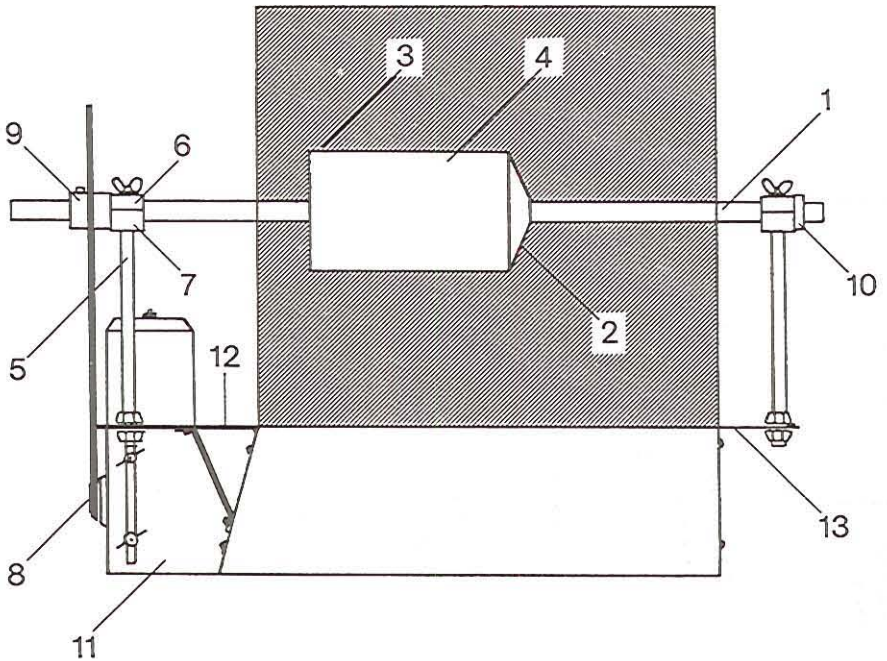

1 Tube axis
2 Bevel cover
3 Cover
4 Sample Vessel
5 Support rod
6 Superior bearing
8 Pinion bushing
9 Crown wheel bushing
10 Limiter ring
11 Motor support
12 Front support
13 Rear support

Fig. 2.3/19: Calcination: Schematic Drawing of the Rotating Tube in the Muffle Furnance

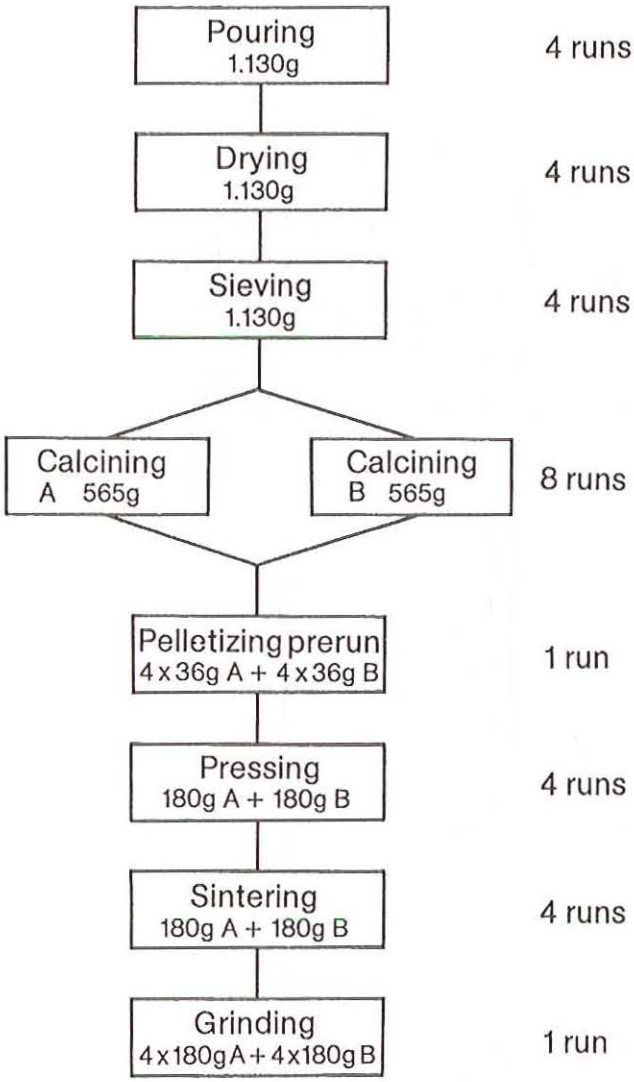

Fig. 2.3/20: Flowsheet for the Process Validation Test

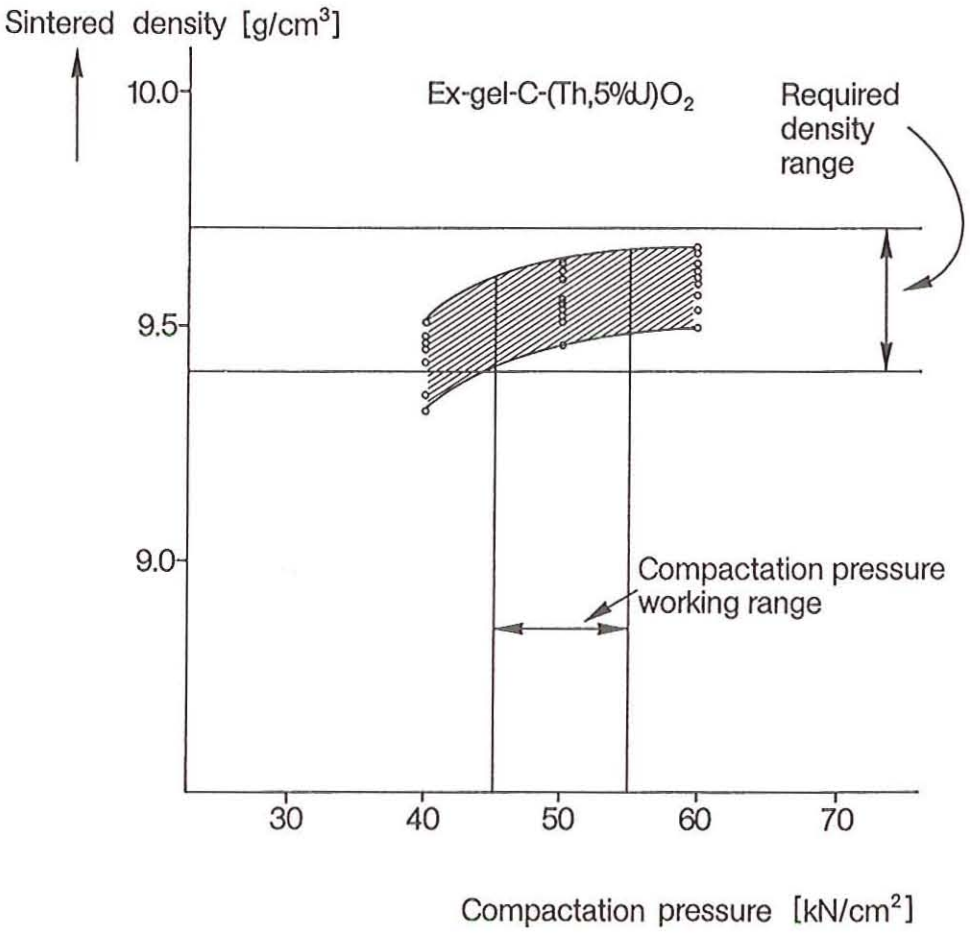

Fig. 2.3/21: Pelletizing Prerun of the Process Validation Test for $(Th,U)O_2$-Pellets

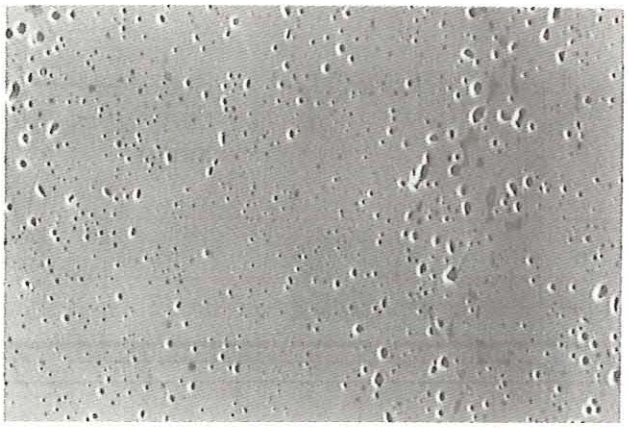

Typical pore structure

⟼ 10 μm

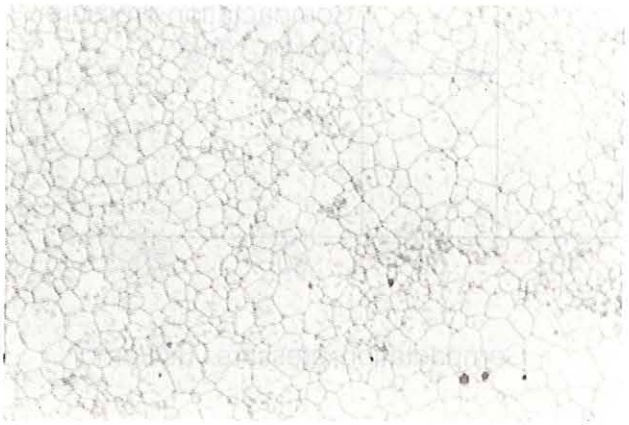

Typical grain structure

1mm ≙ 5μm

Fig. 2.3/22: Pore Structure and Grain Structure from the (Th,U)O_2-Fuel Process Validation Test

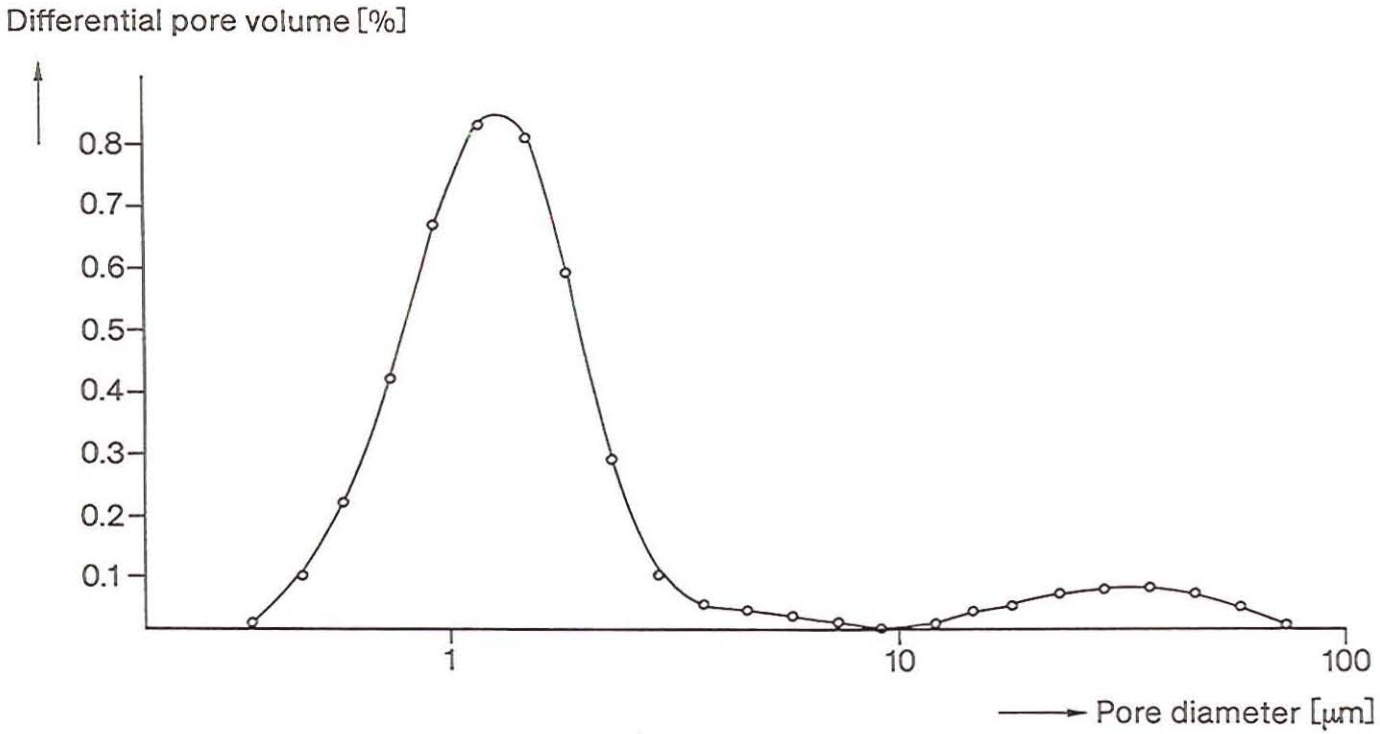

Fig. 2.3/23: A Representative Pellet Pore Size Distribution of $(Th/U)O_2$-Fuel from Validation Test

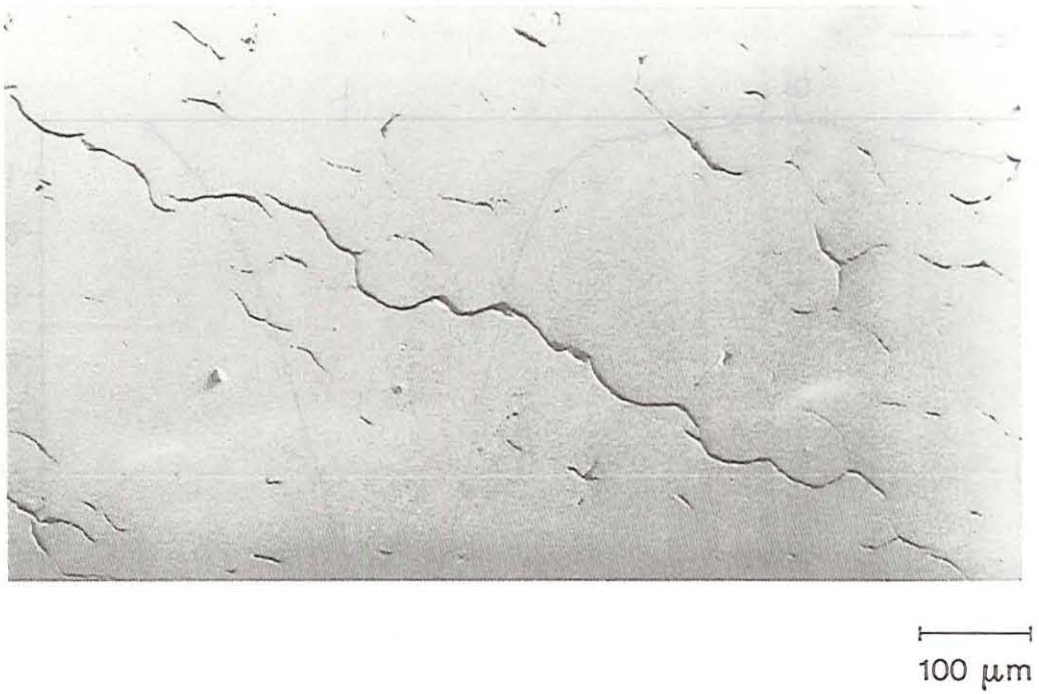

Fig. 2.3/24: Cracks inside of Pellets from Validation Test for (Th,U)O_2-Fuel Manufacturing

2.4 Transfer of $(Th,U)O_2$ Fuel Technology to $(Th,Pu)O_2$ Technology

The advantages of the Th/Pu fuel cycle as outlined in chapter 2.1 lead to the need for developing a suitable manufacturing technology. In the first attempt this has been done using cerium as simulating material for plutonium for reasons of easier handling and cost saving.

2.4.1 Plutonium simulation by means of cerium

ThO_2 forms with CeO_2 – similar as with PuO_2 – a continuous series of solid solution of the fluorite FCC phase for which Vegard's rule is valid [2.4-1, 2.4-2, 2.4-3].

The similarity of the phase diagrams is caused by the isotype of CeO_2 with PuO_2 and the nearly identical cation radii. Besides, the lattice constants (0.5395 nm for PuO_2 and 0.5411 nm for CeO_2 compared to 0.5597 nm for ThO_2) are close together [2.4-2, 2.4-3].

A further similarity of PuO_2 and CeO_2 shows up in the behaviour against hydrogen at higher temperatures, where in both cases up to stoichiometric oxides of the formula PuO_{2-x} and CeO_{2-x} (with x less or equal to 0.3) may occur [2.4-2, 2.4-3].

First of all the applicability of Ce as a simulator for Pu in the mixed system with ThO_2 has to be proven with respect to phase diagrams and physical and chemical properties.

Physical properties

Due to the valency change of the cerium ion two oxides exist: CeO_2 and Ce_2O_3. They can be converted into each other in the temperature range between 700 and 1,250°C by reaction with H_2 or O_2.

CeO_2 is a brown white powder. The oxide forms a fluorite lattice, the density is 7.1 g/cm^3.

Ce_2O_3 is a green gray powder. The oxide forms a hexagonal lattice like La_2O_3, the density is 6.9 g/cm^3. High temperature X-ray diffraction graphs revealed in pure H_2 that hexagonal Ce_2O_3 is present at 1,150°C [2.4-4].

CeO_2 is isomorphic like UO_2, PuO_2 and ThO_2.

Chemical properties

Starting material for the coprecipitation with $Th(NO_3)_4$ is $Ce(NO_3)_3$ with trivalent cerium since a nitrate with 4-valent cerium does not exist.

By precipitation with ammonia a white cerium (III) oxide hydrate ($Ce_2O_3.xH_2O$) is received that can already be oxidized in air.

Formation of CeO_2

The heat treatment of cerium (III) oxide hydrate in air leads to the generation of CeO_2 in the range between 700 and 1,000°C.

Formation of Ce_2O_3

Ce_2O_3 is generated by reduction of CeO_2 with H_2 above 1,000° C. The equilibrium pressures P_o over CeO_x (in the range $1.72 < x < 2.0$ for the temperature range from 650 to 1,300° C are presented graphically in [2.4-4].

The system ThO_2-CeO_2

A deviation from the ideal behaviour of the mixed crystal ThO_2-CeO_2 is observed only at high temperatures in vacuum and under hydrogen. As known from the literature [2.4-1, 2.4-3] the 4-valent cerium in the system $Th_xCe_{1-x}O_2$ is partly reduced to trivalent cerium by hydrogen at temperatures between 800 and 1,400° C. The cerium (III) fraction increases with increasing temperature. For all systems investigated in the range of the boundary composition $Th_{0.75}Ce_{0.25}O_{1.97\text{-}1.89}$ and $Th_{0.2}Ce_{0.8}O_{1.82\text{-}1.63}$ single phase areas were found with fluoride structure.

As can be seen in the preliminary and very incomplete phase diagram of the system ThO_2-CeO_2-Ce_2O_3 at 1,200° C (Figure 2.4-1) the phase boundary in the ternary system lies close to the binary system ThO_2-CeO_2. The solubility of Ce_2O_3 in ThO_2 amounts to about 45 mol%.

In completion of the investigations carried out at the ThO_2-CeO_2-Ce_2O_3 system at temperatures up to 1,200° C (see [2.4-5 and 2.4-6]) the following systems were measured by X-ray diffractometry after a two hours' temperature treatment up to 1,200° C in hydrogen atmosphere:

a) thorium oxide;
b) thorium oxide + 6.5 mol % cerium oxide;
c) thorium oxide + 29.3 mol % cerium oxide.

The evaluation of the X-ray diffraction graphs led to the following results:

a) the system thorium oxide 6.5 mol% cerium oxide exhibits a single phase CaF_2 structure like pure ThO_2;

b) the respective lattice constants are:
for the ThO_2 crystal $a_o = 0.5600 \pm 0.0001$ nm (3)
(literature value 5.597 ± 0.001 nm)
for the Th/Ce mixed oxide $a_o = 0.5596 \pm 0.0002$ nm (5)

Behind the a_o value the number of measurements is given in brackets which were considered at the standard deviation calculation.

In contrast to the above system the X-ray diffraction graphs of the system ThO_2/29.3 mol % cerium oxide show additional reflexes indicating a second fluorite lattice structure ThO_2/Ce_2O_3 mixed crystal. The lattice constants calculated from these graphs are:

a_o (ThO_2/CeO_2): 0.5554 ± 0.0006 nm (10)
a_o (ThO_2/Ce_2O_3): 0.5611 ± 0.0004 nm (3)

The numbers in brackets behind the a_o values indicate the number of measurements considered for the standard deviation calculation.

While the solid solution of the system ThO_2/6.5 mol % cerium oxide could only be detected in the monophase area, two mixed oxide phases exist side by side in the system ThO_2/29.3 mol % cerium oxide: ThO_2/CeO_2 and ThO_2/Ce_2O_3.

On the base of these results the following statements can be made:

a) in the system thorium oxide/cerium oxide with a cerium oxide content of 29.3 mol% the ThO_2/Ce_2O_3 solid solution is just barely detectable by X-ray diffractometry;

b) in the case of the thorium oxide/cerium oxide system containing 6.5 mol % cerium oxide, however, no second phase can be detected by X-ray diffractometry, obviously because of the too low cerium concentration.

In a new work [2.4-7] the system CeO_{2-x} ($x \leq 0.3$) is investigated by means of mathematical models, assuming that a mixture of two species exists in the fluorite lattice due to the large deviation from stoichiometry (e.g. CeO_2 and $Ce_{0.8}O_{1.2}$) one of which exhibiting oxygen defects. As a result the presence of a miscibility gap deficiency at 704°C is stated.

2.4.2 Basic technologies for plutonium processing

The powder production for Pu-containing fuel has to take into account different starting material, the ability to recycle fabrication returns in oxide form, and the requirement to have the plutonium soluble in nitric acid. The plutonium is delivered either in the form of a nitrate solution or in the form of PuO_2 powder.

2.4.2.1 The mixed oxide concept

The fabrication methods for the pressfeed mixed oxide (MOX) powder or particles comprise the following [2.4-8]:

a) mechanical mixing of the oxide powder;

b) co-precipitation of $(U,Pu)O_2$ powder;

c) preparation of spherical particles (e.g. by the gelation process).

The first of these processes has been routinely applied since 1965 by KWU/ALKEM for BWRs, PWRs and PHWR (MZFR Karlsruhe). The PuO_2 powder manufactured by the oxalate process [2.4-9] was mixed into flowable UO_2 powder from the AUC process. Pelletizing and in-reactor behaviour were at least comparable with that of standard UO_2 fuel. However, results from reprocessing of such fuel showed a residual insolubility of the plutonium in nitric acid exceeding that of spent UO_2 fuel. To improve the dissolution behaviour of spent MOX fuel, the simple mechanical mixing of the pure oxide powders UO_2 and PuO_2 was replaced by two modified manufacturing processes:

a) the AUPuC Ammonium Uranyl Plutonyl Carbonate) co-conversion process and

b) the OCOM (Optimized Co-Milling) process [2.4-10].

The flowsheets of these processes including pelletizing are shown in Figure 2.4/2.

For the AUPuC co-conversion process, plutonium nitrate and uranyl nitrate are mixed and oxidized. Then in analogy to the AUC conversion process [2.4-10, 2.4-11] the precipitation, filtration and calcination is performed. The chemical equations are:

a) for the precipitation of AUPuC:
$(U,Pu)O_2(NO_3)_2 + 6NH_3 + 3CO_2 + 3H_2O \longrightarrow (NH_4)_4[(U,Pu)O_2(CO_3)_3] + 2NH_4NO_3$

b) for the calcination:

$$(NH_4)_4[(U,Pu)O_2(CO_3)_3] + H_2 \longrightarrow (U,Pu)O_2 + 4NH_3 + 3CO_2 + 3H_2O$$

The resulting $(U,Pu)O_2$ powder exhibits a complete solid solution of uranium and plutonium oxide and a particle size distribution and particle morphology comparable to UO_2 powder from the AUC conversion process. The co-converted MOX powder shows good flowability properties, high sintering activity, low impurity content and leads to MOX pellets with a solubility greater than 99%. The powder properties are controlled by the process parameters of the precipitation and calcination steps.

The OCOM process is used in the case of plutonium supply in the oxide form. The press-feed is obtained by co-milling UO_2, PuO_2 or $(U,Pu)O_2$ in a ball mill with a milling aid. Since this procedure is applicable not only for powders, larger amounts of hard scrap can be recycled by the use of the OCOM process.

Processing and sintering of MOX pellets follow the same techniques as are usual for UO_2 and UO_2/Gd_2O_3. The only difference is the use of a non-burnable mixture of hydrogen with nitrogen or argon as sintering atmosphere which is required for a safe operation in the glove-boxes.

The quality control of UO_2/PuO_2 pellets is in principle equivalent to that of pure UO_2 and UO_2/Gd_2O_3, but two special characteristics of UO_2/PuO_2 fuel have to be considered separately:

a) the Pu-homogeneity;
b) the Pu-dissolution during reprocessing.

The **Pu-homogeneity** is defined by its macroscopic distribution, i.e. the Pu-content of individual pellets and by the maximum diameter of Pu-containing particles. As an example the Pu-content is specified with a tolerance limit of +2.5% relative to a Pu_{fiss}-content of 3.5 %.

The **Pu_{fiss}-content** is defined by

$$\frac{Pu_{fiss} \times 100}{U + Pu} \text{ \% (mass fraction)},$$

where Pu_{fiss} is the sum of fissile isotopes. The measurement of the Pu_{fiss}-content is performed by Pu isotopic analysis (either by mass or by gamma spectrometry), by Pu and (U+Pu) analysis. (U+Pu) is gravimetrically determined. At ALKEM various test methods for the determination of the Pu content have been compared to each other with respect to accuracy and expense [2.4-12]. Gamma-spectrometry, photometry and potentiometry turned out to have the best cost-benefit relationship.

The microscopic Pu distribution, after having been qualified by extended microprobe investigations [2.4-13], is now routinely determined by alpha-autoradiography from microsections of the pellet. The maximum allowable particle diameter is approximately 300 µm when the Pu_{fiss} content in the particle is 30% (mass fraction).

The **Pu solubility** is defined by

$$\left(1 - \frac{\text{Pu mass not dissolved}}{\text{Pu mass in the sample}}\right) \cdot 100 \text{ (\% mass fraction)}$$

The test conditions for a standard test [2.4-14] are the following: initial HNO_3 concen-

tration 7 mol, boiling temperature with backflow, 6 hours dissolution time, 1 hour cooling time below 60° C, sample size about 30 g, filtration with a 1 μm filter. UO_2/PuO_2 pellets from the AUPuC and OCOM process showed a Pu solubility greater than 99.5% when investigated in hot cell solubility tests [2.4-15].

2.4.2.2 The master-mix concept

In the MOX fabrication route for LWR usually the master-mix concept is applied rather than the homogeneous oxide concept. Because of the low Pu_{fiss} content of about 3 to 4 wt% in LWR fuel, in the case of homogeneous oxide the total amount of fertile material (UO_2 or ThO_2) with more than 90% has to be handled under remote conditions which increases the fabrication costs.

By using the master mix concept, the amount of remote handled fertile material can substantially be lowered: the Pu is mixed in a high amount to UO_2 or ThO_2 to give the so-called master-mix preproduct, which then is admixed in a suitable concentration to pure UO_2 or ThO_2 (see Figure 2.4/2).

The master-mix can be prepared

a) by direct co-precipitation of 40% Pu-nitrate and 60% U-nitrate via A(U,Pu)C-process;

b) by co-milling of 30% of PuO_2 and 70% UO_2 where Pu-containing scrap up to high amounts can be processed simultaneously according to the OCOM-process. Though the co-milled master-mix is not free flowing, it can be homogeneously mixed to free flowing UO_2-powder which becomes the flowable MOX pressfeed powder without any separate granulation step.

In the case of a gelation technique for fuel fabrication, the application of the master-mix concept should be feasible in the same way as used in the A(U,Pu)C-process. Only the admixing behaviour of two different types of microspheres has to be proven.

2.4.3 Objectives, problems and solutions

2.4.3.1 Requirements for PWR fuel pellets

The basic requirements for Pu-containing fuel pellets for PWR are the same as discussed in section 2.3.2.1 for UO_2 and $(Th,U)O_2$. This relates also to the oxide phase structure. In the case of the mixed oxide concept, where the gelation-process ensures a homogeneous Pu-distribution, the requirements are inherently fulfilled. Fuel which is fabricated via the master mix concept shows microscopically inhomogeneous Pu_{fiss} distribution with the consequence that local fissioning in the Pu-containing kernels is higher than in the surrounding pure fertile material. These so-called „hot-spots" have to be limited in size and Pu_{fiss}-concentration. The resulting specification values can be seen in Table 2.4.1 together with all boundary conditions, which are of concern in the master-mix concept. The question of good chemical solubility of Pu-containing fuel during reprocessing is not relevant for $(Th,Pu)O_2$.

2.4.3.2 Scoping studies

The mixed oxide concept

In a first attempt, (Th,6% Ce)O_2 ex-gel pellets were manufactured. Preparation of the feed solution, pouring, drying and calcining have been performed with the (Th,U)O_2 standard conditions, the properties of the kernels showed to be similar to those of (Th,U)O_2. Pressing of the kernels at usual green densities of about 50% TD and sintering under standard conditions (1,720° C – 2h – H_2) yielded high sintered densities, but a tendency for the formation of cracks all over the pellet volume has been observed. A first idea, that this should be due to stoichiometry effects during heat up and/or cooling down and consequently should be compensated for by adjusting the oxygen potential in the sintering gas, or by the use of high heating and cooling rates during sintering, was revealed to be true.

The master mix-concept

(Th,Ce)O_2 with the master concentration of 13% cerium and pure ThO_2 have been prepared under standard conditions to perform a pelletizing feasibility test for the master-mix concept. It was soon revealed that ThO_2 kernels had different properties than the (Th,Ce)O_2 kernels, especially a higher fracture strength and a different sintering behaviour resulting in another pore structure. Thus, emphasis should be given to the adaptation of the ThO_2 kernel properties.

2.4.3.3 Solutions to be investigated

The following possibilities have been investigated

a) co-precipitated mixed oxide concept;
b) „master-mix" concept.

The co-precipitated mixed oxide concept has been investigated in the cerium concentration range of 4 to 6 w/o as required for PWR reactors.

The master-mix concept has been investigated at the master concentration of 13 w/o cerium with the mixing ratio ThO_2/(Th,13w/oCe)O_2 of 1.17/1.

Mixed oxide concept

The manufacturing of (Th,4-6 w/o Ce)O_2 gel kernels has been performed under the standard pouring conditions:

a)	Heavy metal content	: 200 g/l
b)	PVA content	: 5 g/l
c)	FR-101 carbon black content	: 30-60 g/l
d)	Ethanol content	: 56.5 g/l
e)	Ammonia concentration	: 3-5 M
f)	Nozzle diameter	: 391 µm
g)	Frequency	: 1,200 hertz
h)	Flowrate	: 14-15 ml/min

Several batches of calcined kernels have been manufactured. The calcination conditions ranged within 700 to 950° C /2 to 24 h. The characterization data are shown in Table 2.4.2. Figure 2.4/3 shows a typical microstructure of these kernels.

Sintered pellets have been manufactured. The sintering characteristic curve is shown in Figure 2.4/4.

The results have shown:

a) in general very high sintered density even at low green densites. In moist sintering atmosphere the density is 0.1 g/cm^3 higher than in a dry H_2-atmosphere;

b) crack formation in some pellets (Figure 2.4/5).

A way to decrease the pellet density has not been investigated. Two possible ways are by:

a) decreasing the specific surface of the kernels by increasing the calcining temperature;

b) controling the sintering kinetics by varying the oxygen partial pressure of the sintering atmosphere.

The crack formation has been extensively investigated. The results have shown that the crack formation is reproducible only in a moist atmosphere. Examples for the crack standards are shown in Figure 2.4/5 in comparison with crackfree pellets, Figure 2.4/6. The cracks should be due to the already presumed relation between pellet cracks and stoichiometry during the sintering cycle. This behaviour is known in other mixed fuel systems such as U-Gd-O which has been analysed by means of noise emission techniques.

The explanation is based on the possibility that during the heating of the pellets the temperature gradient that is formed, is overlapped with an O/M – gradient (Figure 2.4/7). Both gradients, because of the related lattice expansion or contraction, lead to tension or compression in the pellet which at the worse overlapping result as a crack.

In the case of (Th,Ce)O_2, dried H_2 as sintering gas seems to stabilize the stoichiometry more rapidly than an H_2/H_2O mixture. No quantitative statement is possible because there are insufficient thermodynamic data available for the system Th-Ce-O.

Master-mix concept

The pouring of (Th,13 w/o Ce)O_2 gel kernels has been performed by setting the flowrate at 12 ml/min and adding a less viscous and dense organic liquid (e.g. n-duodecanol) to the ammoniacal solution in the column. The other parameters have been settled according to the standard pouring conditions.

The pouring of the ThO_2 gel kernels has been performed according to the standard pouring conditions.

Several batches of calcined kernels have been manufactured. The calcination conditions ranged within 900 to 1,100°C/2h. The characterization data are shown in Table 2.4.3. Figure 2.4/8 shows a typical microstructure of these kernels.

Sintered pellets have been manufactured. Kernels of ThO_2 and (Th,13w/oCe)O_2 have been put into a plastic bottle and mixed by rotating it around the longitudinal and perpendicular axes by hand for approximately 5 minutes.

Two groups of kernels have been pressed:

a) group I (different densities):
ThO_2 kernels of 4.6 g/cm³ density
+ (Th,13w/oCe)O_2 kernels of 4.2 g/cm³ density

b) group II (similar densities):
ThO_2 kernels of 4.1 g/cm³ density
+ (Th,13w/oCe)O_2 kernels of 4.2 g/cm³ density

The sintering characteristic curves are shown in Figure 2.4/9. The sintered densities of the group II are higher. A typical microstructure is shown in Figure 2.4/10. Ce-rich zones show more porosity than Ce-poor ones. Several cracks can be identified. These features should be the result of different kinetics of ThO_2 and (Th,13w/o Ce)O_2 kernels.

To investigate the sintering kinetics of ThO_2 and (Th,13w/oCe)O_2 kernels separately, two kinds of experiments have been performed:

a) manufacturing of pellets of pure ThO_2 and (Th,13w/oCe)O_2 pellets;

b) dilatometric tests of both.

Figure 2.4/11 shows the sintering characteristic curves of the (Th,13w/oCe)O_2 and ThO_2 pellets. (Th,13w/oCe)O_2 pellets have higher densities. Figure 2.4/12 shows the typical microstructures of these pellets.

Figure 2.4/13 shows the result of the dilatometric investigations. Different (Th,13w/oCe)O_2 kernel batches have been investigated in comparison with one kind of ThO_2 kernels. The sintering kinetics of (Th,13w/oCe)O_2 kernels have shown to be a function of the calcining parameters.

In summary, all these results have shown that the kernel characteristics of both ThO_2 and (Th,13 w/o Ce)O_2 must be adapted to each other in order to get similar sintering characteristics. Possible ways to adapt the kernel characteristics are by:

a) varying the FR-101 carbon black content of the feed-solution;

b) varying the calcining parameters.

2.4.4 Conclusions

The investigations for the transfer of (Th,U)O_2 fuel technology to (Th,Pu)O_2 fuel technology have shown that:

a) the use of Ce as a simulator for Pu based on the available physical and chemical data of the Th-Ce-O and Th-Pu-O systems is justified for scoping studies,

b) the feasibility of pellet manufacturing for the homogeneous mixed oxide concept was successfully tested with (Th,Ce)O_2 on the basis of the (Th,U)O_2 results,

c) the results for the master-mix are encouraging. However, a closer adaptation of the ThO_2-kernels properties to those of the (Th,Ce)O_2-kernels is necessary.

References

[2.4-1] Thorium, System-Nr. 44
Ergänzungsband Teil C2 (1976) S. 78-81

[2.4-2] Pepin, J.G., G.J. McCarthy
Phase relations in crystalline ceramic nuclear waste forms: The system UO_{2+x} – CeO_2-ZrO_2-ThO_2 at 1200° C in air.
J. Am. Ceram. Soc. 64, 9 (1981) 511-516

[2.4-3] Peterson, S., C.E. Curtis
Thorium Ceramics Data Manual
ORNL-4503, Vol. i (1970)

[2.4-4] Seltene Erden, System-Nr. 39
Ergänzungsband Teil C1 (1974) S. 219-226

[2.4-5] Whitfield, H. J., D. Roman, A.R. Palmer
X-ray study of the system ThO_2-CeO_2-CeO_2
J. Inorg. Nucl. Chem. 28, (1966) 2817 '2825

[2.4-6] Hoch, M., H. Sub Yoon
Non-stoichiometry in CeO_{2-x}
Proc. 4th Conf. Rare Earth Res., Phoenix Ariz., (1965)
665-675

[2.4-7] Hillert, M., B. Jansson
Thermodynamic model for nonstoichiometric ionic phases-application to CeO_2-x
J. Am. Ceramic. Soc. 69, 10 (1986) 732-734

[2.4-8] H. Roepenack, F.U. Schlemmer, G.J. Schlosser
Development of Thermal Plutonium Recycling,
to be published in Nucl. Techn.

[2.4-9] H. Roepenack, V.W. Schneider, W.-G. Druckenbrodt,
Am. Ceram. Soc. Bull 63 (1984) 1051/3 and P. 1061

[2.4-10] R. Loeb et al., German P. pending

[2.4-11] H. Assmann, M. Becker,
Trans. Am. Nucl. Soc. 31 (1979) 147/8

[2.4-12] K. Gruber, G. Latzel, H. Roepenack,
Fabrication and Quality Control of Mixed Oxide LWR Fuel with Regard to Homogeneity of Fissile Content,
Report IAEA-SR-102/23, in: KfK 3777 (1984) 353/64

[2.4-13] D. Hanus, H. Keykamp,
J. Nucl. Mat. 106 (1982) 199/210

[2.4-14] S. Baumann, W. Dams,
J. Nucl. Mat. 106 (1982) 101/8

[2.4-15] R. Wuertz,
Atomwirtschaft 32(1987) 190/92

Table 2.4.1: The master-mix concept at ALKEM/SIEMENS

Requirements for $(U,Pu)O_2$-fuel		gives Pu-master concentration of*):
Manufacturing technology:	handling of the lowest possible amounts of Pu-containing material	100%
Reprocessing:	good solubility of Pu in spent fuel	< 40%
Operational behaviour:	– limitation of hotspots	$d < 10^4/Pu_{fiss}$ (µm) d: master particle diameter (e. g.: 280 µm at 40% Pu)
	– limitation of fission gas release due to local high burn-up	–20%

*) Pu concentration in mol.% Pu_{tot}; Pu_{fiss} approx. 0.7 Pu_{tot} depending on the isotope vector

Table 2.4.2: Properties of (Th, 4-6 w/o Ce)O_2 calcined kernels

Composition	Apparent Density (g/cm^3)	Specific Surface (m^2/g)	Fracture Strength (N/kernel)	Diameter (µm)	Carbon Content (ppm)	Sulphur Content (ppm)
(Th, 4w/o Ce)O_2	3.85	52.6	0.7	299	575	470
	3.82	38.9	0.3	309	500	176
	5.17	15.5	0.7	290	840	600
	4.17	11.9	0.3	316	390	730
(Th, 6w/o Ce)O_2	3.79	51.8	–	289	1.050	–
	4.29	34.4	–	284	650	–
	4.82	18.4	–	273	470	–
	2.71	53.7	–	330	845	–
	3.02	36.6	–	326	655	–
	3.51	20.5	–	313	395	–

Table 2.4.3: Properties of ThO_2 and (Th,13w/o Ce)O_2 calcined kernels

Composition	Apparent Density (g/cm^3)	Specific Surface (m^2/g)	Fracture Strength (N/kernel)	Diameter (μm)	Carbon Content (ppm)	Sulphur Content (ppm)
ThO_2	4.57	6.7	0.5	284	290	690
	4.56	8.5	–	284	690	700
	4.08	10.7	0.3	302	690	820
	2.52	–	–	371	–	580
	2.92	6.8	–	367	–	–
(Th,13w/o Ce)O_2	4.97	17.4	1.0	271	–	–
	4.21	16.8	0.7	276	340	750
	4.24	–	0.7	270	760	740
	3.57	–	0.4	–	–	–
	3.48	14.8	0.4	–	–	–
	3.94	9.55	0.4	337	–	–
	4.02	3.9	0.4	330	–	–

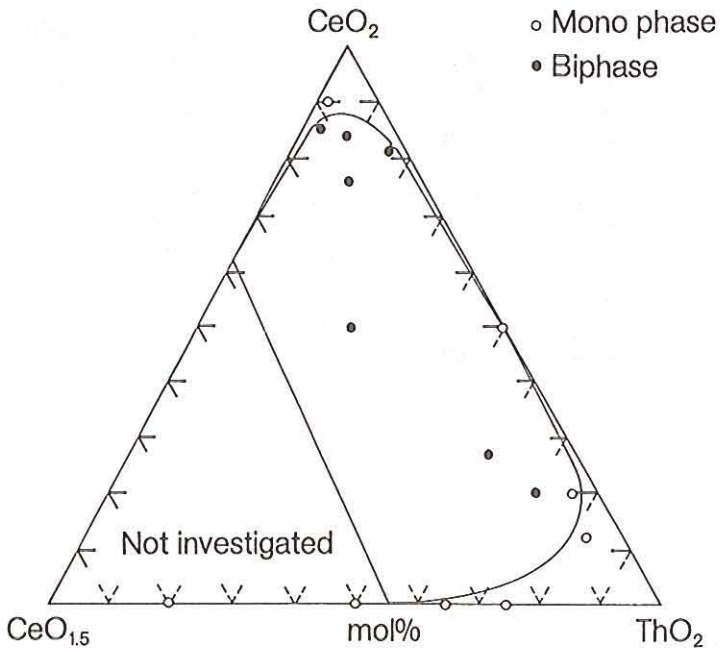

Fig. 2.4/1: Preliminary Phase Diagram of the System $ThO_2 - CeO_2 - Ce_2O_3$ ($T = 1.200°$ C, [2.4-1])

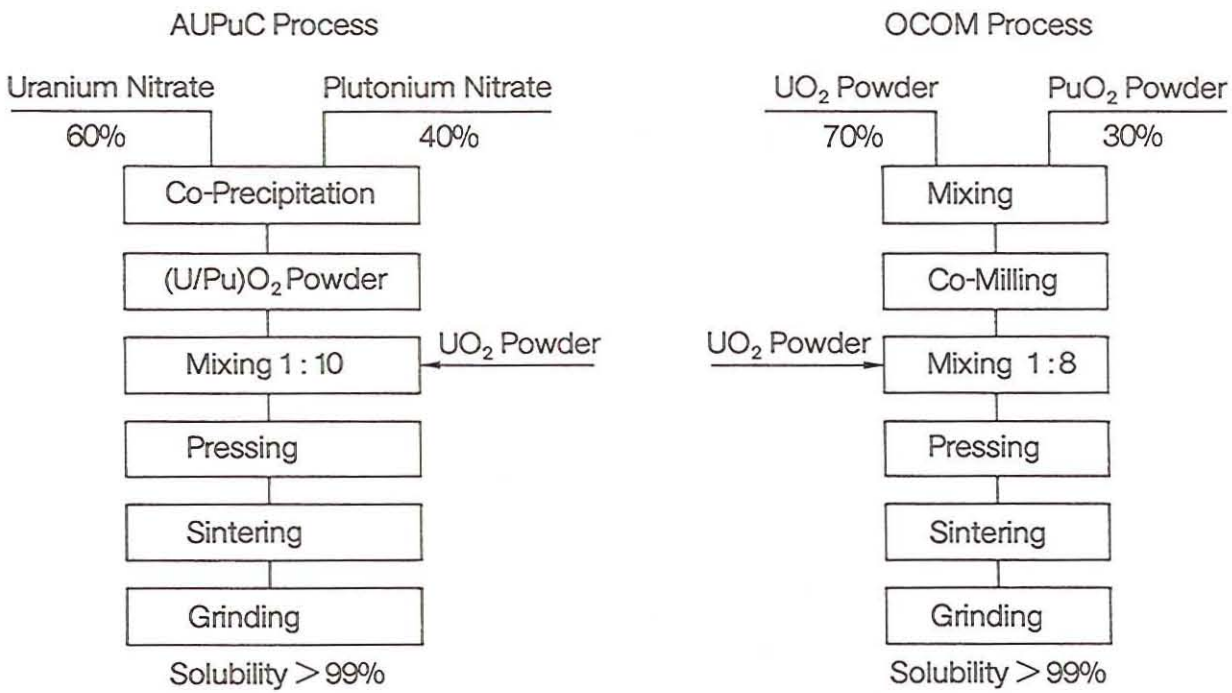

Fig. 2.4/2: Schematic of Alkem Processes for $(U,Pu)O_2$ Pellet Manufacture (Master-Mix-Concept)

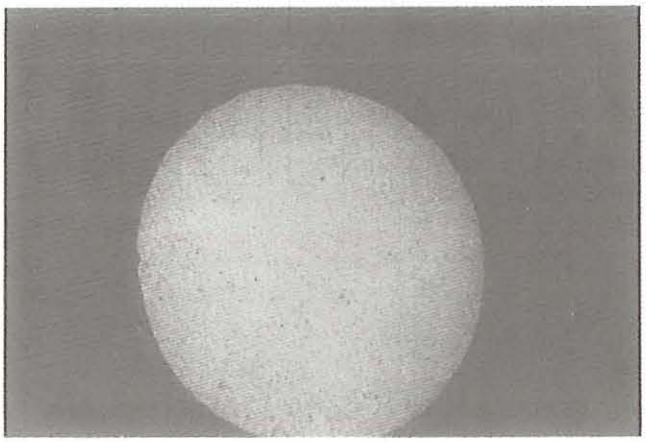

Fig. 2.4/3: Typical Microstructure of (Th, 4^{w}/o Ce)O_2

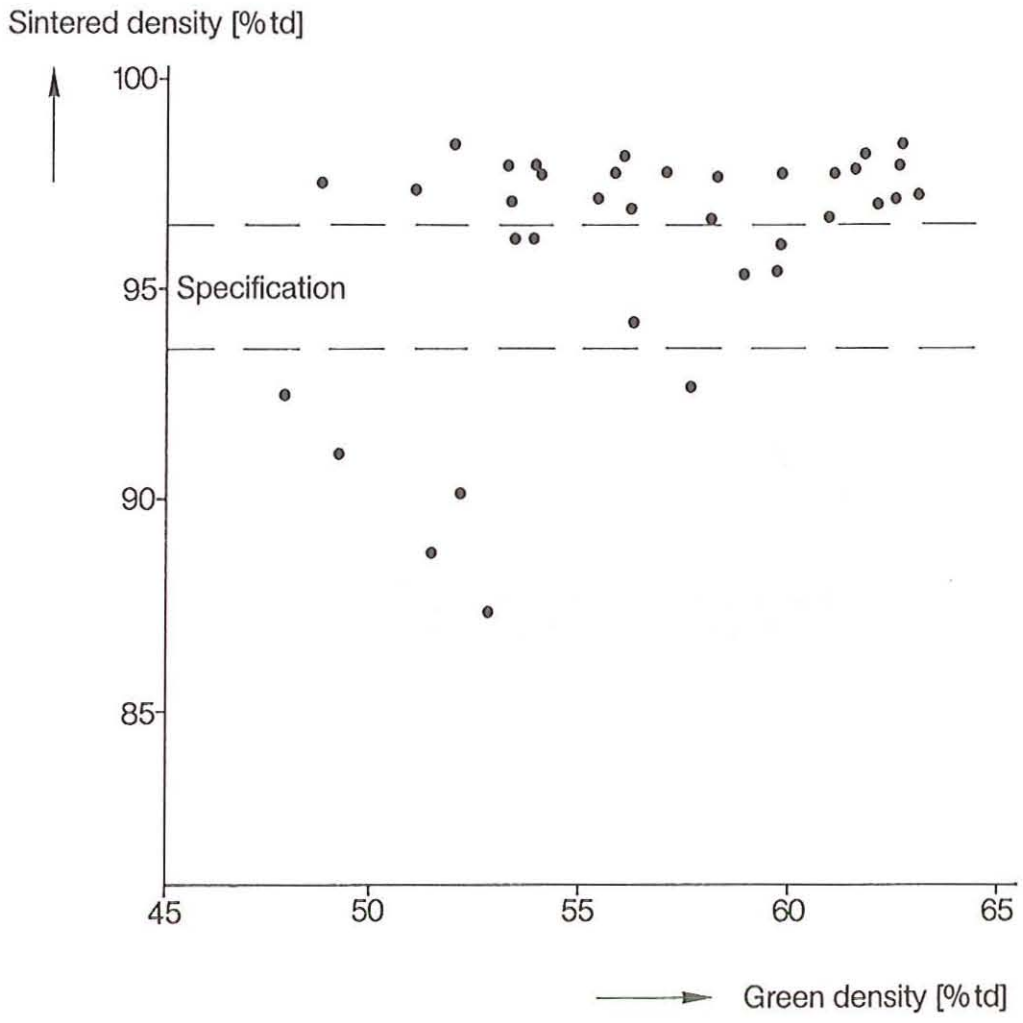

Fig. 2.4/4: Sintering Characteristics of Co-precipitated (Th, 4-6 w/o Ce)O_2 Fuel

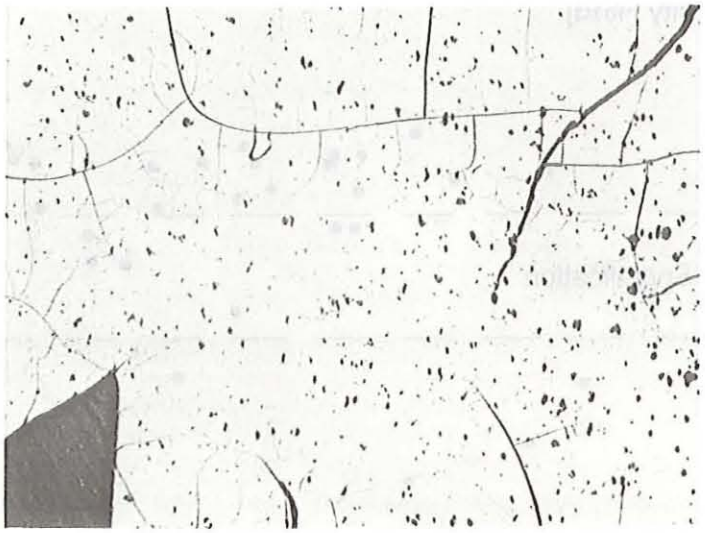

12x

$(Th, 6^{w}\%\,Ce)O_2$ Sintering gas: H_2 / H_2O

$T_{calc.} = 100\,°C$ $\varrho = 9{,}65\ g/cm^3$ (98,8% td)

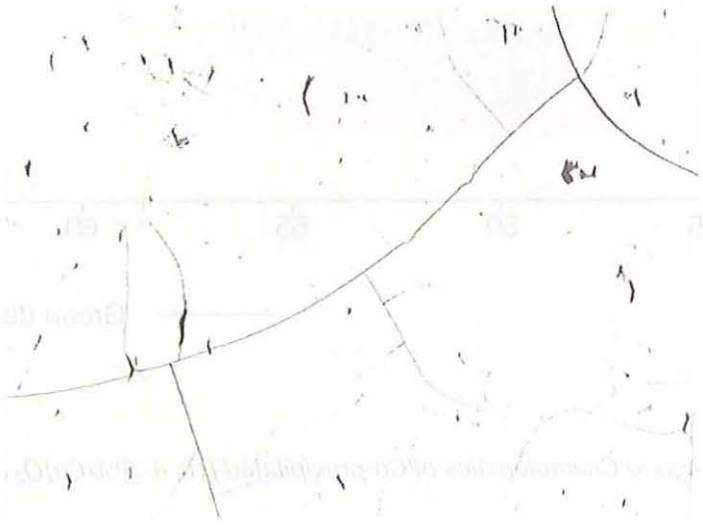

50x

Fig. 2.4/5: Microstructure of a $(Th, 6^{w}\%\,Ce)O_2$ Pellet with Cracks

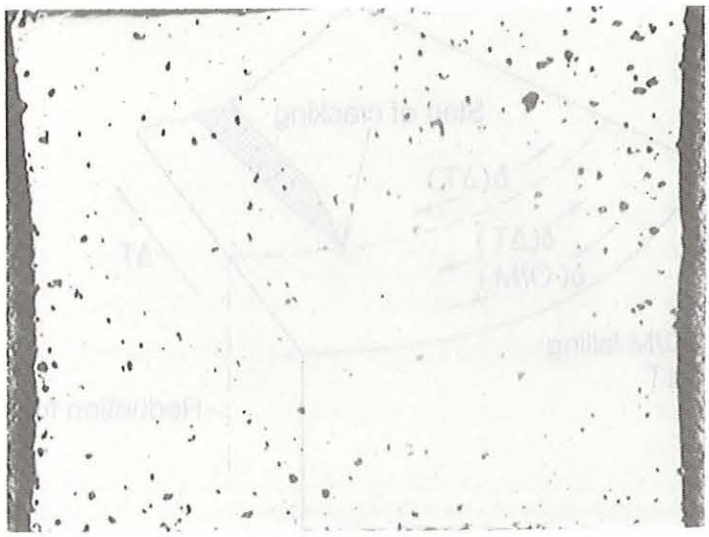

12x

$(Th,6^{w}\%Ce)O_2$ Sintering gas: dried H_2

$T_{calc.} = 700\,°C$ $= 9.56\ g/cm^3$ (98% td)

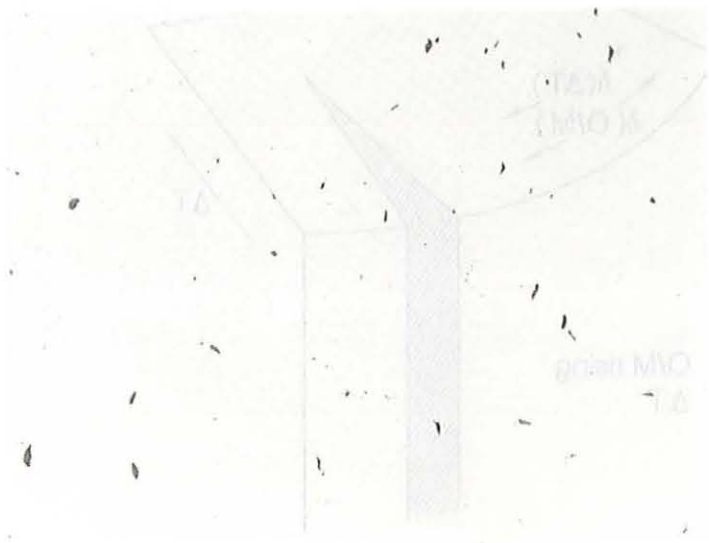

50x

Fig. 2.4/6: Microstructure of a (Th, 6^{w}% Ce)O_2 Pellet without Cracks

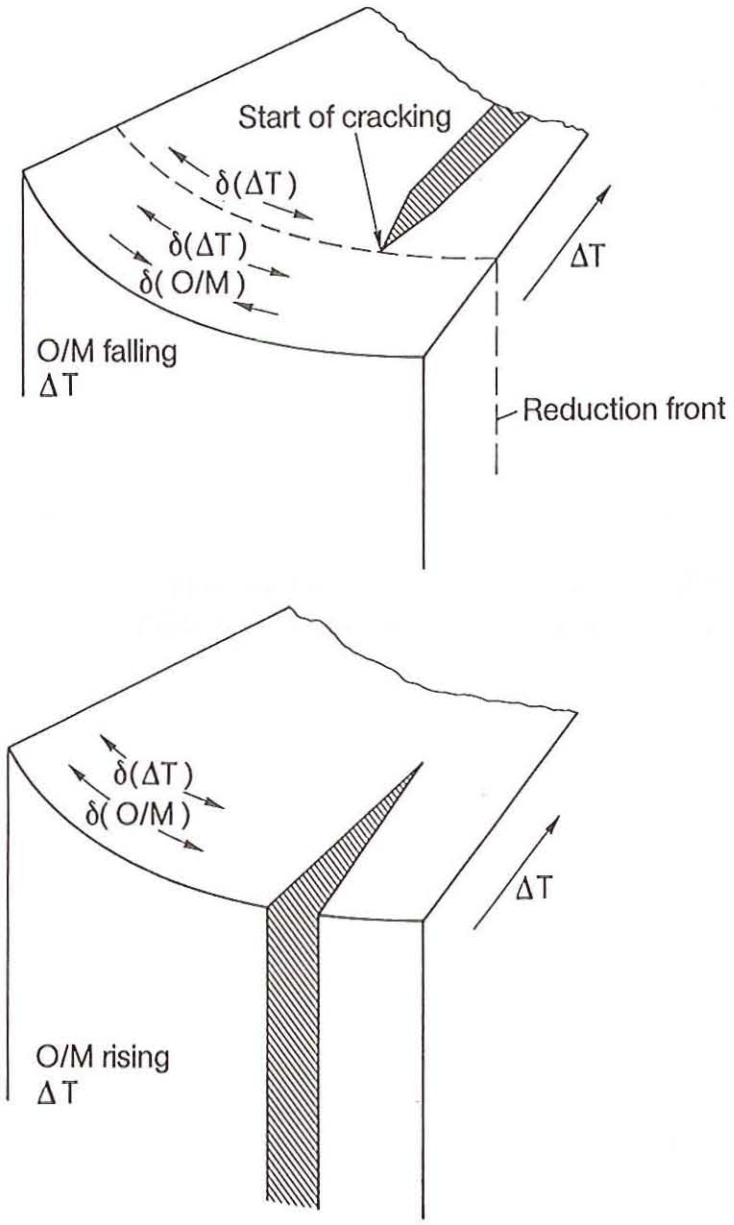

Fig. 2.4/7: Simplified Scheme of Crack Formation due to Non-stabilized O/M

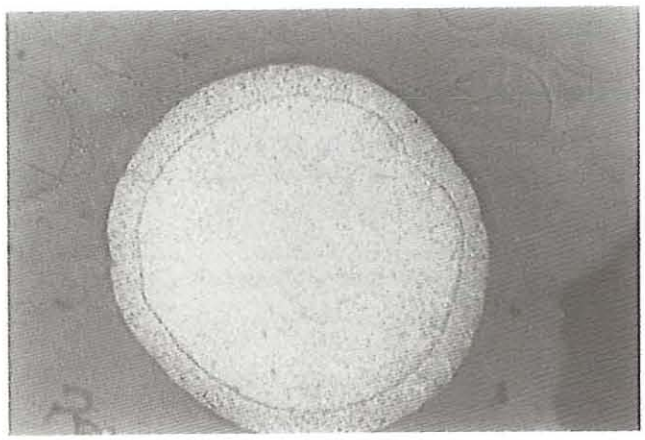

Fig. 2.4/8: Typical Microstructure of (Th, 13^{w}/o Ce)O_2 Kernels

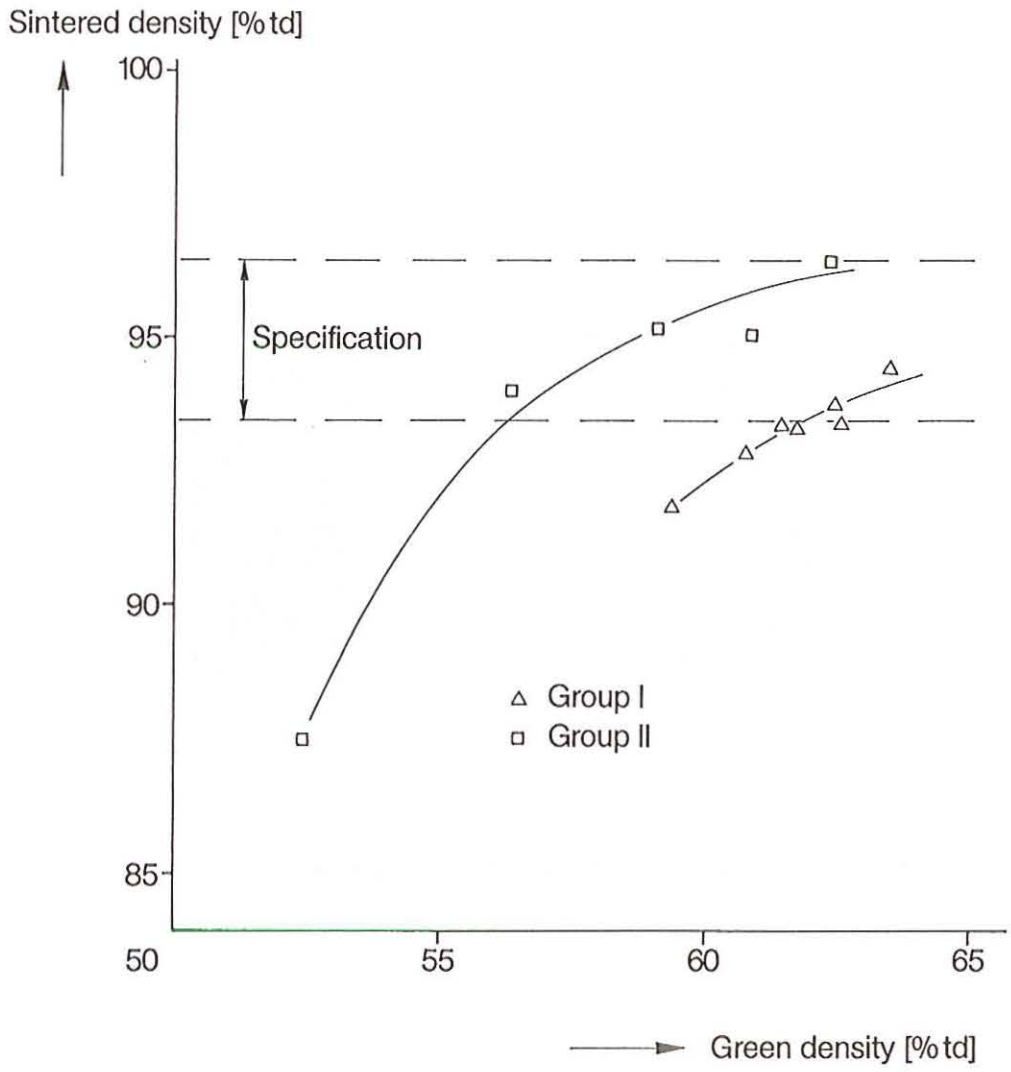

Fig. 2.4/9: Sintering Characteristics of "Master-Mix" Pellets

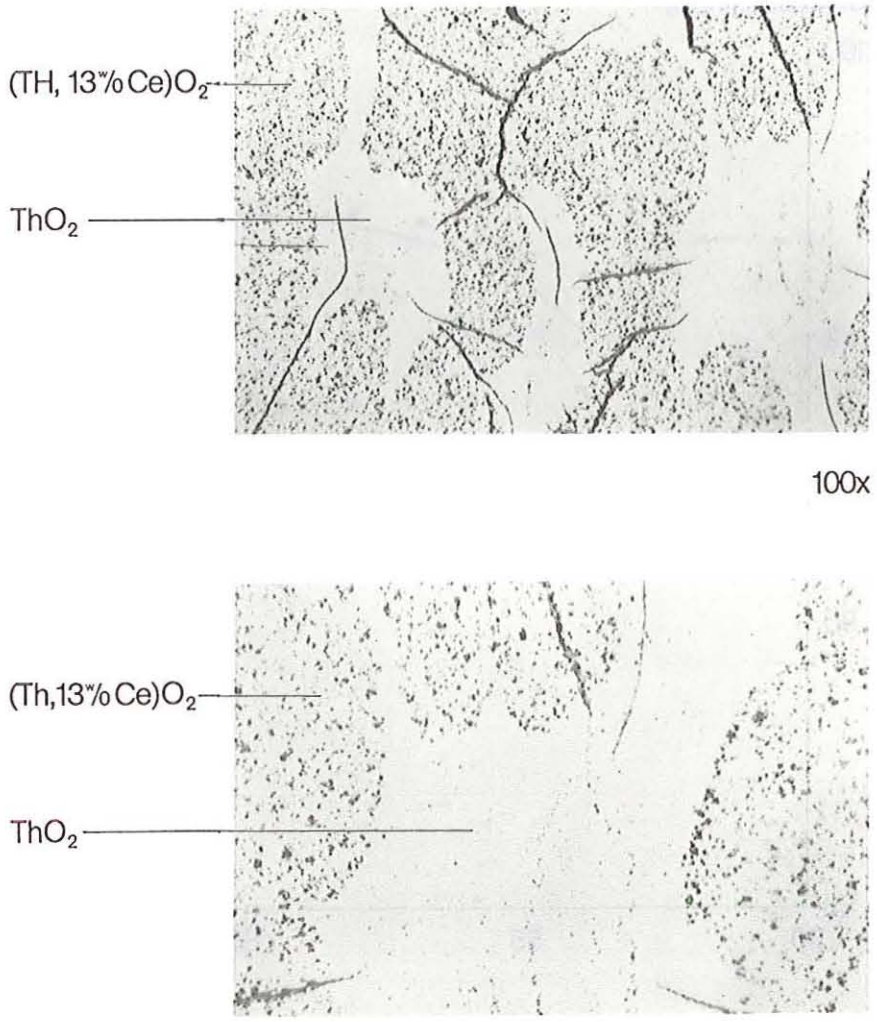

Fig. 2.4/10: Typical Microstructure of a ThO_2 + (Th, 13^w/o Ce)O_2 Pellet (Master-Mix-Concept)

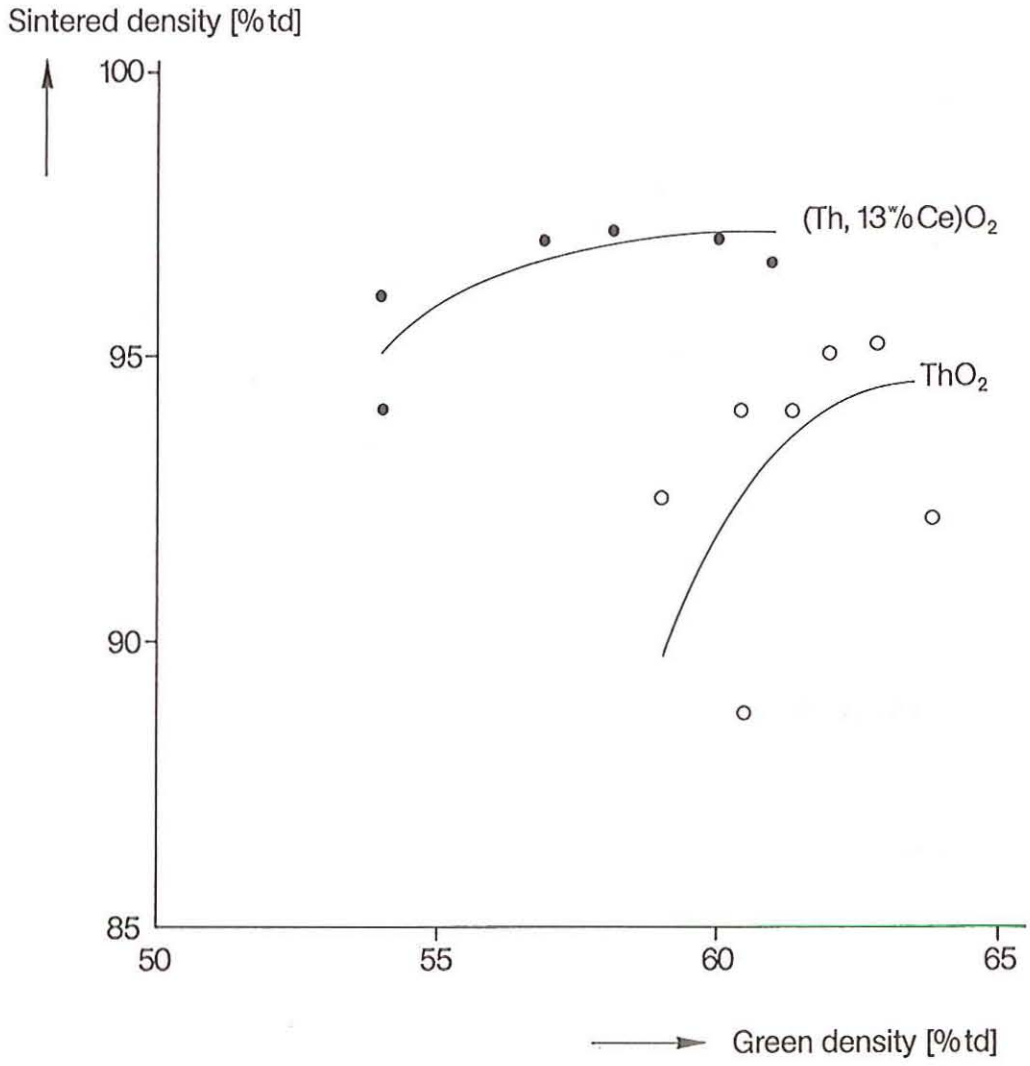

Fig. 2.4/11: Sintering Characteristic Curves of ThO_2 and (Th, 13w% Ce)O_2 Pellets

$(Th, 13\%Ce)O_2$

100x

ThO_2

100x

Fig. 2.4/12: Microstructure of ThO_2 and $(Th, 13^{w}/o\ Ce)O_2$ Pellets

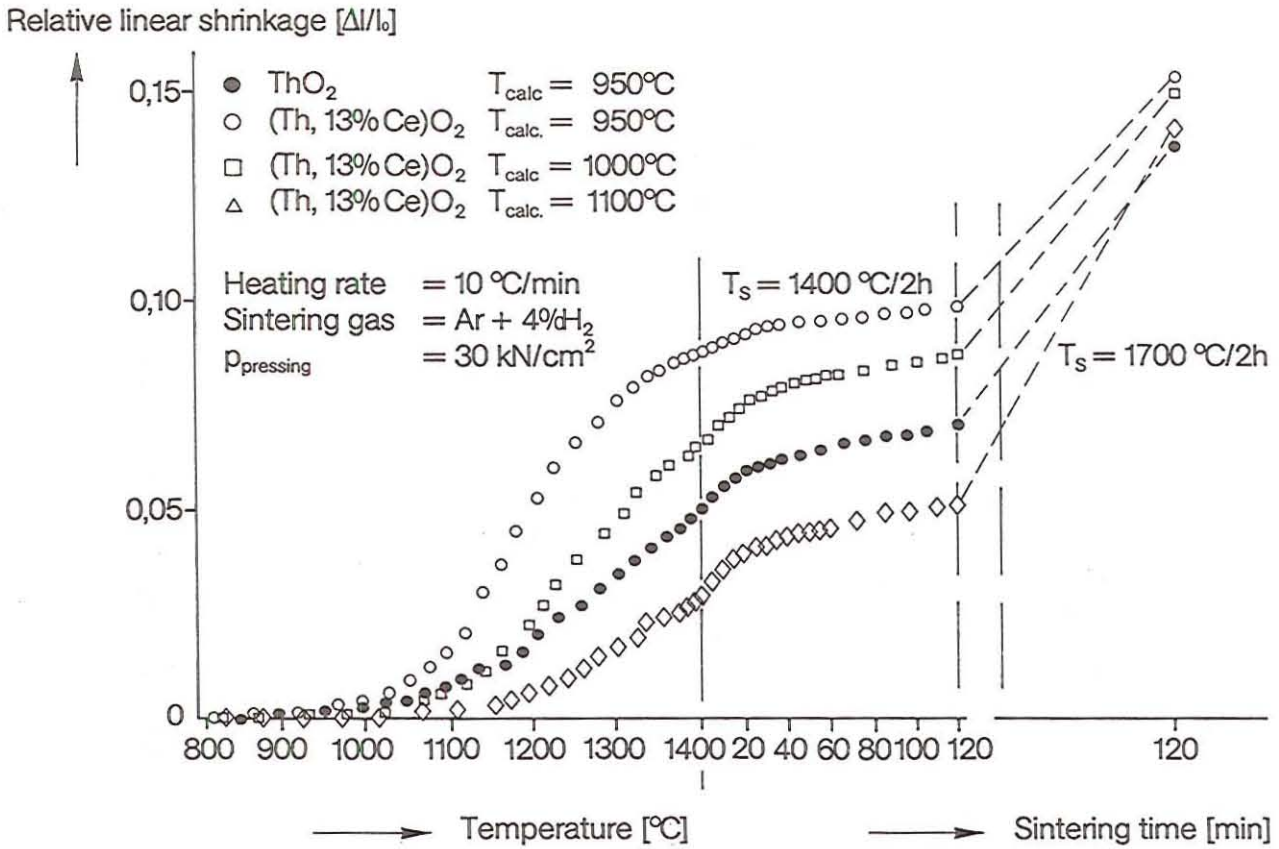

Fig. 2.4/13: Anisothermal Linear Shrinkage of ThO_2 and (Th, 13%o Ce)O_2 Pellets

2.5 Irradiation Testing

Irradiation experiments with six test fuel rods under simulated PWR conditions have been performed in the research reactor FRJ-2 in Juelich, Germany in order to investigate the irradiation behaviour of the new thoria/urania fuel (Th,5%U)O_2 as an advanced nuclear fuel manufactured by novel methods. Hereby, the fuel was qualified and some basic fuel properties were measured. Part of the experimental data could be obtained in the course of the irradiation, but the larger part of the information required could only be gained in the course of the post-irradiation examination (PIE).

A pathfinder irradiation of segmented fuel rods containing (Th,U)O_2 fuel pellets in the power reactor Angra-1 have been prepared to be carried out.

2.5.1 Irradiation experiments in the research reactor FRJ-2

2.5.1.1 Objectives, facilities and procedures

Three rigs with two test fuel rods each have been irradiated in the boiling water loop LV9 in the research reactor FRJ-2 in Juelich.

Objectives

The objective of these three irradiation experiments including test fuel rods with final heavy metal burnups of 1.5, 8.8 and 9.9 MWd/kg, respectively, was to get first information and understanding of the in-pile suitability and properties of the new fuel. Mainly the following features have been investigated by the methods below:

No.	Feature	Method
1.	Fission gas release of the fuel, behaviour of the internal pressure of the test fuel rod	measuring the internal rod pressure during irradiation, measuring the gas volume and composition after irradiation
2.	Restructuring of the fuel	ceramography after irradiation
2.1	Resintering, densification, change of pore size distribution	measuring the fuel density after irradiation
2.2	Grain growth and bubble development by fission gas accumulation	
2.3	Columnar grain growth, pore/gas bubble migration, development of central channel	
2.4	Development of fuel pellet crack pattern	

3.	Fuel temperature in dependence of power and burnup	measuring the central fuel temperature during irradiation
4.	Fuel-to-cladding interaction	measuring of the cladding diameter and cladding metallography after irradiation
4.1	Mechanical interaction (deformation of the cladding)	
4.2	Chemical interaction (fission products attack to the cladding)	
4.3	Chemical and mechanical interaction (stress corrosion cracking)	
5.	Material transport in the fuel	alpha-autoradiography of cross-sections after irradiation and analysis of fuel samples
5.1	Change of the Th/U-ratio	
5.2	Migration of solid fission products	gamma-scan and gamma-spectrometry

A further main objective was to verify a computer code for modelling the fuel rod irradiation behaviour.

Facilities

Two test fuel rods were loaded axially one above the other into the pressure vessel of the irradiation rig (see Figure 2.5/1). The rods were held by three guides of the disc carrier and fixed by the socket at the middle guide. Three axial comb-shaped slats held the discs of thin zirconium sheet.

The discs surrounding the rods limited the size of the steam bubbles, suppressed primary coolant convection, ensured uniform heat transfer conditions, and so prevented the formation of a steam film on the test fuel rods.

The pressure vessel was a seamless $AlMg_3$ tube enclosing the test fuel rods and the disc carrier. It was carried by the pressurized water pipes which, in turn, were led through the central hole of the stainless steel shielding plug and were connected to the head of the rig at the upper end. The pressure vessel was centered within the outer container by means of spacer knobs provided on the flow guiding tube of the cooling water circuit.

This circuit with water of low pressure connected to the rig cooled back the pressurized water through the wall of the pressure vessel. The cooling water flew down through the outer annulus at the outside of the shielding plug and the flow guiding tube to the bottom of the rig and returned through the inner annulus cooling the pressure vessel on this way. It traversed the shielding plug via the central hole up to the connection head.

The outer container which surrounded the cooling water channel could be exchanged during the irradiation pauses. There were two material types, $AlMg_3$ and stainless steel, used to adapt the fuel rod power by different neutron capture of the container material. A further power adaptation was possible by changing the irradiation channel.

For irradiation, the rig was inserted into a 2 inch vertical channel of the FRJ-2 and was connected to the experimental cooling circuit of the reactor and to the pressurized water circuit as well as to the measuring cables of the boiling water loop LV9, which is described in detail in [2.5-1].

The power released by the test fuel rods was determined during irradiation by measuring the temperature increase and the flow rate of the cooling water. The central fuel temperatures in both rods as well as the internal pressure of the lower rod were measured continuously and recorded together with other irradiation data by the computer SIEMENS-R10 for later evaluation.

The important parameters for irradiation testing controlled by the research reactor facility are:

a) reactor power;
b) temperature of the moderator (D_2O);
c) control rods position;
d) massflow, inlet and outlet temperature of the loop cooling water;
e) water pressure inside the equalization vessel;
f) inner gas pressure of the test rods;
g) fuel centreline temperature of both test fuel rods.

Procedures

Preparing the irradiation experiment and its performance has been done by collaboration of the partners as follows:

No.	Working step	Partner
1.	Fabricate the fuel powder and the fuel pellets according to the specifications of section 2.3	NUKEM
2.	Control the fuel quality and pre-characterize the fuel pellets	NUKEM + KWU
3.	Design the test fuel rods	NUCLEBRAS + KWU + KFA
4.	Manufacture the end plugs of the test fuel rods, partly with the pressure transducer and with the tantalum protection tube for the thermocouple, respectively.	KFA
5.	Develop and supply the equipment for pressurizing the test fuel rods, measuring the rod internal free volume	KFA
6.	Supply the qualified cladding tubes	KWU

7.	Fabricate the 8 test fuel rods (2 spare rods included)	RBU
8.	Control the quality of the test fuel rods	RBU
9.	Measure the internal pressure of the test fuel rods	KFA
10.	Measure the diameter and the length of the test fuel rods prior to irradiation	KFA
11.	Fabricate the irradiation rigs	KFA
12.	Install the test fuel rods into the irradiation rigs	KFA
13.	Control the quality of the irradiation rigs	KFA
14.	Irradiate the test fuel rods	KFA
15.	Examine the test fuel rods after irradiation	KFA
16.	Evaluate the irradiation data and the results of the post-irradiation KFA examination	NUCLEBRAS + KFA
17.	Final documentation of data and results	NUCLEBRAS + KFA + KWU

2.5.1.2 Test fuel rod manufacturing and quality control

The test fuel pellets for the irradiation testing were fabricated in 1983 according to the state of the art on $(Th,U)O_2$ fuel technology ex-gel reached in Phase 1 of the program. The test fuel rods including the test fuel were fabricated in accordance with specified processes and proper specifications.

Pellet fabrication

The green pellets were fabricated by pressing (mechanical press TPA35, pressure 500 MPa) of the homogeneous $(Th,U)O_2$ kernels from one batch. A suitable number of these fuel pellets were fabricated with a central bore to accommodate the thermocouple. The sintering step was made in a high vacuum furnace under hydrogen atmosphere at 1,700° C. The specified outer diameter of the fuel pellet was achieved by centerless surface grinding. The inner diameter of the hollow pellets was bored with a diamant-pin.

Pellet properties

Basis for the specification of $(Th,U)O_2$ pellet fuel was the PWR standard specification for UO_2. The required properties relevant for the in-pile behaviour and limitation of impurity contents significant for avoiding rod defects have been maintained. This concerns:

a) thermal stability;
b) density;
c) microstructure (pore and grain size distribution);
d) dimensions (diameter, length);
e) surface properties (roughness, integrity);
f) chemical compositon (Th- and U-content, U-isotope fractions, stoichiometry, moisture and H_2-content, residual gas content, impurity content).

Emphasis was placed on the carbon content of the fuel pellets because of the use of organic precipitation aids and pure carbon addition to feed solution of the ex-gel process. Additionally sulphur was brought into the process by the pore former and was specified as impurity in content. The boron equivalent, mainly given by the rare earth elements, was measured, too, because of the use of thorium for $(Th,U)O_2$ production deviating from the specification of enriched uranium fuel. A list of all chemical analysis methods used for proving the specified pellet data is given in Table 2.5.1. Most of these methods were available as standard examination at NUKEM.

The pellet density was determined by a penetration-immersion method. For the evaluation of the pore size distribution, the quantitative analysis of the pore sizes was applied. Figure 2.5/2 shows the microstructure of a test fuel pellet.

The test frequency as well as the statistical requirements of the statistically controlled properties were given in the specifications. The documentation was performed in accordance to DIN 50049 in a 3.1 B certificate.

Fuel rod manufacturing

The claddings of the test fuel rods (length = 295 and 308 mm, resp.) were manufactured from Zircaloy-4 tube supplied by NRG (Nuklearrohr-Gesellschaft). The manufacture of 8 test fuel rods was started with assembling the end plug with tantalum tube and the cladding by TIG-welding. After the loading of the dried $(Th,U)O_2$ fuel pellets into the cladding, the fuel rods were closed with the spring-side end plug by TIG-welding. Both welding steps were made without addition of welding material. The fuel rods were filled with helium and the filling-hole was sealed with a Zircaloy-4 pin and TIG-welding. The manufacture steps and the quality requirements are summarized by Table 2.5.2.

Compliance with the requirements of the specification and the drawing was certified in an Acceptance-Test-Certificate DIN 50049-3.1 B. All tests and measured data of the 8 fuel rods and of the prerun fuel rods were reported in the Manufacturing and Quality Assurance Report.

Test fuel rod description and data

The test fuel rods (see Figure 2.5/3) had Zircaloy-4 cladding with 10.76 + 0.01 mm outside diameter and 9.30 mm inside diameter. They contained 24 $(Th,U)O_2$ fuel pellets each of PWR standard dimensions (see Figure 2.5/4). The uranium content was 5.03 % of the heavy metal mass, the ^{235}U enrichment was 44.95 weight %. The pellets were 9.105 $\pm$ 0.002 mm in diameter and 11.74 $\pm$ 0.05 mm in length. The first pellet adjacent to the test rod spring was properly shortened to get the specified fuel column length of 275.2 $\pm$ 0.2 mm. The diametric gap was 195 $\pm$ 40 µm. Five fuel pellets had central holes of 2.8 mm diameter to take the protection tube of tantalum of 2.6 mm outside diameter and the thermocouple wires of W5%Re-W26%Re held in a 2-hole insulation-

rod of thoria. The lower rod, positioned nearly symmetrically in the neutron flux profile of the reactor core (see Figure 2.5/5), had been equipped with an additional pressure transducer assembled in the lower end plug. By that, the internal pressure of the lower test fuel rod could be measured during irradiation. The fuel column was axially separated from the metallic components by Al_2O_3-pellets for thermal insulation. A spring of stainless steel located the fuel column in the fuel rod and protected it against transport damages. The test fuel rods were pressurized with highly pure helium of 2.18 ± 0.05 MPa at 293 K.

2.5.1.3 Pre-irradiation measurements

After the transport of the test fuel rods to KFA, the internal helium pressure of the rods with pressure transducer was measured. The diameter and the length of all test fuel rods were measured prior to and after irradiation with the same measuring bench in the hot cell laboratory of KFA in order to accurately determine the change of the dimensions as an effect of irradiation.

2.5.1.4 Irradiation data

The three irradiation experiments were performed between November 1983 and September 1985. Details of the test fuel rods, the irradiation conditions and the results are given in Table 2.5.3. A survey of the measured linear power, the central fuel temperature and the internal gas pressure is given in Figure 2.5/6 for the test fuel rod TDT81.

A decrease of the internal gas pressure was observed in the rod TDT81 after 47 days of irradiation and in the rod TDT83 after 10 days. A leak in the tantalum protection tube and a sealing failure allow the internal gas to flow into the pores of the insulation material of the connection cable of the thermocouple without leaking into the pressurized water circuit. Further tests performed at the PIE have shown that the fuel rod and connection cable system were tight, i.e., a well cooled free gas volume has been added to the internal free rod volume.

The third irradiation experiment with the rods TT84 and TDT85 had to be finished before reaching its burnup goal due to a leak in the cladding of the upper rod TT84. The reason was pressurized water penetrating into the fuel rod through a leak in the connection piece of the thermocouple cables and destroying the tantalum protection tube by corrosion. The tantalum was oxidized and swelled so much that the cladding failed. However, the $(Th,U)O_2$ fuel behaved neutrally in the defective test fuel rod and did not promote failing of the rod cladding by swelling.

2.5.1.5 Post-irradiation examination

After a cooling time of at least 5 weeks the irradiation rigs have been transported within a shielded transportation flask to the fuel cell laboratory (Brennstoffzellenlabor—BZL) of the hot cells of KFA. Here, the rigs have been dismantled and the fuel rods have been examined. If not otherwise remarked the following investigations have been fulfilled in the BZL.

Cladding

The **length** of the fuel rods between the two measurement slots has been measured

before and after irradiation in the bench of the BZL with a resolution of 0.02 mm. A relative axial length increase up to 4.8E-4 has been determined.

Helical, circumferential and length-wise measurements of the **cladding** diameter were made before and after the irradiation by using a displacement transducer. A circumferential diameter diagram is given in Figure 2.5/7. A length-wise diameter diagram is given in Figure 2.5/8.

Fuel

The **ceramography** of the irradiated fuel did not show any irradiation induced change of the fuel microstructure, not even at the highest linear power (see Figure 2.5/9). The development of the $(Th,U)O_2$ fuel crack pattern is similar to the behaviour of the UO_2 fuel. Even at the highest linear power of more than 400 W/cm the dishing is not deformed (see Figure 2.5/10).

For **burnup analysis** two irradiated fuel samples of the rod TDT81 located near the highest linear power have been investigated by mass spectrometry in the Institute of Chemical Technology (KFA-ICT). The results are given in Table 2.5.4. They are important to control the breed and burnup calculations for the fuel nuclides.

For determining the **fuel dimensional behaviour,** on 16 fuel samples, from six individual rods the fuel densities were measured in the hot cells of KfK Karlsruhe. The fuel pellet volume shrank 1.7 $\pm$ 0.7% independently of the fuel temperature (900 to 1,550 K) and burnup (0.6 to 9.6 MWd/kg).

Fuel rod

The cold inner gas pressure of the test fuel rod TT80 was measured in the hot cells after irradiation. Two gas samples of the rod TT80 were analysed in the hot cells of KWU by mass spectrometry. The **fission gas release** calculated from the measured gas volume and the relative Xe + Kr content was 0.17 %. One gas sample of the rod TT80 was analysed in the Central Department for Chemical Analysis (KFA-ZCH) by a specially adapted gas chromatography for SO_2. Since no SO_2 could be detected, the SO_2-content of the gas inventory of the fuel rod was lower than 0.5 volume %, the sensitivity of gas chromatography.

A **gamma scan** of the rod TT80 is given in Figure 2.5/11.

Gamma spectra were taken at three different points of each rod in order to investigate the axial distribution of the radioactive nuclides and their migration behaviour. The activity of 9 nuclides in the test fuel rods TT80 and TDT81 recalculated from the gamma scan peaks to the end of the irradiation time are given in Table 2.5.5.

2.5.2 Pathfinder irradiation technology

2.5.2.1 Objectives, facilities and procedures

The target of the irradiation test to be performed at the Angra-1 nuclear power plant should be to confirm the good operational behaviour and the basic design and fabrication principles of fuel rods containing $(Th,U)O_2$ fuel as established in irradiation tests carried out in the research reactor FRJ-2. For this purpose segmented and full-length

test fuel rods should be loaded into a carrier fuel assembly and should be inserted into the power plant.

The fuel rods should be irradiated for up to four operational cycles and should be examined in the spent fuel pond of the plant after each cycle. Hot cell examinations on these fuel rods were intended, too.

During examination in the spent fuel pond, the integrity of the test fuel rods should be confirmed by wet sipping of the carrier assembly including the test rods and by eddy current testing of the individual test rods. Measuring of the fuel rod dimensions, i.e. diameter and length, should inform on fuel pellet dimensional stability, influencing the diameter changes of the fuel rods.

During hot cell examination of the test fuel rods the results of the spent fuel pond examination should be confirmed and the power and burnup distribution of the rods should be determined. By metallographic and ceramographic examinations, dimensional changes, relocation and crack pattern of the fuel pellets should be determined in detail and microstructural changes of the fuel should be investigated.

Furthermore, puncturing of the fuel rods during hot cell examination should give data on fission gas release of the $(Th,U)O_2$ fuel for the different operational and burnup stages.

Table 2.5.6 summarizes the nuclear fuel service required for the planned irradiation testing.

In order to facilitate the access to the test fuel rods without removing any end piece of the carrier assembly, the top end piece of the assembly was modified by introducing a cross-shaped cut-off seal prior to assembly loading. Thus, during any shutdown or refueling period, the rods may be removed from the carrier assembly through that cut-off open end and may be submitted to non-destructive testing in the spent fuel pond by using the special measuring and examination device (Figure 2.5/12).

2.5.2.2 Irradiation strategy

The irradiation test was planned to determine the operational behaviour of $(Th,U)O_2$ fuel rods in a commercial nuclear power plant. Four segmented test fuel rods and one full-length fuel rod were designed and should be licensed and fabricated for loading into the carrier fuel assembly and into the power reactor Angra-1. The segmented fuel rods should consist of seven short test fuel rodlets each axially screwed to each other.

To get information on the fuel performance in the whole burnup range of up to 45 MWd/kg, the segmented fuel rods should be irradiated for 1 to 4 operational cycles, i.e., one segmented fuel rod should be unloaded during each refueling shutdown of the power plant.

The full-length fuel rod should be irradiated for altogether 4 operational cycles. The test fuel rods should be finally examined in the spent fuel pond of the power plant. Intermediate examinations were planned to be performed during each refueling shutdown.

2.5.3 Conclusions

The irradiation testing of $(Th,U)O_2$ fuel and the subsequent post irradiation examination have brought the following results:

a) a complete irradiation database to characterize the $(Th,U)O_2$ behaviour and performance under simulated PWR conditions up to 10 MWD/kg (Th + U), and

b) the demonstration of the newly developed methods for $(Th,U)O_2$ fuel pellet fabrication which provides an adequate alternative nuclear fuel for PWR's.

The preparation of a pathfinder irradiation technology in a power reactor in Brazil enhanced the transfer of specific know-how from Siemens to NUCLEBRAS. This comprised the design, made by NUCLEBRAS, of a carrier fuel assembly and components for a pathfinder irradiation test in Angra-1 power reactor and the elaboration of documents required for licensing the irradiation test.

References

[2.5-1] K. Reichardt and M. Neumann,
„Irradiation of Water- Cooled Fuel Rods in Boiling Water Loops",
Kerntechnik 10 (1968), Nr.6, pages 331-337.

[2.5-2] H. Knaab,
In: „Onsite Nondestructive Examination Techniques for Irradiated Water Cooled Power Reactor Fuel",
IAEA, Vienna, 1981, (IAEA-TECDOC-245).

Table 2.5.1: Chemical analysis methods for quality control of the fuel

No.	Method	Elements									Ratio	Gas		
		Th	U	F	Cl	C	S	B	Si	Gd	O/U	N_2	H_2/H_2O	residual gas
1	Complexometric titration	+												
2	Gravimetry	+												
3	Controled potential coulometry		+								+			
4	Oximetric titration		+											
5	Photometry		+	+	+							+		
6	Ion selective electrode			+	+									
7	Infra red absorption					+	+							
8	Inductively coupled plasma spectrometry					+	+			+				
9	Emission spectrometry							+	+					
10	Atomic absorption spectrometry							+		+				
11	Gas chromatography											+		
12	Carrier gas method (LECD)												+	
13	Hot extraction													+

Table 2.5.2: Manufacture steps and quality requirements of the test fuel rods

Process step	Quality requirement	Test scope
1. Welding zone of end plug with tantalum tube		
1.1 metallography	correlated standard for LWR	1 welding sample
1.2 X-ray	pore diameter smaller than specified value	all TFRs*
1.3 corrosion test	correlated standard for LWR	1 welding sample
1.4 surface near welding	correlated standard for LWR	all TFRs
2. Fuel pellet stack		
2.1 pellet stack length and weight measuring	in accordance with specified value and tolerance	all TFRs
3. Welding zone of end plug at spring-side		
3.1 metallography	correlated standard for LWR	1 welding sample
3.2 X-ray inspection	pore diameter smaller than specified value	all TFRs
3.3 corrosion test	correlated standard for LWR	1 welding sample
3.4 inspection of the surface of the weld area	correlated standard for LWR	all TFRs
4. Fill gas pressure and sealing of the rods		
4.1 He leak test	leaking rate smaller than specified value	all TFRs
4.2 moisture and H_2-content determination	measurement smaller than specified value	1 qualification rod
4.3 free gas volume measurement	within the specified range	all TFRs with pressure transducer
4.4 fill gas pressure measurement	pressure documentation	all TFRs with pressure transducer
4.5 surface inspection	maximal scratch depth smaller than specified value	all TFRs

*TFRs = test fuel rods

Table 2.5.3: Survey of the irradiation data of all six test fuel rods

Irradiation rig	Test fuel rod	Linear rod power	Fuel temperature	Internal rod pressure	Irradiation time	Burnup of heavy metal	Cold internal pressure		
		max.	max.	max.		max.	initial	min	final
		W/cm	Kelvin	MPa	days	MWd/kg	MPa	MPa	MPa
LU9.6-E60	TT80	319	1405	–	116	6.82	–	–	–
	TDT81	438	1575	7.23	116	8.22	2.105	1.243	1.288
LU9.6-E61	TT82	241	1490	–	194	8.25	–	–	–
	TDT83	307	1365	7.07	194	9.88	2.172	1.183	1.213
LU9.6-E62	TT84	212	1105	–	34	1.26	–	–	–
	TDT85	259	1210	6.25	34	1.53	2.208	1.838	–

water pressure: 9.0 ± 0.05 MPa
rod surface temperature: 582 K = 309°C

*Table 2.5.4: Fuel analysis by mass spectrometry**

Height above mid plane of reactor core	H = –8.5 ± 1.2 cm	H = –10.9 ± 1.2 cm
nuclide	heavy metal burnup A = 8.086 MWd/kg	heavy metal burnup A = 8.342 MWd/kg
^{233}U	11.481%	11.33 %
^{234}U	0.596%	0.589%
^{235}U	27.463%	27.641%
^{236}U	3.120%	3.087%
^{238}U	57.34 %	57.35 %
^{238}Pu	0.461%	
^{239}Pu	82.475%	
^{240}Pu	14.583%	
^{241}Pu	2.051%	
^{242}Pu	0.430%	

*Fuel samples of the test fuel rod TDT81

Table 2.5.5: Activity of 9 nuclides in the test fuel rods TT80 and TDT81 within a disk of 0.2 mm thickness at the end of irradiation

	Test fuel rod	TT80			TDT81		
	Spectrum nr.:	1	2	3	1	2	3
nuclide	energy	nuclide activity A/GBq					
^{95}Zr	724 keV	3.5	5.6	6.1	6.5	7.3	7.7
^{103}Ru	497 keV	2.2	3.3	3.5	3.7	4.1	4.4
^{106}Ru	622 keV	0.084	0.11	0.10	0.13	0.13	0.14
^{134}Cs	605 keV	0.008	0.013	0.019	0.023	0.028	0.031
^{137}Cs	662 keV	0.063	0.10	0.11	0.12	0.13	0.14
^{140}Ba	537 keV	6.0	7.0	8.3	14	16	19
^{144}Pr	696 keV	1.2	1.8	2.1	2.5	2.4	2.8
^{182}Ta	1221 keV	0	0	1.7	1.6	0	0
^{233}Pa	312 keV	48	85	100	110	120	120

Table 2.5.6: Nuclear fuel service for the irradiation testing

Objectives	Activities	Available Equipment
Detective fuel assembly detection	Fuel assembly sipping	Sipping equipment for PWR
Fuel rod exchange	Substitution of a test fuel rod for a standard fuel rod or dummy rod	Fuel assembly handling equipment Working stations and special tools Fuel rod exchange device
Pool site examination	Eddy current testing	Eddy current testing equipment
	Dimensional measurements of fuel rods	Dimensional measurement equipments
	Outer oxide layer thickness measurement	Layer thickness gauge
	Gamma scanning	Gamma scanning device
Hot cell examination	Fission gas analysis	Standard hot cell equipment
	Determination of the internal free volume the fuel rods	
	Profilometry and metallography/ ceramography	
	Burnup and chemical analysis	Radio chemical methods

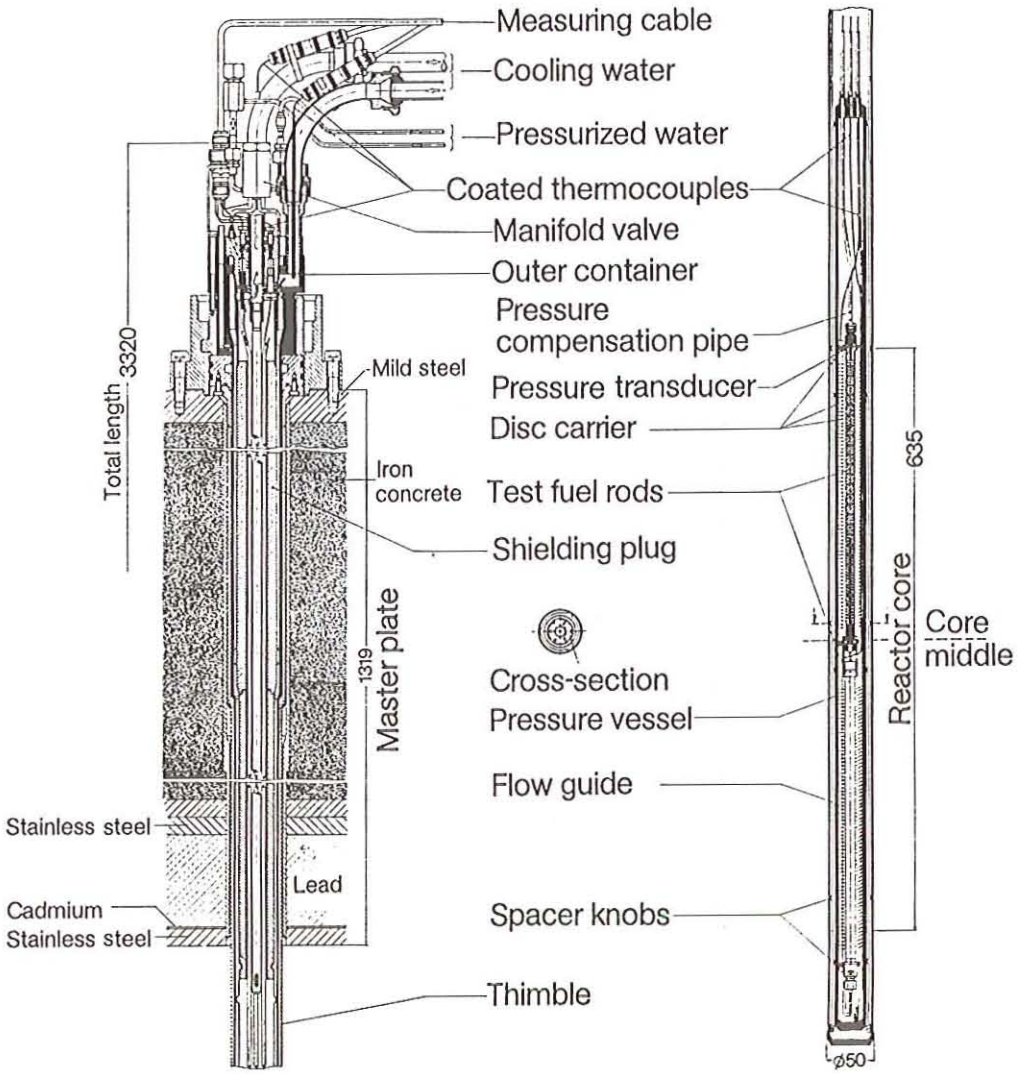

Irradiation rig for test fuel rods
cooled by pressurized water
Pressure of water: 6 to 13 MPa
Linear power: up to 800 W/cm

Fig. 2.5/1: Irradiation Rig with the Two Test Fuel Rods

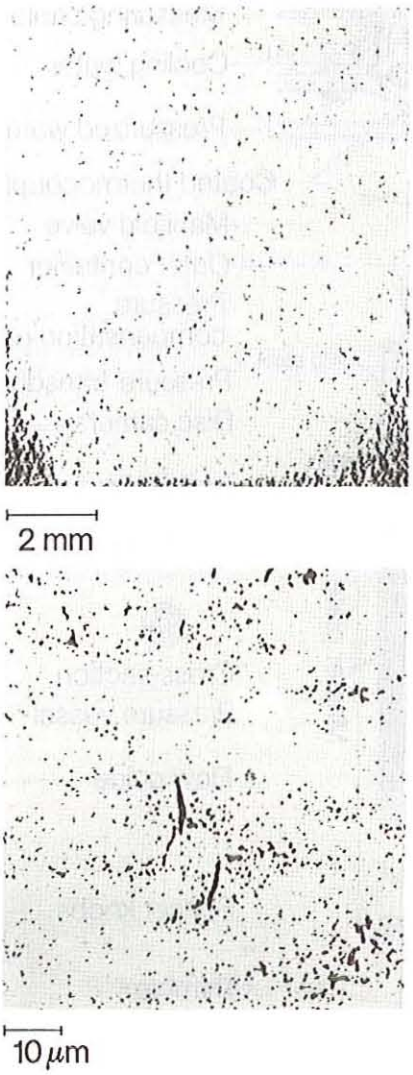

Fig. 2.5/2: Microstructure of a $(Th,U)O_2$ Fuel Pellet before Irradiation

Upper rod TT80 with thermocouple

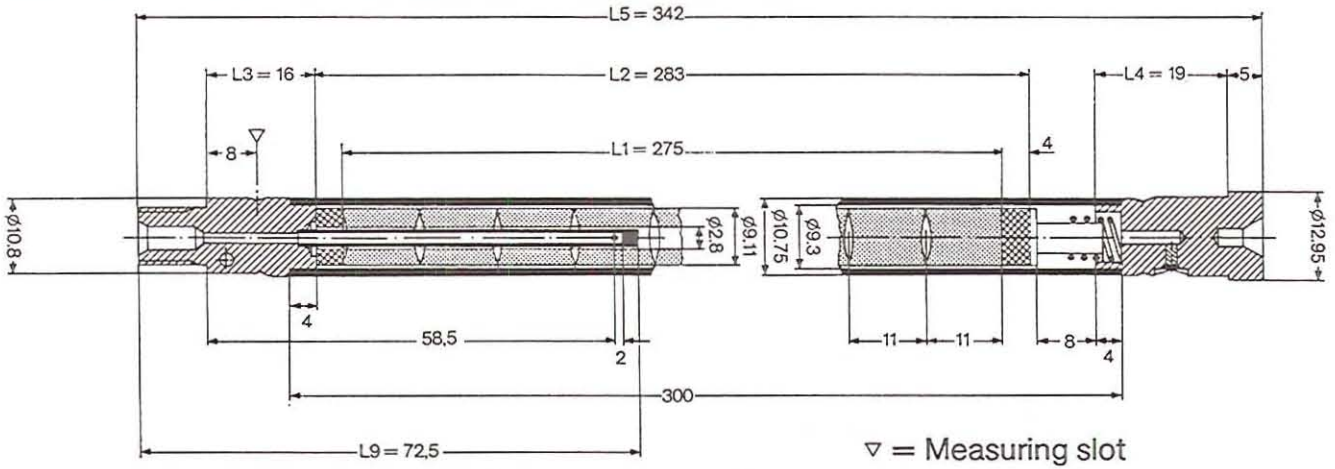

Lower rod TDT81 with thermocouple and pressure transducer

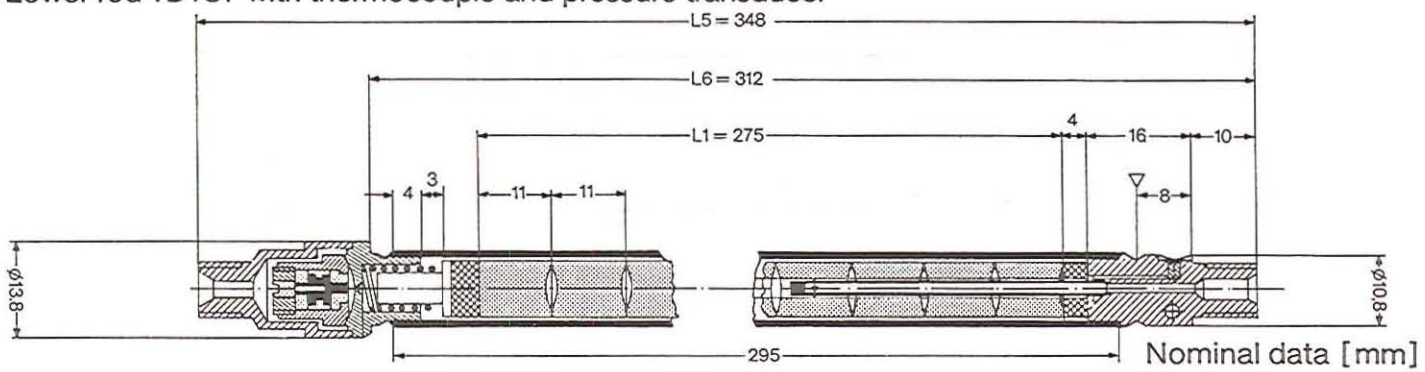

Fig. 2.5/3: Instrumented Test Fuel Rods

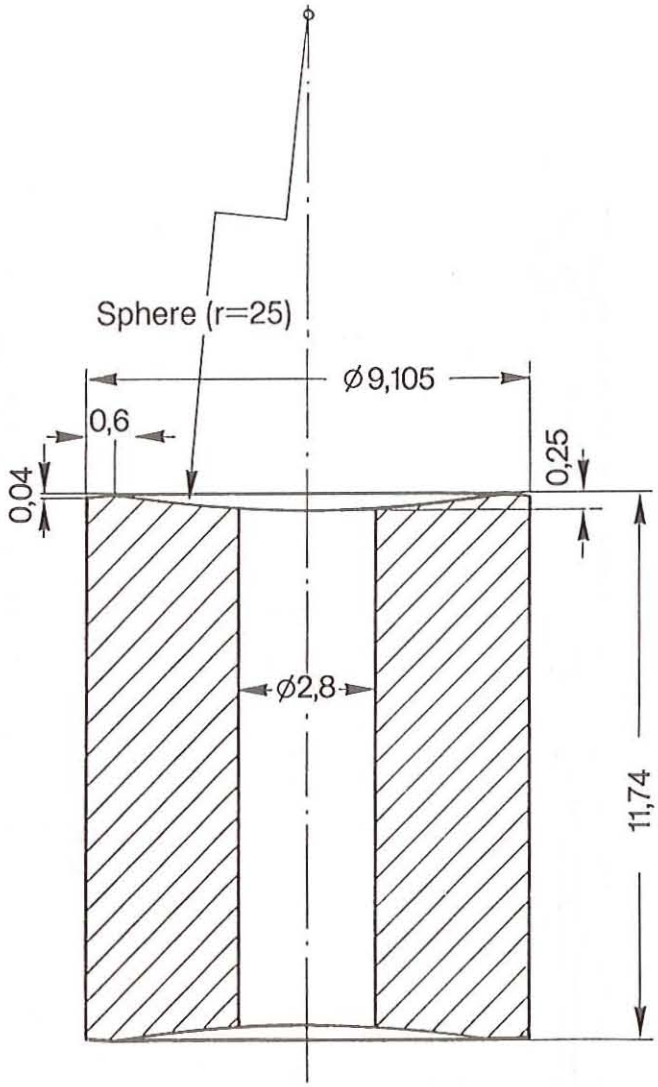

Hole only in 5 of the 24 pellets of each test fuel rod
[mm]

Fig. 2.5/4: Fuel Pellet (Th, 5% U)O_2

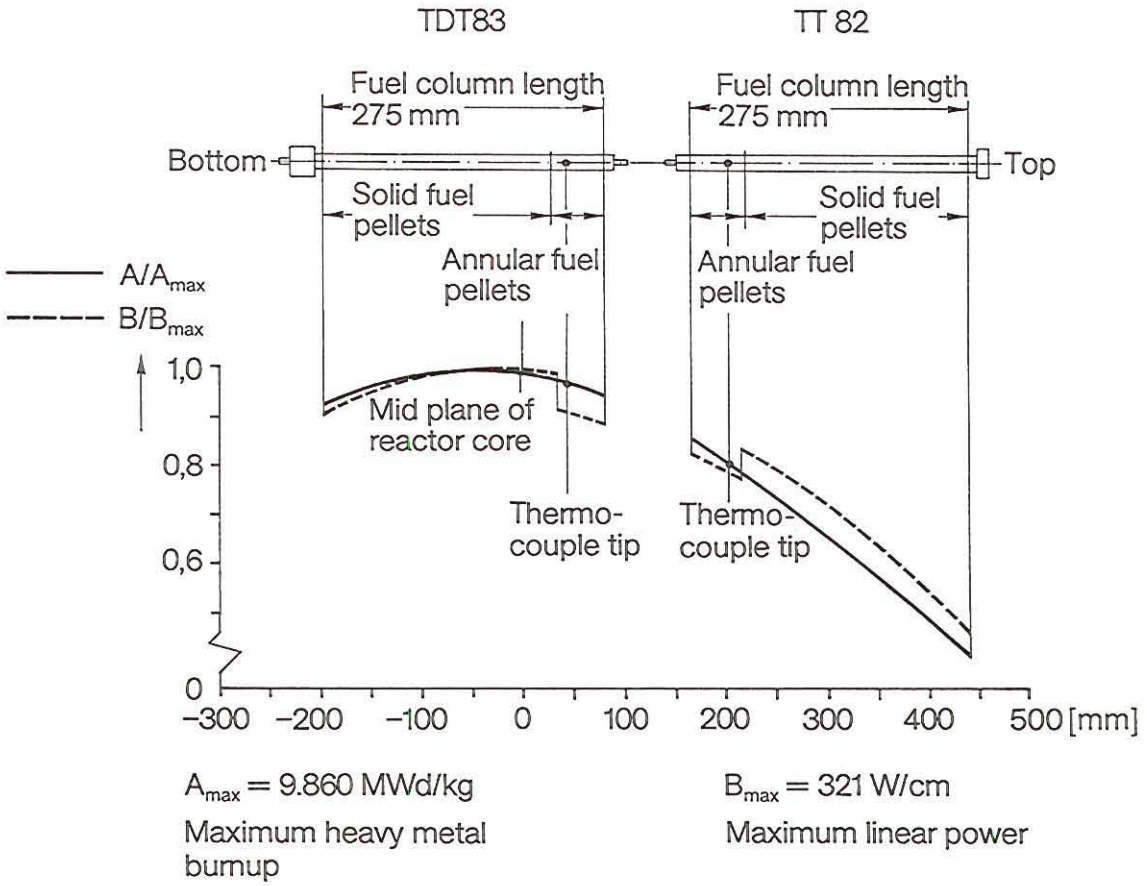

Fig. 2.5/5: Axial Profile of Burnup and Linear Power of the Test Fuel Rods TT82 and TDT83

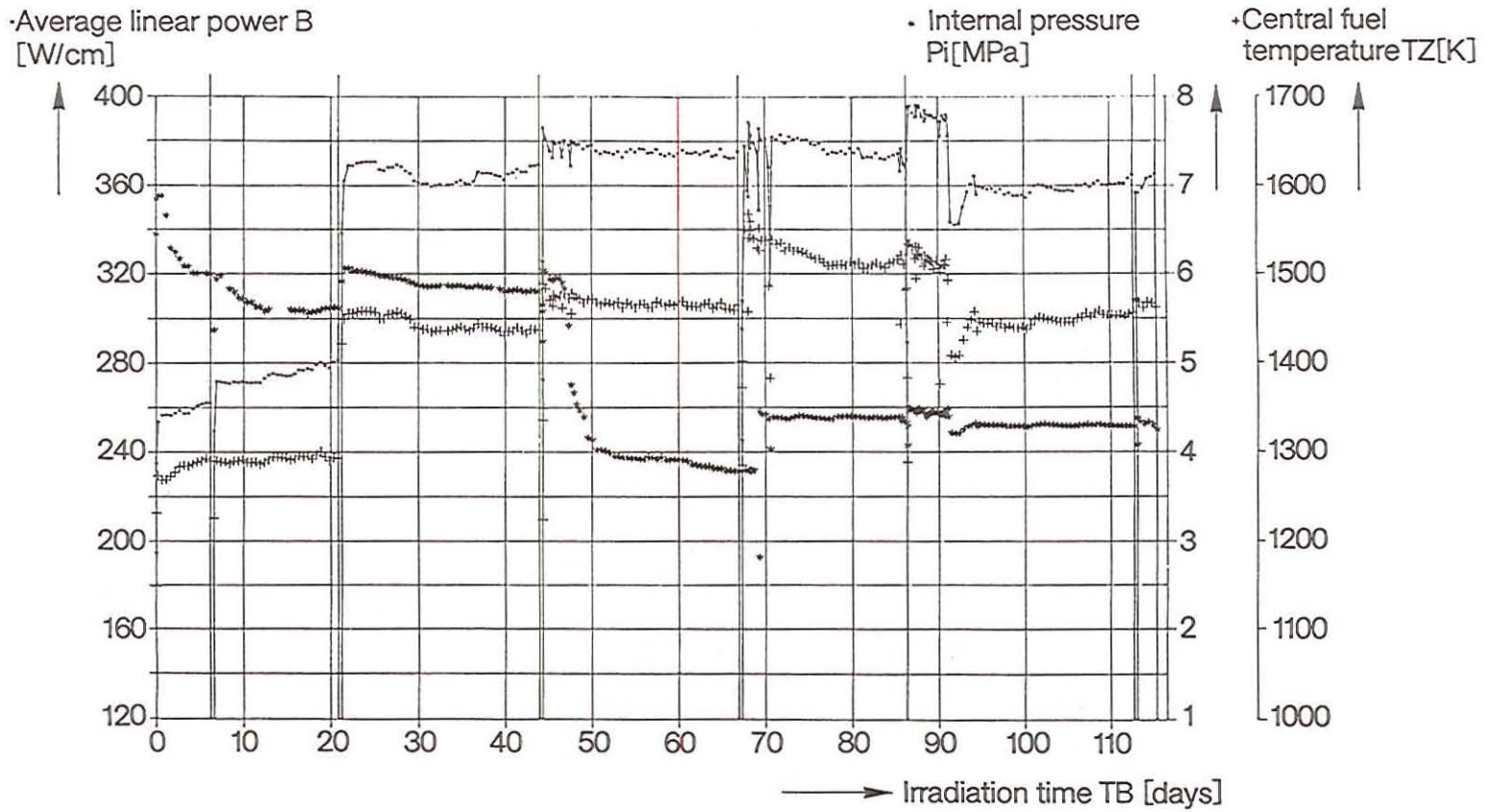

Fig. 2.5/6: Survey of the Irradiation Conditions of the Test Fuel Rod TDT81

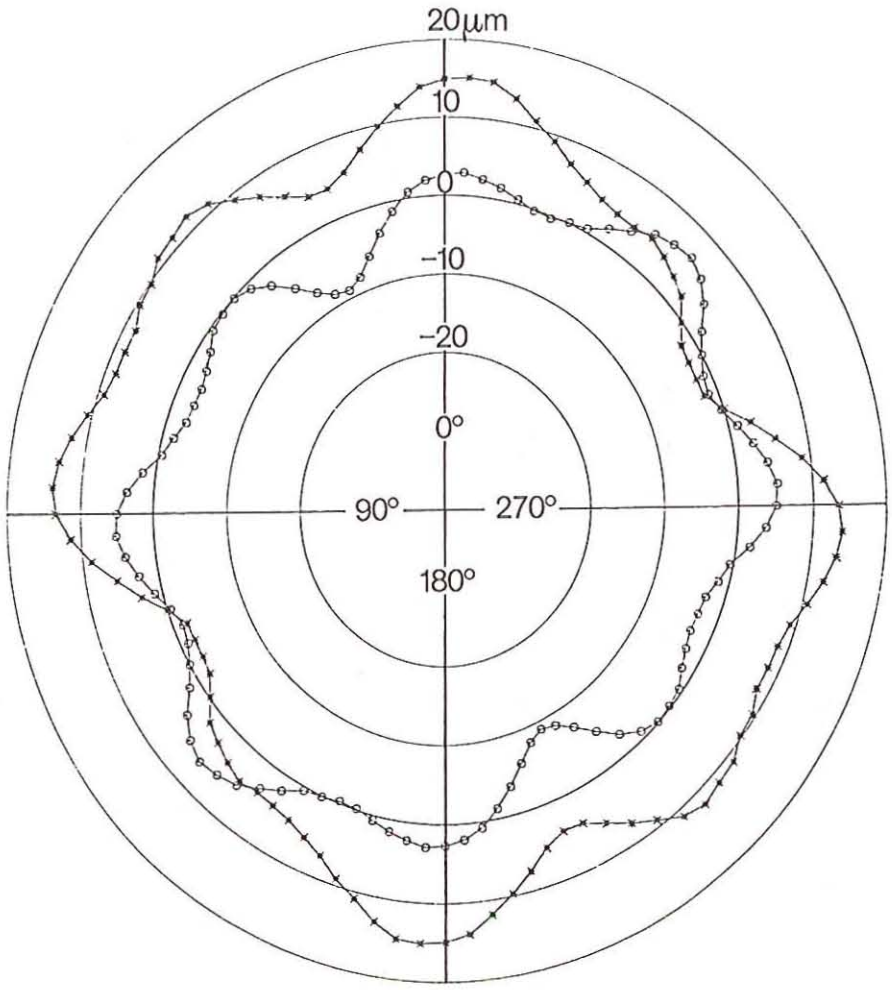

∘ Before irradiation
After irradiation

Deviation from the average diameter before irradiation (10.759mm)

Fig. 2.5/7: Circumferential Diameter Profile of the Test Fuel Rod TDT81

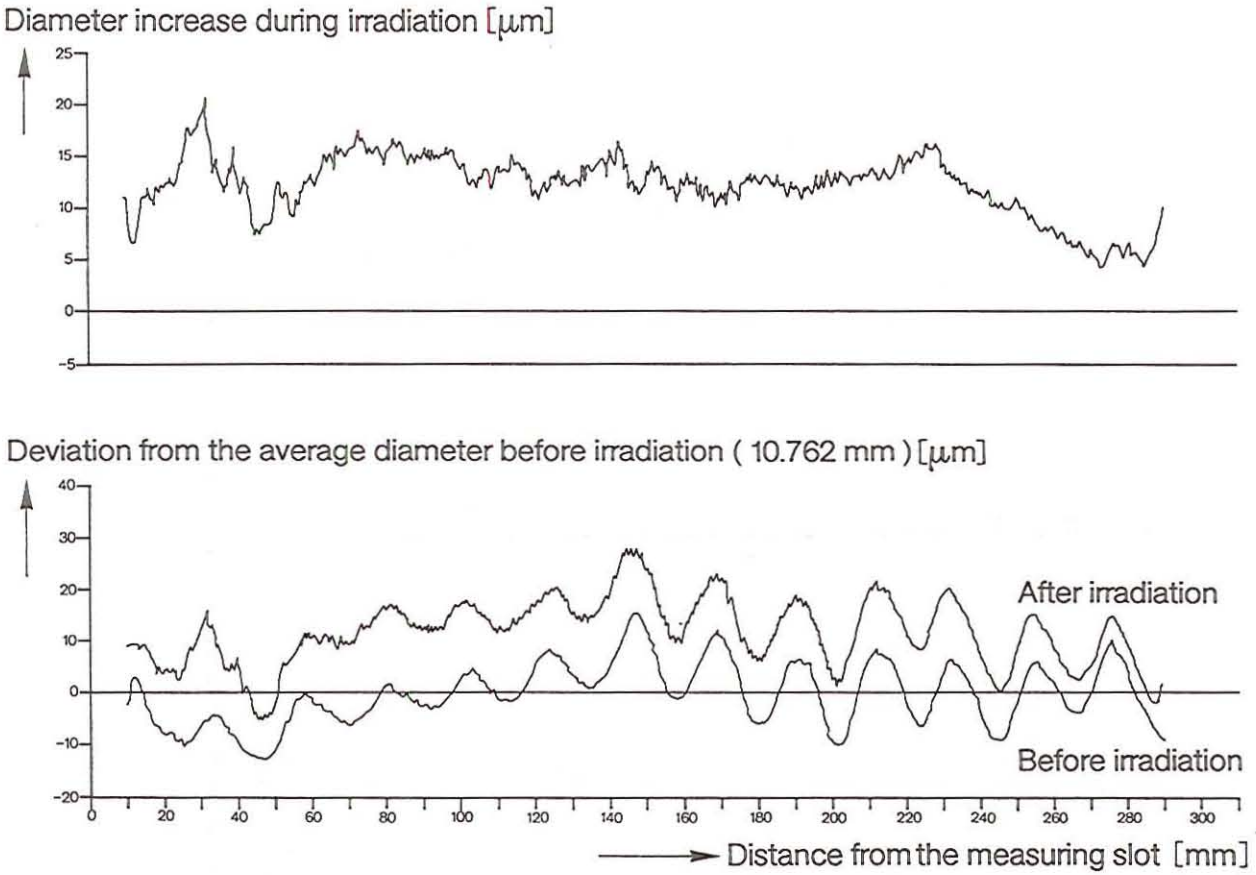

Fig. 2.5/8: Axial Diameter Profile of the Test Fuel Rod TDT81

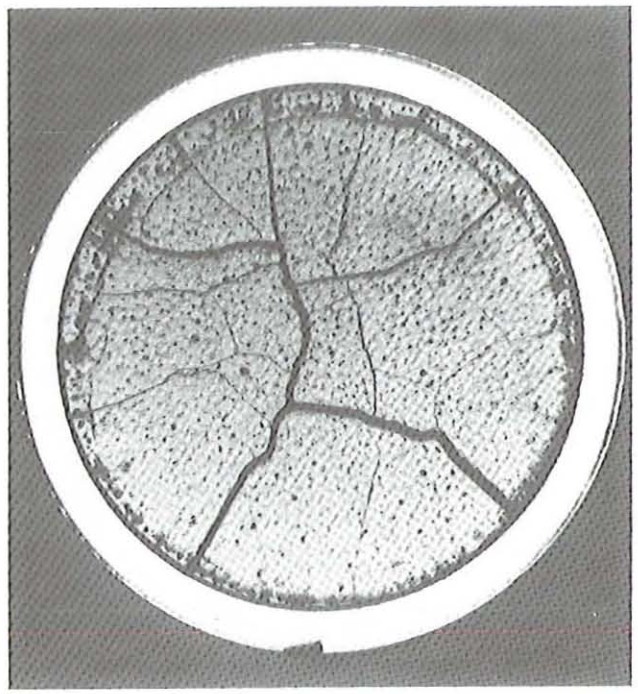

2 mm

Maximum linear power = 438 W/cm

Fig. 2.5/9: Cross-Section of the Test Fuel Rod TDT81

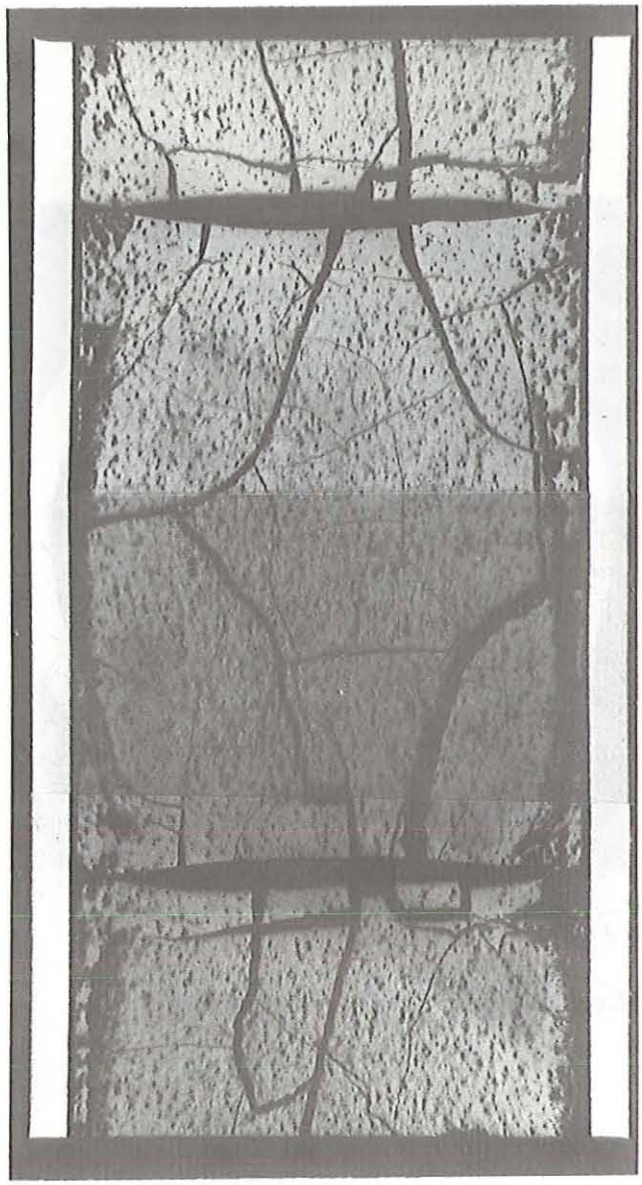

Fig. 2.5/10: Longitudinal Section of the Test Fuel Rod TDT81

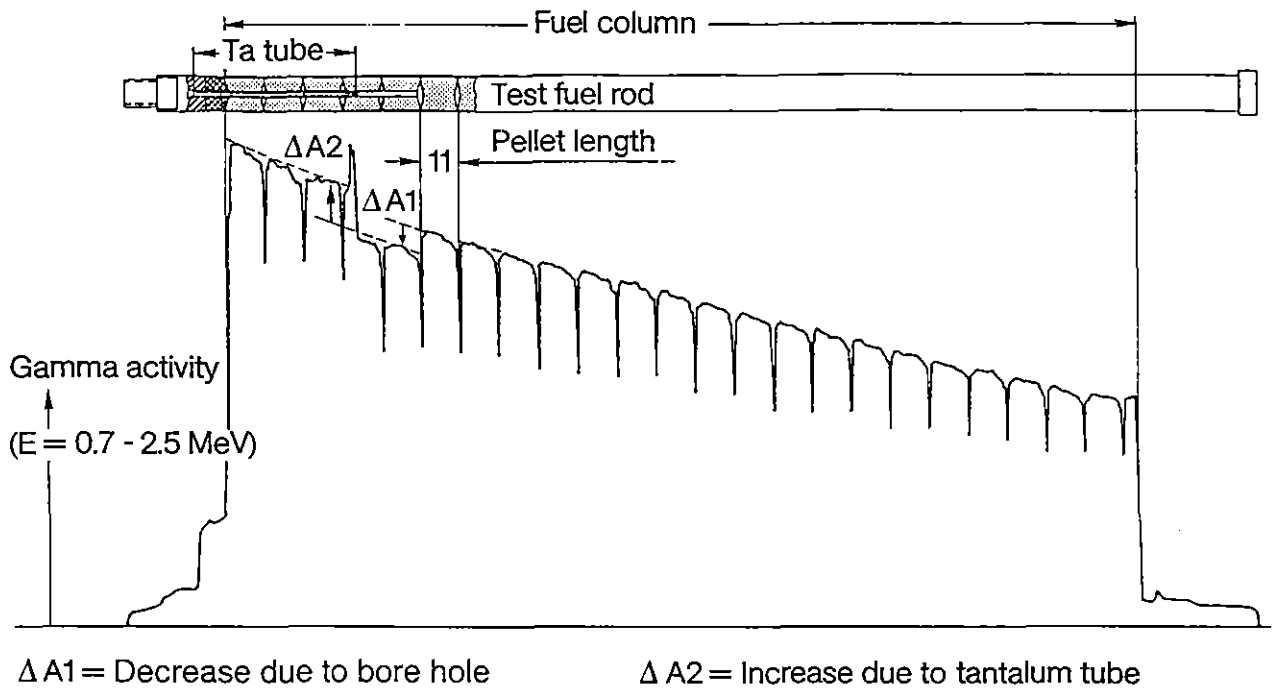

Fig. 2.5/11: Gamma-Scan of the Test Fuel Rod TT80

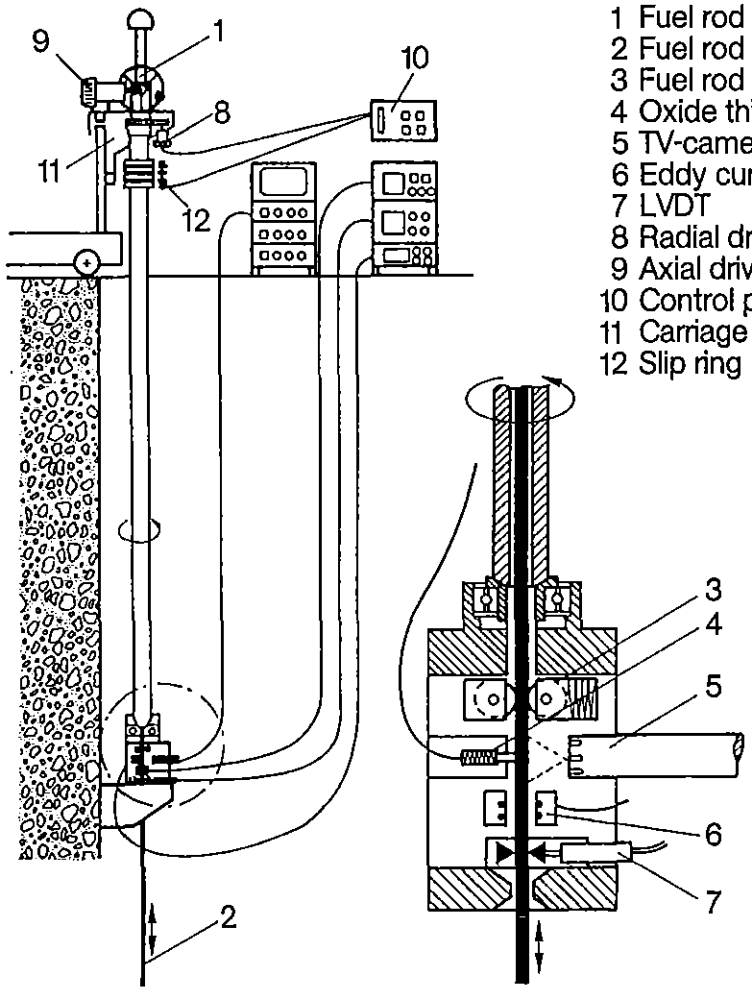

Fig. 2.5/12: Fuel Rod Measuring and Examination Device with Simultaneous Eddy-Current Testing, Measurement of Oxide Layer Thickness and Fuel Rod Diameter, Visual Inspection

2.6 Fuel Storage and Reprocessing

2.6.1 Spent fuel storage assessment

2.6.1.1 Description of the spent fuel storage assessment

Dry storage is the most promising technology of spent fuel storage. Dry storage in an inert atmosphere enables the highest storage temperatures and according to that the shortest pre-storage times in water pools. Therefore, the spent fuel storage assessment has been performed for dry storage in an inert atmosphere.

Figure 2.6/1 features a compilation of all noteworthy mechanisms potentially affecting the fuel rod cladding integrity. Only four of them are of real importance for the fuel rod integrity [2.6-1]:

a) cladding hoop strain;
b) iodine stress corrosion;
c) cladding oxidation from outside;
d) crack propagation.

Experimentally based empirical correlations for these phenomena have been combined to the TRAB code. The computer program calculates the creep strain, the probability of failing by iodine stress corrosion cracking, the cladding oxidation, and the growth of individual cracks as a function of time and at a given temperature/time history [2.6-2]. It has been demonstrated by recalculations of experiments that the TRAB code describes the spent fuel rod behaviour conservatively [2.6-2].

2.6.1.2 Description of the EOL conditions of a Th-fuel pin

The design data of a test fuel rod destinated for an irradiation test in the Angra-1 reactor have been chosen as input data for the TRAB code calculations [2.6-3]. The burnup after four cycles has been estimated to be 53,000 MWd/tU. An end-of-life cold internal pressure of 41 bar has been selected as reference case for the TRAB calculations.

The following geometrical fuel pin data (at room temperature) have been used as input data:

cladding outside diameter:	9.50 mm
cladding inside diameter:	8.22 mm
cladding length:	3840. mm
internal gas volume:	20.5 cm^3

2.6.1.3 Storage performance predictions of a representative spent Th-fuel pin

The calculations have been performed using characteristic data of an independent storage facility of the GORLEBEN type. There, the spent fuel assemblies are stored in metal casks. A cask with a storage capacity of 10 PWR fuel assemblies has been used as reference cask for the calculations. The internal free volume of the loaded cask is 4 m^3. The cask is filled with helium; the oxygen partial pressure is 2 mbar at the beginning of dry storage.

The dry storage behaviour has been analyzed on the basis of a border-line temperature function (Figure 2.6/1). The dry storage starting temperature is 410°C. In a very conservative manner, it is assumed that the temperature is uniform along the fuel rod axis and for all fuel rods in the cask. In reality, the temperature decreases from the midplane to the upper and lower end and from the center to the periphery. Some calculations have also been performed using a temperature which is constant in time.

It has been assumed that the maximum crack depth is 100 µm for the internal surface of the Zircaloy-4 cladding after reactor operation, which is also a conservative value. 25 runs of the TRAB code have been performed (Table 2.6.1) under variation of the outer diameter of the cladding, the internal pressure, the starting temperature and the temperature-time behaviour (decreasing and constant, respectively).

Figures 2.6/2 to 2.6/8 show the results of the calculations for the so-called standard dry storage conditions (border-line temperature function of Figure 2.6/2 and internal cold pressure of 41 bar). The total hoop strain is 0.31 % and its value is nearly obtained after 1 year (Figure 2.6/3). The iodine stress corrosion cracking is not active. The mean crack length remains constant and is far below the mean crack length at perforation (Figure 2.6/4), which results in a perforation probability P of $< 10^{-4}$ (Figure 2.6/5) and in a safety function of practically 1 (Figure 2.6/6). The oxygen content in the cask gas is consumed after 4 months and leads to an increase of the oxide layer of less than 2 µm (Figure 2.6/7). There is no propagation of cracks caused by purely fracture-mechanical mechanisms (Figure 2.6/8).

The results of all calculations – for a storage time of 7 years – are shown in Table 2.6.1. At decreasing temperature the dry storage is safe up to a starting temperature of 450°C at an internal cold pressure of 41 bar. The variation of the internal pressure at the standard temperature function results in failing by Iodine Stress Corrosion Cracking (ISCC) above 60 bar and in exceeding the 1% strain limit above 70 bar. The dependence of total strain from starting temperature and internal pressure is shown in Figure 2.6/9. At constant temperature the fuel rod fails by ISCC above 350°C.

To see the influence of cladding wall thickness, some calculations have been performed for an outer diameter of 9.25 mm corresponding to a wall thickness of 0.52 mm. The results show that the failure limit is now at slightly lower starting temperatures and at slightly lower internal pressures.

2.6.2 Reprocessing studies for (Th, U)O_2 PWR fuel

In the frame of the program one of the objectives was to study the closing of thorium fuel cycle by reprocessing of spent Th-containing PWR fuel elements. However, the demonstration of the closing of the fuel cycle has been considered from the very beginning to be beyond the scope of the program.

An overall conclusion of the performed literature survey at the program beginning was that the program could use to a large extent the existing technologies and available know-how for reprocessing. That is the case with fuel reprocessing from HTR and head-end treatment from LWR [2.6-4]

Following this extensive literature survey cold laboratory tests on reprocessing were initiated. They had as major objective the verification of the applicability of the two-cy-

cle THOREX reprocessing scheme derived for $(Th,U)O_2$ HTR fuel irradiated to burnup of up to 100,000 MWd/tHM [2.6-5] to the $(Th,U)O_2$ pellet fuels considered within the scope of this program.

Cold dissolution experiments have shown that during the dissolution of $(Th,U)O_2$ fuels in THOREX solution, the Zircaloy-4 cladding is also dissolved to some extent and, due to this, the dissolution time is distinctly increased. Hot dissolution tests showed that the dissolution time of $(Th,U)O_2$ fuel decreases substantially compared to the results of cold tests.

For an optimization of the solvent extraction processes, distribution data for the system HNO_3, Th, U covering the whole range of interest have been evaluated. Interpolations and extrapolations are possible by a computer program [2.6-6]. Considerations about the radioactivity of reprocessed ^{233}U fuel from power reactors on the one side, and the experience gained so far with the THOREX process variants on the other side, lead to the selection of a single-cycle THOREX process as the most suitable variant.

Pulsed columns are the preferred extraction apparatus because this equipment produces less TBP degradation products due to the shorter contact time. In addition, pulsed columns are less sensitive against process disturbances by any crud formation [2.6-7]. For extraction a continuous organic phase, for re-extraction a continuous aqueous phase operation in pulsed columns should be selected [2.6-4].

2.6.2.1 Dissolution and feed adjustment of $(Th,U)O_2$ fuel with Zircaloy-4 clad

Cold dissolution tests

The existing technology with available know-how applicable to the head-end treatment in the reprocessing of thorium and uranium mixed oxide with Zircaloy-4 cladding is the chop-leach process, used for PWR reactors. The fuel rod is cut in 2-5 cm pieces, which are processed in a dissolver provided with a basket. The final solution of thorium and uranyl nitrate is adjusted to the requirements of the solvent extraction feed.

A good number of factors affect the reprocessing of ceramic fuels and the first work was to analyse the physico/chemistry side of the system ThO_2/HNO_3-HF [2.6-8]. The dissolution of oxide fuels largely depends on the material microstructure and density, which depend on the fabrication process. For materials with a homogeneous microstructure and regular pores, the total dissolution time is long and it increases with the density. Three types of $(Th,5\%U)O_2$ pellets were used in the experimental work, with different densities and microstructures. The dissolution tests were performed with a ratio of solid to solvent that yields 1 mol Th/l solution after complete dissolution.

The first pellets, with density of 8.3 g/cm^3, were fabricated without carbon black addition and they presented very irregular microstructure with great and interconnected pores. They were completely dissolved between 10-14 hours: the scatter in the total dissolution time may be explained by the variations of material characteristics. The second type were pellets with density 9.3 g/cm^3 and they were fabricated with carbon black addition. They had a little more homogeneous microstructure, but they still displayed great and deformed pores. They were completely dissolved in about 15 hours. The last pellets of the tests had density of 9.4 g/cm^3 and they were also fabricated with carbon black addition. They took more than 50 hours to dissolve, that was the consequence of a good microstructure, without great pores and with a homogeneous pore

distribution. The dissolution of the three types of (Th,5%U)O_2 pellets is described in detail in [2.6-9].

The presence of zirconium slows down the dissolution, that means it reduces the initial reaction rate and increases the total dissolution time of the pellet. Since zirconium forms strong complexes with the fluoride ions, its presence decreases the available fluoride concentration in the THOREX solution. Then, it becomes less effective as ThO_2 dissolution agent. The pellet dissolution time increased by about 30% when Zircaloy-4 was present and the weight loss in the first hours of the reaction decreases between 5 and 20%, depending on the pellet fabrication data.

The (mass of solid/volume of dissolvent solution) ratio is important for the dissolution process and its increase, to a certain extent, reduces the time needed to obtain a solution with the required concentration. When this ratio was increased by 50%, the time to obtain I mol Th/l solution decreased by 65%.

In the dissolution of ThO_2 pellets, 90% of a batch may be dissolved in a few hours, whereas the other 10% may require substantially longer time. With the heel technique, in which the refractory material is contacted with fresh dissolvent, the total processing time is effectively reduced [2.6-10]. By using this technique, it was possible to dissolve a mass of 4 pellets of (Th,5%U)O_2 with density 9.3 g/cm^3 in 10 hours of processing and 1 mol Th/l solution was obtained.

Cold dissolution tests provide basic essential information about the chemical system and reaction mechanism. Nevertheless, the irradiation changes the fuel structure significantly and, therefore, only hot tests can furnish necessary data about dissolution.

Hot dissolution tests

Hot dissolution tests were performed with samples from the first irradiation test in the research reactor FRJ-2 in KFA-Juelich. The pellets had a density of 9.53 g/cm^3 (95% of the theoretical density) before the irradiation. The samples came from the fuel rod TDT 81. Figure 2.6/10 shows the exact place from where the samples for the dissolution tests were taken.

Two dissolution tests were performed having as main objectives to determine the total dissolution time and to check for the presence of insoluble residues. In the first test, the fuel rod pieces number 1 and 2 were used, while for the second one the samples 3 and 4 were taken. The cooling time before the dissolution was 7 months for the first test, and 8 months for the second.

For each test, the two pieces of the rod were weighed with the Zircaloy-4 cladding and dissolved in 50 ml of the THOREX reagent, until only the cladding material remained and no more than a small residue of the fuel material. The thorium concentration in the final solution was about 1 mol/l. The dissolution was followed by thorium and uranium analysis using an X-ray fluorescence spectrometer. Gamma-spectrometry was also carried out. For this it was necessary to dilute the samples up to 1,500 times, to enable their direct handling.

Figure 2.6/11 shows the dissolution curve obtained in the hot tests, and, for comparison, the curve for fresh pellets from the same fabrication batch. The irradiated material was completely dissolved in about 20 hours, while non-irradiated material took more than 35 hours. Such behaviour has already been reported by other authors [2.6-11].

This confirms that the general observations known for UO_2-fuels are also valid for $(Th,U)O_2$. The main point to explain the different behaviour of the irradiated material is its physical state. Figures 2.5/9 and 2.5/10 show the test fuel rod as presented for the post-irradiation examination. The irradiated material had big cracks and it was broken in pieces or partially powdered during the shear process. Then the material had a specific surface for the chemical reaction substantially larger than the one provided by the fresh material, thus dissolving faster.

The top of the Figure 2.6/11 shows that the largest release of the fission product krypton-85 measured at the stack of the hot cells occurs in the first hours of the dissolution process.

Small amounts of insoluble residues were obtained in both dissolution tests. The residues had a bright black colour and they constituted fine particles, which could be retained in filter papers for 0.2 µm particles. Gamma-spectrometric analysis have revealed that the niobium-95 was mainly responsible for the high specific gamma-activity of the residues.

2.6.2.2 Solvent extraction by THOREX process

Selection of the process

The THOREX process was developed for processing irradiated thorium to separate ^{233}U and thorium and decontaminate them from fission products. Like the PUREX process, the different variants of the THOREX process use a 30% solution of TBP in an organic solvent such as kerosene.

The form of the THOREX process first developed at the Knolls Atomic Power Laboratory (KAPL) and the Oak Ridge National Laboratory (ORNL) used aluminum nitrate as salting agent to enhance the distribution coefficients of uranyl and thorium nitrates [2.6-12]. It was used to process thorium irradiated in the U.S. AEC's Savannah River production reactors. Because the $Al(NO_3)_3$ used as salting agent added undesirably to the nonvolatile material in the high-level wastes, it was replaced by nitric acid in the acid THOREX process developed by ORNL in the early 1960s [2.6-12]. Thorium may also be salted out by HNO_3, which is relatively easy to recycle and destroy, and virtually all of the processes taken into consideration today use this acid as a salting agent. The ORNL process uses a feed solution of 1.1 mol/l $Th(NO_3)_4$, a special feature being the acid deficiency of about – 0.15 mol/l. The scrub solution is 1 mol/l HNO_3. The acid deficiency is adjusted by steam stripping of the feed solution. Fission product decontamination (particularly with respect to zirconium) is reported to be improved due to the low acid concentration. On the other hand, undesirable precipitates can be encountered during feed adjustment of high burnup fuels [2.6-13].

Particularly zirconium hydroxide is precipitated almost quantitatively during the acid deficient feed adjustment. This makes a liquid/solid separation necessary with involved losses of heavy metals. This problem is intensified if the solution contains not only the zirconium produced by fission but also the zirconium from Zircaloy-4 as discussed in section 2.6.2.1.

To avoid the problem of the formation of a precipitate in the early 1970s, Farbwerke Hoechst [2.6-5, 2.6-12] developed a dual cycle process to fuel irradiated to burnups to 100,000 MWd/t. The flowsheet was demonstrated in hot-laboratory runs at the

KFA-Jülich on 1 kg/day of fuel irradiated to burnups up to 54,000 MWd/t.

This process uses a 1 mol/l HNO_3 feed solution in the first cycle and a 0.1 mol/l HNO_3 scrub, thus avoiding hydrolytic precipitates during feed adjustment. After having separated the main volume of fission products in the first cycle, an acid deficient feed solution is used in the second cycle to reach the desired decontamination factors. In this cycle the scrub is 1 mol/l HNO_3 [2.6-5].

The acid THOREX process and the acid deficient THOREX process differ very much in their HNO_3 supply via feed solution and scrub. The low HNO_3 concentration of the incoming scrub solution in the acid THOREX process suggests that there is a substantially lower HNO_3 concentration in the scrub section. The question arises whether both flowsheets can be stable in such different process configurations [2.6-4].

Cold experiments have shown the feasibility of both extraction variants. Recovery of 99.9% of the heavy metals is possible without problems. In any case, from the standpoint of easiness of processing the acid feed solution should be preferred because feed adjustment is simpler [2.6-4].

The reextraction of the heavy metals (U,Th) can be, in general, carried out either as joint stripping of both elements or by selectively stripping first the thorium and then the uranium. In the two cycle process of Farbwerke Hoechst co-stripping is done in the first, partitioning of thorium and uranium is accomplished in the second cycle.

Investigations have revealed a serious problem of reextraction. At the low acidity necessary for the process, a crud is formed. It disturbs the function of the extraction apparatus. This has been observed in mixer-settlers as well in pulsed columns [2.6-4]. To avoid the crud safely, it is necessary to reextract at even higher acidity.

Therefore, partitioning should be the preferable procedure, since in this kind of reextraction only thorium is stripped into the aqueous phase while the uranium remains in the organic phase [2.6-4].

Development of the process

Extraction

In designing a THOREX flowsheet, it must be recognized that a second organic phase (third phase) is precipitated if a too high loading of the organic phase occurs. This perturbs the function of the extraction apparatus due to its physical properties. Thus, the formation of this third phase must be avoided with certainty. Maximum loadings of thorium in the organic phase should be limited to about 30% of the theoretical capacity, that is 35g Th/l, since the molar ratio TBP to thorium is about 2.3 for saturated solutions [2.6-13].

Due to the relatively low extractability of thorium, a comparatively high flow-ratio of the organic to the aqueous phase is required. At a working temperature of 20-25° C the feed concentration must be limited to about 1 mol/l of thorium, to avoid the third phase formation. However, since the formation of the third phase is also influenced by the acid concentration, it is also necessary to limit the overall supply of HNO_3 via the feed solution and scrub. The too low supply of acid via these solutions will lead to high thorium losses via the waste flow due to the poor extractability of thorium. For this reason, concentrated HNO_3 is added to the aqueous stream shortly before it leaves the

extraction apparatus. Here the formation of the third phase is not possible due to the low concentration of thorium in the extraction section of the contactor. With the resulting acid concentrations, the thorium losses are reduced to an acceptable level. Uranium, much better extracted than thorium, is practically absent in the raffinate stream [2.6-4].

As seen previously, the THOREX process with acid deficient feed solution was proposed to improve the decontamination factors for fission products such as Zr, Nb and Ru. Both THOREX processes with acid and deficient feed solution differ very much in their HNO_3 supply via feed solution and scrub. However, an analysis of the acid profile in a mixer-settler provided the following result (Figure 2.6/12): although the acid concentration in the vicinity of the scrub inlet is lower than in the acid THOREX process, it is still considerably higher than the expected one and it will then quickly rise to higher values than in the acid deficient process. Moreover, the differences between the acid concentrations in the scrub section of the two extraction processes only produce a minor effect, because the influence of the salting agent HNO_3 on thorium distribution is negligible for the thorium concentrations around 0.1 mol/l found in the scrub section [2.6-4].

Cold experiments have shown that an aqueous/organic (a/o) flow ratio of 0.23 is suitable for the extraction step, providing a recovery close to 99.99% for both heavy metals, for the acid THOREX flowsheet [2.6-14].

Special attention has to be taken at the start-up: the solution containing Th and U cannot be fed into the mixer-settler till a suitable acidity is achieved in the system.

In view of the slightly different acidity profile of the acid and the acid deficient process the question arises whether the acid deficient process can actually result in better decontamination factors as reported by Farbwerke Hoechst and other authors [2.6-5, 2.6-10]. Better decontamination can only be achieved if the hydrolysed species generated during acid deficiency adjustment do not have enough time to react with the acid during the extraction process: the residence time is too short and the temperature is too low.

Batchwise and continuous experiments demonstrated clearly that for both processes similar fractions of zirconium are extracted into the organic phase, if the acid concentrations are the same. The different zirconium decontamination factors observed in the continuous experiments can be simply explained by the different acid profile in both processes. If the Zr-profiles shown in Figure 2.6/13 are compared with the acid profiles (see Figure 2.6/12), it becomes clear that there is a close relationship between Zr-extractability and acidity of the aqueous phase.

It becomes evident that those low extractable hydrolysed species of zirconium are converted rapidly to more extractable non-hydrolysed ones, due to the present HNO_3. The time involved in such transformation is shorter than the residence time of the aqueous phase in the mixer-settler. The conclusion drawn from this fact is: if a mixer-settler is used, there is no actual advantage in employing an acid-deficient feed solution for the THOREX process. This question is still open when the extractor is a pulsed column, since here the contact time between the two phases is short.

With respect to the influence of fluoride anion on the zirconium decontamination, it is interesting to note the increment of the Zr-concentration in the organic phase, if fluoride is present in the system.

The literature reports that zirconium forms a highly extractable monofluoride complex, under special conditions [2.6-15, 2.6-16]. It was concluded that, within the range of thorium, zirconium and fluoride concentrations of interest for the extraction step of the THOREX process, the zirconium is mainly present as a monofluoride complex and almost all the residual fluoride is associated to the thorium. Also, it was seen that an increase of the fluoride content beyond a certain value mainly has as a consequence the increase of the thorium monofluoride concentration, and it does not contribute to the inhibition of the zirconium extraction.

Thorium and uranium partitioning

In the dual cycle process of Farbwerke Hoechst the co-stripping of thorium and uranium is performed in the first cycle, while their partitioning is accomplished in the second one. However at the low acidity necessary for the reextraction of both thorium and uranium, a crud is formed which disturbs the function of the extraction apparatus. The crud is induced by the formation of a $Th(DBP)_4$ precipitate, as was concluded from the chemical analysis [2.6-4].

The dibutylphosphate (DBP) is formed by radiolysis or hydrolysis of TBP during the extraction step, at nitric acid concentrations up to 4 mol/l and it is transported into the next step by the loaded organic phase. Here the $Th(DBP)_4$ precipitates, because the acidity is low (0.01 mol HNO_3/l) according to the Farbwerke Hoechst flowsheet. At this acidity, the operation of an extraction apparatus is only possible for hours, otherwise the crud blocks either the orifices (in mixer-settler) or causes flooding (pulsed columns) [2.6-4].

The crud formation can be avoided, however, if the acidity of the aqueous phase is maintained above 0.3 mol HNO_3/l, as revealed in batchwise experiments; if there is no thorium in the system or if the acidity is high, crud is not formed in cold laboratory tests. But at a higher acidity than the one in the co-stripping step of Hoechst process, it is very difficult to reextract uranium, which remains mainly in the organic phase. Because of this behaviour, it was concluded that the preferable procedure should be the partitioning rather than the co-stripping. So, the crud could be safely avoided with the use of an acidity high enough for the partitioning.

Several cold partitioning tests were performed using thorium-stripping solutions with higher concentrations than that in the Hoechst flowsheet. For instance, using a stripping solution with 0.5 mol HNO_3/l no crud formation was observed independently of the aqueous/organic flow ratio. Unfortunately this high acidity had as result a relatively high loss of thorium in the uranium organic effluent. But it was clear that the correct way to solve the problem of crud formation in the partitioning is to use higher acidity. Then, the questions were the best a/o flow ratio and the best strip solution concentration for an efficient thorium-uranium separation.

The partitioning must be very well controlled, to avoid or at least to minimize the thorium presence in the organic effluent. Since the TBP-degradation products are also transported via the organic phase to the next step of uranium re-extraction, they can form a complex with the residual thorium, resulting in crud formation.

The investigations demonstrated that the organic phase should not be kept loaded more than a few days, to avoid the crud formation. The aging of loaded TBP solutions seems to favour this formation during the next stripping step either for thorium or for

uranium. The right procedure is to process immediately the organic solutions or to perform continuously the whole flowsheet.

According to the Hoechst flowsheet, the first cycle consists of an extraction step using an acid feed solution and an a/o-ratio equal to 0.23, followed by a thorium-uranium co-stripping step.

The second cycle constitutes an extraction step using an acid-deficient feed solution with an a/o flow ratio equal to 0.28, followed by the thorium-uranium partitioning and then the uranium reextraction. As seen, however, the cold tests showed that the best aqueous/organic flow ratio for the extraction step for both acid and acid-deficient feed solution is 0.23 [2.6-14]. For flow-ratios greater than 0.23 the system has a tendency towards the conditions at which the third phase is formed, at room temperature.

As a consequence of the changing in the a/o – ratio for the extraction step that precedes the partitioning, this step has now a feed organic solution containing about 26 g Th/l and 1.3 g U/l; these concentrations are lower than those established in the Hoechst flowsheet. In these new conditions and using a stripping solution with 0.01 mol HNO_3/l, fluctuations of the uranium concentration in the organic effluent stream were observed, even after a time sufficient for the steady-state in the mixer-settler to be reached. The runs were monitored through the thorium concentration in the aqueous product. The consequences are an instability of the whole system and higher thorium and uranium losses. At this unstable condition, the uranium concentrations inside the extractor reached values up to 10 times higher than the one in the organic feed solution of the partitioning step. This fact must be taken into account for a critically safe design of the extraction apparatus.

This uranium fluctuation phenomenon, identified as uranium reflux, has already been reported in the literature [2.6-10, 2.6-17]. Cold laboratory tests have revealed that two main factors influence the uranium reflux: the acidity and the uranium load of the system. Also, the use of a small scale air-pulsed mixer-settler have favoured the uranium reflux, if compared with a mechanically stirred one.

The uranium reflux could be avoided by increasing the nitric acid concentration in the thorium stripping solution. That means, the problems of crud and uranium reflux could be solved by the same way. This simplified the investigations. Some variants of the partitioning step with higher HNO_3 concentration have been tested, aiming at its optimization. Experiments were carried out using, for instance, a 0.5 mol HNO_3/l solution with a/o flow-ratio of 1, 0.66, 0.56 and 0.46. They resulted in no crud formation, as seen above, and no uranium reflux. However undesirable losses of uranium (up to 2%) and a relatively high thorium concentration in the organic effluent were observed. Good results have been obtained with the thorium strip solution of 0.2 mol HNO_3 /l and overall a/o = 0.6; no crud was formed, no uranium reflux was observed and the losses were 0.06% for thorium and 0.06% for uranium. For this last condition, the profiles for acid, thorium and uranium in the mixer-settler in equilibrium for the partitioning step are shown in Figures 2.6/14 and 2.6/15.

Uranium reextraction [2.6-4, 2.6-14]

Uranium is reextracted from the loaded organic stream leaving the partitioning step by a counter-current contact with a low acid content solution.

Since the beginning of this study crud formation has been observed during the urani-

um stripping. Many times the precipitation of this crud has even led to an interruption of the running test. Then, the main efforts were concentrated in looking for operational conditions at which no crud formation was possible and which provided the maximum recovery of uranium.

Two methods were investigated to achieve these objectives. First, the acidity of the stripping solution was increased to 0.3 mol HNO_3/l, and a/o flow ratios equal to 0.5, 3 and 5 were tested. Such conditions reduced the crud formation, but they did not eliminate it completely. In addition, they resulted in a significant loss of uranium in the organic stream.

The second method investigated was the addition of fluoride to a 0.05 mol HNO_3/l stripping solution. The purpose of the fluoride should be the formation of a complex with the residual thorium, instead of the TBP-degradation products, thus suppressing the crud formation. However, at a/o = 1, stripping solutions with 0.1, 0.05 and 0.01 mol F^-/l produced precipitates (ThF_4), which disturbed the stripping process again.

After these disappointing results, it was decided that the best was to improve the thorium-uranium partitioning, as it was reported previously.

If there is very low thorium content in the organic effluent of the partitioning, no crud formation is to be expected during the uranium stripping process, even for a strip solution of low acidity (0.01 mol HNO_3/l). For an a/o flow ratio of 0.50, the uranium concentration in the organic effluent was below the detection limit of the analytical method, or corresponded to a uranium loss lower than 0.1 % for this step.

Recommended flowsheet [2.6-4, 2.6-5]

The dual cycle THOREX process was developed for reprocessing high-burnup fuel for reasons mentioned before. As demonstrated by Kuechler [2.6-5] in hot cell experiments high decontamination factors up to 10^7 for uranium and up to 10^6 for thorium were obtained. The uranium losses to the thorium product and to the organic raffinates of the first and second cycle were 120 ppm and 40 ppm, respectively. The thorium losses to the uranium product came to 250 ppm.

However, when looking at the entire thorium fuel cycle, the question arises, whether such high decontamination factors are required at all. It is known that bred ^{233}U always contains a few hundred ppm ^{232}U, which has some very radioactive daughters. During refabrication, large amounts of ^{233}U can only be handled in hot cells, so that a solvent extraction decontamination factor above 10^2 to 10^3 is not necessary.

The same applies to reprocessed thorium which contains considerably more ^{228}Th than its equilibrium value. Thorium, if recycled immediately, must be processed in hot cells in the same way as ^{233}U. On the other hand, reprocessed thorium can also first be stored for 10 half-lives of ^{228}Th, i.e. for about 20 years, so as to reach the radioactivity of unirradiated thorium again. However, high decontamination factors are probably not worthwhile for this concept either. The most disturbing radionuclide, ^{95}Zr, with a half-life of 64 days, will have decayed completely. It is also doubtful that a very good purification of thorium by solvent extraction will provide advantages with respect to other radionuclides.

These considerations lead to the proposal to use in this case a single-cycle THOREX process for reprocessing thorium-bearing fuel. An optimized process with acid feed

solution (1 mol HNO_3/l) should be capable of providing the required decontamination factors of up to about 10^3 for both uranium and thorium. As previously discussed, an acid deficient feed solution cannot be used in a single cycle operation due to the formation of precipitates in the feed adjustment.

Reextraction should be carried out as partitioning of thorium and uranium, i.e., first reextraction of thorium alone, followed by uranium stripping in a second step. As mentioned before, the formation of a crud can be avoided with this procedure. Furthermore, the flexibility of the fuel cycle requires a partitioning anyway.

Table 2.6.16 shows a flowsheet which reflects the results obtained in the cold tests during the last years. However, hot cell experiments with irradiated fuel are necessary in addition in order to study the influence of the various fission products and radiation effects.

Application for fuel recovery from (Th,5%U)O_2 pellet scraps

During the fabrication of thorium-uranium mixed oxide pellets scraps will occur, and as a consequence, a significant loss of fissile uranium.

Since the beginning of the program, the solvent extraction THOREX process has been studied to reach the best conditions for thorium-uranium separation and purification, in the frame of the reprocessing studies. In view of the results achieved, it was decided to apply the single cycle THOREX process for the purpose of heavy metal recovery from the fabrication scraps (Figure 2.6/16).

The dissolution of the material scraps to be recycled and the adjustment of the solvent extraction feed solution were carried out as seen in section 2.6.2.1.

For the continuous operation of the whole solvent extraction flowsheet, three mixer-settlers were placed in positions so that the load organic phase leaving the extraction step flowed by gravity, to the next partitioning battery, and similarly from this, the organic current flowed to the uranium reextraction battery. The facility is, however, flexible, being possible to operate only one of each step of the process separately, if necessary.

The capacity of the solvent extraction facility in heavy metal separation and purification is 61.5 g thorium (associated to 3.2 g uranium) per 8 hours.

When operating continuously the whole flowsheet, undesirable losses of thorium were observed in the aqueous raffinate of the extraction step, and of uranium in the thorium product stream of the partitioning. These losses occurred at the start-up of the test runs. They were minimized only after about 4 hours of operation, when the nitric acid concentration in the mixer-settlers achieved the required values to provide the extraction. Then, some modifications were introduced in the start procedure so that the losses reached an acceptable level.

During the tests another difficulty presented itself in the occurrence of a white-green gelatinous precipitate in the uranium product solution. The fresh solutions were quite clear, and after some days, they presented a turbid aspect. An analysis revealed that most of the precipitate was volatile material, and it also contained less than 2% of uranium, thorium and phosphorus. The phosphorus originated from the TBP, which is slightly soluble in nitric acid solutions [2.6-18].

Although the TBP is a very stable solvent, it degradates in contact with the nitric acid solutions of the process, by a reaction of hydrolysis. The largest part of the degradation products generated in the extraction step of the THOREX process follow the thorium product stream of the partitioning. This behaviour can be explained by the low acidity present in the thorium-uranium partitioning step [2.6-19].

To avoid surely the formation of such precipitates, the dissolved TBP must be eliminate from the uranium solutions. Furthermore, the phosphorus must be eliminated anyway to obtain a product within the specification for directly recycling in the pellet fabrication process.

2.6.3 Conclusions

The analysis of the dry storage behaviour has been performed for a cask storage facility of the GORLEBEN type. Anticipating realistic EOL conditions, the storage of spent Th fuel pins is safe up to starting temperatures of 450° C. There is a broad safety margin for higher internal pressure or lower cladding wall thickness related to the starting temperature of 410° C as licensed for GORLEBEN. A constant temperature should be limited to 340° C to prevent fuel rod degradation.

The dry storage performance of the spent Th-fuel is very similar to that of the spent U-fuel. It is obvious that all the knowledge of the storage behaviour of U-fuel can be transferred to the Th-fuel rods without any restrictions.

To a large extent the reprocessing studies used existing technologies and available know-how for reprocessing, such as the chemical reprocessing from HTR fuels and the head-end treatment from LWR fuels.

Cold laboratory experiments have shown that during the dissolution of $(Th,U)O_2$ fuels by THOREX solution, the Zircaloy-4 cladding is also dissolved to some extent. The observed dissolution time was increased by about 30% in the presence of Zircaloy-4. Hot dissolution tests showed that the dissolution time of $(Th,U)O_2$ fuel irradiated to about 8000 MWd/t decreases to half related to cold tests.

As a result of theoretical and cold experimental work the single cycle THOREX process has been selected as a reference for reprocessing thorium bearing-fuel from power reactors. An optimized flowsheet with acid feed solution (1 mol HNO_3/l) should be capable of providing decontamination factors of up to about 10^3 for both uranium and thorium, as required when looking at the entire thorium fuel cycle. The reextraction step of the process should be carried out as partitioning of thorium and uranium, i.e. first reextraction of thorium alone, followed by uranium stripping in a next step.

For an optimization of the solvent extraction processes, distribution data covering the whole range of interest have been evaluated. Pulsed columns should be preferred as extraction apparatus because this equipment produces less TBP degradation products due to the shorter contact time and it is less sensitive against process disturbances by any crud formation.

As an extension of the reprocessing studies, the single cycle THOREX process was applied to recover thorium and uranium from scraps. The parameters for the dissolution of the fuel, the feed adjustment and the solvent extraction were defined.

References

[2.6-1] Peehs, M., Kuehnel, R., Kaspar, G.,
„Spent Light-Water Reactor Fuel Properties in Relation to Actual Long Term Storage Concepts",
Siemens Forsch. – U. Entwickl. – Ber. 11 (1982) 301-305

[2.6-2] Peehs, M., Kaspar, G., Steinbeg, E.,
„Experimentally Based Spent Fuel Dry Storage Performance Criteria",
Third Int. Symp. on Spent Fuel Storage Technology, Seattle, Washington – April 8-10, 1986

[2.6-3] Pinto, L.C.M., Santos, A.M.M.,
„Preliminary Design Calculations of (Th,5%U)O_2 Test Fuel Rods to be inserted in Angra-1",
DETS.CN-007/86, Nuclebras, B.Horizonte, Brasil, June 86

[2.6-4] Kernforschungsanlage Jülich; Empresas Nucleares Brasileiras, B. Horizonte, Kraftwerk Union, Erlangen; NUKEM, Hanau.
Program of research and development on the thorium utilization in PWRs final report for Phase 1 (1979-1983)
Jülich, Kernforschungsanlage Jülich, 1984.(Jül. SPEZ-266 NUCLEBRAS/CDTN-471/84)

[2.6-5] Kuechler, L. et alii.
The THOREX two-stage process for reprocessing thorium reactor fuel with high burn-up.
Kerntechnik, 13 (7/8): 319-22, 1971

[2.6-6] Nakashima, T. Zimmer, E.
Die Verteilung von $Th(NO_3)_4$, $UO_2(NO_3)_2$ und HNO_3 zwischen wässeriger Phase und organischer Tributylphosphat-Phase.
Jülich, Kernforschungsanlage Jülich, 1984. (JUEL-1920 ISSN- 0366-0885)

[2.6-7] Fumoto, H. et alii.
Thorium fuel reprocessing with pulse columns II.
Atomkernenergie – Kerntechnik, 41: p.273, 1982

[2.6-8] Filgueiras, S. A. C.
„Dissolucao de oxido misto de torio e uranio em solucao de acido nitrico- acido fluoridrico".
B. Horizonte, Centro Desenvolvimento da Tecnologia Nuclear, 1984. Tese de mestrado.
Universidade Federal de M. Gerais (NUCLEBRAS-CDTN-473)

[2.6-9] Lopes, M.J.O. Filgueiras, S.A.C.
„Dissolucao de ThO_2 e (Th,U)O_2 em solucao de acido nitrico e acido fluoridrico".
In: Congresso Brasileiro de Engenharia Quimica, VI, Campinas, 15-18 Jul, 1984 – Belo Horizonte, NUCLEBRAS/CDTN, 1985 (NUCLEBRAS/CDTN-519)

[2.6-10] Long, J. T.
„Engineering for nuclear fuel reprocessing".
New York, American Nuclear Society, 1978

[2.6-11] Goode, J.H. Flanary, J.R.
„Dissolution of irradiated, stainless-steel-clad $ThO_2 - UO_2$ in fluorid-catalysed nitric acid: hot-cell studies on pelletized, arc-fused and sol-gel derived oxides".
Oak Ridge, Tenn., Oak Ridge National Laboratory, 1965. (ORNL-3725)

[2.6-12] Benedict, M. et al.
„Nuclear chemical engineering".
New York, McGraw-Hill, 1981

[2.6-13] Siddal, T.H.
„Solvent extraction processes based on tri-n-butyl phosphate".
In: Flagg, John F., ed. Chemical processing of reactor fuels. New York, Academic Press, 1961, 530 p.p. 199-248

[2.6-14] Oliveira, E. F.
„A separacao de torio e uranio no reprocessamento quimico de combustivel irradiado de oxidos mistos de torio e uranio"

Belo Horizonte, Centro Desenvolvimento Tecnologia Nuclear, 1984 Tese de Mestrado. Universidade Federalde M. Gerais (NUCLEBRAS/CDTN-512)

[2.6-15] Hickok, R. L. Cannon, R. D.
„Zirconium extraction by tributyl phosphate"
Idaho, Idaho Operations Office, 1959. (IDO – 14487)

[2.6-16] Schlea, C.S. Lowe, J.T.
„Fluoride complexing of U (VI) and Pu (IV) in solutions containing Al(III) and Zr(IV)".
Aiken, S.C., E.I. du Pont de Nemours, 1964 (DP-842)

[2.6-17] Buck et alii.
Chemical processes at U.K. Atomic Energy Authority Works, Dounreay.
In: International Conference on The Peaceful Uses of Atomic Energy, 2., Geneva, 1-13 Sept., 1958. Proceedings... Geneva, United Nations,1959. V.17,p.25-45.

[2.6-18] Leroy, P.
Etude du solvant phosphate tributylique 30% – dodecane.
Centre D'Etudes Nucleaires de Fontenay-aux- Roses, 1976. (CEA-R-3207)

[2.6-19] Cunha, J.W.S.D.
„Influencia da acidez e da dose de radiacao na degradacao hidrolitica e radiolitica do TBP em sistemas de TBP 30% (v/v)-dodecano/H_2O-HNO_3."
Rio de Janeiro, Universidade Federal Rio de Janeiro, 1978. Tese de mestrado.

Table 2.6.1: Input data and results of TRAB code calculations

d(mm)	T_o(°C)	Temp.	P_o(bar)	$_{tot}$(%)	x(mm)	X_{perf}(mm)	P	S	x(mm)
	370			0.12					
	390			0.19					
9.50	410	decr.	41	0.31	0.008	2.56	< 1.E-4	1	0.1
	430			0.49					
	450			0.85					
			31	0.18	0.008	2.56	< 1.E-4	1	
			41	0.31	0.008	2.56	< 1.E-4	1	
9.50	410	decr.	51	0.46	0.008	2.56	< 1.E-4	1	0.1
			61	0.70	0.06	2.56	1	0.97	
			81	1.49	> 4	3.93	1	0	
	300			0.06	0.008	2.56	< 1.E-4	1	
	320			0.10	0.008	2.56	< 1.E-4	1	
9.50	340	const.	41	0.16	0.008	2.56	< 1.E-4	0.99	0.1
	360			0.26	> 4	2.86	1	0	
	380			0.48	> 4	> 4	1	0	
	400			0.91	> 4	> 4	1	0	
	370			0.17					
	390			0.27					
9.25	410	decr.	41	0.45	0.008	2.07	< 1.E-4	1	0.1
	430			0.78					
	450			1.40					
			31	0.26	0.008	2.07	< 1.E-4	1	
			41	0.46	0.008	2.07	< 1.E-4	1	
9.25	410	decr.	51	0.75	0.1	2.07	1	0.97	0.1
			61	1.19	1.3	2.1	1	0.99	
			81	2.99	> 4	> 4	1	0	

Table 2.6.2: Recommended THOREX flowsheet for high burnup fuel (approximate values for concentrations and flowrates)

Extraction		Relative Flowrates (a/o)
Feed:	1.0 mol/l Th; 0.5–1.0 mol/l HNO_3	1.0
Scrub:	0.1 mol/l HNO_3	1.0
Salting acid:	13.0 mol/l HNO_3	0.2
Solvent:	30% TBP/dodecan	9.0
Partitioning		
Feed:	0.1 mol/l Th; 0.15 Mol/l HNO_3	4
Strip:	0.5 mol/l HNO_3	5
Scrub:	30% TBP dodecan	1
U-Stripping		
Strip:	0.01 mol/l HNO_3	0.5

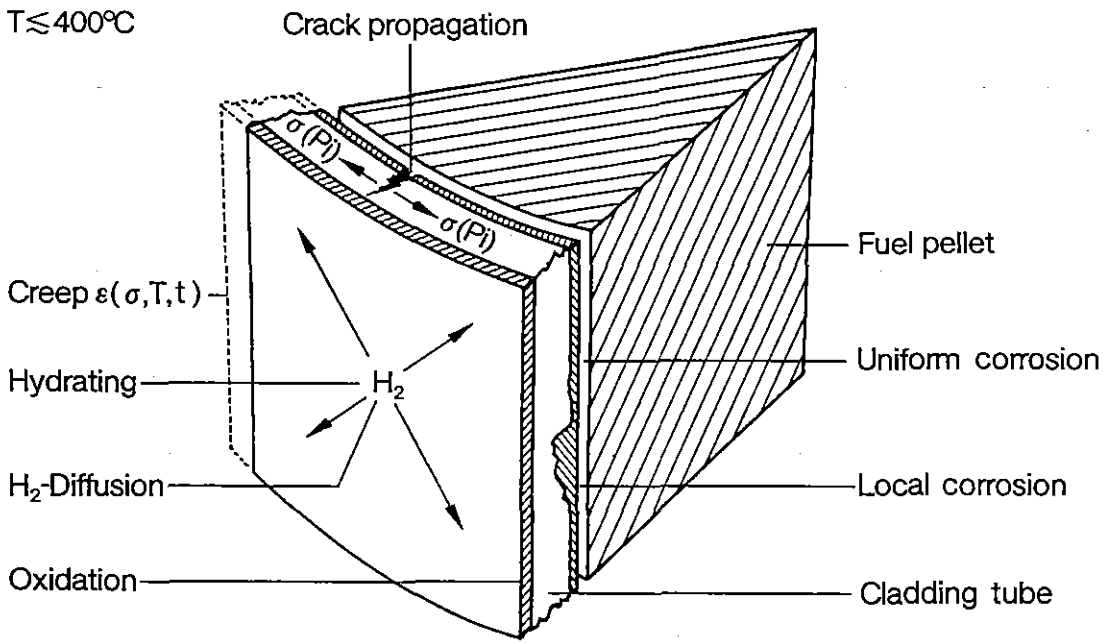

Fig. 2.6/1: Mechanisms Affecting Spent Fuel Cladding Performance during Dry Storage

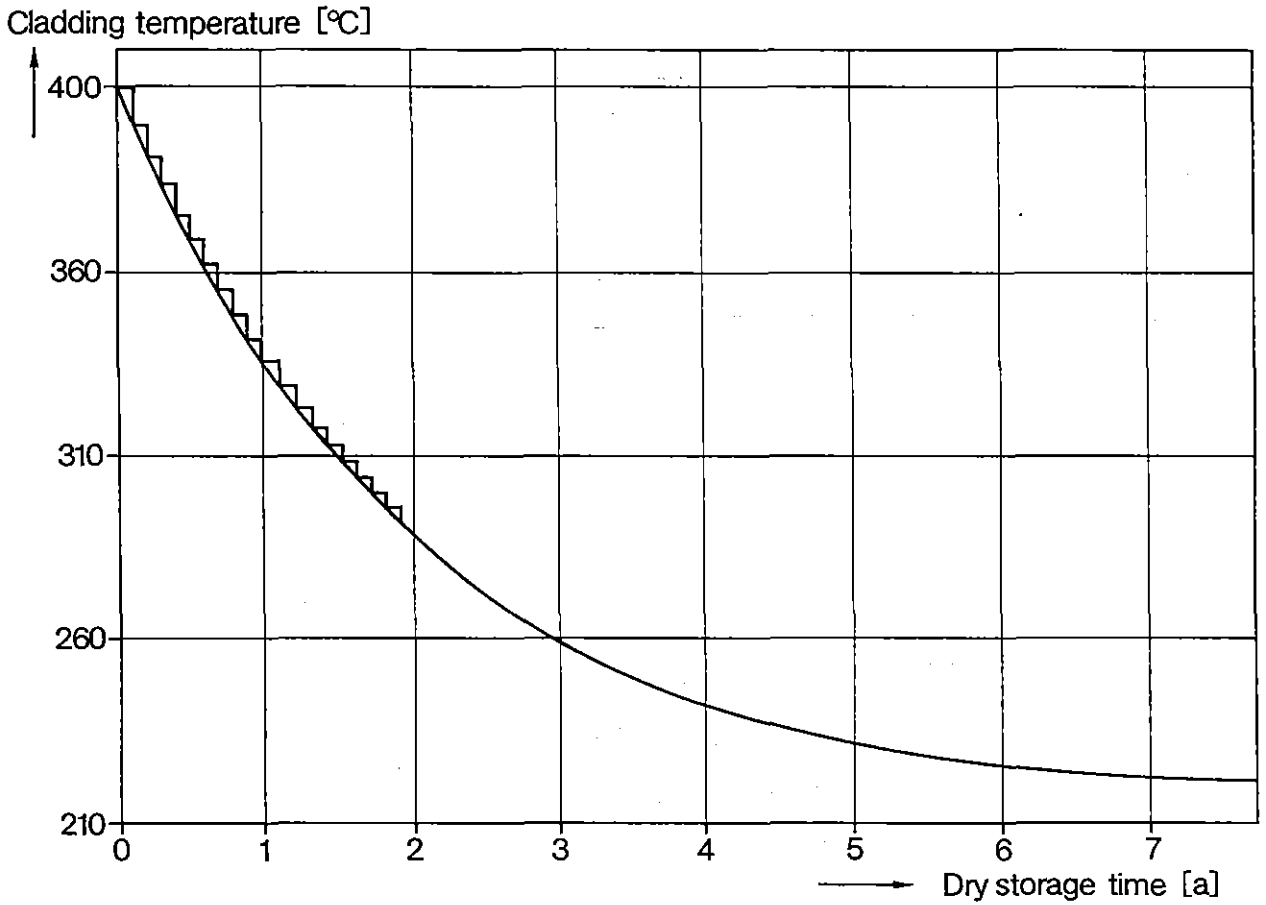

Fig. 2.6/2: Border-line Temperature Function for Dry Storage in Casks

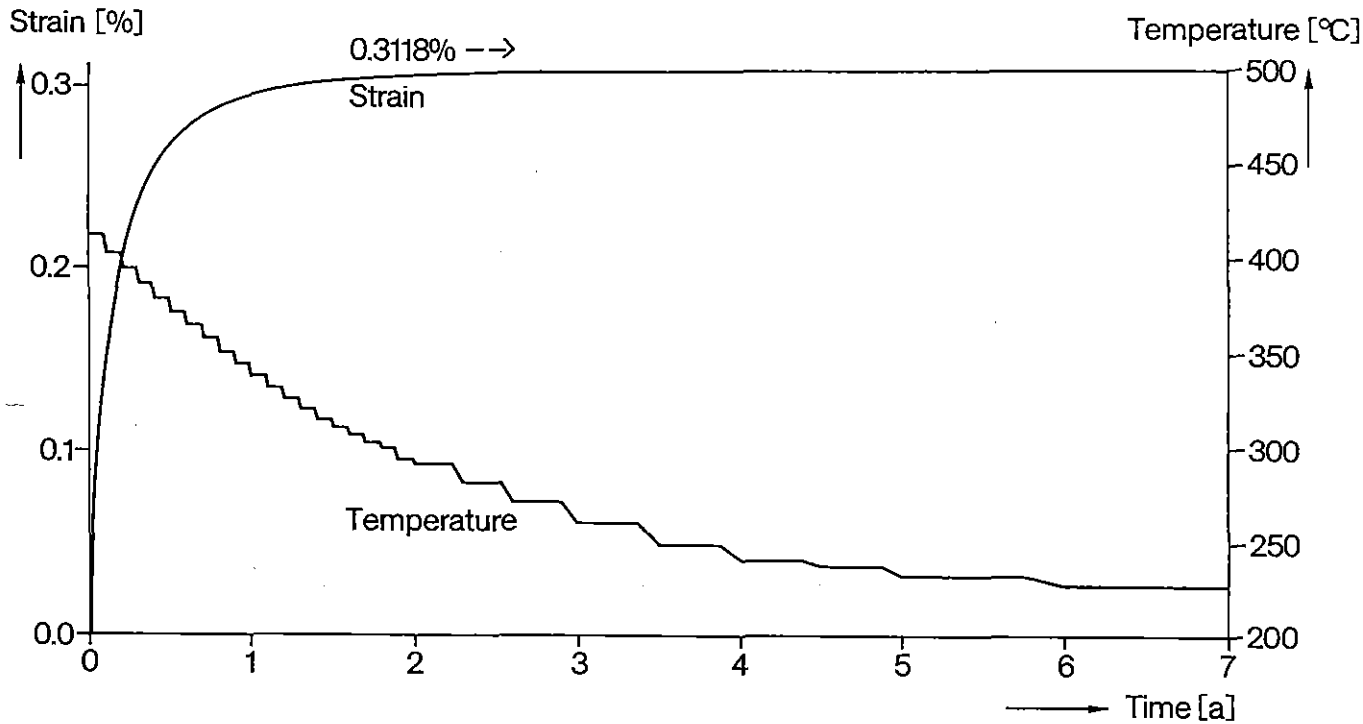

Fig. 2.6/3: Hoop Strain of a Th Fuel Rod at Standard Dry Storage Conditions

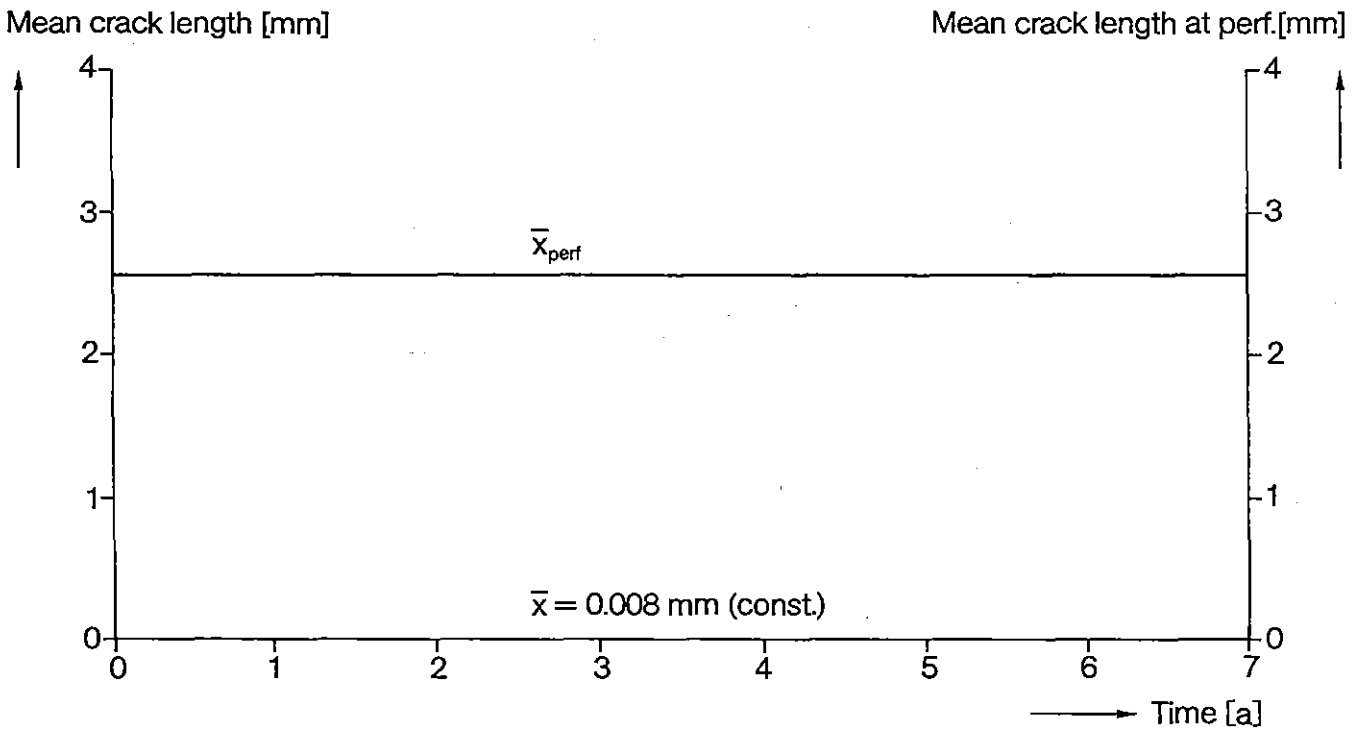

Fig. 2.6/4: "Mean Crack Length" and "Mean Crack Length at Perforation" of a Th Fuel Rod at Standard Dry Storage Conditions

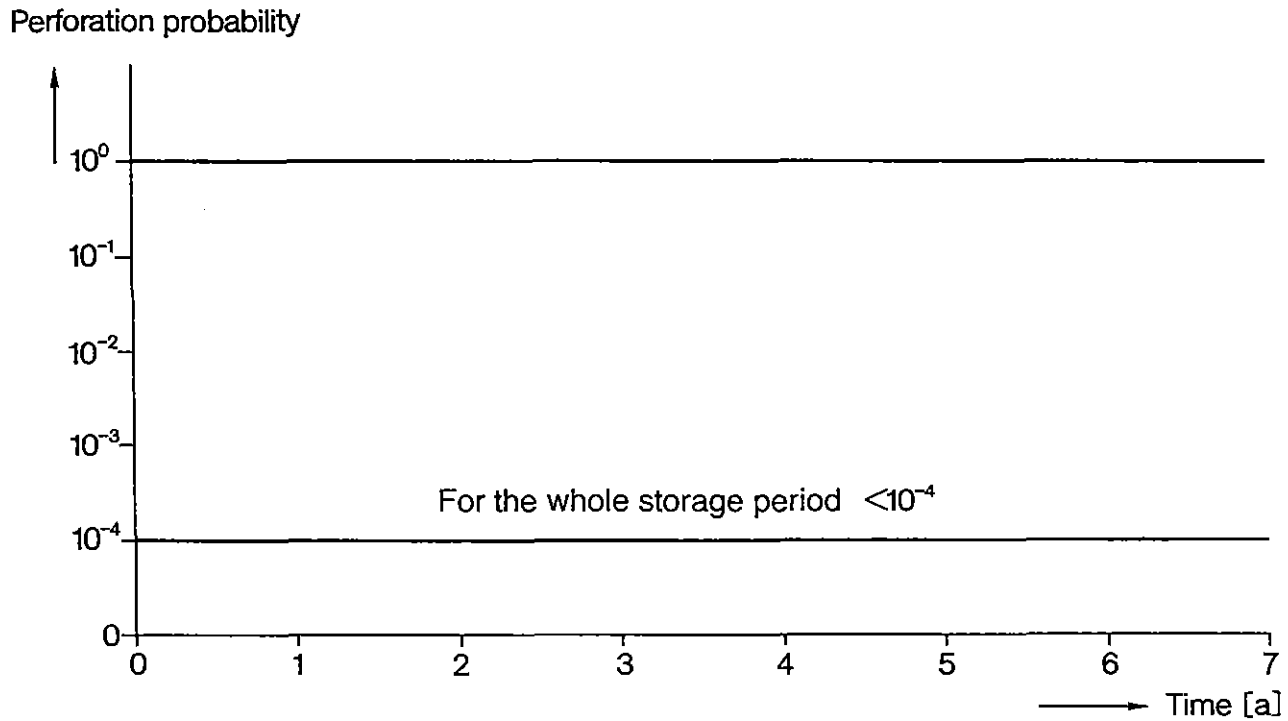

Fig. 2.6/5: Perforation Probability for the Th Fuel Assemblies in a Cask at Standard Dry Storage Conditions

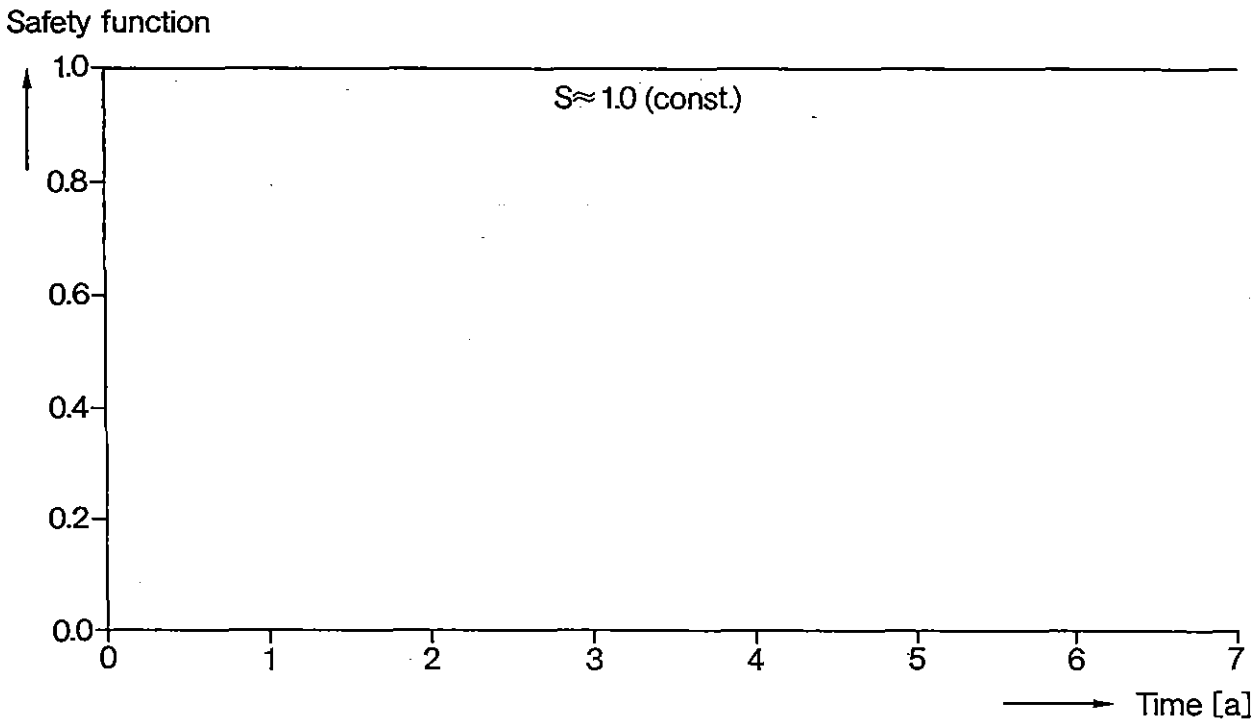

Fig. 2.6/6: ISCC Safety Function s for the Th Fuel Assemblies in a Cask at Standard Dry Storage Conditions

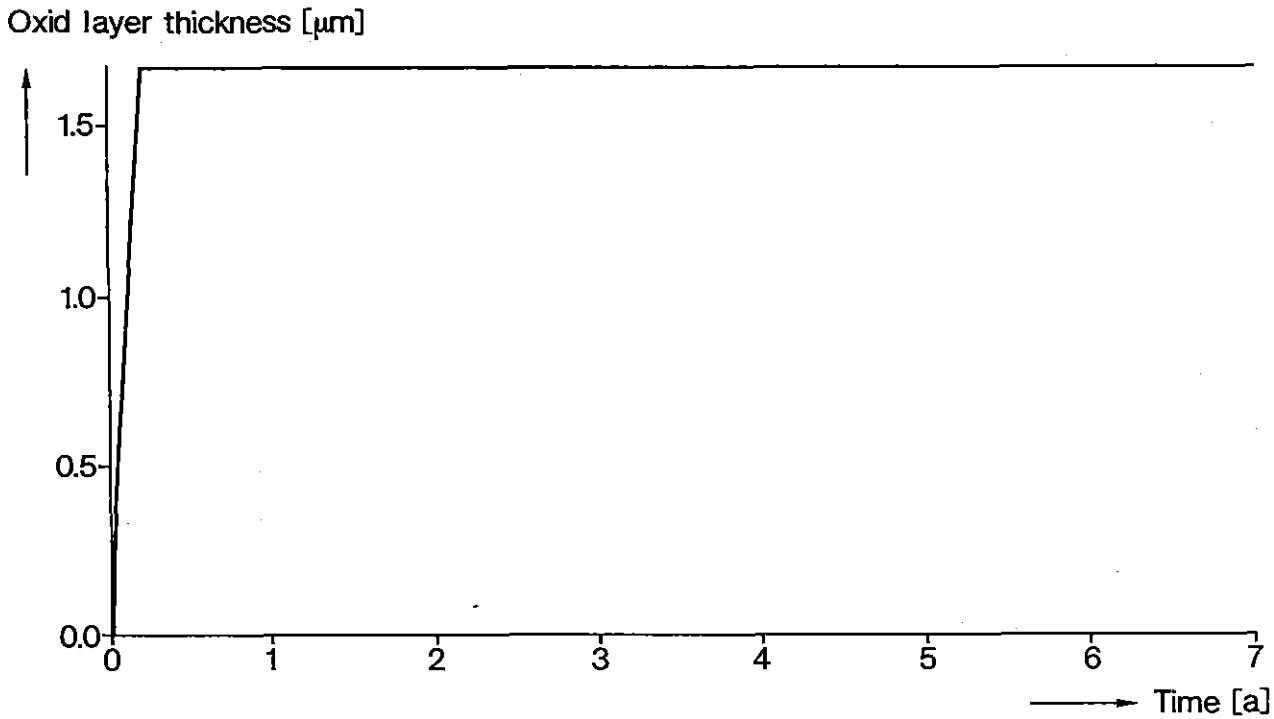

Fig. 2.6/7: Growth of the Oxide Layer of a Th Fuel Rod at Standard Dry Storage Conditions

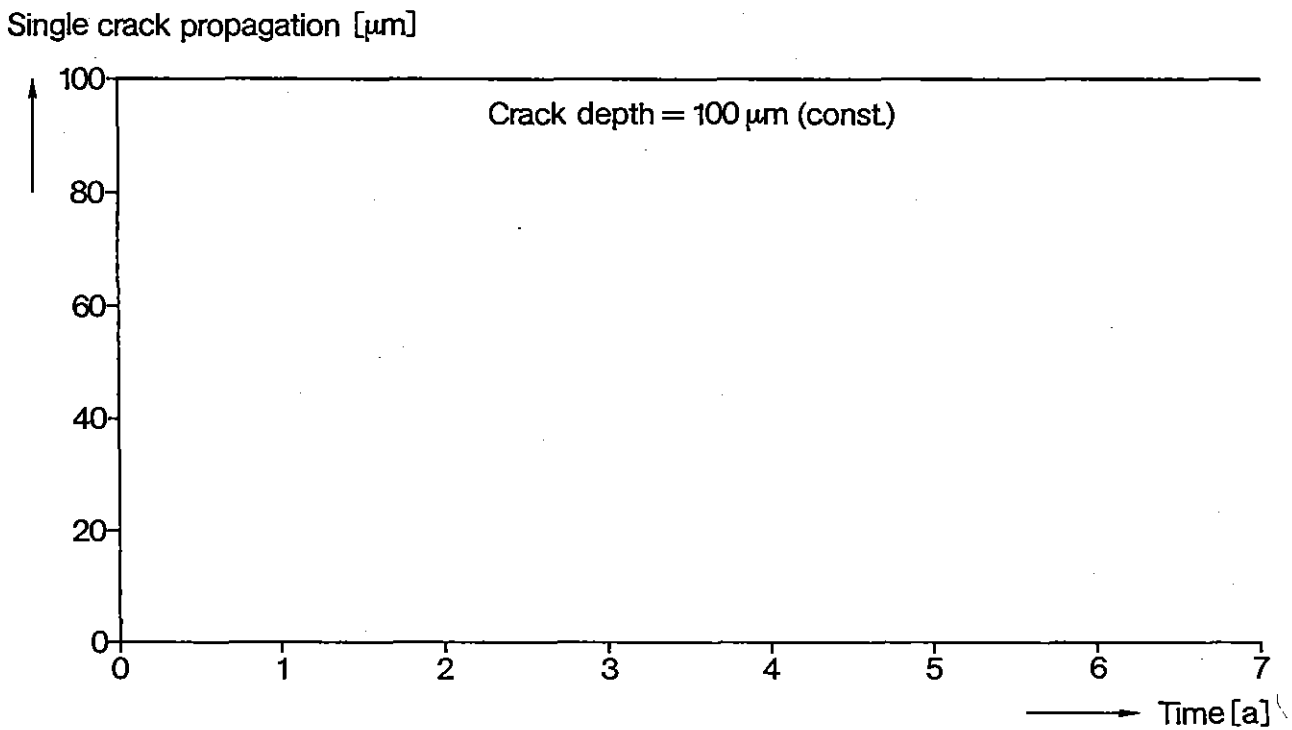

Fig 2.6/8: Propagation of a Singular Crack (100 µm Initial Depth) in a Th Fuel Rod at Standard Dry Storage Conditions

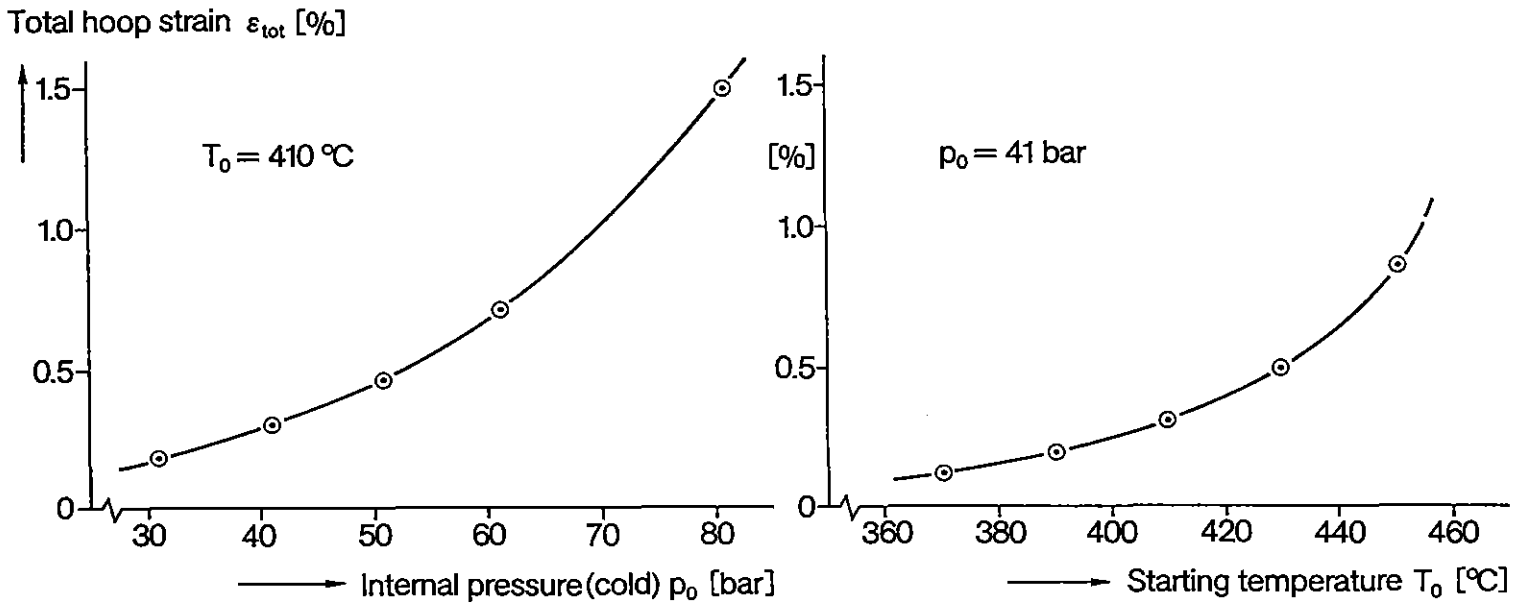

Fig. 2.6/9: Total Hoop Strain in Dependance of Starting Temperature Resp. of Internal Pressure at Decreasing Temperature Function

Data of the fuel sample:
— Fuel rod TDT-81 (1st irradiation test)
— Irradiation time : 11,61d
— Burnup: max. 8,2 kWd/g
— Cooling time: 7-8 months
— Sample length: 1,2cm
— Sample weight: 8,7g ($(Th,U)O_2$ + Zry-4)

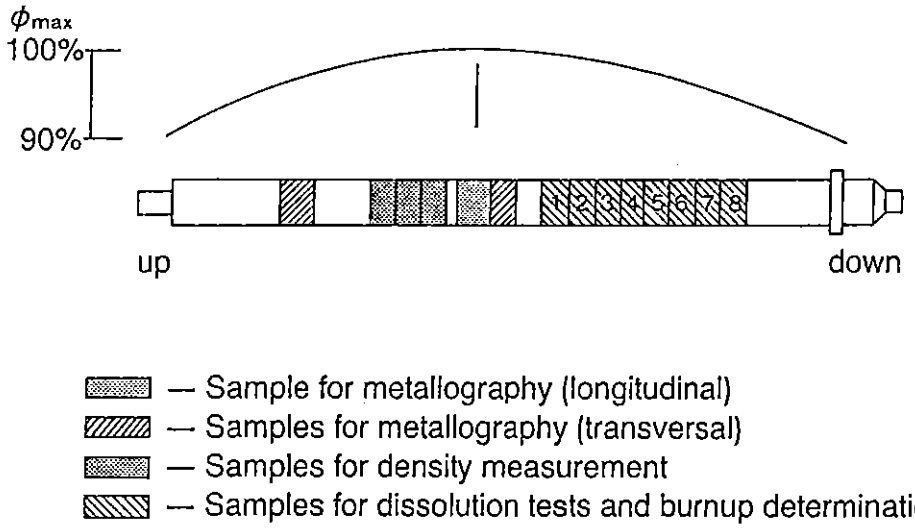

Fig. 2.6/10: Sampling of the Fuel Rod TDT-81

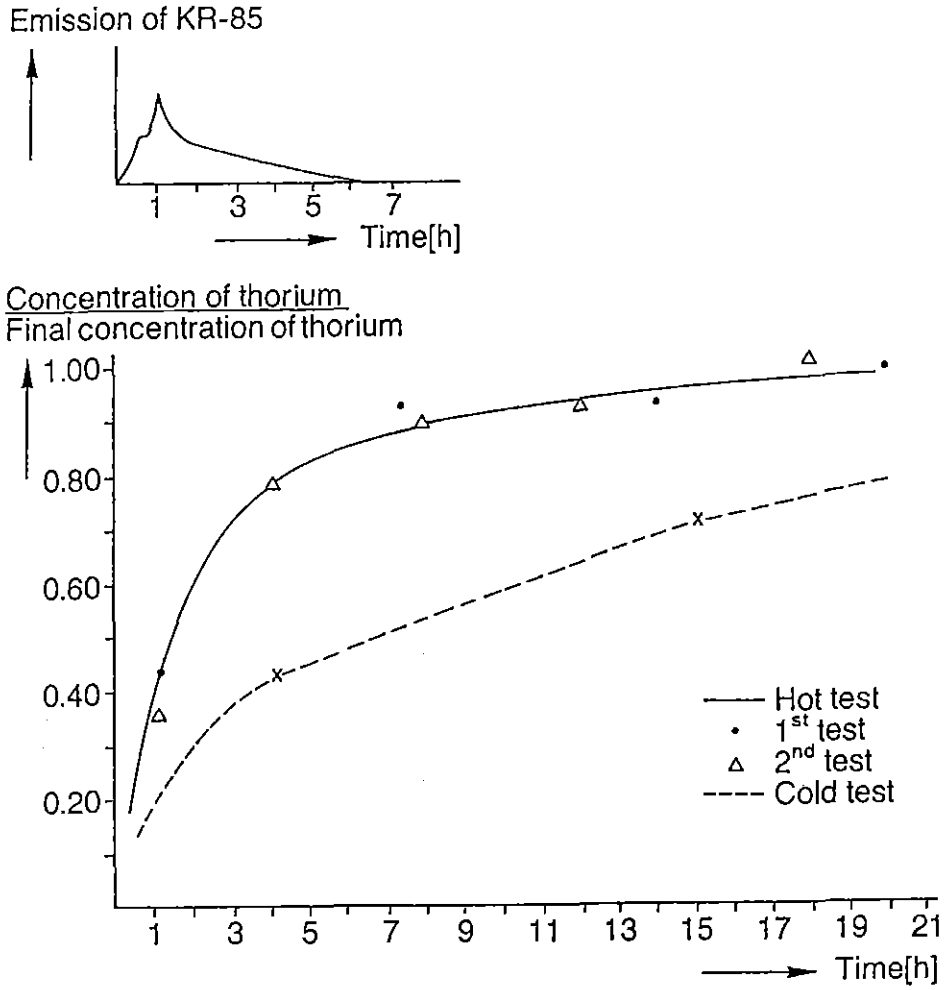

Fig 2.6/11: Dissolution of Irradiated (Th, 5% U)O_2 in Thorex Solution

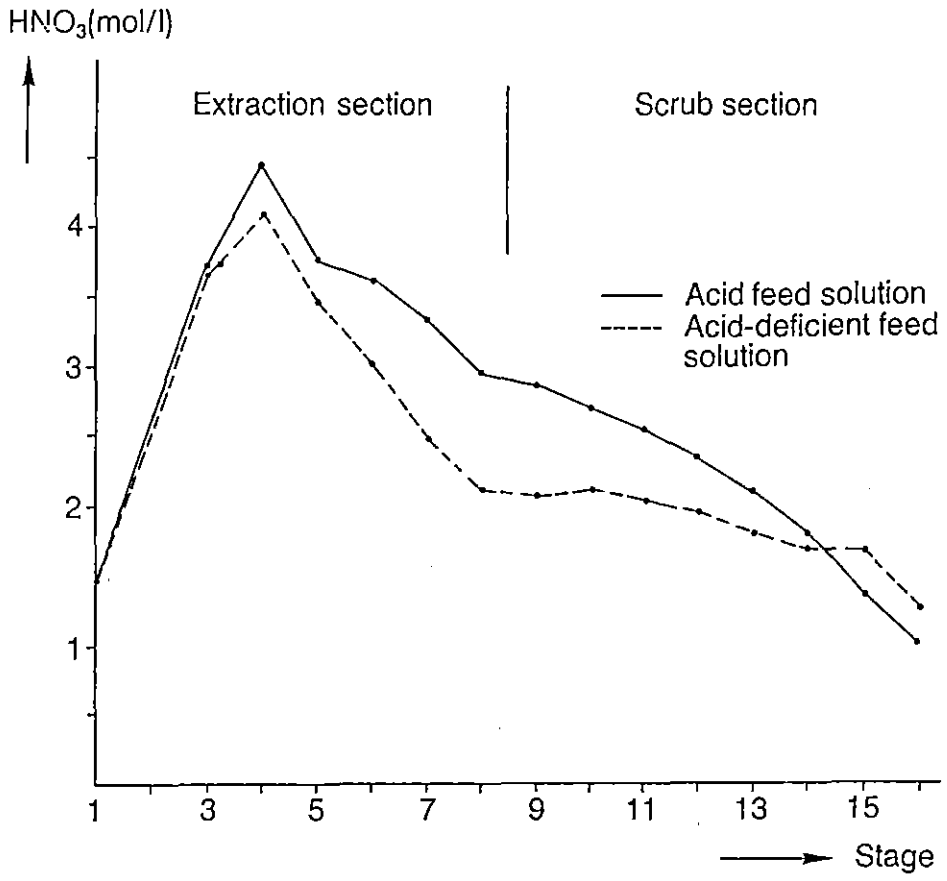

Fig. 2.6/12: HNO_3 Profile in Thorex Process-Extraction (Mixer-Settler)

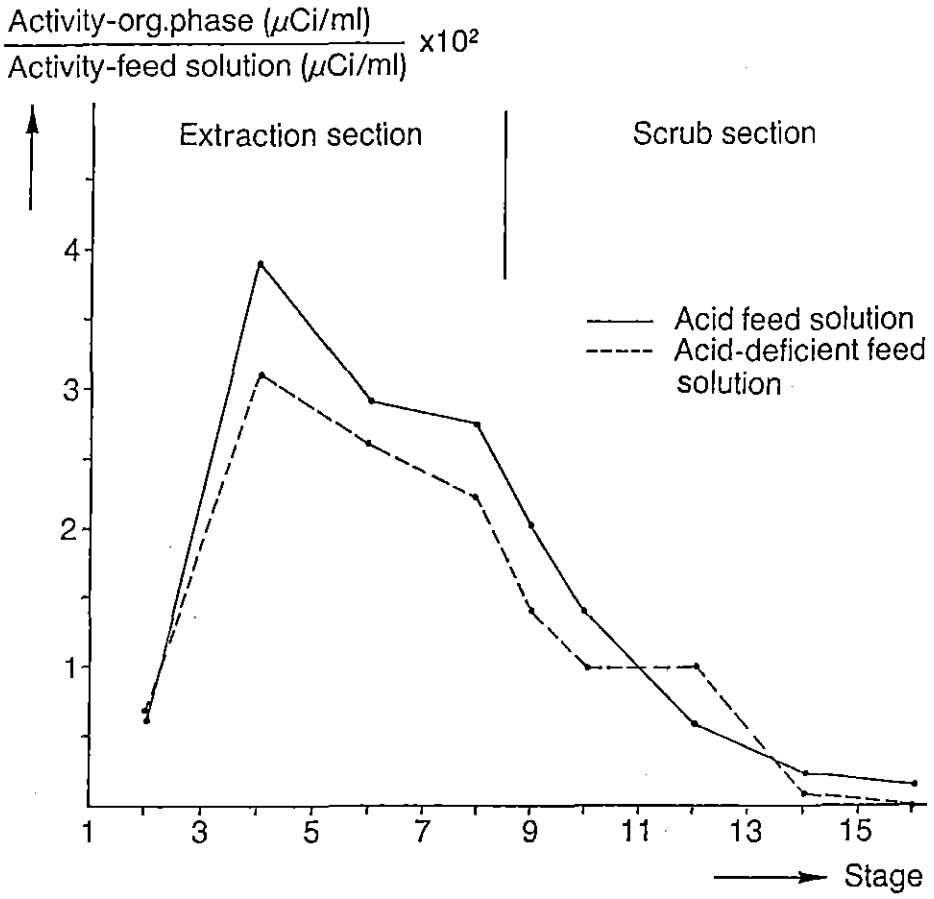

Fig. 2.6/13: Zr-95 Profile in Thorex Process-Extraction (Mixer-Sttler)

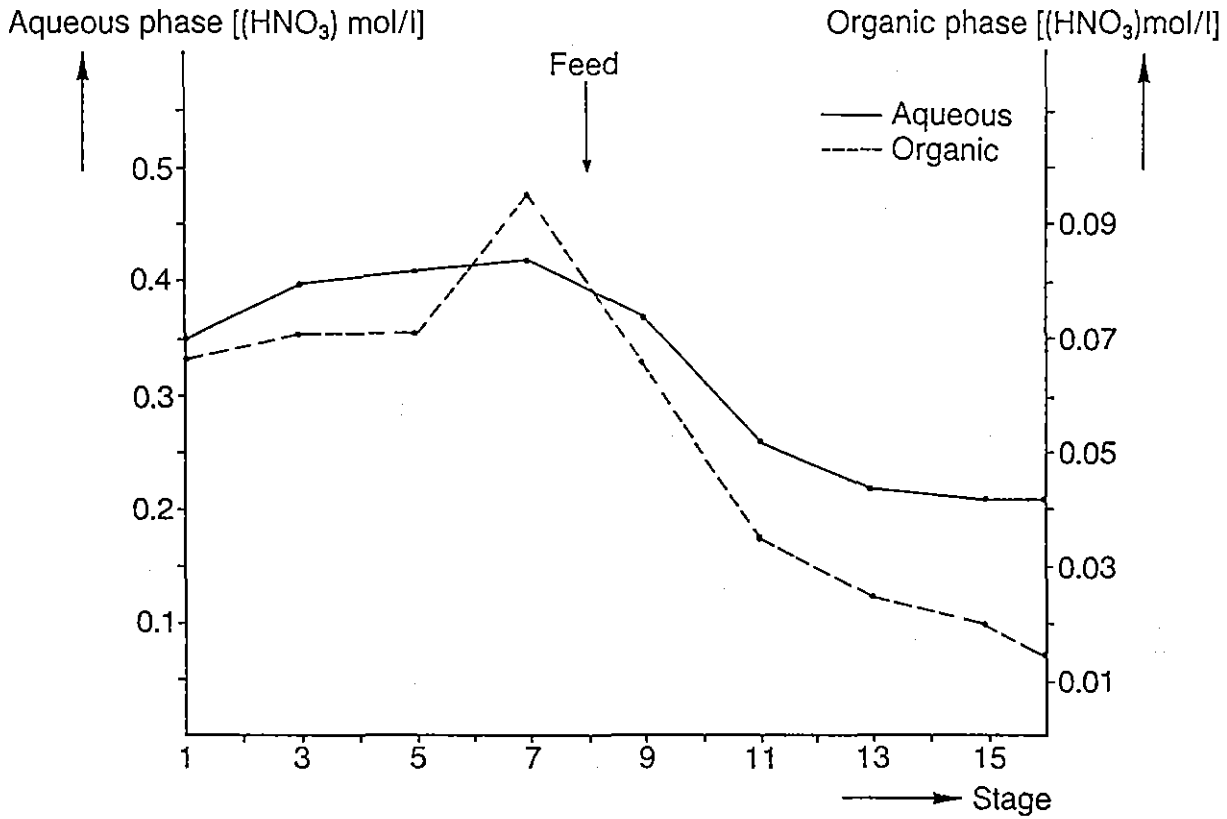

Fig. 2.6/14: HNO_3 Profile in Thorex Process: Partitioning (Mixer-Settler)

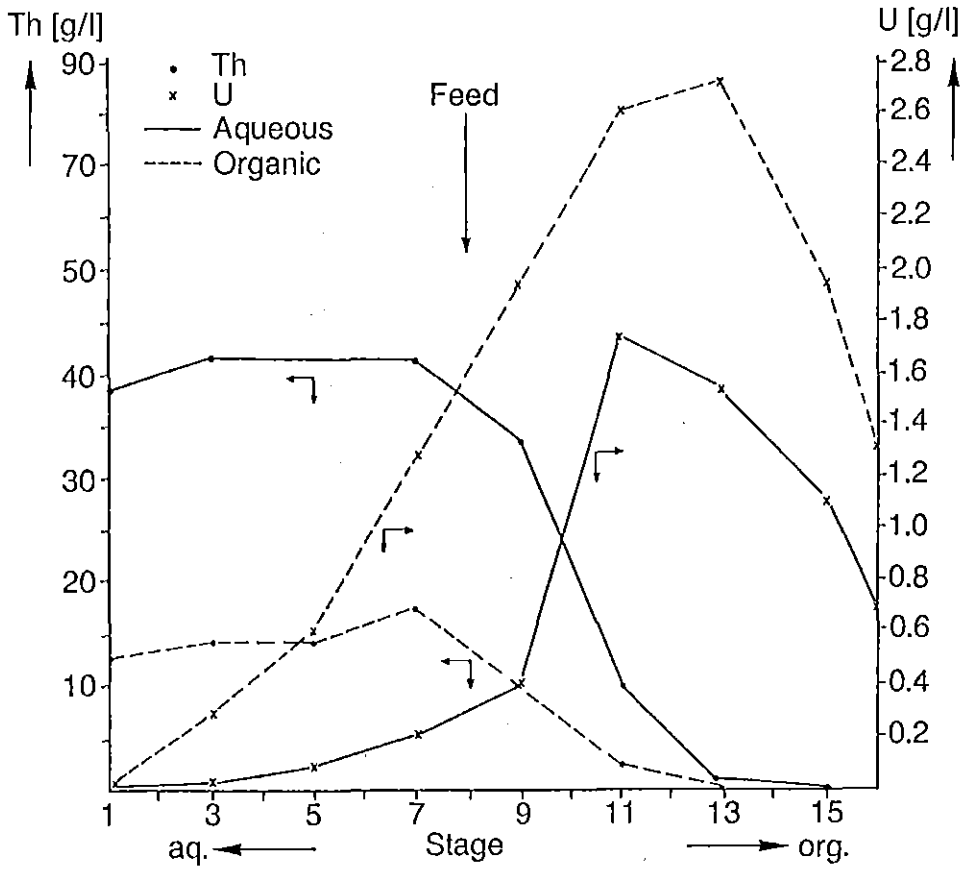

Fig. 2.6/15: Th and U Profiles in Thorex Process: Partitioning (Mixer-Settler)

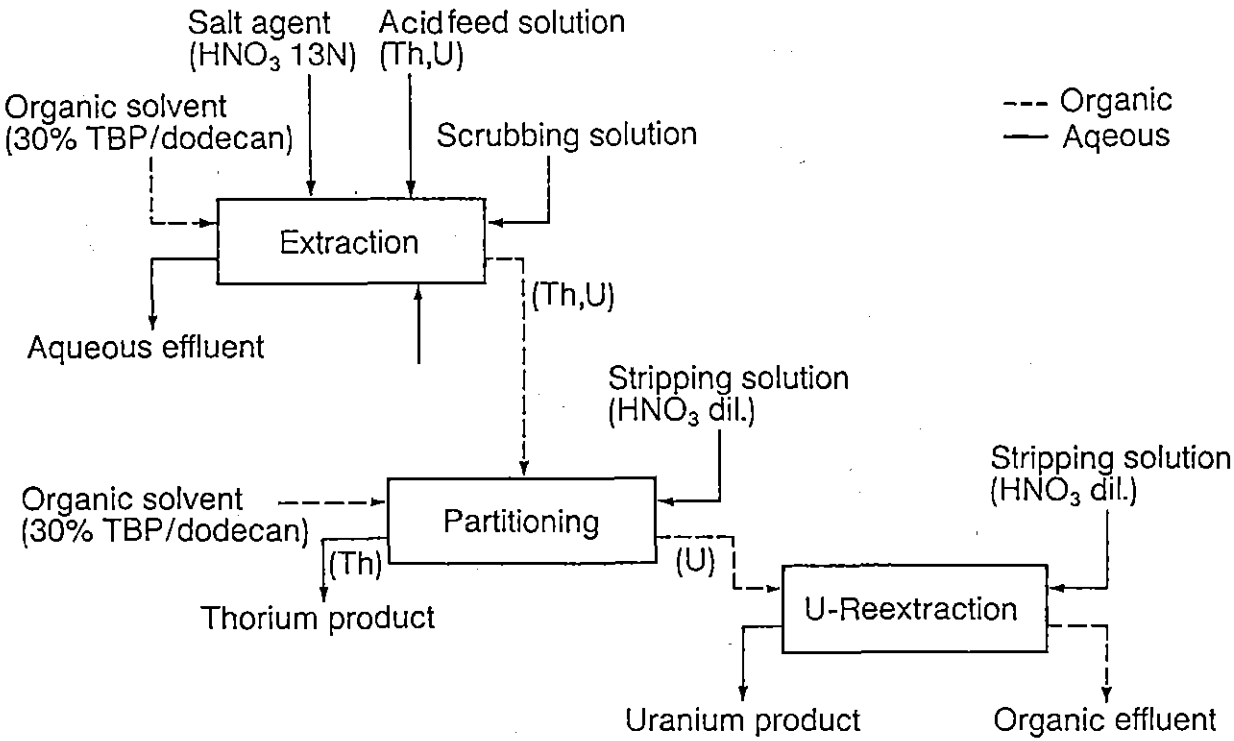

Fig. 2.6/16: One cycle Thorex Process

Vertrieb: KFA Jülich GmbH, Zentralbibliothek
Postfach 1913 · D-5170 Jülich
Telefon: 02461/61-5367 · Telex: 833556-70 kfa d

ISBN 3-89336-019-0